DUAL TRANSITION METAL/PHOTOREDOX CATALYSIS FOR THE SYNTHESIS OF QUATERNARY CARBON STEREOCENTERS

Sijing Xue

UNIVERSITAT ROVIRA i VIRGILI

Dual Transition Metal/Photoredox Catalysis for the Synthesis of Quaternary Carbon Stereocenters

SIJING XUE

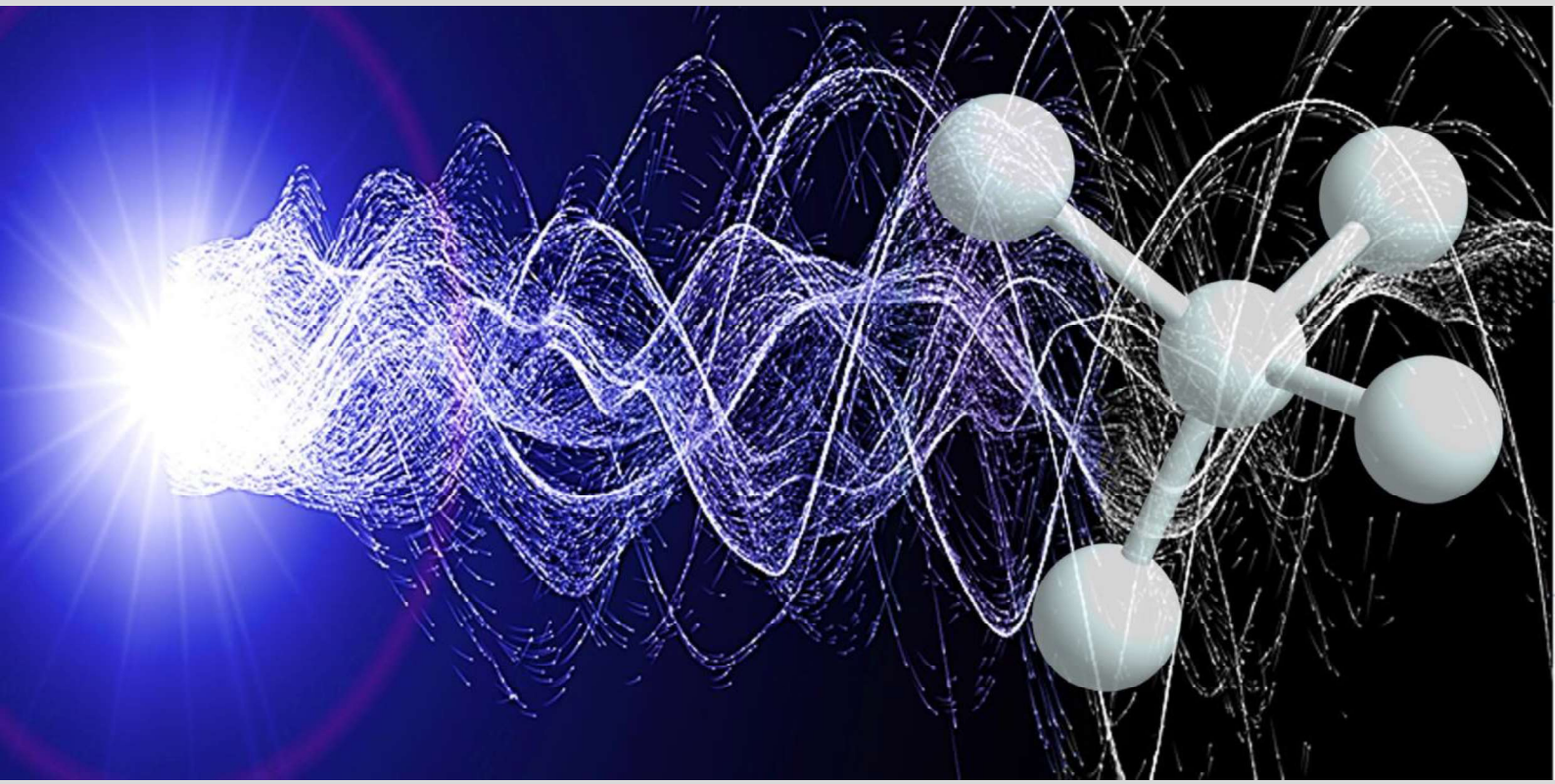

DOCTORAL THESIS

2021

PhD Thesis

"Dual Transition Metal/Photoredox Catalysis for the Synthesis of Quaternary Carbon Stereocenters"

Sijing Xue

Supervised by Prof. Dr. Arjan W. Kleij

Tarragona

December 2021

UNIVERSITAT ROVIRA i VIRGILI

ICIQ

Prof. Dr. Arjan W. Kleij, Group Leader at the Institute of Chemical Research of Catalonia (ICIQ) and Research Professor at the Catalan Institution for Research and Advanced Studies (ICREA),

I STATE that the present Doctoral Thesis, entitled "**Dual Transition Metal/Photoredox Catalysis for the Synthesis of Quaternary Carbon Stereocenters**" presented by Sijing Xue to receive the degree of Doctor, has been carried out under my supervision at the Institute of Chemical Research of Catalonia (ICIQ).

Tarragona, December 2021

Doctoral Thesis Supervisor

Prof. Dr. Arjan W. Kleij

Curriculum Vitae

Sijing Xue was born on February 11 in 1992 in Fujian, China. She obtained her BSc degree in July 2014 at Harbin University of Science and Technology, majoring in material chemistry. Then she started her MSc degree in the Shanghai Institute of Organic Chemistry (SIOC), CAS under the supervision of Prof. Kuiling Ding, during which she was working on Rh(I) catalyzed asymmetric hydrogenation of trisubstituted acrylic acids. In July 2017, she obtained her MSc degree and then she joined the Institute of Chemical Research of Catalonia (ICIQ), Tarragona, to pursue her doctoral studies under the supervision of Arjan W. Kleij. Her research was financially supported by ICIQ and ICIQ predoctoral fellowship. Her PhD research focused on dual transition metal/photoredox catalysis for the synthesis of quaternary carbon stereocenters, and these results are presented in this thesis. Part of this PhD research was communicated as a poster at the XXXVII Reunión Bienal de la Real Sociedad Española de Química in Donostia-San Sebastián in 2019.

Acknowledgments

Till this very moment I was not fully convinced that I would have my thesis ready to be defended on time. This dissertation would not have been possible without all the support of many people. I would like to take this precious opportunity to express my deepest gratitude to those who gave me all the support over the last four years.

First and foremost, I would like to thank my supervisor Prof. **Arjan W. Kleij** for giving me such a great opportunity to join his research group and for all the support he has given me throughout the whole PhD studies. Your optimism, kindness and your faith in me inspired me especially when I was in a dilemma. Again, would like to take this opportunity to give you my sincere gratitude.

Secondly, I would like to thank all the former and current colleagues of the Kleij group. I really cherish all the great time we have spent together and all the knowledge you have been sharing with me: **Jeroen Rintjema**, **Sergio Sopeña**, **Mariachiara Cozzolino**, **Rui Huang**, **Wusheng Guo**, **Sarah Dechent**, **Michela Marchese**, **Josefine Sprachmann**, **José Enrique Gómez (Kike)**, **Aijie Cai**, **Jianing Xie**, **Christian Böhmer**, **Àlex Cristòfol**, **Cristina Maquilón (Cris)**, **Kun Guo**, **Chang Qiao**, **Alèria García**, **Nicola Zanda**, **Bart Limburg**, **Francesco Della Monica**, **Alexander Lücht**, **Debasish Ghorai**, **Alba Villar**, **Xuetong Li**, **Jixiang Ni**, **Qian Zeng**, **Arianna Brandolese**. In addition, I would like to give my sincere gratitude to those with whom I have cooperated: **Jianing Xie**, **Alexander Lücht**, **Àlex Cristòfol** and **Bart Limburg**. Besides, **Ingrid**, thank you for all the paper work you prepared for me throughout my PhD.

During these four years, I shared lots of unforgettable memories with my friends. **Wusheng**, even though I did not get much time to work with you in the lab, it was really a pleasure to get to know you and you will always have my admiration. **Rui**, your optimistic lifestyle and sense of humor always made me feel comfortable to hang out with you. **Kike**, I really appreciated your offer of sharing the fumehood with me. Your enthusiasm in chemistry really inspired me a lot and I enjoyed all the discussions we had. **Aijie**, you were always full of energy and enthusiasm which motivated me in the lab, especially when I came across difficulties. **Jianing**, thank you for helping me fit in the lab when I started my PhD here at ICIQ, and I appreciated all the knowledge you transferred to me. **Cris**, I really cherished all the great time we spent together, the climbing gym, la Móra *etc*. I wish that we still have the chance to hang out together like the old days when I am still in Spain. And I am so happy for you that you could start your

new journey eventually. There would never be enough grateful to **Chang**, my dear, dear **Chang**. You are really a mentor to me in life. Whenever I came across problems, I know that you will always be there. I cherished all the delicious food you prepared for me and all the great time we have spent together. **Alèria**, it has been a pleasure to work with you in the same fume hood. I wish you all the best in the future and I wish you can reunite with your boyfriend soon. **Qian**, I wish you a fruitful PhD throughout the next years.

I would like to express my gratitude to the financial support from ICIQ. I would also like to thank all the ICIQ research support units. Especially, I would like to express my gratitude to **Marta** and **Meritxell** from the Chromtae unit for helping me with the HPLC and electrochemical analyses; **Gabriel**, **Israel** and **Germán** from the NMR unit for helping me with the NMR analyses; **Jordi** from the X-ray unit for your patience and thorough small course on X-ray diffraction, and I admired your strict way of doing research; **Xisco** from the HTE unit for your highly efficient help with the high-throughput experimentation; **Noemí** from the HRMS unit, and **Mariona** from the SMCU unit for your help on the use of various instruments. There are also lots of people who helped me during my PhD who I did not mention yet. I would like to give them my sincere gratitude. I could not have done it without your help.

Last but not the least, I would like to give my high appreciation to my family for their support and love. I wish in the near future I would be able to do something for them in return. And my husband **Xinyi**, I know it has not been easy for both of us to have such a long-distance relationship and thank you for all your support in whatever way. And I am looking forward to our new life together.

I really appreciated my experience here in Spain at in ICIQ. Ever since I arrived in Tarragona, I have had a cosy apartment with friendly roommates. I cherish all the failed and successful experiences during my research work, as I learned a lot during this process being more resilient and self-reliant. I am sure this will help me in my future career.

Sijing, 2021

List of Publications

The results described in this doctoral thesis are based on the following publications:

- **S. Xue**, A. Lücht, J. Benet-Buchholz, A. W. Kleij, *Chem. Eur. J.* **2021**, *27*, 10107-10114.
- **S. Xue**, B. Limburg, D. Ghorai, J. Benet-Buchholz, A. W. Kleij, *Org. Lett.* **2021**, *23*, 4447-4451
- **S. Xue**,[+] À. Cristòfol,[+] B. Limburg, A. W Kleij, A Dual Cobalt/Organophotoredox Catalyst for Diastereo- and Regio selective 1,2-Difunctionalization of 1,3-Diene Surrogates Creating Quaternary Carbon Centers, to be submitted.

Other publications:

- J. Xie, **S. Xue**, E. C. Escudero-Adán, A. W. Kleij, *Angew. Chem. Int. Ed.* **2018**, *57*, 16727-16731.

List of Abbreviations

In this doctoral thesis, the abbreviations and acronyms most commonly used in organic chemistry are based on the recommendations of the ACS "Guidelines for authors" which can be found and consulted at *https://www.cas.org/support/documentation/references/cas-standard-abbreviations#listinga*.

Table of Contents

Chapter 1.

Introduction

1.1. Transition metal catalyzed asymmetric allylic alkylation forging quaternary carbon centers

1.1.1. Construction of all carbon quaternary stereocenters

Significant efforts have been made in the asymmetric construction of quaternary carbon centers which are widely existing in natural products and bioactive pharmaceuticals.[1] However, controlling the configuration of quaternary carbon stereocenters still represents a daunting synthetic challenge due to their congested nature. Although 21 compounds out of the top 200 drugs in the 2012 US retail sales[1b] contained quaternary stereocenters, all were derived from natural product precursors (Scheme 1.1).

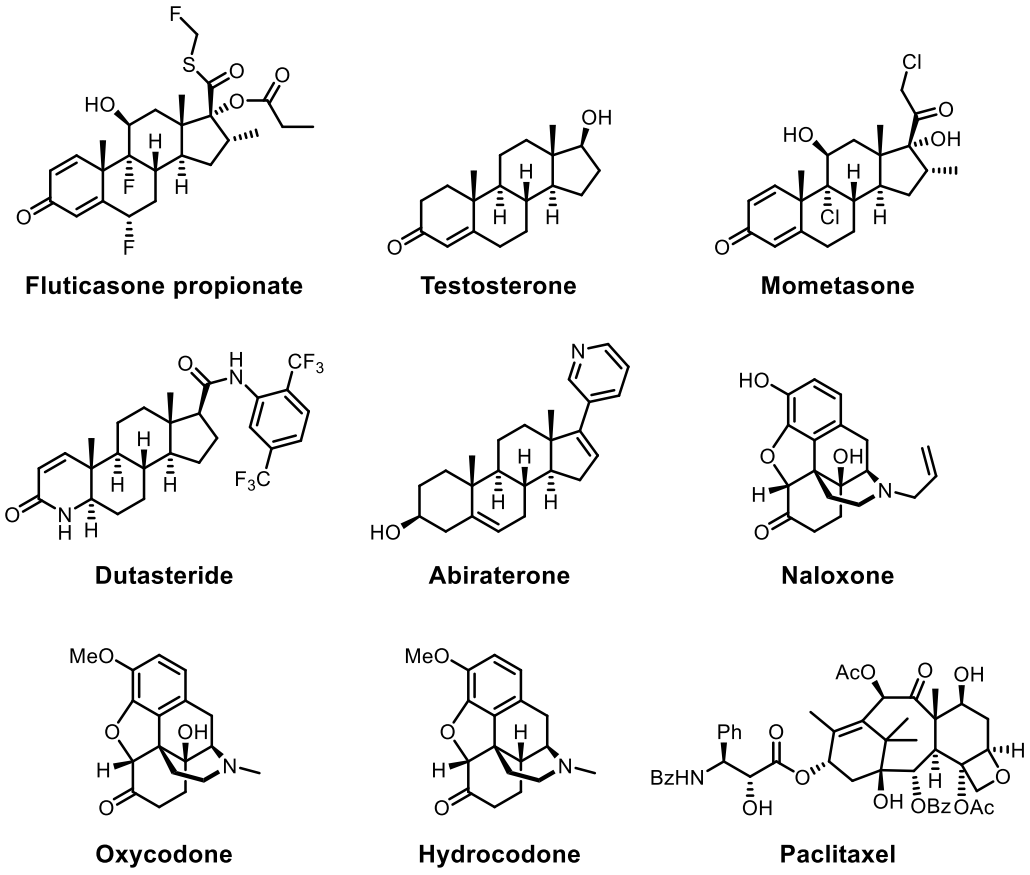

Scheme 1.1. Drug molecules containing quaternary stereocenters

(1) a) J. T. Mohr, M. R. Krout, B. M. Stoltz, *Nature* **2008**, *455*, 323-332; b) Y. Liu, S.-J. Han, W.-B. Liu, B. M. Stoltz, *Acc. Chem. Res.* **2015**, *48*, 740-751; c) M. Büschleb, S. Dorich, S. Hanessian, D. Tao, K. B. Schenthal, L. E. Overman, *Angew. Chem. Int. Ed.* **2016**, *55*, 4156-4186; d) L. Tian, Y.-C. Luo, X.-Q. Hu, P.-F. Xu, *Asian J. Org. Chem.* **2016**, *5*, 580-607; e) C. R. Jamison, J. J. Badillo, J. M. Lipshultz, R. J. Comito, D. W. C. MacMillan, *Nat. Chem.* **2017**, *9*, 1165-1169; f) Q. Zhang, F.-M. Zhang, C.-S. Zhang, S.-Z. Liu, J.-M. Tian, S.-H. Wang, X.-M. Zhang, Y.-Q. Tu, *Nat. Commun.* **2019**, *10*, 2507-2507; g) C. Li, S. S. Ragab, G. Liu, W. Tang, *Nat. Prod. Rep.* **2020**, *37*, 276-292.

1.1.2. Transition metal catalyzed allylic alkylation

Transition metal (TM) catalyzed allylic alkylation reactions have been among the most powerful transformations for the construction of carbon–carbon bonds.[2] With respect to carbon-based nucleophiles, the way in which necleophiles perform the nucleophilic attack on η^3-π-allyl-TM intermediates (Scheme 1.2, **1.1**) can be categorized on the basis of their pK_a.[3] The first class is represented by stabilized or "soft" nucleophiles (i.e., those derived from pronucleophiles with a pK_a < 25), and the second class embodies non-stabilized or "hard" nucleophiles (i.e., those from pronucleophiles with pK_a´s > 25).

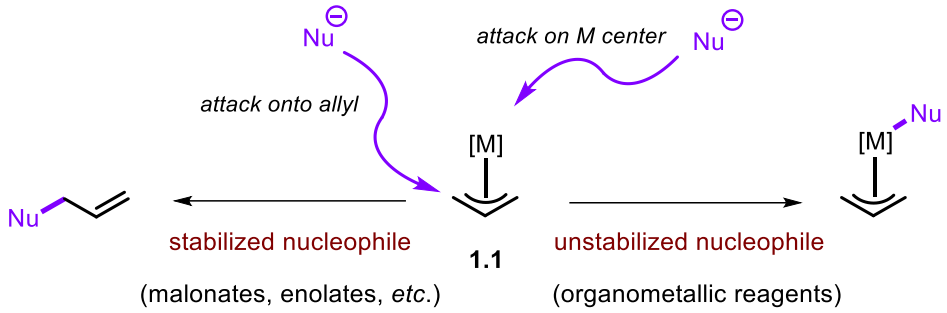

Scheme 1.2. Stabilized versus non-stabilized nucleophiles in allylic substitution reactions. [M] stands typically for a transition metal

Soft nucleophiles are usually involved in direct nucleophilic attack on one of the carbon centers of the π-allyl-TM species (Scheme 3, **1.3**) to afford the target allylation product with net retention of the stereochemistry (Scheme 1.3, right). Transmetalation between hard nucleophiles and the π-allyl-TM species **1.3** leads to the formation of the organometallic species **1.6**, followed by the reductive elimination to deliver the desired product **1.8** with the overall inversion of stereochemistry (Scheme 1.3, left).[4]

(2) a) Z. Lu, S. Ma, *Angew. Chem. Int. Ed.* **2008**, *47*, 258-297; b) J. C. Hethcox, S. E. Shockley, B. M. Stoltz, *ACS Catal.* **2016**, *6*, 6207-6213; c) J. Qu, G. Helmchen, *Acc. Chem. Res.* **2017**, *50*, 2539-2555; d) M. B. Thoke, Q. Kang, *Synthesis* **2019**, *51*, 2585-2631; e) L. Junk, U. Kazmaier, *ChemistryOpen* **2020**, *9*, 929-952.
(3) B. M. Trost, J. E. Schultz, *Synthesis* **2019**, *51*, 1-30.
(4) A. H. Cherney, N. T. Kadunce, S. E. Reisman, *Chem. Rev.* **2015**, *115*, 9587-9652.

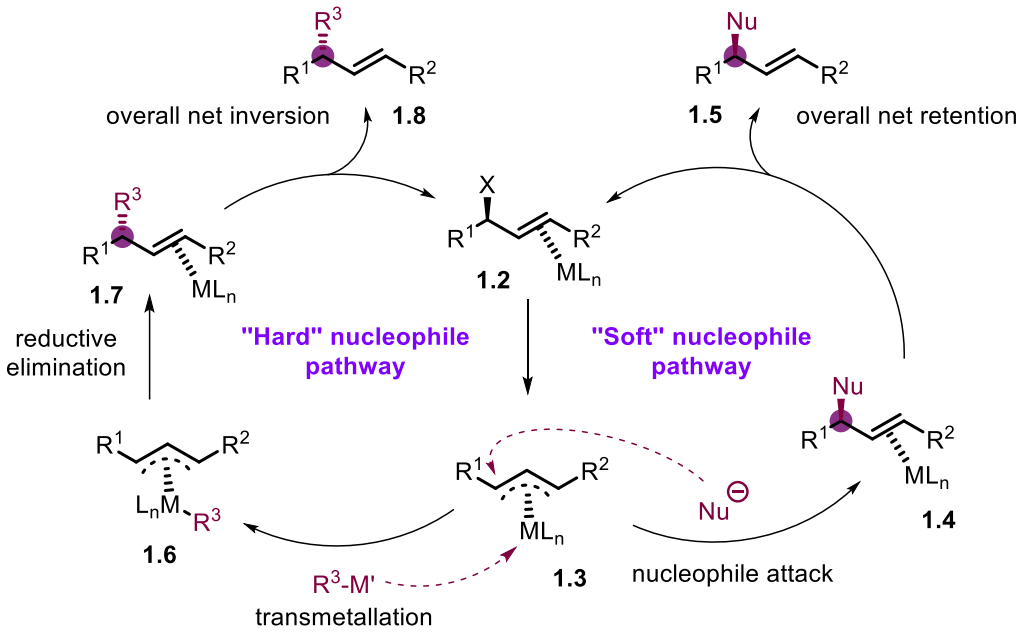

Scheme 1.3. Mechanistic pathways for the regio- and stereospecific transition metal catalyzed allylic substitution

With suitable prochiral nucleophiles or prochiral π-allyl-TM electrophiles, quaternary carbon stereocenters can be generated in either the nucleophilic or electrophilic reaction partner (Scheme 1.4).[5] In the case of prochiral nucleophiles (Scheme 1.4, pathway a), both branched and linear products can be formed featuring quaternary carbon stereocenters. With respect to prochiral π-allyl-TM electrophiles (Scheme 1.4, pathway b), only branch regioselectivity would result in the formation of a quaternary carbon stereocenter.

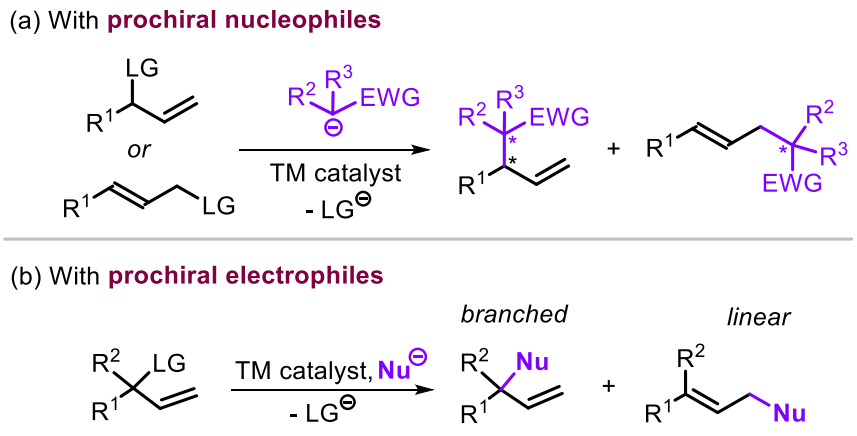

Scheme 1.4. Strategies for the construction of quaternary carbon stereocenters by asymmetric allylic alkylation (AAA). TM = transition metal, LG = leaving group

(5) a) L. Süsse, B. M. Stoltz, *Chem. Rev.* **2021**, *121*, 4084-4099; b) B. M. Trost, C. Jiang, *Synthesis* **2006**, *2006*, 369-396; c) A. Y. Hong, B. M. Stoltz, *Eur. J. Org. Chem.* **2013**, *2013*, 2745-2759.

1.1.3. Pd catalyzed asymmetric allylic alkylation

1.1.3.1. Stereocontrol in prochiral electrophiles forging quaternary carbon stereocenters

The enantiodetermining step in Pd catalyzed asymmetric allylic alkylation with prochiral electrophiles may occur via two mechanisms (Scheme 1.5), namely through the differentiation of enantiotopic olefin faces or via π–σ–π equilibration.[6]

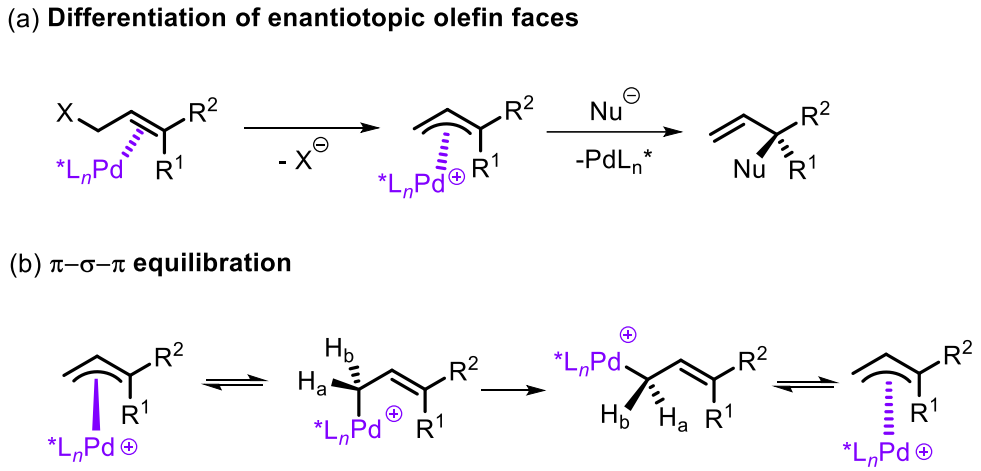

Scheme 1.5. Asymmetric induction approaches based on prochiral electrophiles

Pd catalyzed asymmetric allylic substitution using isoprene monoexpoxide **1.9** (Scheme 1.6) as a prochiral allylic electrophile has been well explored for the construction of C–C,[7] C–O[8] and C–N[9] bonds. Among others, Trost and coworkers established Pd-catalyzed allylic alkylation reactions of nitromethane or β-keto esters with **1.9** to forge acyclic all-carbon quaternary stereocenters (Scheme 1.6).[7] In the case of β-keto ester substrates, the allylic alkylation is followed by a spontaneous cyclization delivering a hemiketal **1.11**, which further reacts via a retroaldol process in the presence of TBAF to provide a product **1.12** having an acyclic quaternary carbon stereocenter.

(6) a) B. M. Trost, D. L. Van Vranken, *Chem. Rev.* **1996**, *96*, 395-422; b) B. M. Trost, M. L. Crawley, *Chem. Rev.* **2003**, *103*, 2921-2944; c) B. M. Trost, M. R. Machacek, A. Aponick, *Acc. Chem. Res.* **2006**, *39*, 747-760.
(7) B. M. Trost, C. Jiang, *J. Am. Chem. Soc.* **2001**, *123*, 12907-12908.
(8) a) B. M. Trost, E. J. McEachern, F. D. Toste, *J. Am. Chem. Soc.* **1998**, *120*, 12702-12703; b) B. M. Trost, E. J. McEachern, *J. Am. Chem. Soc.* **1999**, *121*, 8649-8650.
(9) a) B. M. Trost, R. C. Bunt, R. C. Lemoine, T. L. Calkins, *J. Am. Chem. Soc.* **2000**, *122*, 5968-5976; b) B. M. Trost, C. Jiang, K. Hammer, *Synthesis* **2005**, 3335-3345.

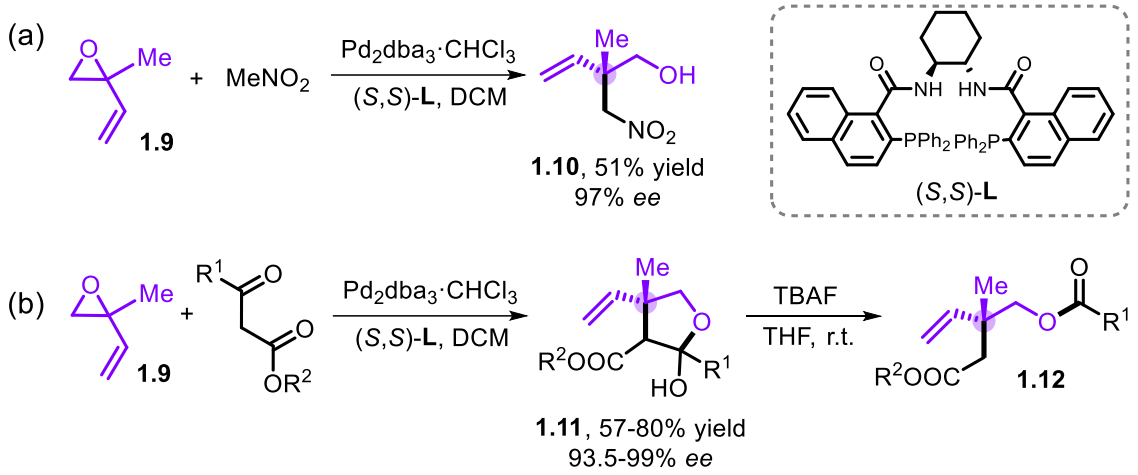

Scheme 1.6. Pd-catalyzed AAA of isoprene monoepoxide **1.9** with carbon nucleophiles

In 2004, the Hou group reported the construction of chiral, quaternary carbon centers through Pd catalyzed asymmetric allylic alkylation with modest to good regio- and enantioselectivities using dimethyl malonate as the pronucleophile (Scheme 1.7).[10]

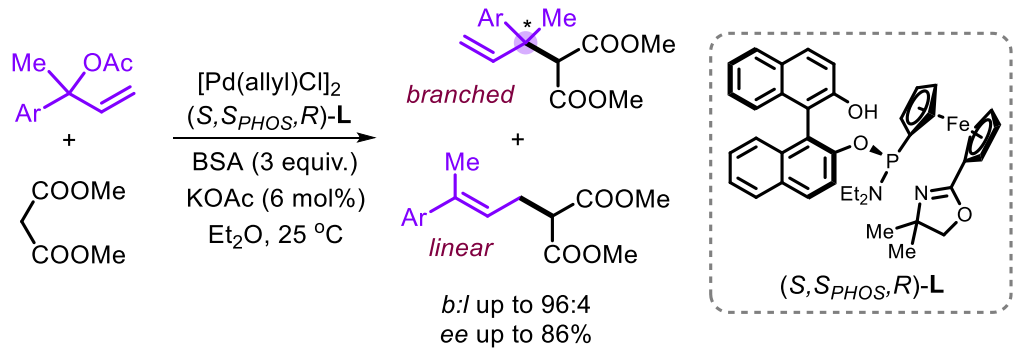

Scheme 1.7. Pd catalyzed AAA of dimethyl malonate leading to the formation of acyclic quaternary carbon stereocenters

Highly regio- and enantio- selective Pd-catalyzed allyl-allyl cross-coupling was realized by Morken et al. to generate all-carbon quaternary and even contiguous quaternary carbon stereocenters.[11] Similar results were observed when (*E*) or (*Z*) configured trisubstituted internal allylic precursors, or terminal allylic precursors (Scheme 1.8) were used. These results indicate that rapid π–σ–π equilibration of the allyl-Pd species was involved before reductive elimination. Mechanistic studies suggested that

(10) X.-L. Hou, N. Sun, *Org. Lett.* **2004**, *6*, 4399-4401.
(11) a) P. Zhang, H. Le, R. E. Kyne, J. P. Morken, *J. Am. Chem. Soc.* **2011**, *133*, 9716-9719; b) M. J. Ardolino, J. P. Morken, *J. Am. Chem. Soc.* **2014**, *136*, 7092-7100.

a 7-membered, 3,3' inner-sphere reductive elimination pathway featuring a bis(η^1-allyl)Pd^{II} complex results in high regio- and enantio-selectivities.

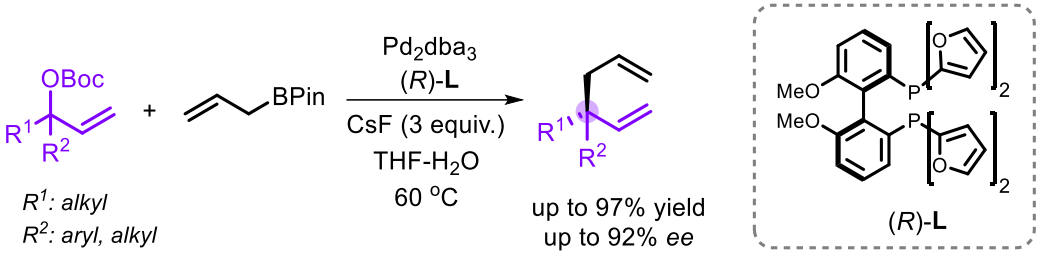

Scheme 1.8. Catalytic enantio- and branch-selective allyl-allyl cross coupling

1.1.3.2. Stereocontrol on prochiral nucleophiles forging quaternary carbon stereocenters

Due to the typical outer-sphere mechanisms involved with the incoming nucleophile remaining distant from the chiral metal-ligand environment, exerting asymmetric induction on prochiral nucleophiles has been traditionally more difficult to achieve compared to prochiral electrophiles with the enantio-selection occurring by discrimination of the prochiral nucleophile faces. Even though significant results have been made in this area, only limited reports discuss the highly enantioselective construction of quaternary carbon stereocenters using prochiral nucleophiles.

Seminal work by the Ito group demonstrated that suitable crown-ether modified chiral ferrocenylphosphine ligands enable the Pd-catalyzed allylic alkylation of β-diketones with moderately high enantioselectivity of up to 75% *ee* (Scheme 1.9).[12] The key objective of this study was to illustrate that by linking a crown-ether to the chiral ligand with a linker having an appropriate chain length would allow for the recognition of the nucleophile counter-ion.

Acyclic amides serving as prochiral nucleophiles have been applied for the allylic alkylation using a Pd/ferrocenyl-based catalyst (Scheme 1.10).[13] Two substrate combinations showed the feasibility of constructing quaternary carbon stereocenters with good enantioselectivity. Extensive optimization indicated that the lithium cation has a crucial influence to control both reactivity and enantioselectivity.

(12) M. Sawamura, H. Nagata, H. Sakamoto, Y. Ito, *J. Am. Chem. Soc.* **1992**, *114*, 2586-2592.
(13) K. Zhang, Q. Peng, X.-L. Hou, Y.-D. Wu, *Angew. Chem. Int. Ed.* **2008**, *47*, 1741-1744.

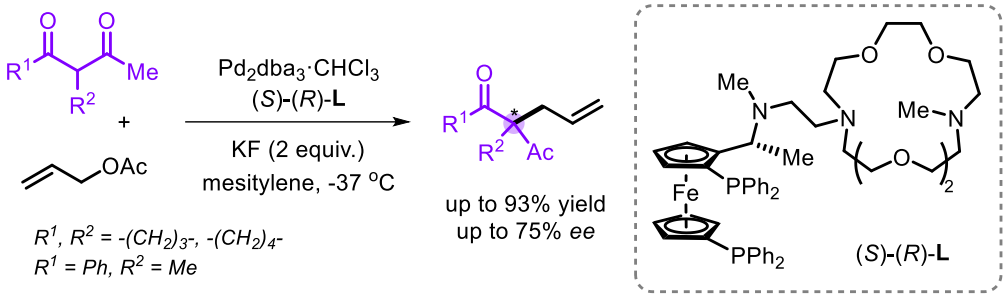

Scheme 1.9. Pd-catalyzed allylic alkylation of β-diketones

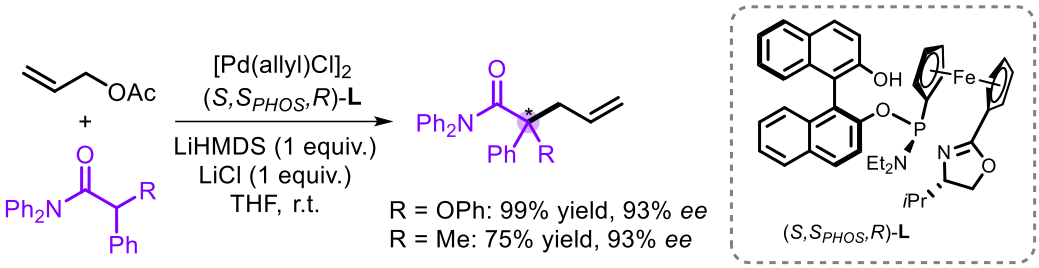

Scheme 1.10. Pd-catalyzed allylic alkylation of *N*,*N*-diphenylamides

In 2011, List and coworker described a direct α-allylation procedure involving prochiral aldehydes with allylic alcohols using a dual Pd/chiral Brønsted acid TRIP/amine based catalyst system (Scheme 1.11).[14] They realized that the low enantioselectivity can be attributed to a reduced geometric control over the *E*- and *Z*- enol isomer formation (**1.13**), which results in the formation of a mixture of enantiomers. Therefore, increasing stereo-control over the enol would deliver the product with enhanced enantioselectivity. Indeed, the addition of amines dramatically increased the enantioselectivity of the process. The aldehyde reagent was conveniently activated by a primary amine to furnish the (*E*)-enamine, while the allylic alcohol was activated by the Brønsted acid **TRIP**. Oxidative addition of Pd(0) onto the activated allylic alcohol enabled the alkylation of the activated (*E*)-enamine involving three catalyst components (**1.14)** through formal asymmetric counteranion-directed catalysis.

(14) G. Jiang, B. List, *Angew. Chem. Int. Ed.* **2011**, *50*, 9471-9474.

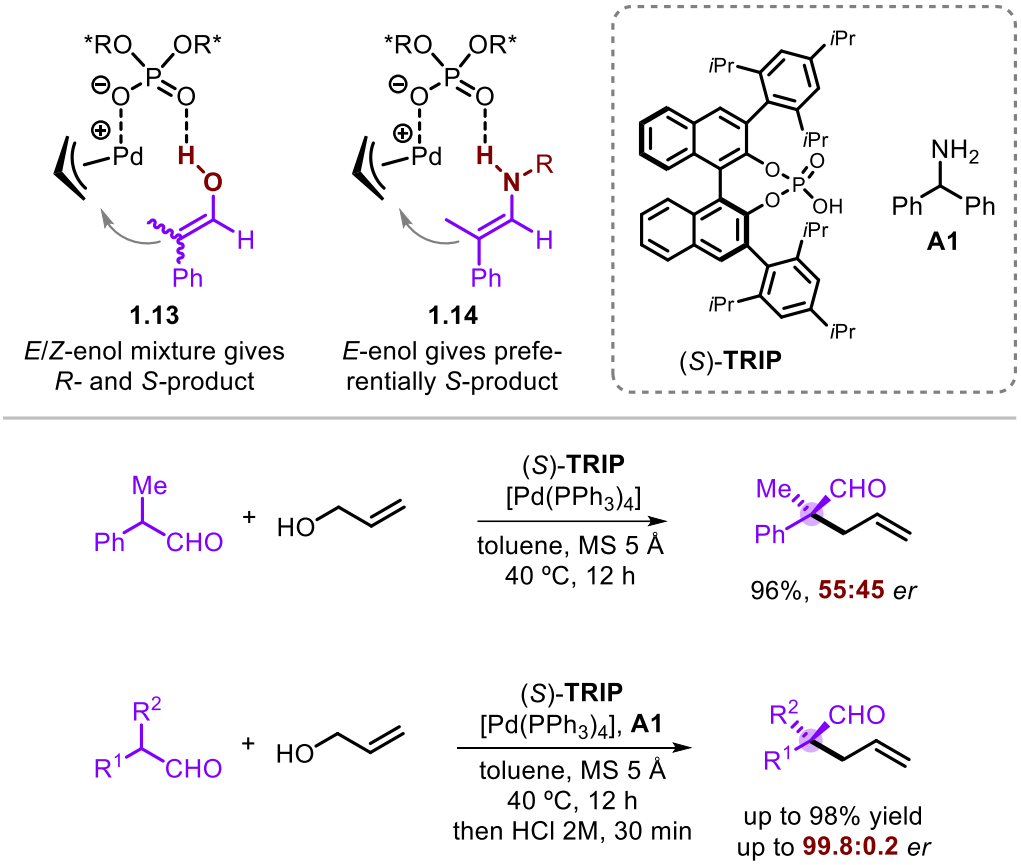

Scheme 1.11. Hypothesized enantioinduction model in the Pd-catalyzed asymmetric α-allylation of different aldehydes

1.1.4. Co catalyzed allylic alkylation

The field of asymmetric allylic substitution has been dominated in the last decades by noble transition metals such as Pd, Ir and Ru, while Co as an earth-abundant, first row TM has been much less explored.[5a,15] This in spite of the fact that Co is cheaper and has an apparent lower toxicity. Early research in the area demonstrated the potential use of Co-catalysis through the allylic alkylation of organometallic reagents and soft nucleophiles (such as β-ketoesters) to deliver the linear allylic product. The development of Co-catalyzed allylic substitution during the recent decades has enabled the reaction process through two main pathways. The first one involves the formation of an electrophilic Co-π-allyl species, which then reacts with a suitable nucleophile to form the allylic products. The second pathway involves the formation of a nucleophilic Co-π-allyl species (cf., umpolung), which then is combined with an electrophilic species.

(15) M. Kojima, S. Matsunaga, *Trends Chem.* **2020**, *2*, 410-426.

1.1.4.1. Reactions with nucleophiles

The Li group reported on a Co-catalyzed allylic alkylation reaction to forge quaternary all-carbon stereocenters by incorporating "soft" carbon nucleophiles such as β-keto esters and malononitriles (Scheme 1.12).[16] Good to excellent regio- and enantioselectivities were realized by using a Co/(*S*,*S*)-Ph-BPE and Co/bis-oxazolinephosphine (abbreviated as NPN) catalyst, respectively. The Zn additive serves as a reductant to generate *in situ* the requisite and envisioned Co^{I}/L species.

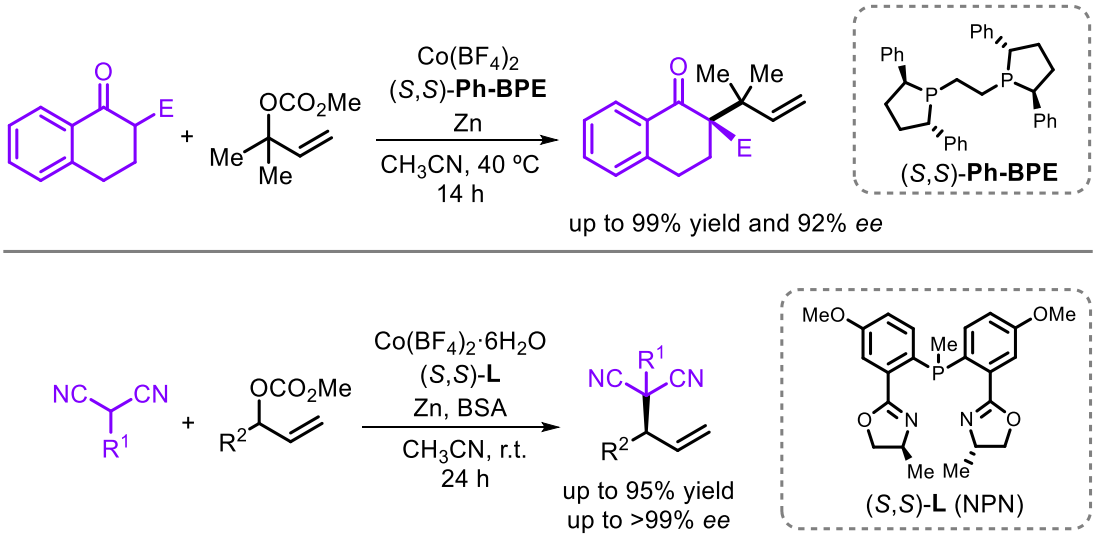

Scheme 1.12. Co-catalyzed allylic alkylation with "soft" carbon nucleophiles

Photoredox catalysis has been widely explored during the last decade providing new synthetic opportunities thereby expanding the toolbox of organic chemists. Photocatalysts typically engage in single electron transfer (SET) events with organic or organometallic substrates upon visible light excitation (Scheme 1.13). These SET events give access to highly reactive radical species under mild conditions, and can effectively 'switch on' other catalyst components that are non-effective in the absence of a photocatalyst. In 2019, the Matsunaga group developed a dual Co/organophotoredox catalyzed allylic alkylation with good regioselectivity.[17] Instead of using zinc as a reductant, photoredox-mediated reduction generates an active Co catalyst to facilitate the catalytic process.

(16) a) M. Sun, J.-F. Chen, S. Chen, C. Li, *Org. Lett.* **2019**, *21*, 1278-1282; b) S. Ghorai, S. Ur Rehman, W.-B. Xu, W.-Y. Huang, C. Li, *Org. Lett.* **2020**, *22*, 3519-3523.
(17) K. Takizawa, T. Sekino, S. Sato, T. Yoshino, M. Kojima, S. Matsunaga, *Angew. Chem. Int. Ed.* **2019**, *58*, 9199-9203.

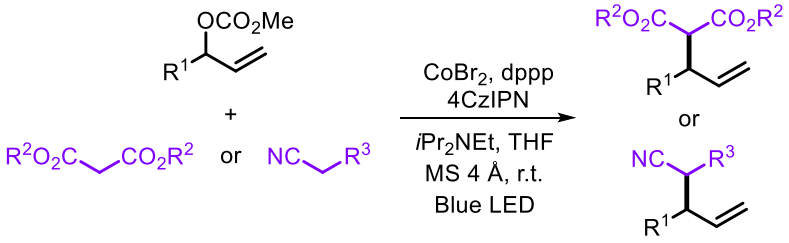

Scheme 1.13. Cobalt-catalyzed allylic alkylation enabled by a dual Co/organophotoredox catalysis approach

1.1.4.2. Reactions with electrophiles

TM-catalyzed allylic alkylation reactions provide an efficient means to forge C–C bonds via a π-allyl-TM intermediate that can undergo alkylation with soft and hard carbon nucleophiles. Additionally, the use of additives and/or designer ligands allows to reverse the polarity of π-allyl-TM metal complex and thus the coupling with electrophiles.[18] For example, in the case of π-allyl-Pd species, the nucleophilic addition to carbonyl compounds and imines have been well developed in the presence of an excess of metal reductant such as Et_2Zn and Et_3B. Below, recent progress of nucleophilic π-allyl/Co species and their synthetic applications will be discussed.

Recently, Cozzi[19] and Shi[20] independently established photocatalytic generation of nucleophilic π-allyl-Co species for the allylation of aldehydes to deliver the target homoallylic alcohols though with moderate diastereo-control. UV-vis spectroscopy studies and control experiments supported the generation of a π-allyl-Co^{II} species (**1.16**, Scheme 1.14). Then, a Co^{I} species is generated through SET by the reduced Ir^{II} photocatalyst, following oxidative addition of the Co^{I} intermediate onto an allyl ester to deliver an electrophilic π-allyl-Co^{III} species (**1.15**). Then as second SET reduction produces a nucleophilic allyl-Co^{II} complex (**1.16**) that attacks the carbonyl substrate through a Zimmerman-Traxler transition state **1.17** to furnish the homoallylic alcohol.

(18) a) M. Yus, J. C. González-Gómez, F. Foubelo, *Chem. Rev.* **2013**, *113*, 5595-5698; b) K. Spielmann, G. Niel, R. M. de Figueiredo, J.-M. Campagne, *Chem. Soc. Rev.* **2018**, *47*, 1159-1173.
(19) A. Gualandi, G. Rodeghiero, R. Perciaccante, T. P. Jansen, C. Moreno-Cabrerizo, C. Foucher, M. Marchini, P. Ceroni, P. G. Cozzi, *Adv. Synth. Catal.* **2021**, *363*, 1105-1111.
(20) C. Shi, F. Li, Y. Chen, S. Lin, E. Hao, Z. Guo, U. T. Wosqa, D. Zhang, L. Shi, *ACS Catal.* **2021**, *11*, 2992-2998.

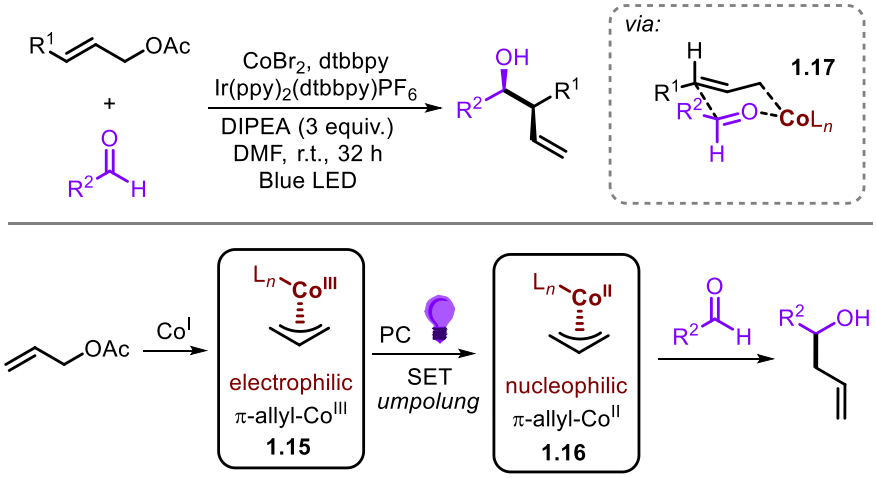

Scheme 1.14. Photocatalytic "umpolung" approach to produce a nucleophilic π-allyl-Co^{II} complex for the allylation of aldehydes

Shortly hereafter, Meng and coworkers reported Co-catalyzed diastereo- and enantioselective carbonyl allylation with a remarkably broad scope of allylic and aldehyde partners (Scheme 1.15).[21] Mn was used as a reductant to convert the allyl-Co^{III} into a nucleophilic allyl-Co^{II} complex. Radical scavenging reactions and radical clock experiments were conducted, which suggested the involvement of an allylic radical intermediate being key in these stereoconvergent transformations.

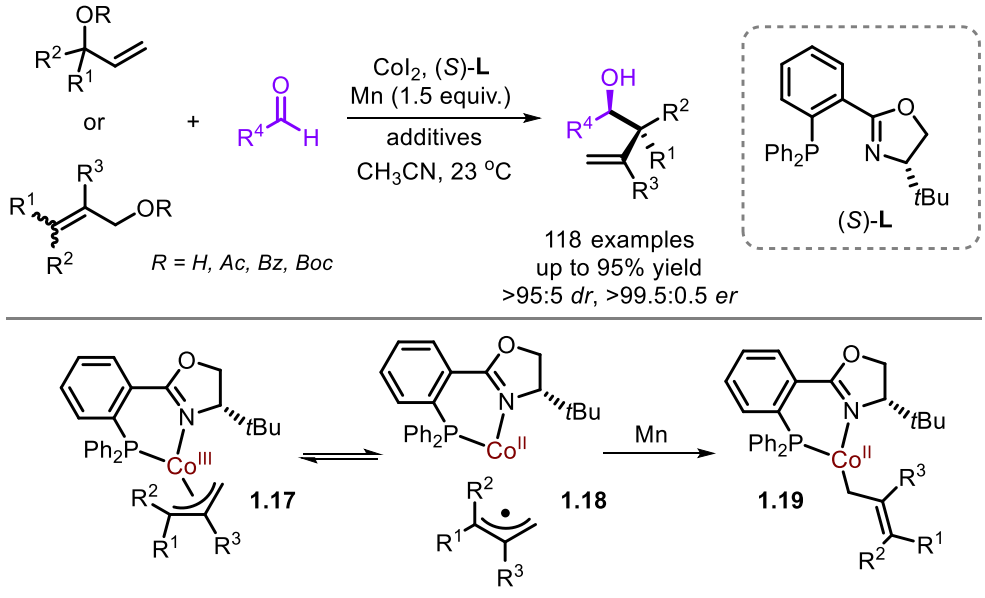

Scheme 1.15. Co-catalyzed diastereo- and enantioselective reductive allylations

(21) L. Wang, L. Wang, M. Li, Q. Chong, F. Meng, *J. Am. Chem. Soc.* **2021**, *143*, 12755-12765.

1.2. The merger of photoredox and TM catalysis

Recently, the field of photocatalysis has undergone a significant renaissance allowing for the development of a wide range of previously inaccessibly transformations in the field of organic chemistry.[22] Upon excitation, an excited-state photocatalyst ($[PC^n]^*$) can engage in photoinduced energy transfer (PEnT) and/or photoinduced electron transfer (PET) processes with an organic substrate. In terms of photoredox catalysis, PET is involved (Scheme 1.16). In the reductive quenching cycle, $[PC^n]^*$ receives an electron from an electron donor followed by oxidation to deliver the ground state PC^n. Alternatively, in the oxidative quenching cycle, $[PC^n]^*$ functions as a reductant to release an electron to an electron acceptor, leading to the formation of an oxidized photocatalyst PC^{n+1}, after which this species can accept an electron completing the catalytic cycle. The resultant excited species could act both as a strong oxidant or reductant simultaneously. These features enable a reaction environment that is unique for organic chemistry.

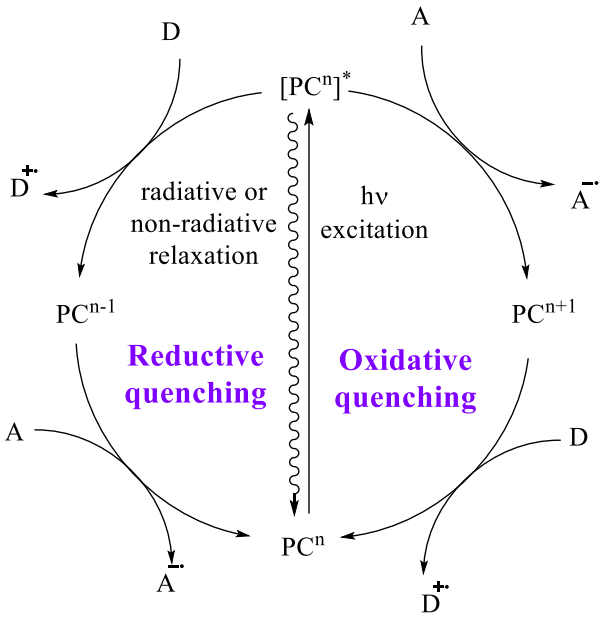

Scheme 1.16. Oxidative and reductive quenching pathways of a photocatalyst

Significant efforts have been made to merge TM and photo-redox catalysis (generally designated as metallaphotoredox catalysis) over the last few decades.[23] Photoredox

(22) a) T. P. Yoon, M. A. Ischay, J. Du, *Nat. Chem.* **2010**, *2*, 527-532; b) J. M. R. Narayanam, C. R. J. Stephenson, *Chem. Soc. Rev.* **2011**, *40*, 102-113.

(23) a) C. K. Prier, D. A. Rankic, D. W. C. MacMillan, *Chem. Rev.* **2013**, *113*, 5322-5363; b) M. N. Hopkinson, B. Sahoo, J. L. Li, F. Glorius, *Chem. Eur. J.* **2014**, *20*, 3874-3886; c) K. L. Skubi, T. R. Blum, T. P. Yoon, *Chem. Rev.* **2016**, *116*, 10035-10074; d) I. Ghosh, L. Marzo, A. Das, R. Shaikh, B. König, *Acc. Chem. Res.* **2016**, *49*, 1566-1577; e) H. H. Zhang, H. Chen, C. Zhu, S. Yu, *Sci. China*

catalysis provide access to reactive radical species under mild conditions typically from abundant functional groups. In combination with TM catalysis, this feature allows direct coupling of non-conventional nucleophilic partners enabling many synthetically useful C–C and C–heteroatom bond formations. In this context, 4-alkyl-1,4-dihydropyridines (4-alkyl-DHPs) have been often used as radical precursors. Therefore, below some basic concepts and benchmark examples will be discussed.

1.2.1. 4-Alkyl-DHPs serving as radical precursors and electron donors

4-alkyl-DHPs, which have recently been established as versatile reagents for the formation of alkyl radical,[24] can be easily prepared from readily available chemicals (*e.g.*, aldehydes) in a single step.[25] 4-alkyl-DHPs can undergo a facile photocatalytic SET oxidation (E_{ox} = + 1.05 V vs SCE),[24c] and subsequent homolysis of the C–C bond at the 4-position to extrude alkyl radicals. A wide range of C–C bond formations have been realized through non-metal involved photoredox catalyzed radical-radical cross-coupling or via radical addition to suitable radical acceptors. Notably, metallaphotoredox catalysis enables the cross-coupling reactions of 4-alkyl-DHPs that formally function as nucleophilic coupling partners.

In 2016, the Molander group described a cross-coupling reaction between a diverse range of (hetero)aryl bromides and 4-alkyl-DHPs towards the formation of $C(sp^2)–C(sp^3)$ bonds using dual Ni/photoredox catalysis (Scheme 1.17).[26] A plausible mechanism was proposed, involving two distinct, yet interconnected catalytic cycles: a photoredox cycle and a metal-promoted cross-coupling cycle. Upon visible light irradiation, the excited state photocatalyst is oxidatively quenched by a 4-alkyl-DHP generating a radical cation, which undergoes homolysis thereby delivering the alkyl radical. The in situ generated carbon-centered alkyl radical is then trapped by a Ni^0 species to give a Ni^I complex. The latter then undergoes oxidative addition in the presence of the aryl bromide to furnish a Ni^{III} intermediate. A subsequent reductive elimination step provides the target cross-

Chem. **2020**, *63*, 637-647; f) M. De Abreu, P. Belmont, E. Brachet, *Eur. J. Org. Chem.* **2020**, *2020*, 1327-1378; g) S. Zheng, Y. Hu, W. Yuan, *Synthesis* **2021**, *53*, 1719-1733.

(24) a) W. Huang, X. Cheng, *Synlett* **2017**, *28*, 148-158; b) P.-Z. Wang, J.-R. Chen, W.-J. Xiao, *Org. Biomol. Chem.* **2019**, *17*, 6936-6951; c) J. A. Milligan, J. P. Phelan, S. O. Badir, G. A. Molander, *Angew. Chem. Int. Ed.* **2019**, *58*, 6152-6163.

(25) a) G. Li, R. Chen, L. Wu, Q. Fu, X. Zhang, Z. Tang, *Angew. Chem. Int. Ed.* **2013**, *52*, 8432-8436; b) W. Chen, Z. Liu, J. Tian, J. Li, J. Ma, X. Cheng, G. Li, *J. Am. Chem. Soc.* **2016**, *138*, 12312-12315.

(26) Á. Gutiérrez-Bonet, J. C. Tellis, J. K. Matsui, B. A. Vara, G. A. Molander, *ACS Catal.* **2016**, *6*, 8004-8008.

coupling product and regenerates a Ni^{I} species, which is reduced to Ni^{0} to complete the overall catalytic cycle.

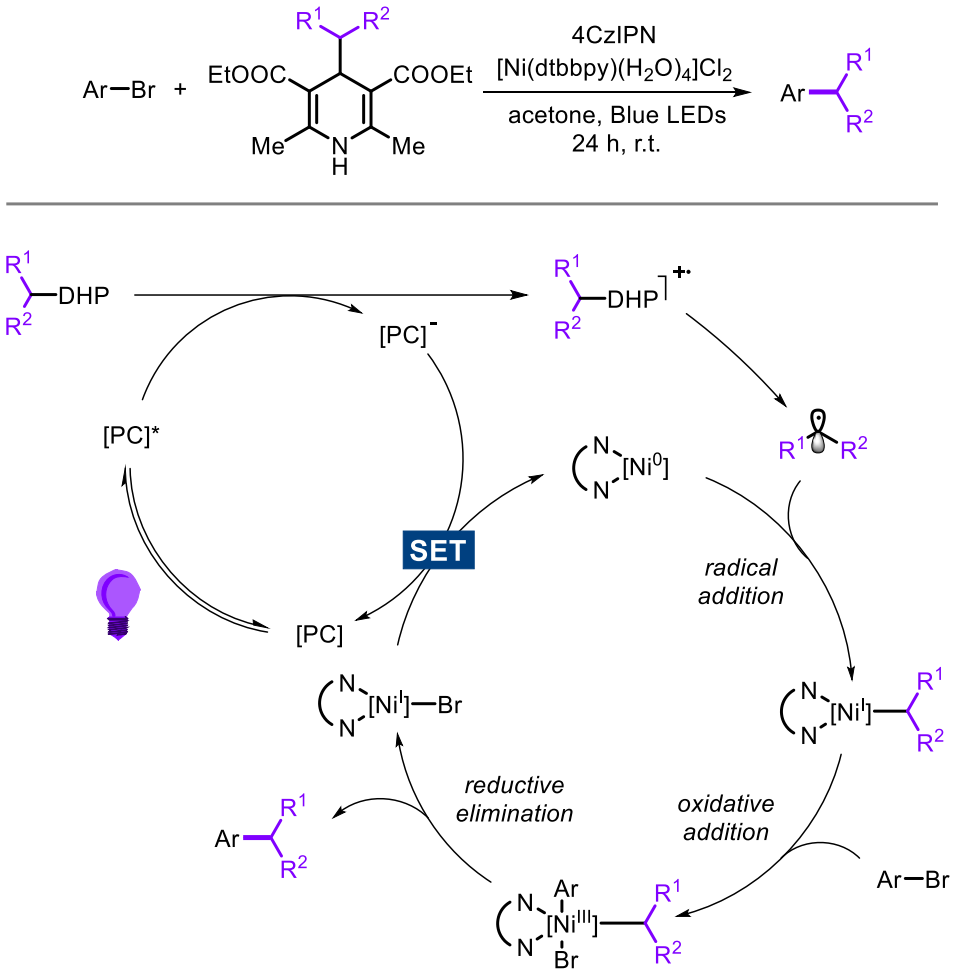

Scheme 1.17. Dual Ni/photoredox catalyzed cross-coupling between (hetero)aryl bromides and 4-alkyl-DHPs

As previously mentioned, allylic alkylation is one of the most powerful strategies for the construction of C–C bonds, however the effective use of carbon-based nucleophiles has been limited to soft nucleophiles or organometallic reagents. The merger of photoredox catalysis and TM-catalyzed allylic alkylation enables the formation of C–C bonds with non-traditional carbon-based nucleophiles. Molander and coworkers disclosed a regio-selective, Ni-catalyzed photoredox based allylation of secondary, benzyl and α-alkoxy radical precursors deliver predominantly linear products. This process is a useful complementary strategy in carbon-carbon formation for the

conventional Pd-catalysed Tsuji-Trost reaction (Scheme 1.18).[27] DFT calculations supported the possible involvement of a Ni^0-Ni^{II}-Ni^{III} redox pathway, and an inner-sphere reductive elimination step.

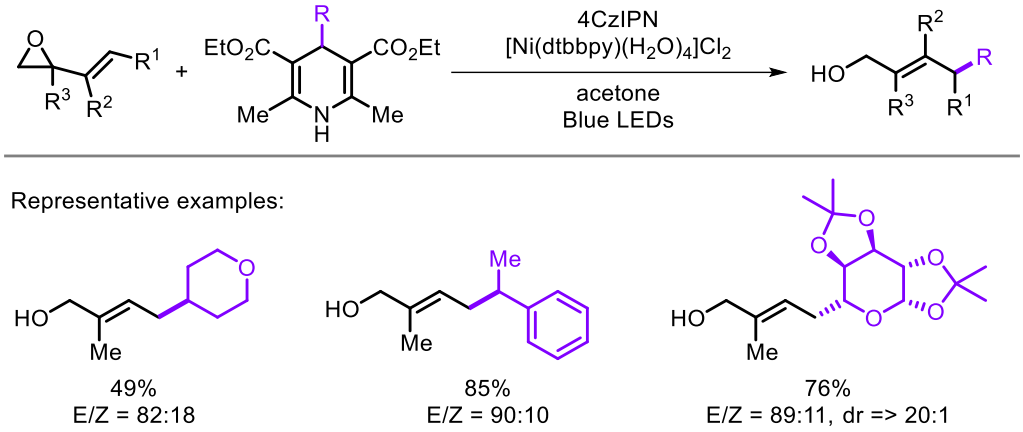

Scheme 1.18. Photoredox/Ni-catalyzed single-electron Tsuji-Trost reactions

Almost simultaneously, Yu and co-workers established the first dual photoredox/Pd catalyzed highly regio- and enantioselective allylic alkylation of 4-alkyl-DHPs (Scheme 1.19).[28] The generality of this method was illustrated through the combination of a variety of allyl esters and 4-alkyl-DHPs. Within the scope, two-substrate combinations displayed the potential of the protocol to deliver products featuring quaternary carbon stereocenters, with appreciable *ee* values. A plausible mechanism was proposed, involving a Pd^0-Pd^{II}-Pd^{III} reaction pathway and forging the key C–C bond through an inner-sphere reductive elimination. Oxidative addition of the allyl ester onto a Pd^0 species provides a π-allyl-Pd^{II} complex, that upon capturing of the *in situ* produced alkyl radical (from the 4-alkyl-DHP) is converted into a Pd^{III} intermediate. The latter undergoes reductive elimination delivering the product along with a Pd^I complex which is reduced to Pd^0 by the reduced photocatalyst.

(27) J. K. Matsui, Á. Gutiérrez-Bonet, M. Rotella, R. Alam, O. Gutierrez, G. A. Molander, *Angew. Chem. Int. Ed.* **2018**, *57*, 15847-15851.
(28) H.-H. Zhang, J.-J. Zhao, S. Yu, *J. Am. Chem. Soc.* **2018**, *140*, 16914-16919.

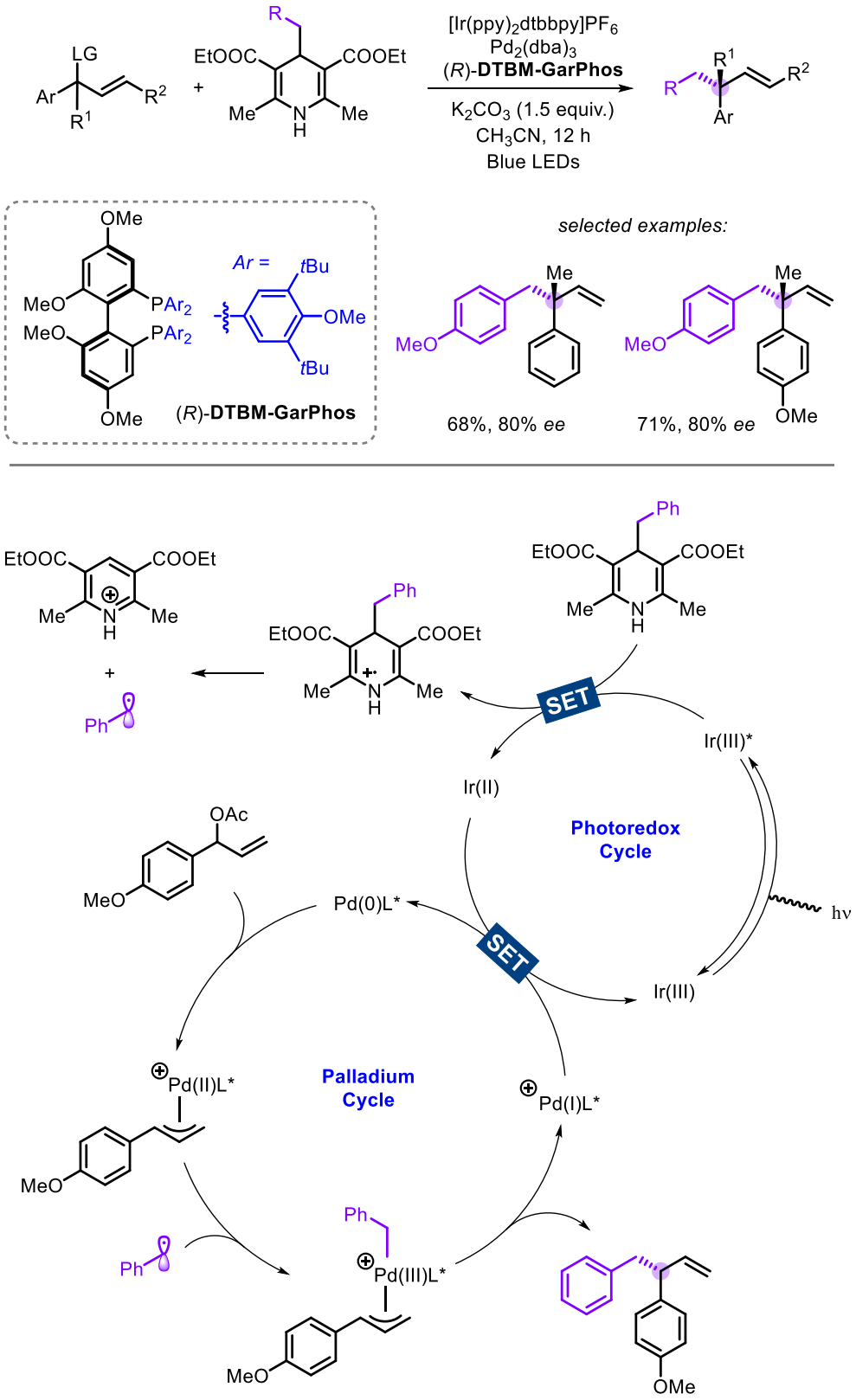

Scheme 1.19. Dual photoredox/Pd catalyzed highly regio- and enantioselective allylic alkylation using 4-alkyl-DHPs

1.2.2. 4-Alkyl-DHPs serving as both radical precursors and photoreductant

The Melchiorre group has been focusing on the development of electronically excited chiral organocatalytic intermediates, which allows to advance unique transformations that are otherwise inaccessible through conventional ground-state pathways (Scheme 1.20).[29] Based on this concept, they disclosed a wide variety of cross-coupling reactions without the need for an external photocatalyst. Upon visible light irradiation, transiently generated chiral enamines can trigger the formation of radicals through SET reduction of organic halides.[29b]

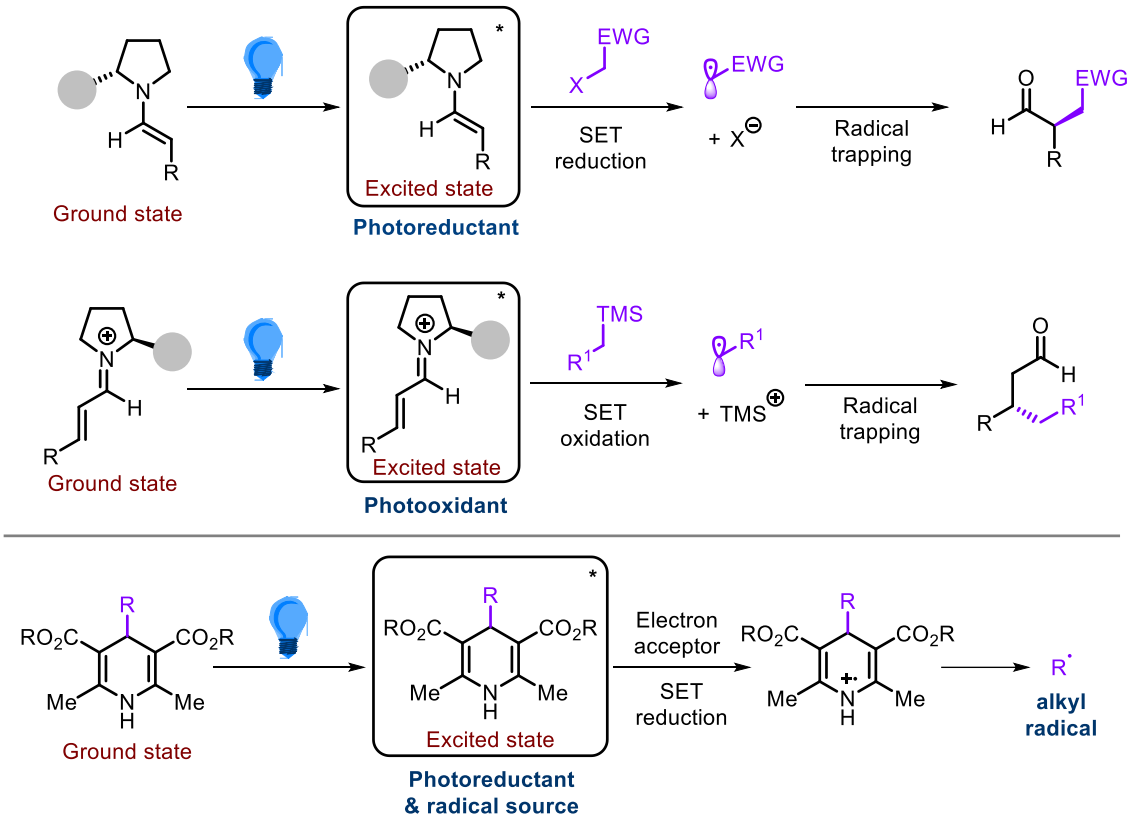

Scheme 1.20. Electronically excited organo-intermediates trigger the formation of radicals

(29) a) J. J. Murphy, D. Bastida, S. Paria, M. Fagnoni, P. Melchiorre, *Nature* **2016**, *532*, 218-222; b) M. Silvi, E. Arceo, I. D. Jurberg, C. Cassani, P. Melchiorre, *J. Am. Chem. Soc.* **2015**, *137*, 6120-6123; c) G. Filippini, M. Silvi, P. Melchiorre, *Angew. Chem. Int. Ed.* **2017**, *56*, 4447-4451; d) M. Silvi, C. Verrier, Y. P. Rey, L. Buzzetti, P. Melchiorre, *Nat. Chem.* **2017**, *9*, 868-873; e) C. Verrier, N. Alandini, C. Pezzetta, M. Moliterno, L. Buzzetti, H. B. Hepburn, A. Vega-Peñaloza, M. Silvi, P. Melchiorre, *ACS Catal.* **2018**, *8*, 1062-1066.

Additionally, photo-active iminium ions can function as strong oxidants in SET processes to furnish alkyl radical species.[29d] Lastly, 4-alkyl-DHPs serve as strong reducing agents upon light excitation and can activate reagents through SET manifolds followed by the homolytic cleavage to generate requisite radicals for C–C coupling.[30]

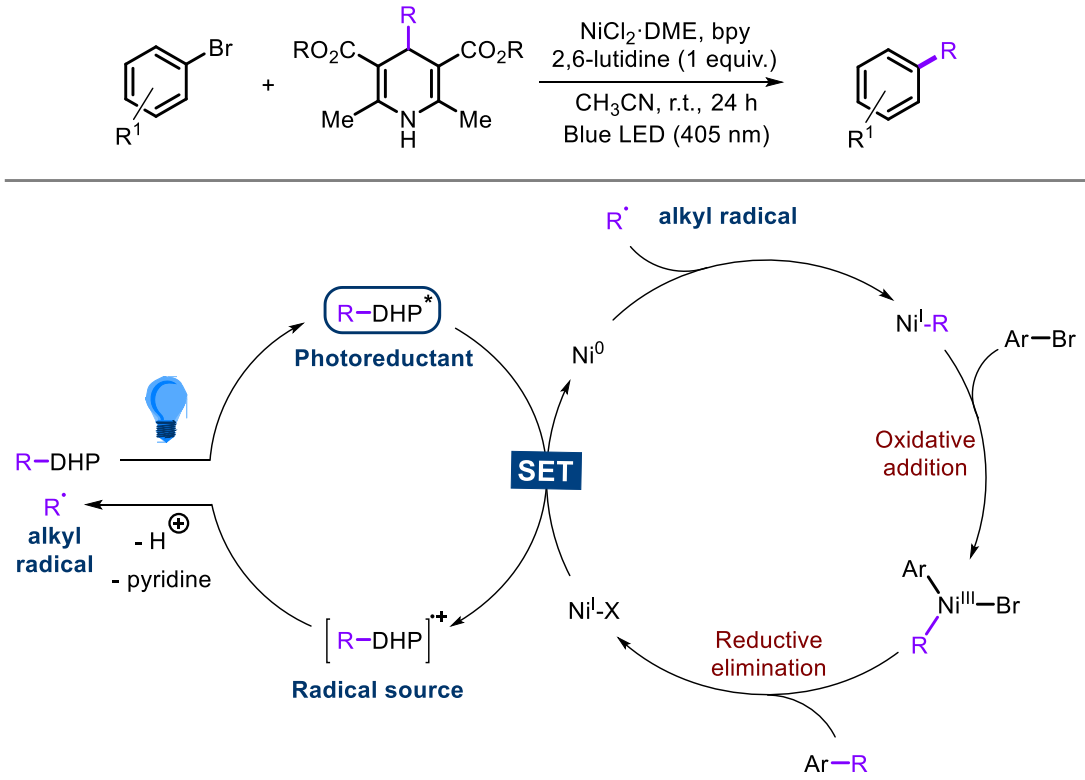

Scheme 1.21. Proposed mechanism for the Ni-catalyzed C(sp^2)–C(sp^3) cross-coupling driven by excited state alkyl-DHPs

In 2017, Melchiorre et al. realized cross-coupling reactions forging C(sp^2)–C(sp^3) bonds by the photoexcitation of 4-alkyl-DHPs combined with a Ni catalyst acting as an electron mediator (Scheme 1.21).[30a] EPR studies and radical quenching experiments with TEMPO suggested the generation of a benzyl radical by photoexcitation of 4-Bn-DHP. Control experiments of 4-Bn-DHP with 4-cyanopyridine or tetracyanobenzene proceeding through a radical coupling mechanism supported the propensity of the DHP derivative to act as a strong reducing agent in the excited state. A plausible mechanism

(30) a) L. Buzzetti, A. Prieto, S. R. Roy, P. Melchiorre, *Angew. Chem. Int. Ed.* **2017**, *56*, 15039-15043; b) B. Bieszczad, L. A. Perego, P. Melchiorre, *Angew. Chem. Int. Ed.* **2019**, *58*, 16878-16883; c) E. Gandolfo, X. Tang, S. Raha Roy, P. Melchiorre, *Angew. Chem. Int. Ed.* **2019**, *58*, 16854-16858; d) G. Goti, B. Bieszczad, A. Vega-Peñaloza, P. Melchiorre, *Angew. Chem. Int. Ed.* **2019**, *58*, 1213-1217; e) T. van Leeuwen, L. Buzzetti, L. A. Perego, P. Melchiorre, *Angew. Chem. Int. Ed.* **2019**, *58*, 4953-4957.

starts with radical formation from the photoactive 4-alkyl-DHP, with the radical being trapped by a Ni^0 intermediate to furnish an alkyl-Ni^I species. Subsequent oxidative addition generates a Ni^{III} complex, and reductive elimination finally gives rise to the cross-coupled product and releases a Ni^I species (which is reduced to Ni^0 by an SET for additional turnover), thereby completing the overall catalytic cycle.

Based on a similar approach (Scheme 1.22), the Melchiorre group further established the photochemical Giese addition of C(sp^3)–centered radicals to a variety of electron-poor olefins[30e] and the cross coupling between anhydrides and 4-alkyl-DHPs[30c] to afford enantioenriched α-substituted ketones with up to 95% *ee*, involving direct excitation of 4-alkyl-DHPs to generate alkyl radicals.

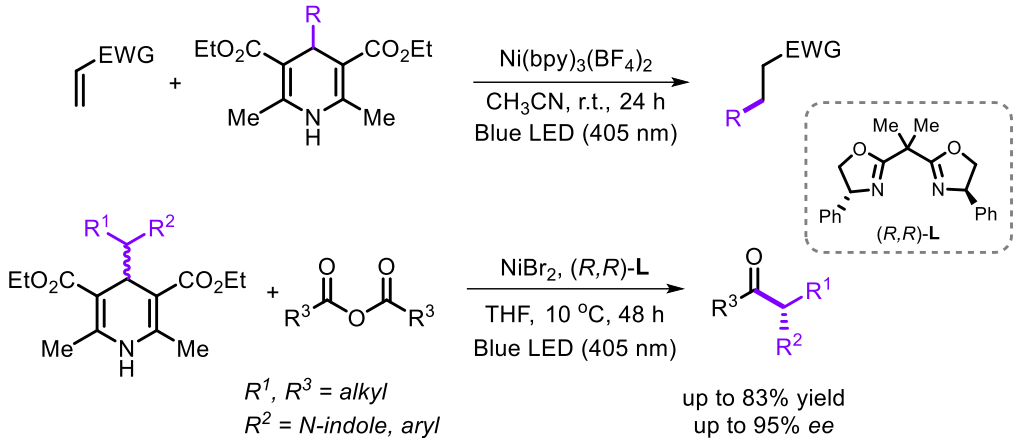

Scheme 1.22. Excited state DHPs in combination with nickel catalyst to realize cross coupling reactions

1.3. TM-catalyzed decarboxylative functionalization of VCCs

Vinyl cyclic carbonates (VCCs) have recently emerged as versatile building blocks for various decarboxylative transformations towards the formation of highly functionalized scaffolds. Key to these transformations is the dipolar character of the Pd(allyl) species that can provide highly reactive intermediates upon CO_2 extrusion (Scheme 1.23).[31] The allyl-Pd^{II} intermediate can function as a 1,3-dipole (pathway a) or 1,5-dipole (pathway b) and undergo cyclization with various unsaturated electrophiles.[32]

(31) W. Guo, J. E. Gómez, À. Cristofol, J. Xie, A. W. Kleij, *Angew. Chem. Int. Ed.* **2018**, *57*, 13735-13747.
(32) A. Khan, Y. J. Zhang, *Synlett* **2015**, *26*, 853-860.

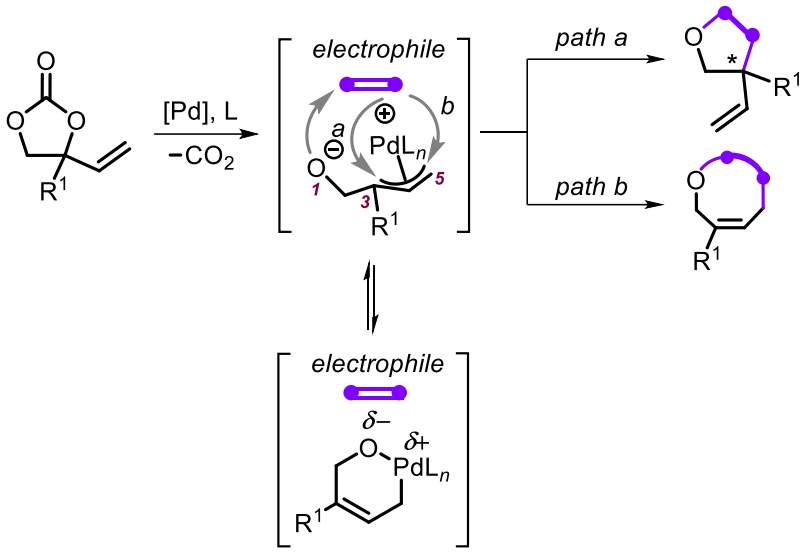

Scheme 1.23. Pd-catalyzed decarboxylative annulation of VCCs in the presence of electrophiles.

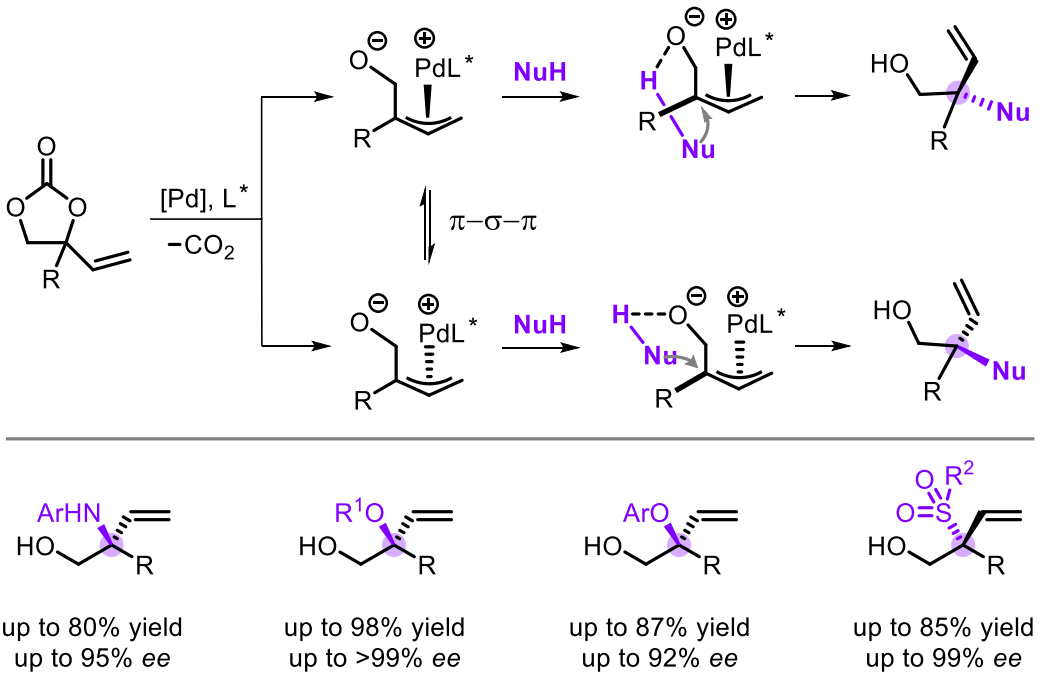

Scheme 1.24. Pd-catalyzed decarboxylative allylation affording branch-selective allylic products

Alternatively, this intermediate can also serve as an electrophilic allylic precursor that may be intercepted by a wide variety of (protic) nucleophiles to deliver branch-selective, enantioenriched products comprising of elusive tetrasubstituted carbon stereocenters,

including α-tertiary amines,[33] alcohols[34] as well as sulfones[35] (Scheme 1.24). In this regard, significant efforts have been made by our group to realize such allylic functionalization reactions.

With respect to C-based nucleophiles, to the best of our knowledge, only soft nucleophiles have been employed to deliver (*Z*)-selective (racemic) linear products through a six-membered palladacycle (Scheme 1.25). For instance, by using nitroalkanes as pronucleophiles,[36] stereoselective synthesis of homoallylic nitroalkanes could be realized and by using β-keto esters, allylic alcohols[37] and amines[38] products featuring quaternary carbon centers could be constructed. This approach is general in terms of the stereoselective construction of tri- and tetra-substituted olefins. However, asymmetric versions of these latter allylic alkylation protocols still remain underexplored.

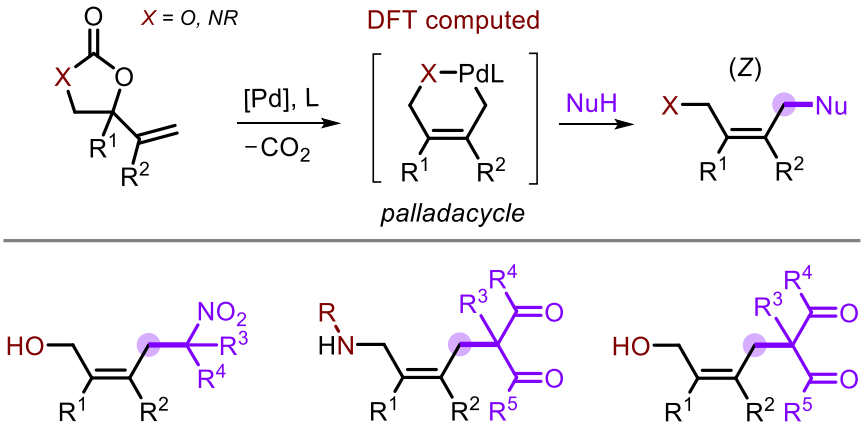

Scheme 1.25. Pd-catalyzed decarboxylative alkylation affording (*Z*)-selective linear allylic products

Apart from the aforementioned reaction manifolds, our group recently reported that upon decarboxylation the VCC itself can produce *in situ* a nucleophilic species that can react with a second molecule of decarboxylated VCC (i.e., a π-allyl-Pd^{II} species; Scheme 1.26), delivering a cross-coupled product with a quaternary carbon center.[39] Shortly hereafter, under cooperative Pd/Ti(O*i*Pr)$_4$ catalysis, the Zhao laboratory also realized

(33) A. Cai, W. Guo, L. Martínez-Rodríguez, A. W. Kleij, *J. Am. Chem. Soc.* **2016**, *138*, 14194-14197.
(34) a) J. Xie, W. Guo, A. Cai, E. C. Escudero-Adán, A. W. Kleij, *Org. Lett.* **2017**, *19*, 6388-6391; b) A. Khan, S. Khan, I. Khan, C. Zhao, Y. Mao, Y. Chen, Y. J. Zhang, *J. Am. Chem. Soc.* **2017**, *139*, 10733-10741.
(35) A. Khan, H. Zhao, M. Zhang, S. Khan, D. Zhao, *Angew. Chem. Int. Ed.* **2020**, *59*, 1340-1345.
(36) À. Cristòfol, E. C. Escudero-Adán, A. W. Kleij, *J. Org. Chem.* **2018**, *83*, 9978-9990.
(37) L. Shi, Y. He, J. Gong, Z. Yang, *Asian J. Org. Chem.* **2019**, *8*, 823-827.
(38) L. Shi, Y. He, Y. Chang, N. Zheng, Z. Yang, J. Gong, *Org. Lett.* **2019**, *21*, 3077-3080.
(39) W. Guo, R. Kuniyil, J. E. Gómez, F. Maseras, A. W. Kleij, *J. Am. Chem. Soc.* **2018**, *140*, 3981-3987.

reversed-polarity coupling of VCCs enabling a highly diastereoselective [4+2] cycloaddition furnishing [6,5]-spirocycles (Scheme 1.26).[40] Notably, by a judicious choice of ligand, the enantio- and diastereoselective cycloaddition could also be achieved (*dr* >20:1, 60% *ee*, 80:20 *er*). This formal umpolung strategy could be further applied to other alkylating agents such as simple allylic acetate in the presence of a sterically demanding Pd(tBu$_3$P)$_2$ (pre)catalyst.[41]

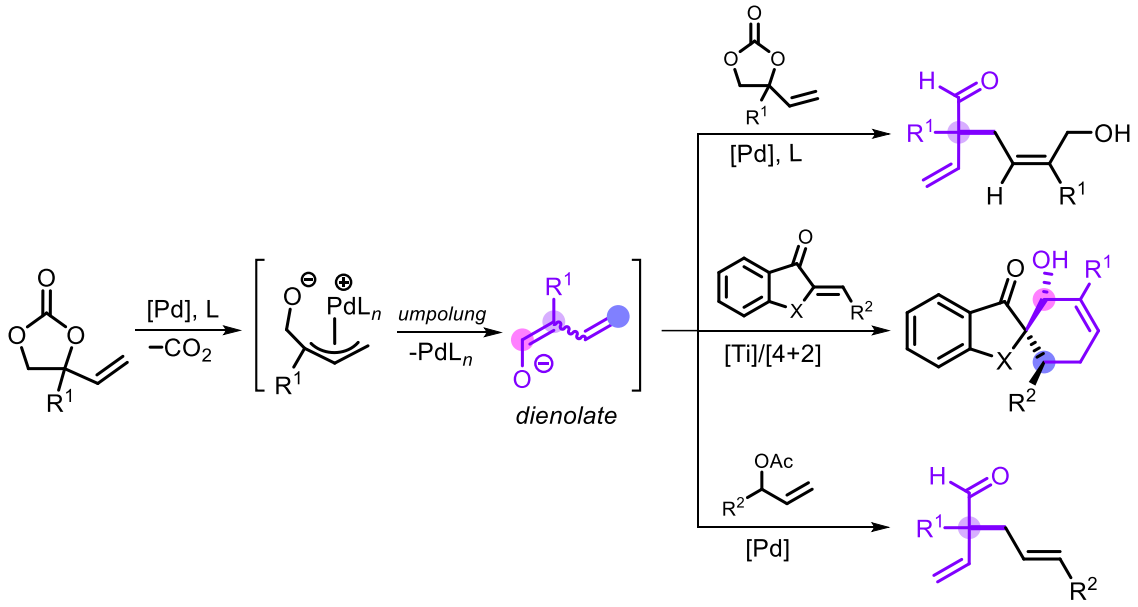

Scheme 1.26. Pd catalyzed decarboxylative umpolung coupling of VCCs

(40) L.-C. Yang, Z. Y. Tan, Z.-Q. Rong, R. Liu, Y.-N. Wang, Y. Zhao, *Angew. Chem. Int. Ed.* **2018**, *57*, 7860-7864.
(41) H. Wang, S. Qiu, S. Wang, H. Zhai, *ACS Catal.* **2018**, *8*, 11960-11965.

1.4. Thesis aims and outline

Quaternary carbon stereocenters are common motifs in pharmaceutical and bioactive molecules. TM catalyzed allylic alkylation has witnessed notable progress in the construction of quaternary carbon stereocenters over the last few decades, while photoredox catalysis has enabled the generation of reactive radical species. Their combination offers thus a powerful combination for the direct coupling of non-conventional nucleophiles under mild conditions. In addition, VCCs have recently emerged as privileged allylic surrogates that upon decarboxylation provide access to a wide variety of highly functionalized cyclic and acyclic scaffolds. Despite these significant advances, highly regio-, enantio-, and/or diastereo- selective allylic alkylation of VCCs for the generation of quaternary carbon stereocenters remained at the beginning of this thesis work remarkably scarce. Therefore, the **main objective** of this doctoral thesis was the design and development of enantio/diastereo-selective synthesis of target molecules with challenging quaternary carbon stereocenters by using dual (photo)catalysis strategies. An outline of the thesis is provided below.

In **Chapter 2**, *the specific aim* was to develop a dual Pd/Cu catalyzed asymmetric synthesis of compounds featuring highly functional, all-carbon quaternary stereocenters, which was realized giving appreciable products yield and *er* values of up to 90:10. In this work, the VCC and the requisite in situ produced nucleophile were simultaneously activated through a formal umpolung of the carbonate substrate. Various control experiments were conducted to clarify the role and importance of the process additives.

In **Chapter 3**, *we aimed* at an asymmetric synthesis of homoallylic alcohols featuring vicinal tetrasubstituted carbon centers that builds on a dual Pd/photoredox catalysis approach. The merger of photoredox and Pd catalysis provided access to the direct coupling of alkyl radicals with the π-allyl-Pd species, delivering branch-selective, highly congested enantioenriched homoallylic alcohols with *er* values up to 94:6.

In **Chapter 4**, *we strived* towards a conceptually new dual Co/organophotoredox approach that allows to perform unique cascade transformations with VCCs as modular 1,3-diene surrogates. In these cascade transformations, a variety of 2-aryl-1,3-dienes are conveniently prepared *in situ*. These are subsequently selectively transformed through catalytic and formal 1,2-hydroalkylation or 1,2-dicarbofunctionalization, delivering a wide scope of homoallylic alcohols featuring quaternary carbon centers.

Chapter 1

Chapter 2.

Pd/Cu Dual Catalyzed Asymmetric Synthesis of Highly Functional All-Carbon Quaternary Stereocenters from Vinyl Carbonates

The results described in this chapter have been published in:

S. Xue, A. Lücht, J. Benet-Buchholz, A. W. Kleij, *Chem. Eur. J.* **2021**, *27*, 10107-10114.

2.1. Introduction

2.1.1. All-carbon quaternary stereocenters

All-carbon quaternary stereocenters are ubiquitous motifs in bio-active natural compounds.[1] The congested nature of these stereocenters poses a major hurdle for their synthesis, while enantioselective synthesis is intrinsically even more challenging.[2] The synthesis of various drug molecules relies on the use of natural product precursors that feature such a quaternary stereocenter.[1a] In this regard, it is not surprising that considerable synthetic efforts have focused on the preparation of such compounds, and exemplary cases involve the development of efficient protocols for hodgkinsine,[3] minalrestat analogues[4] and (+)-bulleyanaline (an isoquinoline alkaloid).[5]

The crowded nature of quaternary carbon stereocenters entails the utilization of powerful and enantioselective carbon–carbon bond formation manifolds such as well-established Diels-Alder reactions,[6] allylic substitution reactions[7] and polyene cyclization cascades.[8] Whereas the focus has long been on the construction of cyclic quaternary stereocenters, more recent attention has been relayed to the formation of elusive acyclic

(1) a) K. W. Quasdorf, L. E. Overman, *Nature* **2014**, *516*, 181-181; b) M. Büschleb, S. Dorich, S. Hanessian, D. Tao, K. B. Schenthal, L. E. Overman, *Angew. Chem. Int. Ed.* **2016**, *55*, 4156-4186; c) C. Li, S. S. Ragab, G. Liu, W. Tang, *Nat. Prod. Rep.* **2020**, *37*, 276-292.

(2) a) B. M. Trost, C. Jiang, *Synthesis* **2006**, *2006*, 369-396; b) Y. Liu, S.-J. Han, W.-B. Liu, B. M. Stoltz, *Acc. Chem. Res.* **2015**, *48*, 740-751; c) L. Tian, Y.-C. Luo, X.-Q. Hu, P.-F. Xu, *Asian J. Org. Chem.* **2016**, *5*, 580-607; d) X.-P. Zeng, Z.-Y. Cao, Y.-H. Wang, F. Zhou, J. Zhou, *Chem. Rev.* **2016**, *116*, 7330-7396; e) T. S. Mei, H. H. Patel, M. S. Sigman, *Nature* **2014**, *508*, 340-344; f) J. J. Murphy, D. Bastida, S. Paria, M. Fagnoni, P. Melchiorre, *Nature* **2016**, *532*, 218-222; g) Q. Zhang, F.-M. Zhang, C.-S. Zhang, S.-Z. Liu, J.-M. Tian, S.-H. Wang, X.-M. Zhang, Y.-Q. Tu, *Nat. Commun.* **2019**, *10*, 2507-2507.

(3) C. R. Jamison, J. J. Badillo, J. M. Lipshultz, R. J. Comito, D. W. C. MacMillan, *Nat. Chem.* **2017**, *9*, 1165-1169.

(4) C. Cheng, B. Wan, B. Zhou, Y. Gu, Y. Zhang, *Chem. Sci.* **2019**, *10*, 9853-9858.

(5) B. M. Trost, C.-I. J. Hung, Z. Jiao, *J. Am. Chem. Soc.* **2019**, *141*, 16085-16092.

(6) a) Y. Shimizu, S.-L. Shi, H. Usuda, M. Kanai, M. Shibasaki, *Angew. Chem. Int. Ed.* **2010**, *49*, 1103-1106; b) L. N. Mander, R. P. Robinson, *J. Org. Chem.* **1991**, *56*, 3595-3601; c) L. N. Mander, R. J. Thomson, *Org. Lett.* **2003**, *5*, 1321-1324; d) H. Oikawa, T. Tokiwano, *Nat. Prod. Rep.* **2004**, *21*, 321-352.

(7) a) B. M. Trost, M. L. Crawley, *Chem. Rev.* **2003**, *103*, 2921-2944; b) J. T. Mohr, M. R. Krout, B. M. Stoltz, *Nature* **2008**, *455*, 323-332; c) A. Y. Hong, B. M. Stoltz, *Eur. J. Org. Chem.* **2013**, *2013*, 2745-2759; d) B. M. Trost, J. Xu, *J. Am. Chem. Soc.* **2005**, *127*, 2846-2847; e) S. Chiba, M. Kitamura, K. Narasaka, *J. Am. Chem. Soc.* **2006**, *128*, 6931-6937; f) B. M. Trost, Z. Zuo, J. E. Schultz, N. Anugula, K. A. Carr, *Chem. Sci.* **2020**, *11*, 2136-2140.

(8) a) S. G. Sethofer, T. Mayer, F. D. Toste, *J. Am. Chem. Soc.* **2010**, *132*, 8276-8277; b) M. A. Schafroth, D. Sarlah, S. Krautwald, E. M. Carreira, *J. Am. Chem. Soc.* **2012**, *134*, 20276-20278; c) K. Surendra, G. Rajendar, E. J. Corey, *J. Am. Chem. Soc.* **2014**, *136*, 642-645; d) L. Fan, C. Han, X. Li, J. Yao, Z. Wang, C. Yao, W. Chen, T. Wang, J. Zhao, *Angew. Chem. Int. Ed.* **2018**, *130*, 2137-2141.

quaternary chiral carbon containing molecules.[9] Typically, the generation of acyclic all-carbon quaternary stereocenters is frustrated due to a higher conformational mobility compared to their cyclic congeners.

2.1.2. Pd-catalyzed decarboxylative allylation reactions

One viable and highly versatile way to produce sterically congested stereocenters via carbon-carbon bond formation is through the use of Pd-catalyzed decarboxylative allylation methods.[10] In 2004, pioneering work by Stoltz[11] and Trost[7d] demonstrated the enantioselective Pd-catalyzed allylic alkylation of ketones by allyl enol carbonates using a PHOX and the Trost ligand, respectively. Both methodologies enabled the formation of allylic compounds featuring quaternary carbon centers with excellent enantio-control.

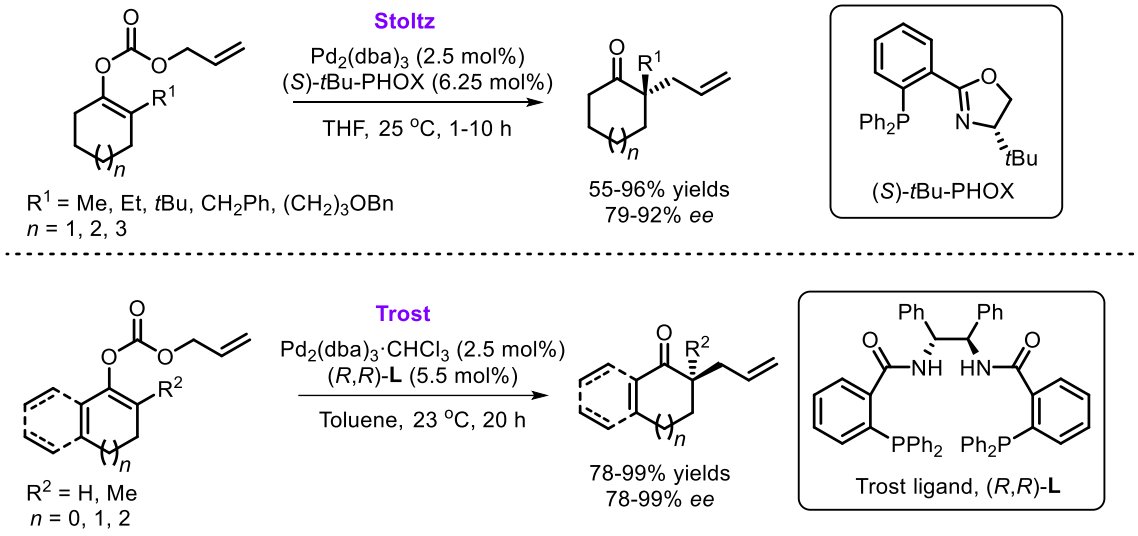

Scheme 2.1. Enantio-selective Pd-catalyzed decarboxylative allylic alkylation of ketones

Such methods have indeed been proven useful to forge acyclic quaternary (carbon) centers in an intramolecular manner.[12] The creation of functionally diverse, quaternary

(9) a) I. Marek, Y. Minko, M. Pasco, T. Mejuch, N. Gilboa, H. Chechik, J. P. Das, *J. Am. Chem. Soc.* **2014**, *136*, 2682-2694; b) J. Feng, M. Holmes, M. J. Krische, *Chem. Rev.* **2017**, *117*, 12564-12580; c) B. M. Trost, J. E. Schultz, *Synthesis* **2019**, *51*, 1-30; d) D. Pierrot, I. Marek, *Angew. Chem. Int. Ed.* **2020**, *59*, 36-49.

(10) a) J. D. Weaver, A. Recio, A. J. Grenning, J. A. Tunge, *Chem. Rev.* **2011**, *111*, 1846-1913; b) N. Rodríguez, L. J. Goossen, *Chem. Soc. Rev.* **2011**, *40*, 5030-5048; c) J. Schwarz, B. König, *Green Chem.* **2018**, *20*, 323-361; d) L. Zuo, T. Liu, X. Chang, W. Guo, *Molecules* **2019**, *24*, 3930; e) J. A. Tunge, *Isr. J. Chem.* **2020**, *60*, 351-359; f) W. Guo, J. E. Gómez, À. Cristòfol, J. Xie, A. W. Kleij, *Angew. Chem. Int. Ed.* **2018**, *57*, 13735-13747.

(11) D. C. Behenna, B. M. Stoltz, *J. Am. Chem. Soc.* **2004**, *126*, 15044-15045.

(12) a) B. M. Trost, J. Xu, T. Schmidt, *J. Am. Chem. Soc.* **2009**, *131*, 18343-18357; b) B. M. Trost, A. Nagaraju, F. Wang, Z. Zuo, J. Xu, K. L. Hull, *Org. Lett.* **2019**, *21*, 1784-1788; c) E. J. Alexy, H. Zhang, B. M. Stoltz, *J. Am. Chem. Soc.* **2018**, *140*, 10109-10112; d) P. Starkov, J. T. Moore, D. C.

carbon stereocenters in an intermolecular fashion remains, however, much less developed,[13] providing thus incentives for the synthetic community.

2.1.3. Aims and objectives

Our group has become interested in the utilization of decarboxylative chemistry to discover new stereoselective manifolds.[10f, 14] The use of vinyl cyclic carbonates in combination with suitable *P*- and *N*-based ligands proved to be key to advance previously considered elusive allylic and propargylic substitution reactions leading to sterically congested stereocenters.[15]

In the course of our investigations we discovered that under certain conditions vinyl cyclic carbonates can be transformed into functionalized compounds with an all-carbon quaternary centre (Scheme 2.1, **2.A** and **2.C**).[16] This formal cascade process features the coupling of a dienolate nucleophile and an allyl electrophile both originating from the same vinyl cyclic carbonate substrate, and the resultant products comprise quaternary carbon centres with a high degree of functionalization. The *in situ* umpolung of the typical electrophilic allyl intermediate thus provided at that time new synthetic impetus but the asymmetric coupling of the key dienolate species has so far not been achieved.[13e, 13f]

Duquette, B. M. Stoltz, I. Marek, *J. Am. Chem. Soc.* **2017**, *139*, 9615-9620; e) W.-B. Liu, C. M. Reeves, B. M. Stoltz, *J. Am. Chem. Soc.* **2013**, *135*, 17298-17301; f) E. J. Alexy, T. J. Fulton, H. Zhang, Brian M. Stoltz, *Chem. Sci.* **2019**, *10*, 5996-6000; g) Y. Ariyarathna, J. A. Tunge, *Org. Biomol. Chem.* **2014**, *12*, 8386-8389; h) I. I. I. A. Recio, J. D. Heinzman, J. A. Tunge, *Chem. Commun.* **2012**, *48*, 142-144; i) B. M. Trost, J. E. Schultz, Y. Bai, *Angew. Chem. Int. Ed.* **2019**, *58*, 11820-11825; j) Z.-W. Zhang, C.-C. Wang, H. Xue, Y. Dong, J.-H. Yang, S. Liu, W.-Q. Liu, W.-D. Z. Li, *Org. Lett.* **2018**, *20*, 1050-1053.

(13) a) L. Shi, Y. He, Y. Chang, N. Zheng, Z. Yang, J. Gong, *Org. Lett.* **2019**, *21*, 3077-3080; b) R. Shintani, M. Murakami, T. Hayashi, *J. Am. Chem. Soc.* **2007**, *129*, 12356-12357; c) J. Meng, L.-F. Fan, Z.-Y. Han, L.-Z. Gong, *Chem* **2018**, *4*, 1047-1058; d) Q.-Z. Li, Y. Liu, M.-Z. Li, X. Zhang, T. Qi, J.-L. Li, *Org. Biomol. Chem.* **2020**, *18*, 3638-3648; e) L.-C. Yang, Z. Y. Tan, Z.-Q. Rong, R. Liu, Y.-N. Wang, Y. Zhao, *Angew. Chem. Int. Ed.* **2018**, *57*, 7860-7864; f) H. Wang, S. Qiu, S. Wang, H. Zhai, *ACS Catal.* **2018**, *8*, 11960-11965.

(14) a) W. Guo, L. Martínez-Rodríguez, R. Kuniyil, E. Martin, E. C. Escudero-Adán, F. Maseras, A. W. Kleij, *J. Am. Chem. Soc.* **2016**, *138*, 11970-11978; b) W. Guo, L. Martínez-Rodríguez, E. Martin, E. C. Escudero-Adán, A. W. Kleij, *Angew. Chem. Int. Ed.* **2016**, *55*, 11037-11040; c) J. E. Gómez, W. Guo, A. W. Kleij, *Org. Lett.* **2016**, *18*, 6042-6045; d) À. Cristòfol, E. C. Escudero-Adán, A. W. Kleij, *J. Org. Chem.* **2018**, *83*, 9978-9990; e) N. Miralles, J. E. Gómez, A. W. Kleij, E. Fernández, *Org. Lett.* **2017**, *19*, 6096-6099.

(15) a) A. Cai, W. Guo, L. Martínez-Rodríguez, A. W. Kleij, *J. Am. Chem. Soc.* **2016**, *138*, 14194-14197; b) W. Guo, A. Cai, J. Xie, A. W. Kleij, *Angew. Chem. Int. Ed.* **2017**, *56*, 11797-11801; c) J. E. Gomez, W. Guo, S. Gaspa, A. W. Kleij, *Angew. Chem. Int. Ed.* **2017**, *56*, 15035-15038; d) J. Xie, W. Guo, A. Cai, E. C. Escudero-Adán, A. W. Kleij, *Org. Lett.* **2017**, *19*, 6388-6391; e) L. Hu, A. Cai, Z. Wu, A. W. Kleij, G. Huang, *Angew. Chem. Int. Ed.* **2019**, *58*, 14694-14702; f) A. Cai, A. W. Kleij, *Angew. Chem. Int. Ed.* **2019**, *58*, 14944-14949; g) B. M. Trost, M. R. Machacek, A. Aponick, *Acc. Chem. Res.* **2006**, *39*, 747-760.

(16) W. Guo, R. Kuniyil, J. E. Gómez, F. Maseras, A. W. Kleij, *J. Am. Chem. Soc.* **2018**, *140*, 3981-3987.

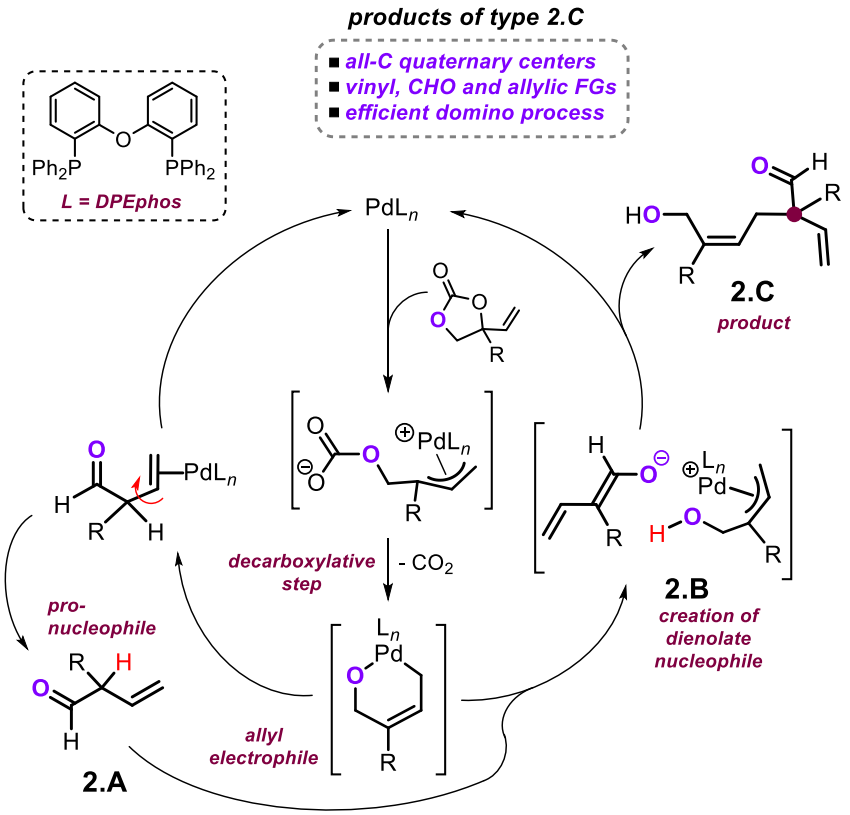

Scheme 2.2 Simplified computed manifold for the formation of racemic products containing a highly functional quaternary carbon center based on a Pd-mediated decarboxylative cross-coupling process. The final product **2.C** contains a quaternary center with aldehyde, vinyl, allylic and substituted aryl groups.

The unique nature of the functionally dense compounds of type **2.C** (Scheme 2.2) made us wonder whether an asymmetric version of this cascade process could be developed. However, several challenges are associated with this endeavor, and above all is the selection of a suitable chiral ligand. Whereas in our previous work on asymmetric allylic substitution monodentate phosphoramidite ligands proved to be highly efficient in directing the regio- and enantio-selectivity towards the "branched" position,[15a, 15b, 15d-g] a preliminary examination revealed that phosphoramidites are not productive ligands in this complex manifold.[16]

Based on the success of a DPEphos-Pd based catalyst to accommodate the formation of the racemic product **2.C** (Scheme 2.2), we sought to use a diphosphine backbone as a linchpin structural ligand motif in our quest to develop an asymmetrically version of this cross-coupling event. The coupling between the dienolate nucleophile and the allylic electrophile (Scheme 2.2, **2.B**) in the presence of more bulky, chiral ligands will likely be

significantly decelerated. In order to overcome the loss of activation potential of the α,β-unsaturated aldehyde by the Pd(allyl) intermediate, a completely new approach needs to be considered while optimizing both the yield and enantio-purity of the target compounds.

In this chapter, we report an extensive screening focusing on the discovery of suitable reaction conditions, chiral ligands and additives to provide enantio-enriched products of type **2.C** that have built-in quaternary functionalized carbon stereocenters. The complex nature and relationship between all components and the effect this has on the formation of the chiral products is further discussed on the basis of the mechanistic description provided in Scheme 2.2.

2.2. Results and discussion

2.2.1. Optimization studies

We anticipated that the asymmetric coupling between the *in situ* formed α,β-unsaturated aldehyde and the palladacyclic species (Scheme 2.2, **2.B**) would likely depend on additives as to increase their reactivity. Since the aldehyde reactant requires deprotonation (and hence a base) prior to the formation of the dienolate nucleophile, simple Lewis acids could help to stabilize the latter by coordination and maximize its concentration in the medium, and subsequent turnover. We also envisioned that boric acid $B(OH)_3$ could be helpful in activating the vinyl cyclic carbonate substrate through electrophilic B–O activation. With these process design elements in mind, we examined the role of the diphosphine on the catalytic performance of *in situ* formed Pd-catalysts derived from $Pd_2(dba)_3 \cdot CHCl_3$.

As a representative and well-known chiral diphosphine, (*S*)-BINAP **L1** was first utilized to pursue reaction conditions that would lead to product formation (Table 2.1). Gratifyingly, in the presence of (*S*)-BINAP **L1** a 39% yield of **2.2a** was achieved having an enantiomeric ratio (*er*) of 67.5:32.5. Then other chiral diphosphines were examined (entries 3-11, **L2**-**L11**), and among these the SegPhos (*cf.*, **L4**) family of ligands provided a first structural clue for further optimization.

Table 2.1. First screening stage of the chiral diphosphine ligand for the Pd-catalyzed conversion of cyclic carbonate **2.1a** into product **2.2a**[a]

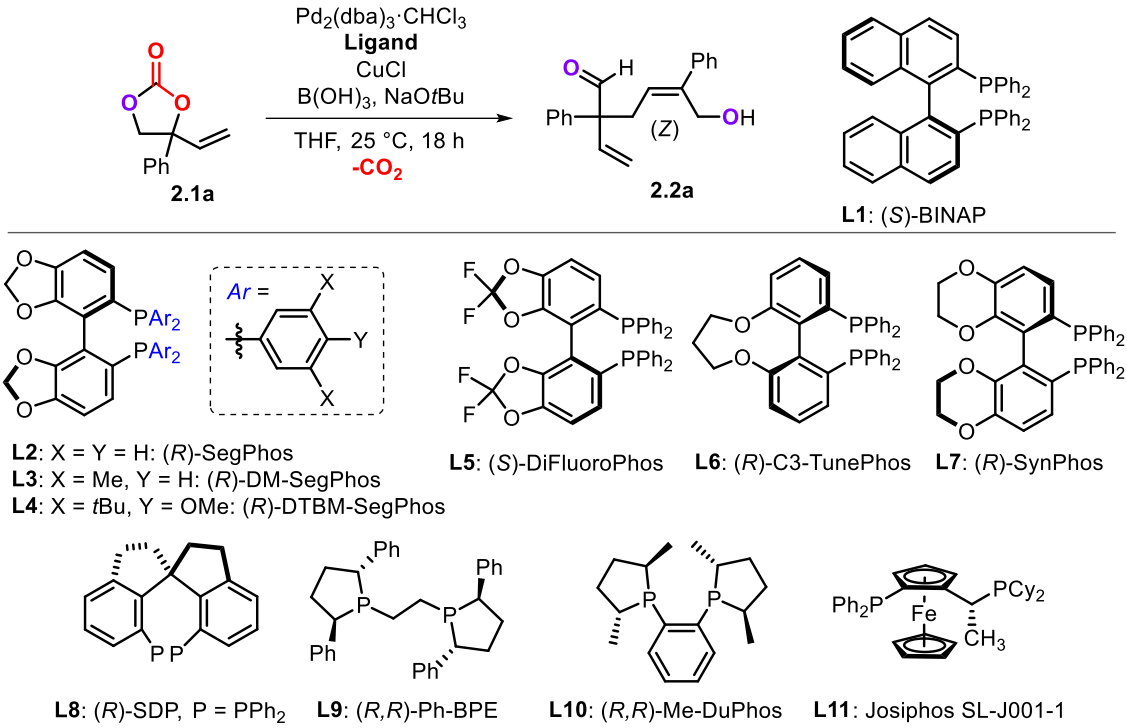

Entry	Ligand	Yield[b]	*er*[c]
1	**L1**	39%	67.5:32.5
2	**L2**	31%	78.5:21.5
3	**L3**	39%	74.5:25.5
4	**L4**	**37%**	**78.5:21.5**
5	**L5**	23%	76.5:23.5
6	**L6**	37%	78.5:21.5
7	**L7**	33%	75:25
8	**L8**	57%	76.5:23.5
9	**L9**	0%	–
10	**L10**	0%	–
11	**L11**	13%	69:31

[a] $Pd_2(dba)_3·CHCl_3$ (2 mol%), ligand (6 mol%), CuCl (5 mol%), $B(OH)_3$ (1.5 equiv.), NaO*t*Bu (1.5 equiv.), THF (0.50 mL), 15 s; then addition of **2.1a** (1.0 equiv.), THF (1.5 mL), 18 h, r.t. [b] Isolated yield after chromatographic purification. [c] The *er* values were determined by UPC2 after converting the product first into its corresponding diol by $NaBH_4$ reduction.

Based on the comparison of both yield and *er* values, we selected (*R*)-DTBM-SegPhos **L4** (Table 2.1, entry 4; 37% yield, *er* = 78.5:21.5,) as the preferred chiral ligand to scrutinize the role of the Lewis acid in more detail (Table 2.2, entries 1-8). Compared with the use of CuCl, the presence of $Cu(OAc)_2$ slightly increased the *er* of **2.2a** (entry 3, 29%, 80.5:19.5 *er*). Several other Lewis acids failed to boost the reaction towards **2.2a** despite the observation of similar levels of asymmetric induction.

Table 2.2. Screening of the influence of the Lewis acid on the Pd-catalyzed conversion of cyclic carbonate **2.1a** into product **2.2a**[a]

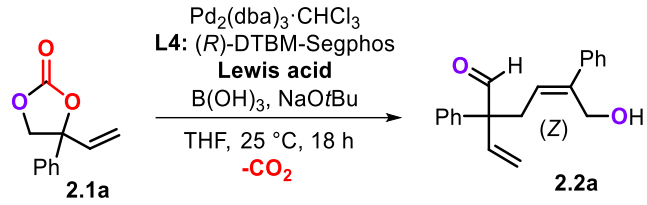

Entry	Lewis acid	Yield[b]	*er*[c]
1	CuCl	37%	78.5:21.5
2	$Cu(OTf)_2$	0%	–
3	**$Cu(OAc)_2$**	**29%**	**80.5:19.5**
4	$CuBr_2$	12%	78:22
5	$CuCl_2$	20%	79.5:20.5
6	$Zn(OAc)_2$	16%	79:21
7	$Mg(OAc)_2$· 4 H_2O	12%	77:23
8	Ti(O*i*Pr)$_4$	0%	–

[a] $Pd_2(dba)_3$·$CHCl_3$ (2 mol%), **L4** (6 mol%), Lewis acid (5 mol%), $B(OH)_3$ (1.5 equiv.), NaO*t*Bu (1.5 equiv.), THF (0.50 mL), 15 s; then addition of **2.1a** (1.0 equiv.), THF (1.5 mL), 18 h, r.t. [b] Isolated yield after chromatographic purification. [c] The *er* values were determined by UPC2 after converting the product first into its corresponding diol by $NaBH_4$ reduction.

Evaluation of the ratio between $B(OH)_3$ and NaO*t*Bu suggested that both reagents have significant influence on the coupling process. Reducing the load of NaO*t*Bu to 1.0 equiv. increased the yield of **2.2a** to 56% with the *er* more or less preserved (Table 2.3, entry 2). Further decreasing the load of NaO*t*Bu gave a lower yield (Table 2.3, entry 3-4). Reducing the load of $B(OH)_3$ to 1.0 equiv. delivered **2.2a** in slightly lower yield (Table

2.3, entry 5), while further decreasing the load failed to give the desired product **2.2a** (Table 2.3, entry 6-7).

Table 2.3. Screening of the ratio between $B(OH)_3$ and NaO*t*Bu for the Pd-catalyzed conversion of cyclic carbonate **2.1a** into product **2.2a**[a]

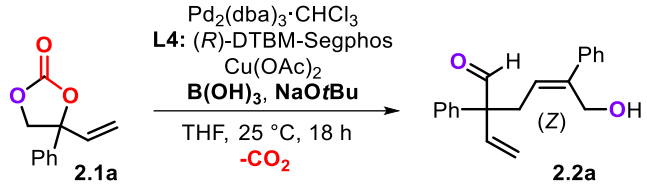

Entry	$B(OH)_3$ (equiv.)	NaO*t*Bu (equiv.)	Yield[b]	*er*[c]
1	1.5	1.5	29%	80.5:19.5
2	**1.5**	**1.0**	**56%**	**79.5:20.5**
3	1.5	0.5	42%	74:26
4	1.5	0.2	0%	-
5	1.0	1.0	52%	79.5:20.5
6	0.5	1.0	trace	-
7	0.2	1.0	0	-

[a] $Pd_2(dba)_3·CHCl_3$ (2 mol%), **L4** (6 mol%), Lewis acid (5 mol%), $B(OH)_3$, NaO*t*Bu, THF (0.50 mL), 15 s; then addition of **2.1a** (1.0 equiv.), THF (1.5 mL), 18 h, r.t. [b] Isolated yield after chromatographic purification. [c] The *er* values were determined by UPC2 after converting the product first into its corresponding diol by $NaBH_4$ reduction.

The solvent appears to have a significant effect. The use of a relatively nonpolar solvent like diethyl ether gave access to **2.2a** with similar levels of enantio-induction, while the utilization of THF provided **2.2a** in 56% yield with 79.5:20.5 *er*. Neither a highly polar solvent (Table 2.4, entries 6-9) nor nonpolar solvents (Table 2.4, entries 10-11) gave rise to product formation.

Table 2.4. Screening of the solvent towards the formation of product **2.2a**[a]

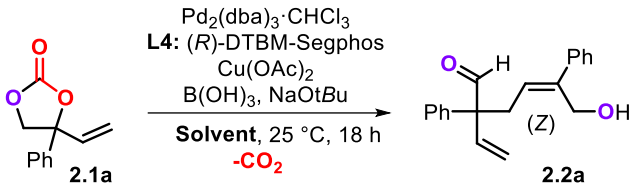

Entry	Solvent	Yield[b]	*er*[c]
1	**THF**	**56%**	**79.5:20.5**
2	2-MeTHF	41%	79.5:20.5
3	Dioxane	15%	77:23
4	MTBE	42%	76:24
5	Diethylether	30%	77:23
6	DMF	17%	80.5:19.5
7	DMA	0%	-
8	MeCN	0%	-
9	MeOH	0%	-
10	CH_2Cl_2	0%	-
11	Toluene	0%	-

[a] $Pd_2(dba)_3·CHCl_3$ (2 mol%), **L4** (6 mol%), Lewis acid (5 mol%), $B(OH)_3$ (1.5 equiv.), NaO*t*Bu (1.0 equiv.), THF (0.50 mL), 15 s; then addition of **2.1a** (1.0 equiv.), THF (1.5 mL), 18 h, r.t. [b] Isolated yield after chromatographic purification. [c] The *er* values were determined by UPC2 after converting the product first into its corresponding diol by $NaBH_4$ reduction.

By increasing the pre-mixing time of the catalyst components from 15 s to 30 min (Table 2.5, entry 2) the formation of the product was further favored with an improved isolated yield of 75%. In the absence of $Cu(OAc)_2$ (entry 3), the yield dropped to only 15%, whereas in the absence of NaO*t*Bu (entry 4) or $B(OH)_3$ (entry 5) virtually no conversion of **2.1a** was observed. In the absence of **L4** no product formation was noted (entry 6). These latter data help to establish that all three additives play an imperative role in the activation and stabilization of the substrate and derived intermediates.

Table 2.5. Deviations from the standard conditions for the Pd-catalyzed conversion of cyclic carbonate **2.1a** into product **2.2a**[a]

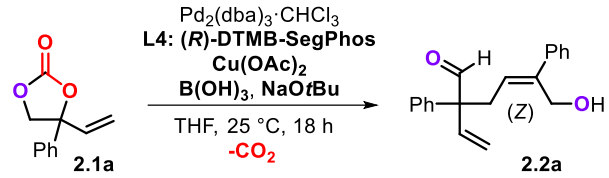

Entry	$Cu(OAc)_2$	NaO*t*Bu	$B(OH)_3$	**L4**	Yield[b]	*er*[c]
1	√	√	√	√	56%	79.5:20.5
2[d]	√	√	√	√	75%	80.5:19.5
3[d]	–	√	√	√	15%	78.5:21.5
4[d]	√	–	√	√	0%	-
5[d]	√	√	–	√	3%	77.5:22.5
6[d]	√	√	√	–	0%	-

[a] $Pd_2(dba)_3·CHCl_3$ (2 mol%), **L4** (6 mol%), Lewis acid (5 mol%), $B(OH)_3$ (1.5 equiv.), NaO*t*Bu (1.0 equiv.), THF (0.50 mL), 15 s; then addition of **2.1a** (1.0 equiv.), THF (1.5 mL), 18 h, r.t. [b] Isolated yield after chromatographic purification. [c] The *er* values were determined by UPC2 after converting the product first into its corresponding diol by $NaBH_4$ reduction. [d] As under [a] but instead of 15 s, 30 min pre-stirring was applied.

Next, the influence of the base on the yield of **2.2a** was studied and these results are summarized in Table 2.6. The performance of each base was benchmarked against the use of NaO*t*Bu (entry 1), and first the cation of the *tert*-butoxide base was varied (entries 2 and 3). Both KO*t*Bu and LiO*t*Bu proved to be less efficient base additives resulting in lower yields for **2.2a** (57 and 43%, respectively). Changing the anion (entries 4 and 5) also did not provoke improved reactivity, and other typical inorganic/organic bases such as Cs_2CO_3, DBU, NEt_3 and K_3PO_4 were ineffective. While LiHMDS initially did not give any improvement (entry 10), we were pleased to find that by adding the base after the pre-mixing time (entry 11) resulted in high yield (92%) for of **2.2a**. The Na and K analogues of LiHMDS were also effective promotors of the reaction though lower yields of **2.2a** were produced, and in the case of KHMDS with slight erosion of the *er* value (75:25). Finally, a comparable amide base (LDA) gave rise to substantially lower yield of the product. Overall, both the type of base as well as cation seem to affect the yield of **2.2a**, and virtually without changing the enantio-induction.

Table 2.6. Screening of the influence of the base on the Pd-catalyzed conversion of cyclic carbonate **2.1a** into product **2.2a**[a]

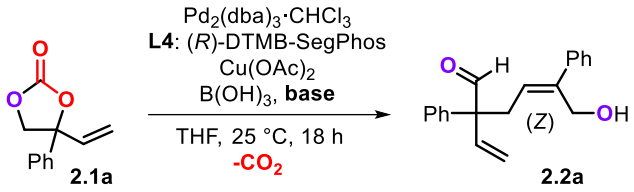

Entry	Base	Yield[b]	*er*[c]
1	NaO*t*Bu	75%	80.5:19.5
2	KO*t*Bu	57%	81:19
3	LiO*t*Bu	43%	80:20
4	NaOMe	9%	77:23
5	NaOEt	16%	79.5:20.5
6	Cs_2CO_3	traces	–
7	DBU	0%	–
8	NEt_3	0%	–
9	K_3PO_4	0	–
10	LiHMDS	42	80:20
11[d]	**LiHMDS**	**92**	**79.5:20.5**
12[d]	NaHMDS	83	80:20
13[d]	KHMDS	69	75:25
14[d]	LDA	45	81:19

[a] $Pd_2(dba)_3$·$CHCl_3$ (2 mol%), ligand **L4** (6 mol%), $Cu(OAc)_2$ (5 mol%), $B(OH)_3$ (1.5 equiv.), base (1.0 equiv.), THF (0.50 mL), 30 min premixing time; then addition of **2.1a** (1.0 equiv.), THF (1.5 mL), 18 h, r.t. [b] Isolated yield after chromatographic purification. [c] The *er* values were determined by UPC2 after converting the product first into its corresponding diol by $NaBH_4$ reduction. [d] All catalyst components except the base were pre-mixed for 20 min, after which 1 equiv. of the base was added following stirring for an additional 10 min; then **2.1a** (1.0 equiv.), THF (1.5 mL), 18 h, r.t.; Note that LiHMDS stands for lithium bis(trimethylsilyl)amide, LDA = lithium diisopropylamide and DBU = 1,8-diazabicyclo[5.4.0]undec-7-ene.

With the yield of **2.2a** optimized, we turned our attention to increase the asymmetric induction by considering ligands with similar types of backbones compared to DTBM-SegPhos (Figure 2.1, **L12-L27**; Table 2.7).

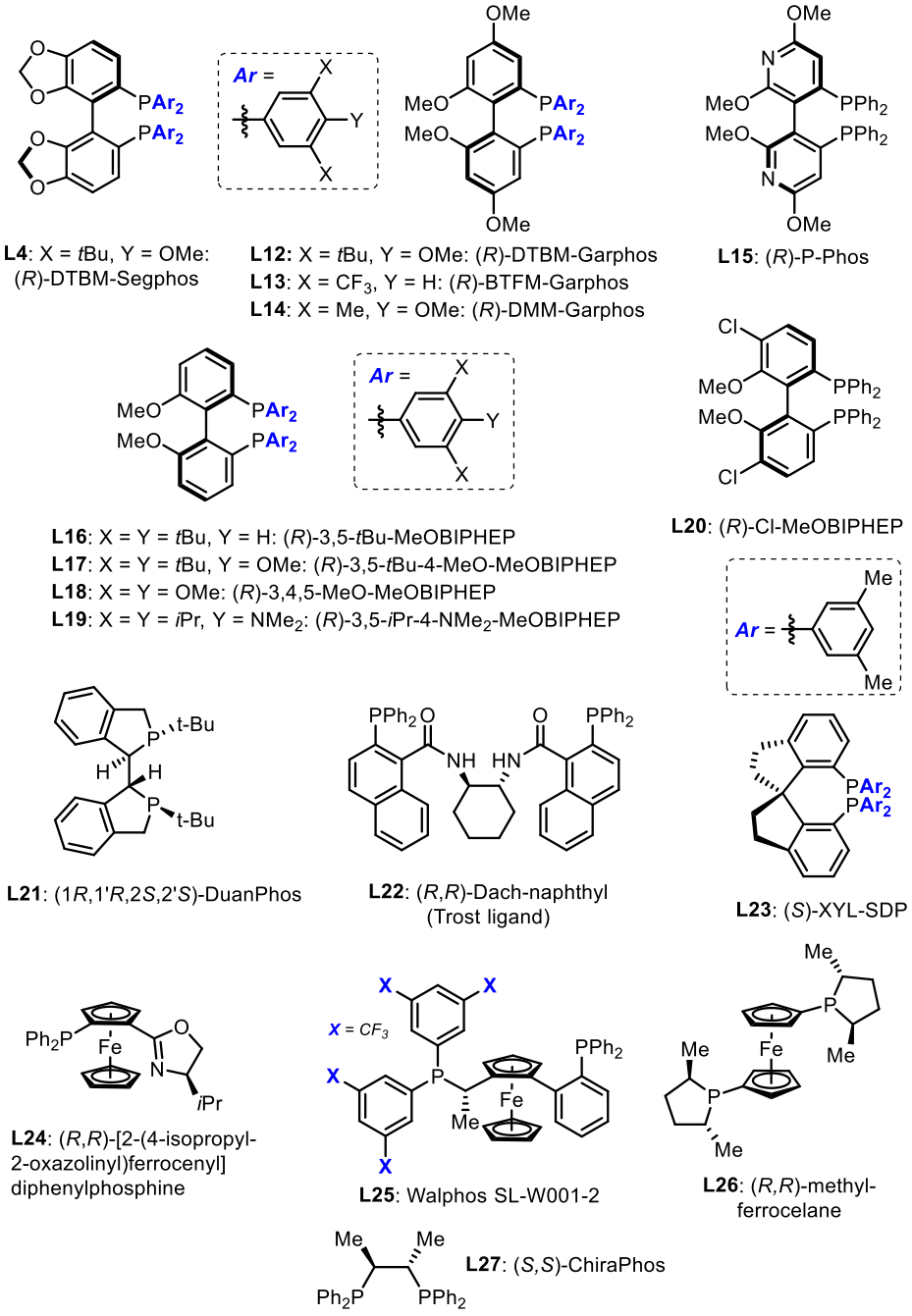

Figure 2.1. Selected chiral diphosphine ligands (**L12-L27**) with backbones similar or related to DTBM-SegPhos used in a second ligand screening phase

Little variation in the *er* value was observed when increasing or decreasing the ligand to metal ratio (entries 2 and 3 versus 1), but the yield of **2.2a** dropped significantly to 48% at a ratio of 1.25, while it was slightly increased to 98% at a ligand/Pd ratio of 2.5. Therefore, in the second ligand screening phase, we maintained the conditions reported in entry 1.

Structurally related ligands (Figure 2.1 and Table 2.7: entries 4-20) were then utilized and their performance carefully reviewed. Whereas none of the other ligand systems were able to produce **2.2a** in a similar high yield, only two ligands stood out in terms of asymmetric induction. The presence of (*R*)-DTBM-GarPhos (entry 4; **L12**, 42% yield, *er* = 82.5:17.5) and (*R*)-3,5-*i*Pr-4-NMe_2-MeOBIPHEP (entry 12; **L19**, 72% yield, *er* = 86:14) gave rise to product formation with slightly improved enantiocontrol compared to (*R*)-DTBM-SegPhos **L4** (entry 1; 92% yield, *er* = 79.5:20.5). With these three ligands in hand, we then further continued to evaluate concentration and temperature effects on the outcome of the cross-coupling reaction.

Table 2.7. Second ligand screening phase for the Pd-catalyzed conversion of cyclic carbonate **2.1a** into product **2.2a**[a]

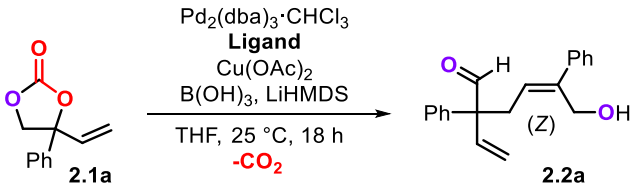

Entry	Ligand	Yield[b]	*er*[c]
1	**L4**	**92**	**79.5:20.5**
2[d]	**L4**	48	73:27
3[e]	**L4**	98	81:19
4	**L12**	**42%**	**82.5:17.5**
5	**L13**	49%	78.5:21.5
6	**L14**	49%	59.5:40.5
7	**L15**	57%	7.8.5:21.5
8	**L16**	32%	81.5:18.5
9	**L17**	75%	80:20
10	**L18**	13%	68.5:31.5
11	**L19**	56%	86:14
12[f]	**L19**	**72%**	**86:14**
13	**L20**	40%	72:28

Table 2.7. *Continued*

14	**L21**	0%	–
15	**L22**	traces	–
16	**L23**	73%	68.5:31.5
17	**L24**	traces	–
18	**L25**	traces	–
19	**L26**	51%	70:30
20	**L27**	0%	–

[a] $Pd_2(dba)_3 \cdot CHCl_3$ (2 mol%) and ligand (6 mol%), ratio ligand/Pd = 1.5; $Cu(OAc)_2$ (5 mol%), $B(OH)_3$ (1.5 equiv.) and THF (0.5 mL) pre-mixed for 20 min; then LiHMDS (1 equiv.) added, mixture further stirred for 10 min, followed by addition of **2.1a** (1.0 equiv.), THF (1.5 mL), 18 h, r.t. [b] Isolated yield after chromatographic purification. [c] The *er* values were determined by UPC2 after converting the product first into its corresponding diol by $NaBH_4$ reduction. [d] Ratio ligand/Pd was 1.25. [e] Ratio ligand/Pd was 2.5. [f] Using freshly purchased LiHMDS.

The use of (*R*)-DTBM-SegPhos **L4** as chiral ligand at a higher or lower than 0.1 M concentration of **2.1a** did not provoke any significant change in the yield and/or *er* value of **2.2a** (Table 2.8, entries 1-4). Next, the reaction temperature was screened (entries 5-9) and at lower reaction temperature (entries 5-8, 5 and 0 ºC), a slight increase in the *er* value was noted though at the expense of the yield of **2.2a**. This effect could be partially compensated by increasing the ligand-to-Pd ratio though extension of the reaction time did not cause any positive effect (entry 6 *versus* 7). Unfortunately, at –20 ºC no reactivity was observed.

Slightly improved levels of enantio-induction were achieved with (*R*)-3,5-*i*Pr-4-NMe_2-MeOBIPHEP **L19** (entries 10-12) providing low-to-moderate yields of **2.2a**. The best *er* value (90:10) was accomplished by working at a temperature of –5 ºC, giving **2a** in 22% isolated yield. Considering the rather complex nature of this cross-coupling process leading to compounds with highly functional quaternary carbon stereocenters, the best enantio-induction (*er* = 90:10, 80% *ee*) is certainly appreciable and promising. For this reason, we started to investigate the scope of this transformation choosing 25 ºC as the reaction temperature.

Table 2.8. Concentration and temperature effects in the Pd-catalyzed conversion of cyclic carbonate **2.1a** into product **2.2a**[a]

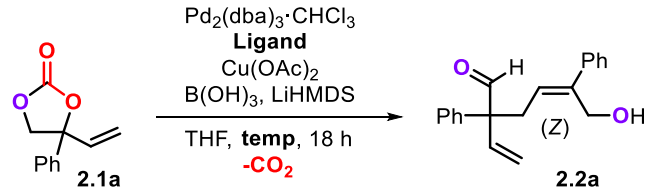

Entry	Ligand	Conc./T [M], [ºC]	Yield[b]	*er*[c]
1	**L4**	0.1, 25	92	79.5:20.5
2	**L4**	0.2, 25	73	76.5:23.5
3	**L4**	0.05, 25	80	82.5:17.5
4	**L4**	0.025, 25	42	78.5:21.5
5	**L4**	0.1, 10	42	81:19
6[d]	**L4**	0.1, 5	52	84:16
7	**L4**	0.1, 0	33	84:16
8[e]	**L4**	0.1, 0	30	84:16
9	**L4**	0.1, –20	0	–
10	**L19**	0.1, 25	56	86:14
11[f]	**L19**	0.1, 5	22	88.5:11.5
12	**L19**	**0.1, –5**	**22**	**90:10**

[a] $Pd_2(dba)_3·CHCl_3$ (2 mol%) and ligand **L4** or **L19** (6 mol%), $Cu(OAc)_2$ (5 mol%), $B(OH)_3$ (1.5 equiv.) and THF (amount depending on the required molarity) pre-mixed for 20 min; then LiHMDS (1 equiv.) added, mixture further stirred for 10 min, followed by addition of **2.1a** (1.0 equiv.), THF (amount depending on the required molarity), 18 h, r.t. [b] Isolated yield after chromatographic purification. [c] The *er* values were determined by UPC2 after converting the product first into its corresponding diol by $NaBH_4$ reduction. [d] Using a ligand/Pd ratio of 2.5, 22 h. [e] After 66 h. [f] Using a ligand/Pd ratio of 2.5.

2.2.2. Product scope of the cross-coupling process

In order to have a productive cross-coupling process (*i.e.*, an acceptable balance between the yield of the product and enantio-induction), we used the conditions reported in Table 2.7 (entry 12) to prepare a wider variety of compounds featuring functionalized quaternary carbon stereocenters (Scheme 2.3, **2.2a–2.2o**). Most of these products could

be obtained in an appreciable yield with rather similar asymmetric induction as compared to the standard formation of compound **2.2a**.

In those cases where the Ar-substituents carry electron-donating groups or weakly withdrawing (**2.2a–2.2f, 2.2k**), the isolated yields (60-84%) and *er* values (77.5 : 22.5 up to 86:14) fall within a relatively small range. With the introduction of (strong) electron-withdrawing groups (**2.2g–2.2j**), there is a clear tendency showing substantially lower yield of product (37-53%) but with the enantio-induction more or less preserved. The presence of heteroatoms in the aryl group (**2.2o**) causes the asymmetric induction to drop (65:35 *er*), which we ascribe to the potential interference of the substrate via Pd-S coordination motifs. Lastly, we also subjected vinyl cyclic carbonates with additional substitution on the double bond and/or carbonate ring to the optimized reaction conditions, but these precursors failed to deliver any observable product. The higher steric impediment within these substrates may be responsible for the lack of productive cross-coupling events.

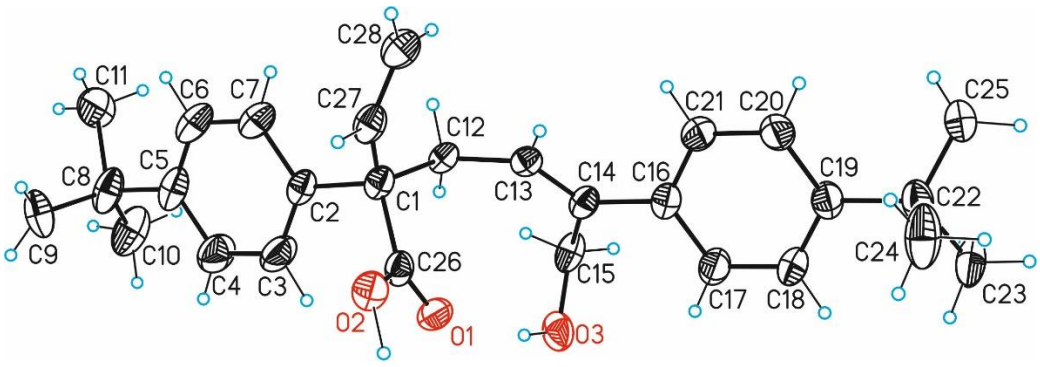

Figure 2.2. X-ray molecular structure determined for the oxidized derivative (*R*)-(*Z*) **2.2p** obtained from **2.2f**.

Whereas the determination of the absolute configuration of **2.2f** failed, its carboxylic acid derivative **2.2p** could be conveniently measured by X-ray crystallography showing it to have an (*R*) configuration (see Figure 2.2).[17]

(17) Several attemps to obtain X-ray quality crystals for **2.2d** and **2.2f** to determine their absolute configutation failed. Oxidation of **2.2f** to **2.2p** (it's corresponding acid) provided finally an indirect way to determine its absolute configuration. See the experimental section for all details.

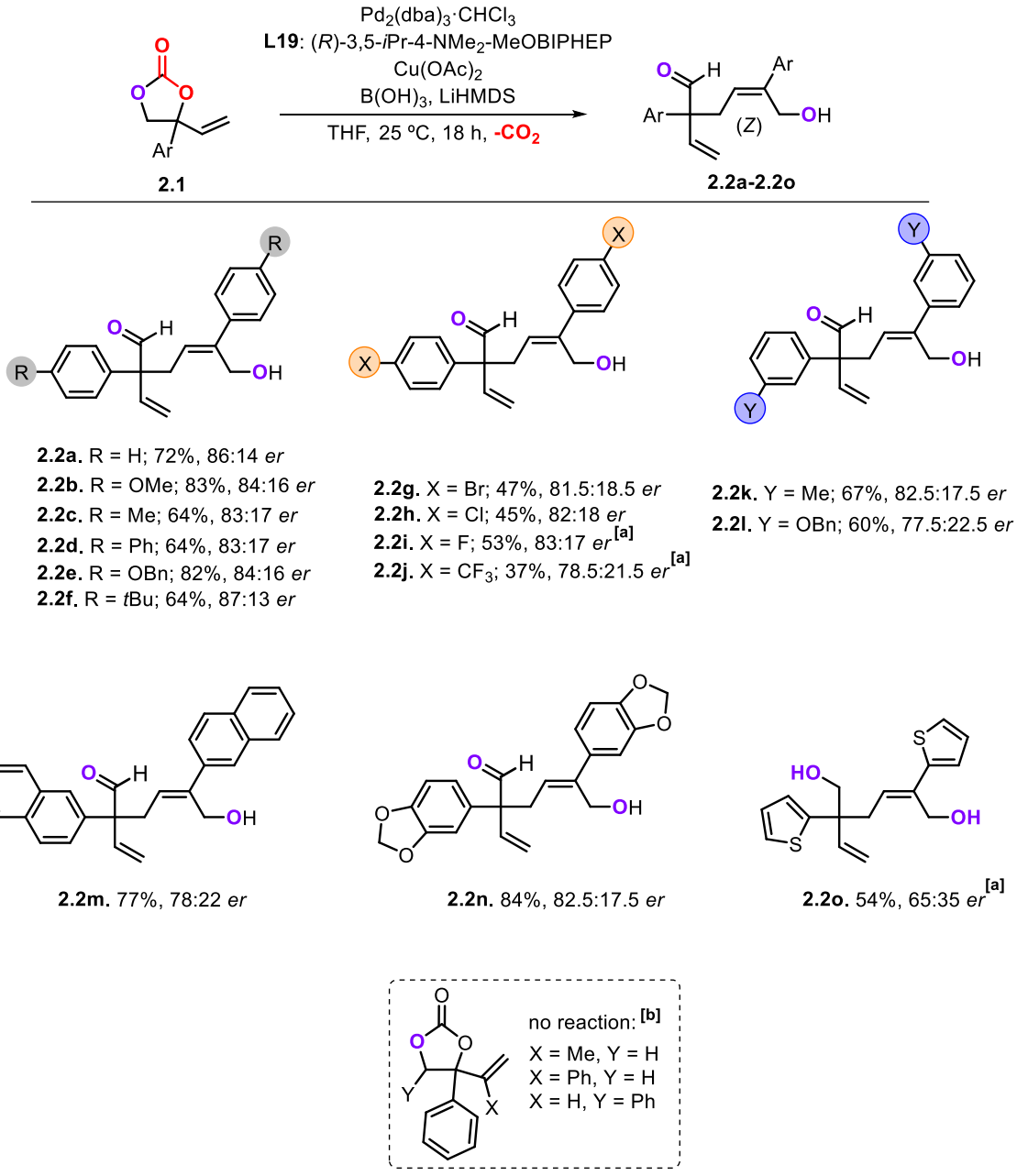

Scheme 2.3. Investigated product scope for compounds having highly functional/substituted quaternary carbon stereocenters (**2.2a–2.2o**) starting from various vinyl cyclic carbonates. The reaction conditions, if not stated otherwise, are those reported in Table 2.7, entry 12. [a] The chiral product was analyzed after reduction of the aldehyde group to the corresponding alcohol. [b] These substituted carbonates were not reactive under the conditions applied.

2.2.3. Mechanistic considerations

A number of control reactions were performed to clarify the role of the additives required in the optimized manifold. As can be expected from this asymmetric version of this sterically demanding formal cross-coupling reaction, the presence of the more bulky chiral ligand (*R*)-3,5-*i*Pr-4-NMe_2-MeOBIPHEP **L19** versus DPEPhos used in the racemic synthesis,[16] further activation/stabilization of the vinyl cyclic carbonate substrate and/or dienolate intermediate was essential.

From Table 2.5 and Scheme 2.4a it can be deduced that the chiral induction is most likely transferred from the *in situ* formed Pd(L*) based catalyst, with the Lewis acid additive playing a minor role in the asymmetric induction during the cross-coupling of the dienolate and Pd(allyl) species (Scheme 2.4a). From the observed data it can be inferred that the type of Lewis acid does play a role to increase the overall efficiency which in the case of $Cu(OAc)_2$ is higher without affecting the enantioselectivity. Importantly, when the reaction was performed in the absence of the Lewis acid additive, much lower conversion was noted but with essentially the same enantio-induction level. Therefore, in the most likely scenario, the role of the Lewis acid additive is to help to stabilize and turn-over the *in situ* formed dienolate species.

Next, the influence of the amount of boron additive and its nature was evaluated (Scheme 2.4b). In the case of boric acid [$B(OH)_3$], lowering the amount to 1 equiv. only had a small effect on the yield of the product, but when it was further decreased to sub-stoichiometric amounts, the transformation became completely ineffective. The use of other boron additives [$B(OMe)_3$ and $BF_3{\cdot}Et_2O$] was unproductive, while the addition of phenyl boronic acid [$PhB(OH)_2$] led to 55% vinyl carbonate conversion but without desired product formation. In this latter case, the boronic ester **2.3** could be isolated in 25% isolated yield.[18]

(18) C. H. Hövelmann, K. Muñiz, *Chem. Eur. J.* **2005**, *11*, 3951-3958.

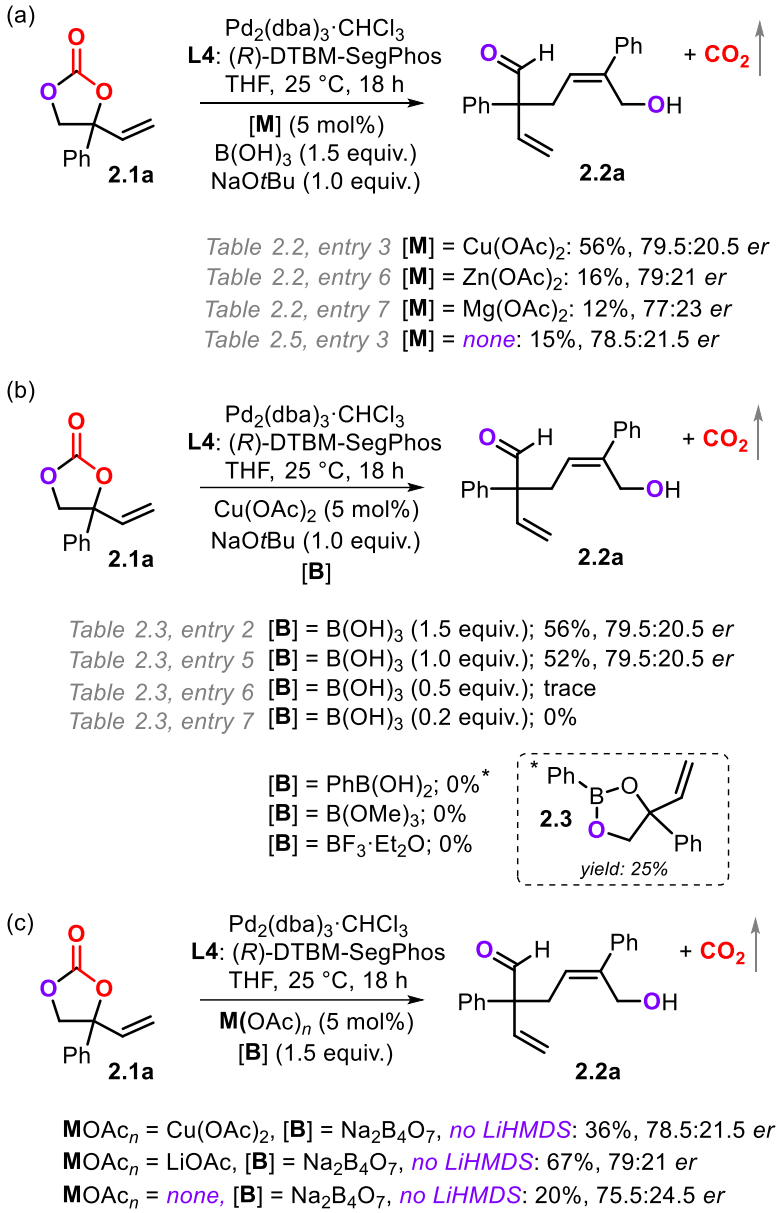

Scheme 2.4. Mechanistic control experiments: (a) Role of the Lewis acid. (b) Role of the boron additive and its amount. (c) Relationship between boric acid and the base.

We assume that the base (LiHMDS) first deprotonates $B(OH)_3$ and eventually forms some kind of lithium borate intermediate (Scheme 2.5)[19] able to stabilize the dienolate.[20]

(19) a) J. C. Vantourout, H. N. Miras, A. Isidro-Llobet, S. Sproules, A. J. B. Watson, *J. Am. Chem. Soc.* **2017**, *139*, 4769-4779; b) J.-C. Xiang, Y. Cheng, M. Wang, Y.-D. Wu, A.-X. Wu, *Org. Lett.* **2016**, *18*, 4360-4363; c) M. Gao, Y. Gan, B. Xu, *Org. Lett.* **2019**, *21*, 7435-7439; d) X.-S. Wu, Y. Chen, M.-B. Li, M.-G. Zhou, S.-K. Tian, *J. Am. Chem. Soc.* **2012**, *134*, 14694-14697; e) B. M. Trost, J. E. Schultz, T. Chang, M. R. Maduabum, *J. Am. Chem. Soc.* **2019**, *141*, 9521-9526; f) Y.-T. Tsoi, Z. Zhou, A. S. C. Chan, W.-Y. Yu, *Org. Lett.* **2010**, *12*, 4506-4509; g) A. Khan, S. Khan, I. Khan, C. Zhao, Y. Mao, Y. Chen, Y. J. Zhang, *J. Am. Chem. Soc.* **2017**, *139*, 10733-10741.

(20) a) E. W. H. Ng, K.-H. Low, P. Chiu, *J. Am. Chem. Soc.* **2018**, *140*, 3537-3541; b) L. Dang, Z. Lin, T. B. Marder, *Organometallics* **2008**, *27*, 4443-4454; c) N. J. Bell, A. J. Cox, N. R. Cameron, J. S. O.

The presence of $Cu(OAc)_2$ provokes a transmetalation process allowing for substrate turnover. Product **2.2a** is finally formed through the nucleophilic attack of the Cu-dienolate onto a Pd(allyl) electrophile following *in situ* protonation (Scheme 2.4).

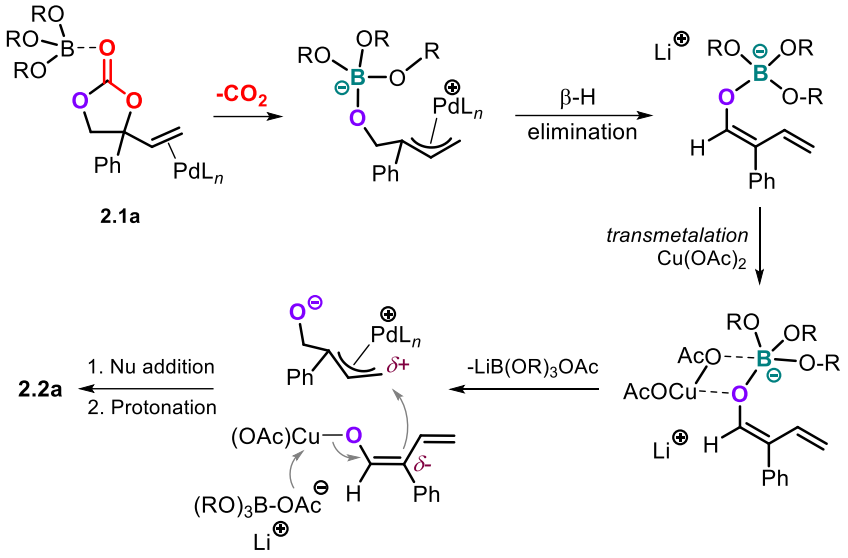

Scheme 2.5. Hypothesized formation of a borate species (here simplified for clarity) involving the dienolate derived from the vinyl carbonate substrate, and proposed manifold towards **2.2a**

To substantiate a possible involvement of a borate/boronate species,[21] some further experiments were carried out (Scheme 2.4c). Upon replacing the $B(OH)_3$/LiHMDS for $Na_2B_4O_7$, a 36% yield of the cross-coupled product was noted and its yield could be improved by replacing the catalytic amount of $Cu(OAc)_2$ for LiOAc (67%). The presence of the latter Lewis acid additive was crucial as in the absence of any, the yield of **2.2a** decreased to only 20%. All these manipulations hardly affected the enantio-induction but the trend noted in Scheme 2.4c aligns well with the results presented in Table 2.6 (entries 11-13), showing the more productive nature of a lithium borate species in this manifold.

Evans, T. B. Marder, M. A. Duin, C. J. Elsevier, X. Baucherel, A. A. D. Tulloch, R. P. Tooze, *Chem. Commun.* **2004**, 1854-1855.

(21) M. Van Duin, J. A. Peters, A. P. G. Kieboom, H. Van Bekkum, *Tetrahedron* **1984**, *40*, 2901-2911.

2.3. Conclusions

In this chapter, we present an asymmetric version of our previously reported formal cross-coupling reaction that involves two molecules of substituted vinyl cyclic carbonate. An umpolung process allows for a dienolate species to be formed that attacks a Pd(allyl) intermediate providing compounds with functionally dense quaternary carbon stereocenters. In this protocol, additives are required to compensate for the lower reactivity of the Pd catalyst that comprises of a sterically more demanding chiral ligand, and a number of control experiments point towards the involvement of a metal boronate as to activate the cyclic carbonate substrate and stabilized a key dienolate species. Appreciable asymmetric induction up to 80% *ee* (90:10 *er*) could be achieved using a Pd catalyst derived from (*R*)-3,5-*i*Pr-4-NMe_2-MeOBIPHEP **L19**, and the scope of products demonstrates that the transformation is reasonably general in terms of asymmetric induction.

This work clearly illustrates that these kinds of sterically highly demanding cross-coupling processes require substantial optimization and ligand fine-tuning, with the latter aspect envisioned to be of crucial importance for the development of new protocols that can expand the synthesis of compounds with quaternary carbon stereocenters.

2.4. Experimental section

2.4.1. General information

Commercially available reagents were used as received without further purification. $Pd_2(dba)_3 \cdot CHCl_3$ was purchased from Aldrich, ligands were purchased from Aldrich and STREM, anhydrous solvents were taken from a commercial SPS solvent dispenser. ^1H NMR, ^{13}C NMR and ^{19}F NMR spectra were recorded on a Bruker AV-400 MHz or a Bruker AV-500 MHz at 20°C and referenced to the residual deuterated solvent signals. All reported NMR data are given in parts per million (ppm). FT-IR measurements were carried out using a Bruker Optics FTIR Alpha spectrometer. Optical rotations were measured with a Jasco P-1030 polarimeter. Mass spectrometric analyses, UPC2 analyses, and X-ray diffraction analyses were performed by the Research Support Area (RSA) at ICIQ.

2.4.2. General procedure for the preparation of vinyl cyclic carbonates

The vinyl carbonates can be easily prepared according to a previous reported procedure with minor modifications.[14a,22] The α-hydroxymethyl ketones were synthesized followed a reported procedure when they were not commercially available.[23] To a solution of the corresponding α-hydroxymethyl ketone (5 mmol, 1 equiv.) in THF (20 mL) was added vinyl magnesium bromide (1.0 M in THF, 2.5 equiv.) at 0 °C. The reaction was stirred under an Ar atmosphere at room temperature (rt) for 2 h. The reaction mixture was then quenched with saturated aqueous NH_4Cl, and extracted with EtOAc. The combined organic layers were dried over anhydrous Na_2SO_4, filtered and concentrated affording a light yellow oil. To a solution of the latter in CH_2Cl_2 (30 mL) was added pyridine (20 mmol, 4 equiv.) and triphosgene (2.5 mmol, 0.5 equiv.) at 0 °C. The reaction was stirred under an Ar atmosphere at room temperature for 2 h. The reaction mixture was then quenched with saturated aqueous NH_4Cl, washed with H_2O, and extracted with CH_2Cl_2. The combined organic layers were dried over anhydrous Na_2SO_4, filtered and concentrated. The residue was purified by flash chromatography on silica to afford the corresponding carbonate.

(22) a) A. Khan, L. Yang, J. Xu, L. Y. Jin, Y. J. Zhang, *Angew. Chem. Int. Ed.* **2014**, *53*, 11257-11260; b) A. Khan, R. Zheng, Y. Kan, J. Ye, J. Xing, Y. J. Zhang, *Angew. Chem. Int. Ed.* **2014**, *53*, 6439-6442.
(23) R. de la Campa, R. Manzano, P. Calleja, S. R. Ellis, D. J. Dixon, *Org. Lett.* **2018**, *20*, 6033-6036.

2.4.3. Typical procedure for the formation of highly functionalized compounds featuring quaternary stereocenters

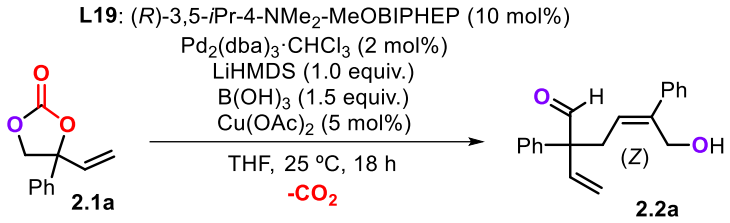

A mixture of $Pd_2(dba)_3{\cdot}CHCl_3$ (4.1 mg, 0.004 mmol, 2 mol%), (*R*)-3,5-*i*Pr-4-NMe_2-MeOBIPHEP (21.8 mg, 0.02 mmol, 10 mol%), $B(OH)_3$ (18.5 mg, 0.3 mmol, 1.5 equiv.) and $Cu(OAc)_2$ (1.8 mg, 0.01 mmol, 5 mol%) in THF was stirred under an Ar atmosphere for 20 min at r.t. LiHMDS (1 M in THF, 1.0 equiv.) was added and the reaction mixture was stirred for further 10 min and then the carbonate **2.1a** (38.0 mg, 0.2 mmol, 1.0 equiv.) was added. The reaction was stirred for 18h at rt and was then quenched with H_2O and extracted with EtOAc. The combined organic layers were dried over anhydrous Na_2SO_4, filtered and concentrated. The residue was purified by flash chromatography on silica to afford the desired product **2.2a**.

2.4.4. Characterization data for all new compounds

(*Z*)-6-hydroxy-2,5-diphenyl-2-vinylhex-4-enal (2.2a)[16]

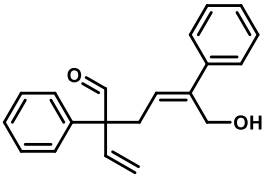

Yellow oil; 72% yield, 86:14 *er*, $[\alpha]_D^{25}$ = -0.65 (c 0.13, $CHCl_3$); **^{1}H NMR** (400 MHz, $CDCl_3$) δ 9.61 (s, 1H), 7.44-7.40 (m, 2H), 7.35, 7.33-7.21 (m, 8H), 6.20 (dd, *J* = 17.9, 11.0 Hz, 1H), 5.72 (t, *J* = 7.8 Hz, 1H), 5.59 (d, *J* = 11.0 Hz, 1H), 5.31 (d, *J* = 17.9 Hz, 1H), 4.41-4.35 (m, 2H), 3.07-2.96 (m, 2H) ppm; **^{13}C NMR** (101 MHz, $CDCl_3$) δ 198.41, 141.36, 140.96, 138.14, 136.27, 129.00, 128.37, 128.23, 127.84, 127.22, 126.34, 126.30, 119.99, 61.92, 59.75, 33.30 ppm; the enantiomeric excess was determined by UPC2 analysis on Chiralpak IA after reduction with $NaBH_4$, mobile phase: CO_2:MeOH 90:10, flow rate 3 mL/min, ABPR 1500 psi, t_R = 3.77 min (major), t_R = 4.54 min (minor).

(*Z*)-6-hydroxy-2,5-bis(4-methoxyphenyl)-2-vinylhex-4-enal (2.2b)[16]

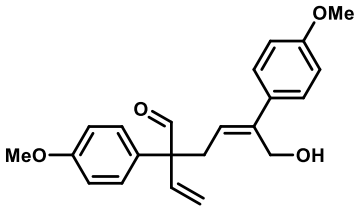

Yellow oil; 83% yield, 84:16 *er*, $[\alpha]_D^{25}$ = +4.36 (c 0.16, $CHCl_3$); **^{1}H NMR** (400 MHz, $CDCl_3$) δ 9.55 (s, 1H), 7.27-7.25 (m, 2H), 7.18-7.16 (m, 2H), 6.94-6.92 (m, 2H), 6.84-6.82 (m, 2H), 6.17 (dd, *J* = 18.0, 11.0 Hz, 1H), 5.64 (t, *J* = 7.8 Hz, 1H), 5.56 (d, *J* = 11.0 Hz, 1H), 5.26 (d, *J* = 17.8 Hz, 1H), 4.42-4.36 (m, 2H), 3.81 (s, 3H), 3.79 (s, 3H), 3.01-2.92 (m, 2H) ppm; **^{13}C NMR** (101 MHz, CDCl3) δ 198.60, 159.09, 158.94, 140.58, 136.76, 133.39, 129.76, 129.38, 127.40, 124.91, 119.54, 114.38, 113.79, 61.19, 59.80, 55.29, 55.26, 33.26 ppm; the enantiomeric excess was determined by UPC2 analysis on Chiralpak IA after reduction with $NaBH_4$, mobile phase: CO_2:MeOH 85:15, flow rate 3 mL/min, ABPR 1500 psi, t_R = 4.19 min (major), t_R = 4.92 min (minor).

(*Z*)-6-hydroxy-2,5-di-*p*-tolyl-2-vinylhex-4-enal (2.2c)[16]

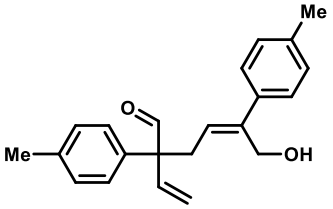

Yellow oil; 64% yield, 83:17 *er*, $[\alpha]_D^{25}$ = +5.05 (c 0.17, $CHCl_3$); **^{1}H NMR** (400 MHz, $CDCl_3$) δ 9.58 (s, 1H), 7.24-7.18 (m, 4H), 7.15-7.10 (m, 4H), 6.18 (dd, *J* = 17.8, 11.0 Hz, 1H), 5.70 (t, *J* = 7.6 Hz, 1H), 5.56 (d, *J* = 11.0 Hz, 1H), 5.28 (d, *J* =17.8 Hz, 1H), 4.41-4.34 (m, 2H), 3.03-2.93 (m, 2H), 2.35 (s, 3H), 2.32 (s, 3H) ppm; **^{13}C NMR** (101 MHz, $CDCl_3$) δ 198.57, 141.04, 138.04, 137.62, 136.95, 136.49, 134.99, 129.67, 129.07, 128.11, 126.17, 125.63, 119.70, 61.57, 59.75, 33.25, 21.02, 20.97 ppm; the enantiomeric excess was determined by UPC2 analysis on Chiralpak IA after reduction with $NaBH_4$, mobile phase: CO_2:MeOH 85:15, flow rate 3 mL/min, ABPR 1500 psi, t_R = 2.86 min (major), t_R = 3.86 min (minor).

(*Z*)-2,5-di([1,1'-biphenyl]-4-yl)-6-hydroxy-2-vinylhex-4-enal (2.2d)[16]

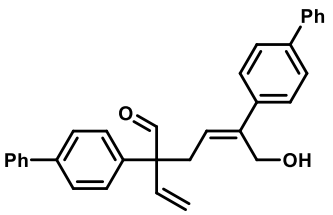

Yellowish solid; 85% yield, 86:16 *er*, $[\alpha]_D^{25}$ = +18.03 (c 0.21, $CHCl_3$); **^{1}H NMR** (400 MHz, $CDCl_3$) δ 9.66 (s, 1H), 7.68-7.64 (m, 2H), 7.61-7.52 (m, 6H), 7.47-7.41 (m, 6H), 7.39-7.31 (m, 4H), 6.25 (dd, *J* = 17.8, 10.9 Hz, 1H), 5.82 (t, *J* = 7.7 Hz, 1H), 5.63 (d, *J* = 10.9 Hz, 1H), 5.36 (d, *J* = 17.8 Hz, 1H), 4.51-4.44 (m, 2H), 3.13-3.03 (m, 2H) ppm; **^{13}C NMR** (101 MHz, $CDCl_3$) δ 198.42, 140.91, 140.72, 140.65, 140.10, 140.08, 139.79, 136.96, 136.33, 128.83, 128.72, 128.65, 127.62, 127.60, 127.22,

127.10, 127.04, 126.92, 126.66, 126.29, 120.01, 61.65, 59.69, 33.31 ppm; the enantiomeric excess was determined by UPC2 analysis on Chiralpak ID after reduction with $NaBH_4$, mobile phase: CO_2:IPA 70:30, flow rate 3 mL/min, ABPR 1500 psi, t_R = 4.15 min (minor), t_R = 4.66 min (major).

(*Z*)-2,5-bis(4-(benzyloxy)phenyl)-6-hydroxy-2-vinylhex-4-enal (2.2e)[16]

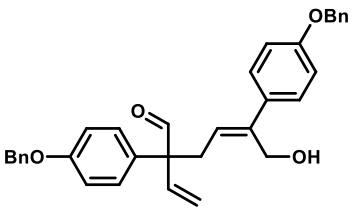

White solid; 82% yield, 84:16 *er*, $[\alpha]_D^{25}$ = +7.64 (c 0.36, $CHCl_3$); **^{1}H NMR** (400 MHz, $CDCl_3$) δ 9.56 (s, 1H), 7.45-7.37 (m, 8H), 7.35-7.31 (m, 2H), 7.28-7.23 (m, 2H), 7.19-7.16 (m, 2H), 7.03-6.98 (m, 2H), 6.93-6.89 (m, 2H), 6.17 (dd, *J* = 17.8, 11.0 Hz, 1H), 5.65 (t, *J* = 7.8 Hz, 1H), 5.55 (d, *J* = 11.0 Hz, 1H), 5.27 (d, *J* = 17.8 Hz, 1H), 5.07 (s, 2H), 5.06 (s, 2H), 4.43-4.34 (m, 2H), 3.02-2.92 (m, 2H) ppm; **^{13}C NMR** (101 MHz, $CDCl_3$) δ 198.55, 158.25, 158.14, 140.58, 136.96, 136.68, 136.66, 133.62, 130.03, 129.40, 128.59, 128.55, 128.03, 127.92, 127.44, 127.41, 127.39, 124.96, 119.57, 115.30, 114.73, 70.03, 69.99, 61.20, 59.73, 33.23 ppm; the enantiomeric excess was determined by UPC2 analysis on Chiralpak IB after reduction with $NaBH_4$, mobile phase: CO_2:EtOH 70:30, flow rate 3 mL/min, ABPR 1500 psi, t_R = 3.05 min (major), t_R = 3.43 min (minor).

(*Z*)-2,5-bis(4-(*tert*-butyl)phenyl)-6-hydroxy-2-vinylhex-4-enal (2.2f)[16]

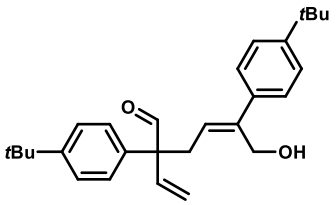

Yellowish solid; 64% yield, 87:13 *er*, $[\alpha]_D^{25}$ = +11.44 (c 0.36, $CHCl_3$); **^{1}H NMR** (400 MHz, $CDCl_3$) δ 9.59 (s, 1H), 7.43 (d, *J* = 8.4 Hz, 2H), 7.36-7.25 (m, 5H), 7.20 (d, *J* = 8.2 Hz, 2H), 6.20 (dd, *J* = 17.9, 10.9 Hz, 1H), 5.75 (t, *J* = 7.7 Hz, 1H), 5.57 (d, *J* = 10.9 Hz, 1H), 5.29 (d, *J* = 17.8 Hz, 1H), 4.45-4.30 (m, 2H), 3.07-2.94 (m, 2H), 1.33 (s, 19H), 1.31 (s, 19H) ppm; **^{13}C NMR** (101 MHz, $CDCl_3$) δ 198.66, 150.82, 150.13, 140.93, 138.00, 136.56, 134.91, 127.90, 125.96, 125.88, 125.80, 125.28, 119.62, 61.50, 59.71, 34.52, 34.43, 33.26, 31.27, 31.23 ppm; the enantiomeric excess was determined by UPC2 analysis on Chiralpak IG after reduction with $NaBH_4$, mobile phase: CO_2:MeOH 70:30, flow rate 2 mL/min, ABPR 2000 psi, t_R = 2.37 min (major), t_R = 2.68 min (minor).

(*Z*)-2,5-bis(4-bromophenyl)-6-hydroxy-2-vinylhex-4-enal (2.2g)

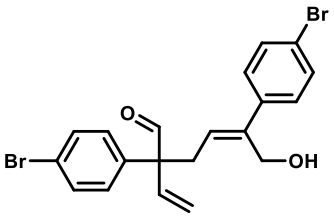

Yellow oil; 47% yield, 81.5:18.5 *er*, $[\alpha]_D^{25}$ = -3.80 (c 0.12, $CHCl_3$); **^{1}H NMR** (400 MHz, $CDCl_3$) δ 9.55 (s, 1H), 7.55-7.52 (m, 2H), 7.45-7.39 (m, 2H), 7.20-7.17 (m, 2H), 7.14-7.11 (m, 2H), 6.13 (dd, *J* = 17.8, 11.0 Hz, 1H), 5.65-5.59 (m, 2H), 5.28 (d, *J* = 17.8 Hz), 4.43-4.36 (m, 2H), 3.02-2.92 (m, 2H) ppm; **^{13}C NMR** (101 MHz, $CDCl_3$) δ 197.88, 140.63, 139.76, 137.01, 135.85, 132.18, 131.50, 129.88, 127.94, 126.47, 122.19, 121.34, 120.45, 61.40, 59.64, 33.15; the enantiomeric excess was determined by UPC2 analysis on Chiralpak IC after reduction with $NaBH_4$, mobile phase: CO_2:IPA 80:20, flow rate 3 mL/min, ABPR 1500 psi, t_R = 3.06 min (minor), t_R = 3.88 min (major); **HRMS-ESI** calcd for $C_{20}H_{18}Br_2NaO_2^+$: 470.9566, found: 470.9557 ($[M+Na]^+$); **IR** (neat) ν = 3410, 2923, 2853, 2719, 1721, 1586, 1485, 1072, 1004, 818, 754 cm^{-1}.

(*Z*)-2,5-bis(4-chlorophenyl)-6-hydroxy-2-vinylhex-4-enal (2.2h)[16]

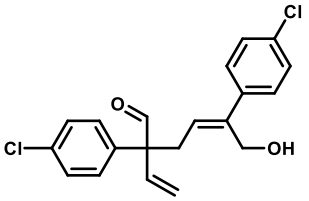

Yellow oil; 45% yield, 82.5:17.5 *er*, $[\alpha]_D^{25}$ = -6.44 (c 0.11, $CHCl_3$); **^{1}H NMR** (400 MHz, $CDCl_3$): δ 9.56 (s, 1H), 7.40-7.38 (m, 2H), 7.26-7.14 (m, 4H), 7.20-7.18 (m, 2H), 6.14 (dd, *J* = 17.8, 10.9 Hz, 1H), 5.63 (t, *J* = 7.6 Hz, 1H), 5.60 (d, *J* = 10.9 Hz, 1H), 5.28 (d, *J* = 17.8 Hz, 1H), 4.43-4.36 (m, 2H), 3.03-2.93 (m, 2H) ppm; **^{13}C NMR** (101 MHz, $CDCl_3$): δ 197.97, 140.55, 139.28, 136.47, 135.95, 134.04, 133.18, 129.55, 129.21, 128.53, 127.59, 126.42, 120.38, 61.33, 59.67, 33.19 ppm; the enantiomeric excess was determined by UPC2 analysis on Chiralpak IC after reduction with $NaBH_4$, mobile phase: CO_2:EtOH 90:10, flow rate 3 mL/min, ABPR 1500 psi, t_R = 4.89 min (minor), t_R = 5.38 min (major).

(*Z*)-2,5-bis(4-fluorophenyl)-6-hydroxy-2-vinylhex-4-enal (2.2i)[16]

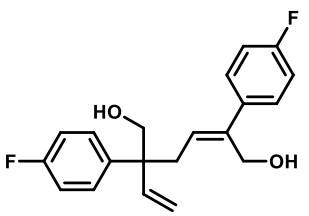

Yellow oil; 53% yield, 83:17 *er*, $[\alpha]_D^{25}$ = -38.37 (c 0.14, $CHCl_3$); **^{1}H NMR** (400 MHz, $CDCl_3$) δ 7.38-7.28 (m, 4H), 7.07-6.96 (m, 4H), 5.96 (dd, *J* = 17.8, 11.0 Hz, 1H), 5.67 (t, *J* = 8.0 Hz, 1H), 5.37 (d, *J* = 11.0 Hz, 1H), 5.17 (d, *J* = 17.8 Hz, 1H), 4.50-4.44 (m, 2H), 3.93 (d, *J* = 11.0 Hz, 1H), 3.84 (d, *J* = 11.1 Hz, 1H), 2.87-2.85 (m, 2H) ppm; **^{13}C NMR** (101 MHz, $CDCl_3$) δ 163.09 (d, *J* = 55.4 Hz), 160.64 (d, *J* = 55.4

Hz), 142.60, 140.92, 138.46 (d, *J* = 3.3 Hz), 137.89 (d, *J* = 3.3 Hz), 128.80 (d, *J* = 7.8 Hz), 127.71 (d, *J* = 7.8 Hz), 127.43, 115.82, 115.35 (d, *J* = 17.5 Hz), 115.14 (d, *J* = 17.5 Hz), 65.64, 60.10, 49.83, 33.42 ppm; **^{19}F NMR** (376 MHz, $CDCl_3$) δ -115.70, -115.95 ppm; the enantiomeric excess was determined by UPC2 analysis on Chiralpak IC, mobile phase: CO_2:IPA 85:15, flow rate 3 mL/min, ABPR 1500 psi, t_R = 1.75 min (minor), t_R = 2.02 min (major).

(*Z*)-2,5-bis(4-(trifluoromethyl)phenyl)-5-vinylhex-2-ene-1,6-diol (2.2j)

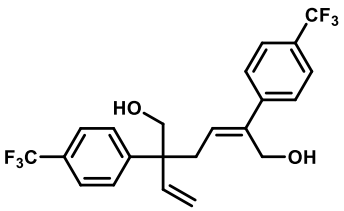

Yellow oil; 37% yield, 78.5:21.5 *er*, $[\alpha]_D^{25}$ = -21.80 (c 0.13, $CHCl_3$); **^{1}H NMR** (400 MHz, $CDCl_3$) δ 7.67-7.43 (m, 8H), 5.97 (dd, *J* = 17.8, 11.0 Hz, 1H), 5.79 (t, *J* = 8.0 Hz, 1H), 5.42 (d, *J* = 11.0 Hz, 1H), 5.20 (d, *J* = 17.8 Hz, 1H), 4.59-4.44 (m, 2H), 3.99 (d, *J* = 11.1 Hz, 1H), 3.89 (d, *J* = 11.2 Hz, 1H), 3.04-2.87 (m, 2H) ppm; **^{13}C NMR** (101 MHz, $CDCl_3$) δ 147.00, 145.36, 141.84, 141.21, 129.28, 129.23 (q, *J* = 32.7 Hz), 127.62, 126.38, 124.19 (q, *J* = 272.2 Hz), 124.04 (q, *J* = 272.0 Hz), 125.47 (q, *J* = 3.8 Hz), 125.35 (q, *J* = 3.8 Hz), 116.50, 65.42, 59.92, 50.34, 33.34 ppm; **^{19}F NMR** (376 MHz, $CDCl_3$) δ -62.22, -62.28 ppm; the enantiomeric excess was determined by UPC2 analysis on Chiralpak IG, mobile phase: CO_2:IPA 90:10, flow rate 2 mL/min, ABPR 2000 psi, t_R = 3.08 min (minor), t_R = 3.53 min (major); **HRMS-ESI** calcd for $C_{22}H_{20}F_6NaO_2^+$: 453.1260, found: 453.1257 ($[M+Na]^+$); **IR** (neat) ν = 3313, 2924, 2854, 1616, 1323, 1113, 1066, 836, 731 cm^{-1}.

(*Z*)-6-hydroxy-2,5-di-*m*-tolyl-2-vinylhex-4-enal (2.2k)[16]

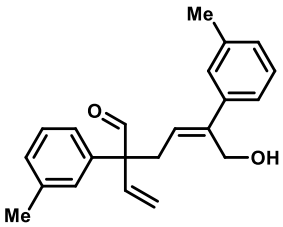

Yellow oil; 67% yield, 82.5:17.5 *er*, $[\alpha]_D^{25}$ = +6.09 (c 0.19, $CHCl_3$); **^{1}H NMR** (400 MHz, $CDCl_3$) δ 9.60 (s, 1H), 7.33-7.29 (m, 1H), 7.21-7.06 (m, 7H), 6.20 (dd, *J* = 17.9, 11.0 Hz, 1H), 5.70 (t, *J* = 7.8 Hz, 1H), 5.58 (d, *J* = 11.0 Hz, 1H), 5.30 (d, *J* = 17.9 Hz, 1H), 4.37-4.34 (m, 2H), 3.04-2.94 (m, 2H), 2.37 (s, 3H), 2.33 (s, 3H) ppm; **^{13}C NMR** (101 MHz, $CDCl_3$) δ 198.53, 141.39, 141.01, 138.72, 138.04, 137.91, 136.34, 128.93, 128.84, 128.55, 128.25, 127.97, 127.07, 126.28, 125.21, 123.41, 119.78, 61.81, 59.78, 33.22, 21.49, 21.45 ppm; the enantiomeric excess was determined by UPC2 analysis on Chiralpak IA after reduction with $NaBH_4$, mobile phase: CO_2:MeOH 85:15, flow rate 3 mL/min, ABPR 1500 psi, t_R = 1.62 min (major), t_R = 2.26 min (minor).

(*Z*)-2,5-bis(3-(benzyloxy)phenyl)-6-hydroxy-2-vinylhex-4-enal (2.2l)[16]

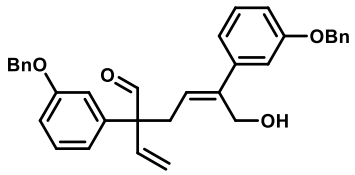

Yellow oil; 60% yield, 77.5:22.5 *er*, $[\alpha]_D^{25}$ = -0.38 (c 0.23, $CHCl_3$); **^{1}H NMR** (400 MHz, $CDCl_3$) δ 9.58 (s, 1H), 7.44-7.31 (m, 11H), 7.21 (t, *J* = 8.0 Hz, 1H), 6.98-6.83 (m, 6H), 6.17 (dd, *J* = 17.8, 11.0 Hz, 1H), 5.72 (t, *J* = 7.8 Hz, 1H), 5.57 (d, *J* = 11.0 Hz, 1H), 5.28 (d, *J* = 17.8 Hz, 1H), 5.06-5.01 (m, 2H), 4.41-4.34 (m, 2H), 3.04-2.93 (m, 2H) ppm; **^{13}C NMR** (101 MHz, $CDCl_3$) δ 198.23, 159.24, 158.83, 142.55, 141.17, 139.65, 136.95, 136.57, 136.16, 129.97, 129.36, 128.58, 128.54, 128.05, 127.92, 127.52, 126.58, 120.64, 119.96, 119.04, 115.44, 113.81, 113.40, 113.23, 70.12, 69.95, 61.77, 59.76, 33.15 ppm; the enantiomeric excess was determined by UPC2 analysis on Chiralpak IC after reduction with $NaBH_4$, mobile phase: CO_2:EtOH 85:15, flow rate 3 mL/min, ABPR 1500 psi, t_R = 9.37 min (major), t_R = 10.09 min (minor).

(*Z*)-2,5-bis(benzo[d][1,3]dioxol-5-yl)-6-hydroxy-2-vinylhex-4-enal (2.2m)[16]

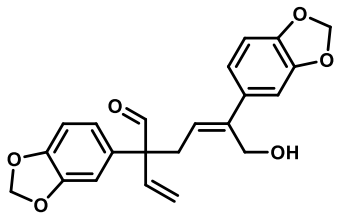

Yellow oil; 84% yield, 82.5:17.5 *er*, $[\alpha]_D^{25}$ = +8.97 (c 0.24, $CHCl_3$); **^{1}H NMR** (400 MHz, $CDCl_3$) δ 9.52 (s, 1H), 6.84-6.80 (m, 3H), 6.76-6.72 (m, 2H), 6.70-6.67 (m, 1H), 6.13 (dd, *J* = 17.8, 11.0 Hz, 1H), 5.97 (s, 2H), 5.92 (s, 2H), 5.58 (t, *J* = 7.6 Hz, 1H), 5.55 (d, *J* = 11.0 Hz, 1H), 5.26 (d, *J* = 17.8 Hz, 1H), 4.43-4.36 (m, 2H), 2.94-2.92 (m, 2H) ppm; **^{13}C NMR** (101 MHz, $CDCl_3$) δ 198.23, 148.41, 147.69, 147.18, 146.85, 140.82, 136.58, 135.25, 131.53, 125.38, 121.67, 119.77, 119.69, 108.55, 108.49, 108.13, 106.95, 101.33, 100.97, 61.33, 59.94, 33.15 ppm; the enantiomeric excess was determined by UPC2 analysis on Chiralpak IF after reduction with $NaBH_4$, mobile phase: CO_2:EtOH 75:25, flow rate 2 mL/min, ABPR 2000 psi, t_R = 2.03 min (major), t_R = 2.53 min (minor).

(*Z*)-6-hydroxy-2,5-di(naphthalen-2-yl)-2-vinylhex-4-enal (2.2n)

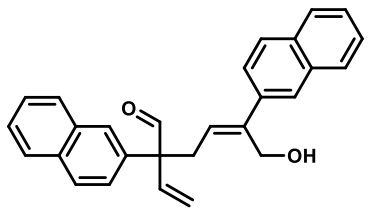

Yellow oil; 77% yield, 78:22 *er*, $[\alpha]_D^{25}$ = +7.20 (c 0.14, $CHCl_3$); **^{1}H NMR** (400 MHz, $CDCl_3$): δ 9.57 (s, 1H), 7.77-7.70 (m, 3H), 7.63-7.57 (m, 5H), 7.40-7.37 (m, 2H), 7.30-7.24 (m, 4H), 6.19 (dd, *J* = 17.8, 11.0 Hz, 1H), 5.73 (t, *J* = 7.8 Hz, 1H), 5.52 (d, *J* = 11.0 Hz, 1H), 5.23 (d, *J* = 17.8 Hz, 1H), 4.43-4.35 (m, 2H), 3.10-2.98 (m, 2H) ppm; **^{13}C NMR** (101 MHz, CDCl3) δ 198.60, 141.32, 138.15, 136.46, 135.37, 133.34, 133.31, 132.60, 132.57, 128.82, 128.04, 128.01, 127.93, 127.62, 127.59,

127.44, 126.90, 126.61, 126.10, 125.75, 125.61, 124.97, 124.59, 120.20, 61.99, 59.83, 33.41 ppm; the enantiomeric excess was determined by UPC2 analysis on Chiralpak IB after reduction with $NaBH_4$, mobile phase: CO_2:IPA 70:30, flow rate 3 mL/min, ABPR 1500 psi, t_R = 2.46 min (minor), t_R = 3.03 min (major); **HRMS-ESI** calcd for $C_{28}H_{24}NaO_2^+$: 415.1669, found: 415.1685 ($[M+Na]^+$); **IR** (neat) ν = 3357, 2921, 2853, 2718, 1720, 1597, 1502, 1016, 814, 744 cm^{-1}.

(*E*)-2,5-di(thiophen-2-yl)-5-vinylhex-2-ene-1,6-diol (2.2o)[16]

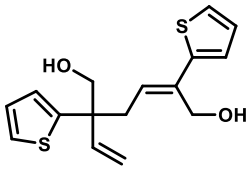

Yellow oil; 54% yield, 65:35 *er*, $[\alpha]_D^{25}$ = -8.76 (c 0.10, $CHCl_3$); **^{1}H NMR** (400 MHz, $CDCl_3$) δ 7.27-7.26 (m, 1H), 7.15-7.11 (m, 2H), 7.03-6.94 (m, 3H), 6.06 (dd, *J* = 17.7, 10.9 Hz, 1H), 6.01 (t, *J* = 8.1 Hz, 1H), 5.35 (d, *J* = 10.9 Hz, 1H), 5.19 (d, *J* = 17.7 Hz, 1H), 4.55 (d, *J* = 12.2 Hz, 1H), 4.47 (d, *J* = 12.2 Hz, 1H), 3.95-3.76 (m, 2H), 3.04-2.75 (m, 2H) ppm; **^{13}C NMR** (101 MHz, $CDCl_3$) δ 147.67, 145.27, 141.89, 136.01, 127.53, 126.86, 125.68, 124.42, 124.29, 123.87, 123.34, 115.76, 66.56, 59.79, 49.35, 34.60 ppm; the enantiomeric excess was determined by UPC2 analysis on Chiralpak IG, mobile phase: CO_2:EtOH 70:30, flow rate 2 mL/min, ABPR 2000 psi, t_R = 4.50 min (minor), t_R = 4.93 min (major).

2,4-diphenyl-4-vinyl-1,3,2-dioxaborolane (2.3)

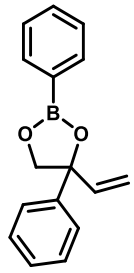

Yellow oil; 25% yield; **^{1}H NMR** (400 MHz, $CDCl_3$) δ 7.95-7.93 (m, 2H), 7.54- 7.50 (m, 1H), 7.46-7.36 (m, 6H), 7.32-7.28 (m, 1H), 6.26 (dd, *J* = 17.1, 10.6 Hz, 1H), 5.37 (dd, *J* = 17.1, 1.0 Hz, 1H), 5.23 (dd, *J* = 10.6, 1.0 Hz, 1H), 4.61 (d, *J* = 8.9 Hz, 1H), 4.48 (d, *J* = 8.9 Hz, 1H) ppm; **^{13}C NMR** (101 MHz, $CDCl_3$) δ 143.36, 141.05, 135.00, 131.68, 128.51, 127.89, 127.55, 124.97, 114.02, 85.47, 77.28 ppm; ^{11}B NMR (128 MHz, $CDCl_3$) δ 30.94 ppm; **HRMS-APCI** calcd for $C_{16}H_{16}O_2B^+$: 251.1238, found: 251.1235 ($[M+H]^+$); **IR** (neat) ν = 2959, 2923, 1603, 1497, 1442, 1351, 1093, 980, 698 cm^{-1}.

2.4.5. The transformation of 2f into its carboxylic acid derivative 2.2p

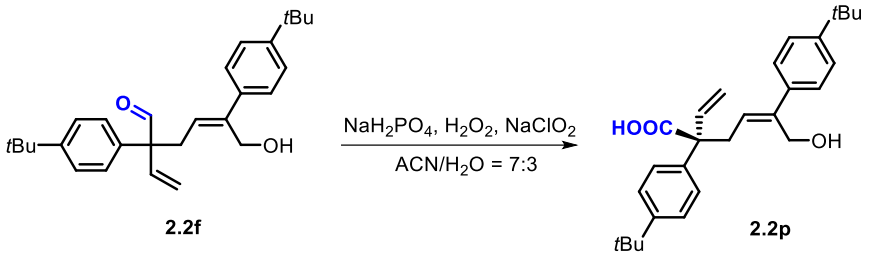

2.2f **2.2p**

To a small vial was added aldehyde **2.2f** (0.31 mmol, 124.8 mg), H_2O_2 (35 μL, 1.1 equiv., 33% w/v solution), $NaClO_2$ (39.3 mg, 1.4 equiv.) and NaH_2PO_4 (9.3 mg, 0.25 equiv.), and then a mixture of acetonitrile/H_2O (7:3, 4 mL) was added. The resultant reaction mixture was stirred at r.t. for 12 h. The pure product **2.2p** (colorless solid, 85.7 mg, 66% yield) was isolated by flash chromatography on silica gel. $[\alpha]_D^{25}$ = -6.75 (c 1.02 , $CHCl_3$); **^{1}H NMR** (500 MHz, $CDCl_3$) δ 7.38-7.34 (m, 2H), 7.33-7.26 (m, 5H), 7.26-7.23 (m, 1H), 6.38 (dd, *J* = 17.7, 10.9 Hz, 1H), 5.82 (t, *J* = 7.7 Hz, 1H), 5.43 (d, *J* = 10.9 Hz, 1H), 5.26 (d, *J* = 17.7 Hz, 1H), 4.45-4.35 (m, 2H), 3.15-2.97 (m, 2H), 1.31 (s, 9H), 1.30 (s, 9H) ppm; **^{13}C NMR** (126 MHz, $CDCl_3$) δ 177.23, 150.31, 150.16, 140.85, 138.98, 138.16, 137.61, 127.06, 126.45, 126.03, 125.33, 125.30, 117.15, 59.80, 57.56, 35.74, 34.46, 34.45, 31.30, 31.28 ppm; **HRMS-ESI** calcd for $C_{28}H_{35}O$: 419.2592, found: 419.2582 ($[M–H]^-$); **IR** ($CDCl_3$) ν = 3399, 3085, 3030, 2960, 2905, 1704, 1511, 1468, 1400, 1269, 1005, 918, 831, 734 cm^{-1}.

2.4.6. X-ray crystallographic studies

General procedure:

The measured crystal of **2.2p** was stable under atmospheric conditions; nevertheless, it was treated under inert conditions immersed in perfluoro-polyether as protecting oil for manipulation. Data Collection: measurements were made on a Bruker-Nonius diffractometer equipped with an APPEX II 4K CCD area detector, a FR591 rotating anode with Mo Kα radiation, Montel mirrors and a Kryoflex low temperature device (T = −173 °C). Full-sphere data collection was used with ω and φ scans. Programs used: Data collection Apex2 V2011.3 (Bruker-Nonius 2008), data reduction Saint+Version 7.60A (Bruker AXS 2008) and absorption correction SADABS V. 2008−1 (2008).

Structure Solution: SHELXTL Version 6.10 (Sheldrick, 2000) was used.[24] Structure Refinement: SHELXTL-97-UNIX VERSION.

Comments for the X-ray measurements for 2.2p: With the aim to confirm the absolute configuration of the major fraction of **2.2p**, different crystals selected from the same vial were measured. Finally, four different crystals were measured and all of them crystallized in same orthorhombic chiral space $P2_12_12_1$. From the measured crystals, three corresponded to complete datasets suitable for absolute structure determination. The absolute structure could be determined reliably for all three crystals with Flack values based on Parsons' quotients of -0.02(5), 0.03(4) and 0.06(6) (references: H. D. Flack, *Acta Cryst*. **1983**, *A39*, 876; S. Parsons, H. Flack, *Acta Cryst*. **2004**, *A39*, S61; S. Parsons, H. D. Flack, T. Wagner, *Acta Cryst*. **2013**, *B69*, 249). The Flack *x* values were determined using 1698 quotients [(I+)-(I-)]/[(I+)+(I-)]). The Flack (Parsons or Hooft) parameter value for the correct absolute structure determination should be 0, whereas the inverted structure would give 1 taking in account the standard deviation. The absolute configuration based on the absolute structure of the measured crystals was always determined as *R* (at C1) and in this way, the absolute configuration of the majority fraction is unambiguously confirmed. The structures are of excellent quality (no A- or B-alerts) with R_1 values of 0.026, 0.037 and 0.039. All three structures have been deposited at the CCDC with corresponding CCDC reference numbers: 2081269-2081271.

Crystallographic data for 2.2p (one selected example):

$C_{28}H_{35}O_3$, M_r = 419.56, orthorhombic, $P2_12_12_1$, a = 9.9184(5) Å, b = 11.0314(5) Å, c = 22.2295(10) Å, $\alpha = \beta = \gamma = 90^o$, V = 2432.2(2) Å^3, Z = 4, ρ = 1.146 mg·M^{-3}, μ = 0.568 mm^{-1}, λ = 0.71073 Å, T = 100(2) K, F(000) = 908, crystal size = 0.30 × 0.20 × 0.10 mm, 2θ(min) = 3.977°, 2θ(max) = 65.156°, 27575 reflections collected, 4195 reflections unique (R_{int} = 0.0331), GoF = 1.076, R_1 = 0.0453 and wR_2 = 0.1294 [$I > 2\sigma(I)$], R_1 = 0.0459 and wR_2 = 0.1308 (all indices), Flack (x) = -0.02(5), min/max residual density = −0.230/0.298 [e·Å^{-3}]. Completeness to 2θ(65.156°) = 100%. CCDC number 2081270.

(24) G. M. Sheldrick, *SHELXTL Crystallographic System*, version 6.10; Bruker AXS, Inc.: Madison, WI, **2000**.

Chapter 3.

Asymmetric Synthesis of Homoallylic Alcohols Featuring Vicinal Tetrasubstituted Carbon Centers via Dual Pd/Photoredox Catalysis

The results described in this chapter have been published in:

S. Xue, B. Limburg, D. Ghorai, J. Benet-Buchholz, A. W. Kleij, *Org. Lett.* **2021**, *23*, 4447-4451.

3.1. Introduction

3.1.1. Acyclic vicinal tetrasubstituted carbon centers

Chiral quaternary carbon centers are ubiquitous in natural products and pharmaceuticals,[1] but their synthesis still represents a big challenge. While significant progress has been made over the recent decades in the asymmetric construction of quaternary carbon stereocenters,[2] the enantioselective formation of acyclic vicinal tetrasubstituted carbon centers represents a more daunting challenge.[1a, 1b,3]Among the strategies that have proven to be both versatile and effective, asymmetric allylic alkylation (AAA) represents one of the most powerful methods for the construction of carbon-carbon bonds resulting in quaternary carbon stereocenters.[2a, 2b,4] Two main AAA approaches are known that exploit stereocontrol over either prochiral nucleophiles[5] or prochiral electrophiles (Scheme 3.1).[6] Although various efficient metal-assisted protocols have been established, to date the enantioselective preparation of organic target molecules comprising acyclic, vicinal tetrasubstituted carbon centers utilizing prochiral electrophiles remains underexplored (Scheme 3.2).[6a, 6d]

(1) a) M. Büschleb, S. Dorich, S. Hanessian, D. Tao, K. B. Schenthal, L. E. Overman, *Angew. Chem. Int. Ed.* **2016**, *55*, 4156-4186; b) R. Long, J. Huang, J. Gong, Z. Yang, *Nat. Prod. Rep.* **2015**, *32*, 1584-1601; c) Y. Liu, S.-J. Han, W.-B. Liu, B. M. Stoltz, *Acc. Chem. Res.* **2015**, *48*, 740-751.

(2) a) L. Süsse, B. M. Stoltz, *Chem. Rev.* **2021**; b) I. Marek, Y. Minko, M. Pasco, T. Mejuch, N. Gilboa, H. Chechik, J. P. Das, *J. Am. Chem. Soc.* **2014**, *136*, 2682-2694; c) J. Feng, M. Holmes, M. J. Krische, *Chem. Rev.* **2017**, *117*, 12564-12580.

(3) a) F. Zhou, L. Zhu, B.-W. Pan, Y. Shi, Y.-L. Liu, J. Zhou, *Chem. Sci.* **2020**, *11*, 9341-9365; b) D. Pierrot, I. Marek, *Angew. Chem. Int. Ed.* **2020**, *59*, 36-49.

(4) a) A. H. Cherney, N. T. Kadunce, S. E. Reisman, *Chem. Rev.* **2015**, *115*, 9587-9652; b) O. Pàmies, J. Margalef, S. Cañellas, J. James, E. Judge, P. J. Guiry, C. Moberg, J.-E. Bäckvall, A. Pfaltz, M. A. Pericàs, M. Diéguez, *Chem. Rev.* **2021**, *121*, 4373-4505; c) H.-M. Huang, P. Bellotti, F. Glorius, *Chem. Soc. Rev.* **2020**, *49*, 6186-6197.

(5) a) B. M. Trost, G. M. Schroeder, *J. Am. Chem. Soc.* **1999**, *121*, 6759-6760; b) B. M. Trost, S. Malhotra, W. H. Chan, *J. Am. Chem. Soc.* **2011**, *133*, 7328-7331; c) J. C. Hethcox, S. E. Shockley, B. M. Stoltz, *ACS Catal.* **2016**, *6*, 6207-6213.

(6) a) X.-L. Hou, N. Sun, *Org. Lett.* **2004**, *6*, 4399-4401; b) P. Zhang, H. Le, R. E. Kyne, J. P. Morken, *J. Am. Chem. Soc.* **2011**, *133*, 9716-9719; c) S. E. Shockley, J. C. Hethcox, B. M. Stoltz, *Angew. Chem. Int. Ed.* **2017**, *56*, 11545-11548; d) J. C. Hethcox, S. E. Shockley, B. M. Stoltz, *Angew. Chem. Int. Ed.* **2018**, *57*, 8664-8667.

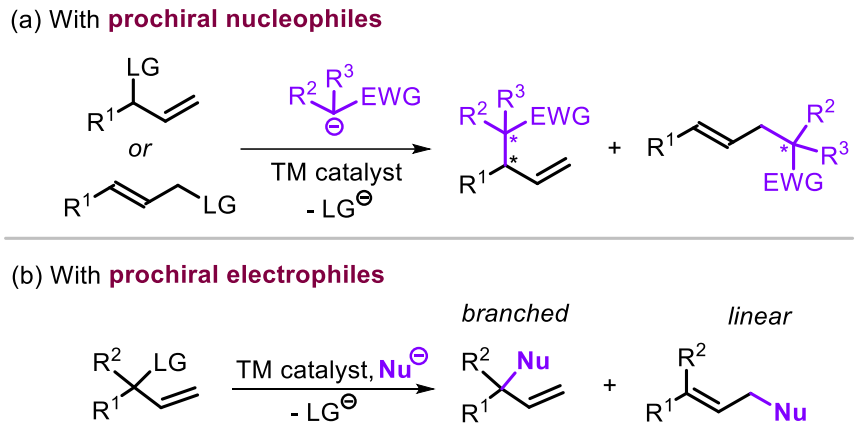

Scheme 3.1. General strategies for the construction of quaternary carbon stereocenters by asymmetric allylic alkylation (AAA). TM = transition metal, LG = leaving group

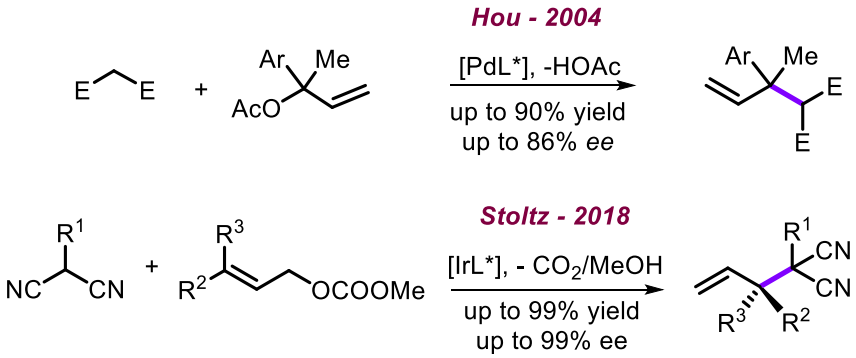

Scheme 3.2. Preparation of compounds with vicinal/acyclic quaternary carbon centers using prochiral electrophiles

3.1.2. The application of VCCs in asymmetric allylic alkylation

Pd-catalyzed asymmetric allylic substitution reactions of vinyl epoxides[7] and vinyl cyclic carbonates (VCCs)[8] serving as prochiral electrophilic allylic surrogates have been recently reported as efficient approaches to forge compounds featuring a tetrasubstituted carbon stereocenter. While only a handful of studies report the efficient use of olefin-

(7) a) B. M. Trost, E. J. McEachern, F. D. Toste, *J. Am. Chem. Soc.* **1998**, *120*, 12702-12703; b) B. M. Trost, R. C. Bunt, R. C. Lemoine, T. L. Calkins, *J. Am. Chem. Soc.* **2000**, *122*, 5968-5976; c) B. M. Trost, C. Jiang, *J. Am. Chem. Soc.* **2001**, *123*, 12907-12908; d) Q. Cheng, H.-J. Zhang, W.-J. Yue, S.-L. You, *Chem* **2017**, *3*, 428-436; e) J. Feng, V. J. Garza, M. J. Krische, *J. Am. Chem. Soc.* **2014**, *136*, 8911-8914.

(8) a) A. Khan, H. Zhao, M. Zhang, S. Khan, D. Zhao, *Angew. Chem. Int. Ed.* **2020**, *59*, 1340-1345; b) A. Khan, S. Khan, I. Khan, C. Zhao, Y. Mao, Y. Chen, Y. J. Zhang, *J. Am. Chem. Soc.* **2017**, *139*, 10733-10741.

substituted VCCs in allylic alkylation (Scheme 1b, R^2–$R^4 \neq H$)[9] and more particularly towards branched allylic products,[9d, 9e] as far as we are aware only two reports exist that briefly discuss the use of more elaborate carbonate ring substituted congeners (Scheme 1b, R^5 and $R^6 \neq H$).[9c] The successful conversion of these latter types of congested substrates in transformations leading to compounds having vicinal tetrasubstituted carbon centers would greatly expand the application potential of VCCs, and advance the synthesis of otherwise elusive carbon stereocenters.

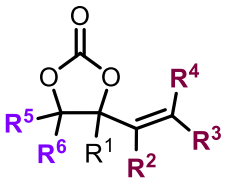

with **R2**, **R3** and/or **R4**: *limited*

with **R5** and/or **R6**: *rare*

Scheme 3.3. Progress with VCCs in (asymmetric) allylic alkylation chemistry

3.1.3. Aims and objectives

Photoredox catalysis has recently emerged as a versatile reactivity platform to provide access to radical species under mild conditions.[10] The merger of photoredox and transition metal catalysis allows the direct coupling of non-traditional nucleophilic partners.[11] In order to expedite the potential of the challenging functional substrates illustrated in Scheme 3.3 in allylic alkylation processes, we envisioned that the use of dual transition metal/photoredox catalysis[12] could offer an alternative yet powerful

(9) a) Y. Wang, J. Chai, C. You, J. Zhang, X. Mi, L. Zhang, S. Luo, *J. Am. Chem. Soc.* **2020**, *142*, 3184-3195; b) X. Wei, D. Liu, Q. An, W. Zhang, *Org. Lett.* **2015**, *17*, 5768-5771; c) L. Chen, H. Quan, Z. Xu, H. Wang, Y. Xia, L. Lou, W. Yang, *Nat. Commun.* **2020**, *11*, 2151; d) H. Wang, S. Qiu, S. Wang, H. Zhai, *ACS Catal.* **2018**, *8*, 11960-11965; e) W. Guo, R. Kuniyil, J. E. Gómez, F. Maseras, A. W. Kleij, *J. Am. Chem. Soc.* **2018**, *140*, 3981-3987.

(10) a) C. K. Prier, D. A. Rankic, D. W. C. MacMillan, *Chem. Rev.* **2013**, *113*, 5322-5363; b) J. M. R. Narayanam, C. R. J. Stephenson, *Chem. Soc. Rev.* **2011**, *40*, 102-113; c) T. P. Yoon, M. A. Ischay, J. Du, *Nat. Chem.* **2010**, *2*, 527-532.

(11) a) M. N. Hopkinson, B. Sahoo, J. L. Li, F. Glorius, *Chem. Eur. J.* **2014**, *20*, 3874-3886; b) M. H. Shaw, J. Twilton, D. W. C. MacMillan, *J. Org. Chem.* **2016**, *81*, 6898-6926; c) J. Twilton, C. Le, P. Zhang, M. H. Shaw, R. W. Evans, D. W. C. MacMillan, *Nat. Rev. Chem.* **2017**, *1*, 0052-0052; d) K. L. Skubi, T. R. Blum, T. P. Yoon, *Chem. Rev.* **2016**, *116*, 10035-10074; e) H. H. Zhang, H. Chen, C. Zhu, S. Yu, *Sci. China Chem.* **2020**, *63*, 637-647; f) W. Liang, Y. Yang, M. Yang, M. Zhang, C. Li, Y. Ran, J. Lan, Z. Bin, J. You, *Angew. Chem. Int. Ed.* **2021**, 3493-3497.

(12) a) S. B. Lang, K. M. O'Nele, J. A. Tunge, *J. Am. Chem. Soc.* **2014**, *136*, 13606-13609; b) S. B. Lang, K. M. O'Nele, J. T. Douglas, J. A. Tunge, *Chem. Eur. J.* **2015**, *21*, 18589-18593; c) J. Xuan, T.-T. Zeng, Z.-J. Feng, Q.-H. Deng, J.-R. Chen, L.-Q. Lu, W.-J. Xiao, H. Alper, *Angew. Chem. Int. Ed.* **2015**, *54*, 1625-1628; d) J. K. Matsui, Á. Gutiérrez-Bonet, M. Rotella, R. Alam, O. Gutierrez, G. A. Molander, *Angew. Chem. Int. Ed.* **2018**, *57*, 15847-15851; e) H. Ye, Q. Ye, D. Cheng, X. Li, X. Xu, *Tetrahedron Lett.* **2018**, *59*, 2046-2049; f) H.-H. Zhang, J.-J. Zhao, S. Yu, *ACS Catal.* **2020**, 4710-4716; g) H.-H. Zhang, J.-J. Zhao, S. Yu, *J. Am. Chem. Soc.* **2018**, *140*, 16914-16919.

approach that could circumvent the limitations encountered in classical catalytic allylic substitution reactions.

In this chapter, we report the combination of photoredox and Pd-catalyzed AAA of vinyl cyclic carbonates using Hantzsch type esters as radical precursors[13] affording homoallylic alcohol products with either α,β-tri/tetra- or α,β-tetra-substituted carbon centers (Scheme 3.4). The developed protocol combines mild reaction conditions, avoids the use of stoichiometric organometallic reagents and produces a series of products with acyclic vicinal tetrasubstituted carbon centers in good yields and under high regio- and enantiocontrol.

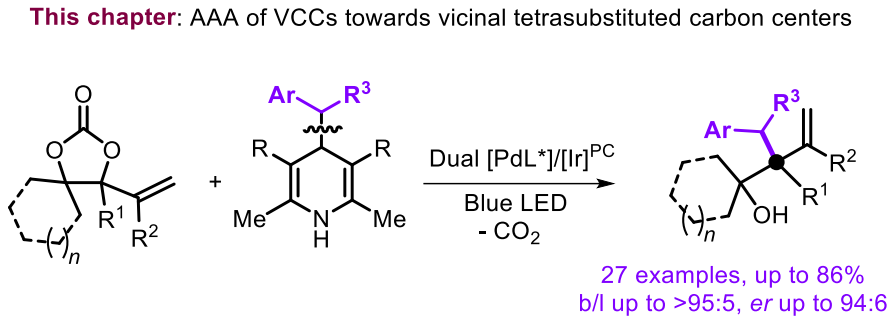

Scheme 3.4. Current approach towards elusive stereocenters using AAA strategies

(13) a) S. Crespi, M. Fagnoni, *Chem. Rev.* **2020**, *120*, 9790-9833; b) J. K. Matsui, S. B. Lang, D. R. Heitz, G. A. Molander, *ACS Catal.* **2017**, *7*, 2563-2575.

3.2. Results and discussion

3.2.1. Optimization studies

We started our investigation by using VCC **3.1a** and substituted Hantzsch ester **3.2a** and examining the envisioned coupling while screening a variety of chiral ligands, photocatalysts (PCs), solvents and base additives (Tables 3.1-3.5). Initial investigation of a number of photocatalysts revealed the feasibility of the allylic alkylation process (Table 3.1). The PC $[Ir(ppy)_2(dtbbpy)]PF_6$ provided a 25% yield of the coupling product **3.3aa** with a 59:41 branch/linear (b/l) ratio (entry 2), while more reducing or oxidizing Ir-based PCs exhibited lower reactivity (entries 1 and 3). Ru-based PCs furnished the allylic allylation product **3.3aa** in lower yield (entries 4-6).

Table 3.1. Screening of the PC for the Pd catalyzed asymmetric allylic alkylation towards product **3.3aa**[a]

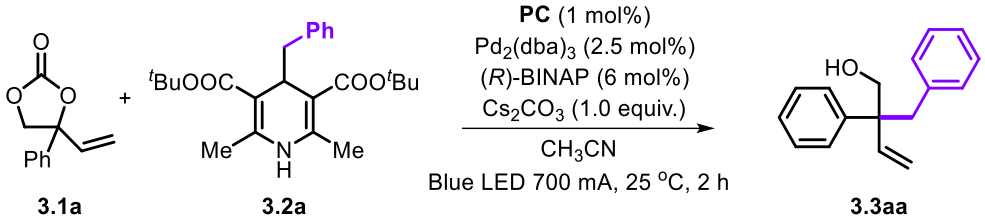

3.1a **3.2a** **3.3aa**

Entry	PC	Yield of **3.3aa**	*er*	b/l
1	$Ir(ppy)_3$	16%	0	55:46
2	**$[Ir(ppy)_2(dtbbpy)]PF_6$**	**25%**	**0**	**59:41**
3	$[Ir(dF(CH_3)ppy)_2(dtbbpy)]PF_6$	16%	0	56:44
4	$Ru(bpy)_3Cl_2 \cdot 6H_2O$	18%	-	59:41
5	$[Ru(dmbpy)_3](PF_6)_2$	12%	-	41:59
6	$[Ru(p\text{-}CF_3\text{-}bpy)_3](BF_4)_2$	0	-	-

[a] **3.1a** (0.10 mmol), **3.2a** (0.15 mmol), PC (1.0 mol%), $Pd_2(dba)_3$ (2.5 mol%), **L1**: (*R*)-BINAP (6.0 mol%), Cs_2CO_3 (0.10 mmol) were combined in CH_3CN (2.0 mL) at 25 °C under blue LED radiation (445 nm, 700 mA, 1.2 μeinstein/s) for 2 h. Yields and b/l ratios were determined by ^1H NMR analysis using CH_2Br_2 as an internal standard. Enantiomeric ratios were determined by UPC2.

A wide variety of chiral diphosphine ligands (Figure 3.1 and Table 3.2) were scrutinized. The use of **L1** (*S*)-BINAP as a chiral ligand (entry 1) did not lead to any asymmetric induction and **3.3aa** was produced in a low yield (25%). The utilization of

SegPhos type diphosphines proved to be more productive (entries 2-4), and variation of the P-aryl groups gave **3.3aa** in 60% yield with excellent regio- (b:l >95:5) and appreciable enantio-selectivity (*er* = 86:14). Structurally related BIPHEP and GarPhos ligands (entries 5-8) also provided good results, with the use of **L5** being most efficient (entry 5: 71%, b:l >95:5, *er* = 89:11). The use of other diphosphine ligands (**L9**-**L15**) did not further improve the process outcome (entries 9-15).

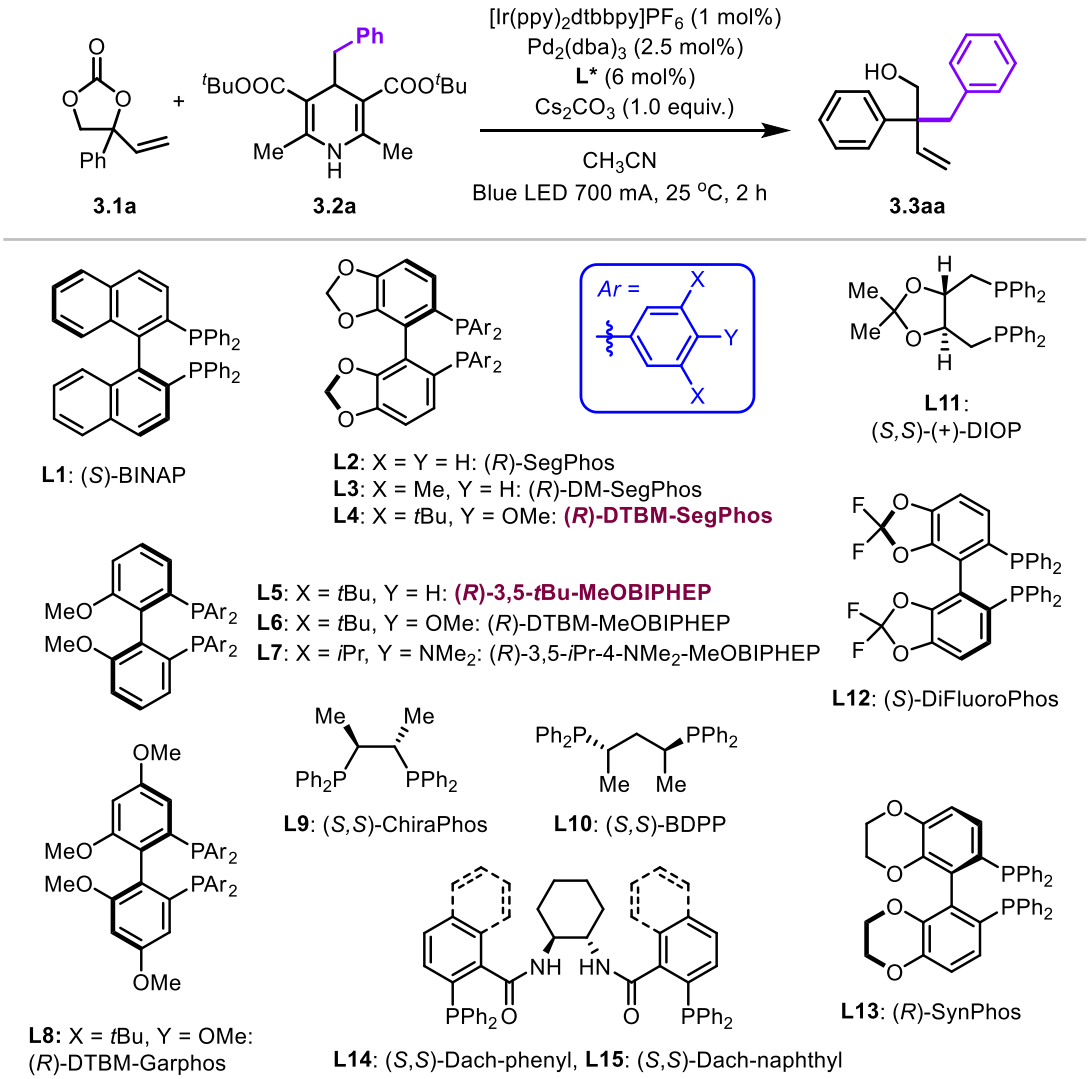

Figure 3.1. Overview of the diphosphine ligands used in the screening stage related to Table 2

Omitting the iridium PC (entry 16) still provided **3.3aa** in 25% yield suggesting that Hantzsch ester **3.2a** could itself serve as a photo-reductant to form a radical cation that subsequently generates, through homolytic cleavage, the requisite alkyl radical for the

C–C coupling.[14] As expected, no product was detected without blue LED irradiation (entry 17).

Table 3.2. Screening of diphosphine ligands **L1**-**L15** for the Pd catalyzed asymmetric allylic alkylation towards product **3.3aa**[a]

Entry	**L***	Yield	*er*	b/l
1	**L1**	25%	0	65:35
2	**L2**	26%	64:36	64:36
3	**L3**	31%	63:37	70:30
4	**L4**	**60%**	**86:14**	**>95:5**
5	**L5**	**71%**	**89:11**	**>95:5**
6	**L6**	66%	84:16	>95:5
7	**L7**	65%	86:14	>95:5
8	**L8**	60%	85:15	93:7
9	**L9**	12%	–	22:78
10	**L10**	16%	50.5:40.5	31:69
11	**L11**	12%	–	28:72
12	**L12**	28%	40:60	73:26
13	**L13**	30%	63:37	61:39
14	**L14**	11%	–	27:73
15	**L15**	12%	–	22:78
16[b]	**L4**	25%	87.5:12.5	61:39
17[c]	**L4**	0	–	–

[a] **3.1a** (0.10 mmol), **3.2a** (0.15 mmol), $Ir(ppy)_2(dtbbpy)PF_6$ (1.0 mol%), $Pd_2(dba)_3$ (2.5 mol%), **L*** (6.0 mol%), Cs_2CO_3 (0.10 mmol) were combined in CH_3CN (2.0 mL) at 25 °C under blue LED radiation (445 nm, 700 mA, 1.2 µeinstein/s) for 2 h. Yields and b/l ratios were determined by ^1H NMR analysis using CH_2Br_2 as an internal standard. Enantiomeric ratios were determined by UPC2. [b] In the absence of $Ir(ppy)_2(dtbbpy)PF_6$. [c] In the dark.

(14) L. Buzzetti, A. Prieto, S. R. Roy, P. Melchiorre, *Angew. Chem. Int. Ed.* **2017**, *56*, 15039-15043.

Further variations of the protocol (Tables 3.3-3.5) were first carried out with (*R*)-DTBM-SegPhos being cheaper than (*R*)-3,5-*t*Bu-MeOBIPHEP, but providing nearly the same regio- and enantiocontrol (cf., entries 4 versus 5). In the absence of base, **3.3aa** was obtained in a slightly higher yield and *er* (Table 3.3, entry 1 versus 3). Decreasing the reaction temperature to 0 ºC failed to increase the *er* value (entry 1 versus 2 and entry 4 versus 5).

Table 3.3. Screening of the influence of the base and temperature on the Pd catalyzed asymmetric allylic alkylation towards the product **3.3aa**[a]

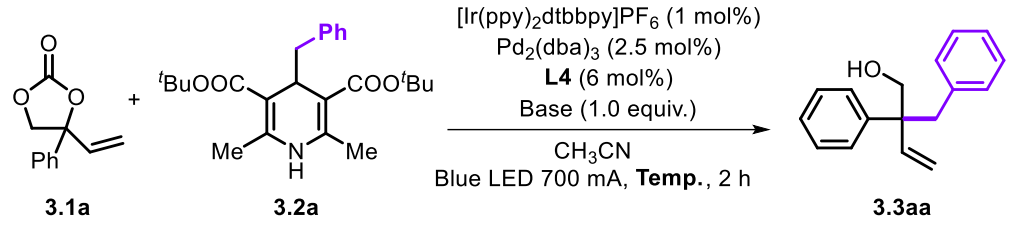

Entry	Base	T	Yield	*er*	b/l
1	**-**	**25 ºC**	**65%**	**87.5:12.5**	**>95:5**
2	-	0 ºC	61%	86.5:13.5	>95:5
3	Cs_2CO_3	25 ºC	60%	86:14	>95:5
4	K_2CO_3	25 ºC	61%	88:12	>95:5
5	K_2CO_3	0 ºC	63%	84:16	>95:5

[a] **3.1a** (0.10 mmol), **3.2a** (0.15 mmol), $Ir(ppy)_2(dtbbpy)PF_6$ (1.0 mol%), $Pd_2(dba)_3$ (2.5 mol%), **L4** (6.0 mol%), base (0.10 mmol or without) were combined in CH_3CN (2.0 mL) at 0 °C or 25 °C under blue LED radiation (445 nm, 700 mA, 1.2 µeinstein/s) for 2 h. Yields and b/l ratios were determined by ^1H NMR analysis using CH_2Br_2 as an internal standard. Enantiomeric ratios were determined by UPC2.

A wide variety of solvents were also investigated. Performing the reaction in polar solvents, such as DMF and acetone, provides give the product **3.3aa** in moderate yield and with slightly lower *er* and b/l ratio, while the use of DCM as medium failed to deliver the desired product (entries 2-4). The reaction carried out in THF as solvent resulted in product **3.3aa** with similar enantioselectivity but with lower yield (entry 7). Poor yields and enantioselectivity were observed when MeOH and Et_2O were used as solvent.

Table 3.4. Evaluation of the influence of the solvent on the Pd catalyzed asymmetric allylic alkylation towards product **3.3aa**[a]

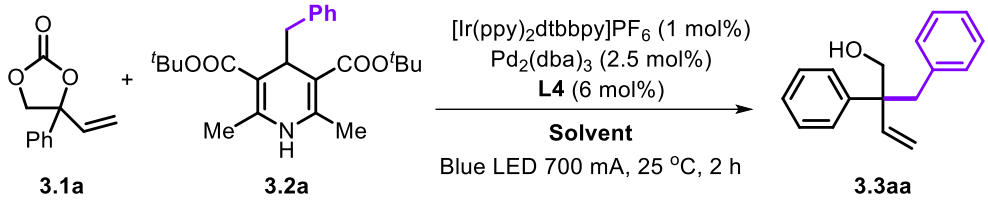

3.1a **3.2a** **3.3aa**

Entry	Solvent	Yield	*er*	b/l
1	**CH_3CN**	**65%**	**87.5:12.5**	**>95:5**
2	DMF	55%	84:16	92:8
3	Acetone	55%	86.5:13.5	92:8
4	DCM	Trace	-	-
5	MeOH	23%	58:42	65:35
6	Et_2O	17%	81.5:18.5	74:26
7	THF	43%	87:13	>95:5

[a] **3.1a** (0.10 mmol), **3.2a** (0.15 mmol), $Ir(ppy)_2(dtbbpy)PF_6$ (1.0 mol%), $Pd_2(dba)_3$ (2.5 mol%), **L4** (6.0 mol%), were combined in solvent (2.0 mL) at 25 °C under blue LED radiation (445 nm, 700 mA, 1.2 μeinstein/s) for 2 h. Yields and b/l ratios were determined by ^1H NMR analysis using CH_2Br_2 as an internal standard. Enantiomeric ratios were determined by UPC2.

By further increasing the light intensity, the yield of **3.3aa** increased to 71% (Table 3.5, entry 3). With these alternative conditions in hand, we then re-used (*R*)-3,5-*t*Bu-MeOBIPHEP **L5** as ligand, which afforded the product in 75% yield and with an *er* of 89:11 (entry 4).

Table 3.5. Evaluation of the influence of the light intensity on the Pd catalyzed asymmetric allylic alkylation towards the product **3.3aa**[a]

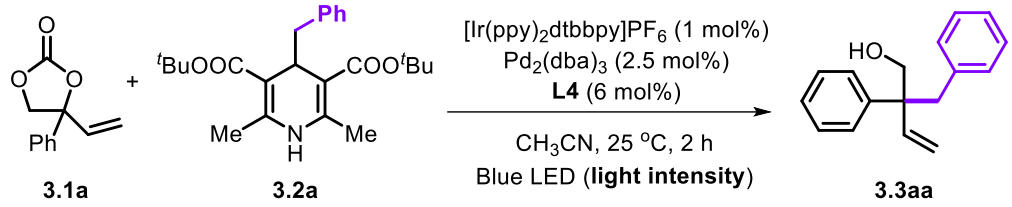

3.1a **3.2a** **3.3aa**

Entry	Current (mA)	Yield	*er*	b/l
1	300	58%	86.5:13.5	>95:5
2	700	65%	87.5:12.5	>95:5
3	**1000**	**71%**	**88:12**	**>95:5**
4[b]	**1000**	**75%**	**89:11**	**>95:5**

[a] **3.1a** (0.10 mmol), **3.2a** (0.15 mmol), $Ir(ppy)_2(dtbbpy)PF_6$ (1.0 mol%), $Pd_2(dba)_3$ (2.5 mol%), **L4** (6.0 mol%), were combined in CH_3CN (2.0 mL) at 25 °C under blue LED radiation (different light intensity) for 2 h. Yields and b/l ratios were determined by ^1H NMR analysis using CH_2Br_2 as an internal standard. Enantiomeric ratios were determined by UPC2. [b] **L5** was used.

3.2.2. Scope of products

With these optimized conditions, we then examined the generality of similar substrate combinations providing homoallylic alcohols with quaternary carbon stereocenters (Scheme 3.5, **3.3aa**-**3.3ja**).[15] Variation of the aryl substituents on the VCC in the presence of Hantzsch ester **3.2a** generally provided the homoallylic alcohols with remarkable branch selectivity (b:l >95:5)[16] and in appreciable isolated yields of up to 78% (**3.3ga**).[17] Good enantio-induction levels of up to 89:11 *er* for the majority of the products were achieved except for **3.3fa**, **3.3ha** and **3.3ja**. Whereas for **3.3ha** the presence of the thiophen-2-yl group could interfere through coordination to Pd(allyl) intermediates, the

(15) Vinyl carbonates with R^3/R^4 substituents or having aliphatic R^1 (Scheme 3.3) groups such as Me gave between a trace amount and 22% NMR yield and were not further considered in the product scope phase.

(16) a) X. Wang, F. Meng, Y. Wang, Z. Han, Y.-J. Chen, L. Liu, Z. Wang, K. Ding, *Angew. Chem. Int. Ed.* **2012**, *51*, 9276-9282; b) X. Wang, P. Guo, Z. Han, X. Wang, Z. Wang, K. Ding, *J. Am. Chem. Soc.* **2014**, *136*, 405-411; c) X. Wang, X. Wang, Z. Han, Z. Wang, K. Ding, *Angew. Chem. Int. Ed.* **2017**, *56*, 1116-1119; d) A. Cai, A. W. Kleij, *Angew. Chem. Int. Ed.* **2019**, *58*, 14944-14949; e) L. Hu, A. Cai, Z. Wu, A. W. Kleij, G. Huang, *Angew. Chem. Int. Ed.* **2019**, *58*, 14694-14702; f) A. Cai, W. Guo, L. Martínez-Rodríguez, A. W. Kleij, *J. Am. Chem. Soc.* **2016**, *138*, 14194-14197; g) H. Li, I. Khan, M. Li, Z. Wang, X. Wu, K. Ding, Y. J. Zhang, *Org. Lett.* **2021**, *23*, 3567-3572.

(17) In some cases, the yield of product was compromised due to formation of the undesired linear product and unidentified, minor products.

use of a VCC with an additional substituent (R^1 = Ph, **3.1j**) on the vinyl group likely increased the steric demand for substrate activation, and as a consequence was detrimental to both the product yield (33%) and optical purity (62.5:37.5 *er*).

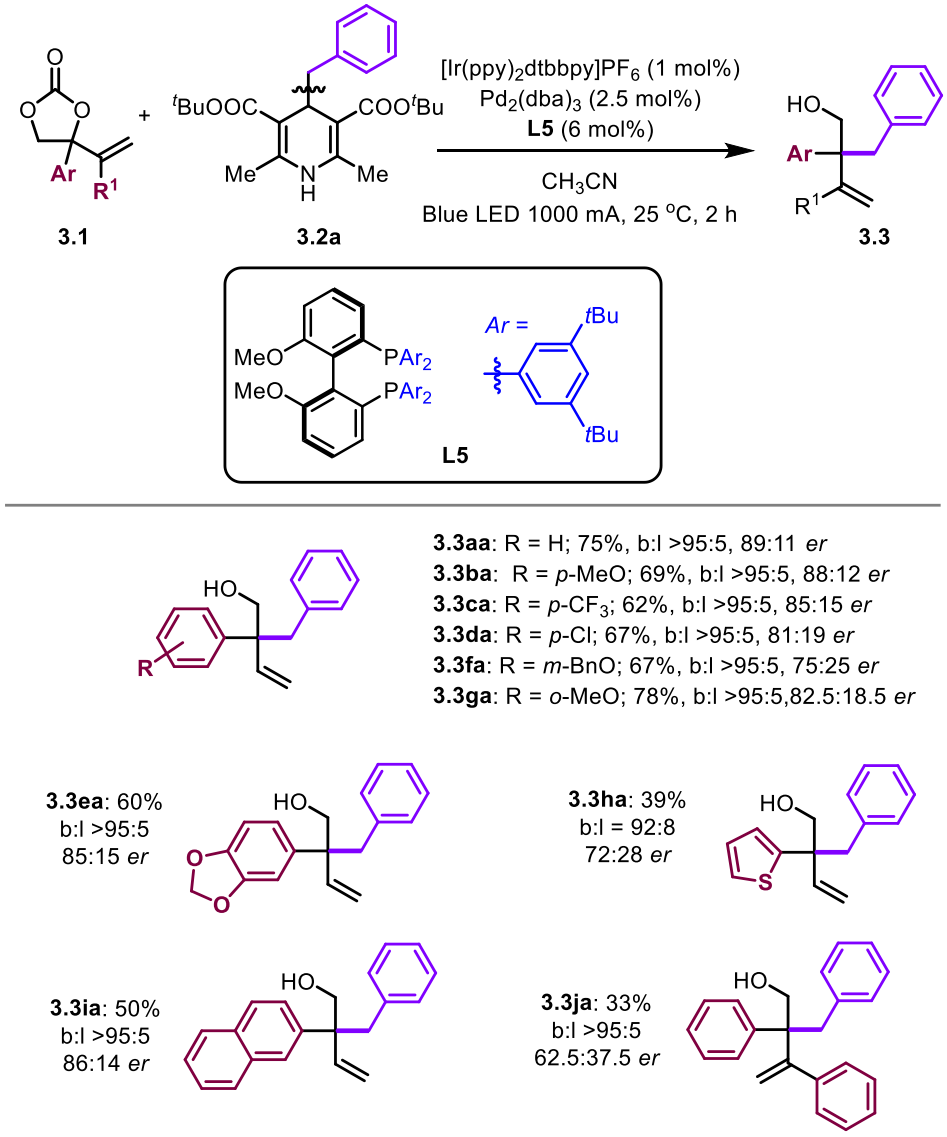

Scheme 3.5. Product scope using various VCCs to generate quaternary carbon stereocenters. Reaction conditions: **3.1** (0.10 mmol), **3.2a** (0.15 mmol), $Ir(ppy)_2(dtbbpy)PF_6$ (1.0 mol%), $Pd_2(dba)_3$ (2.5 mol%), (*R*)-3,5-*t*Bu-MeOBIPHEP **L5** (6.0 mol%), CH_3CN (2 mL), at 25 °C under blue LED radiation (445 nm, 1000 mA, corresponding to a photon flux of 1.6 μeinstein/s) for 2 h. Yields of the isolated, column-purified products are reported. The enantiomeric ratios (*er* values) were determined by UPC2. The b/l ratios were determined by ^{1}H NMR analysis.

In a second, more dedicated embodiment of the substrate scope we primarily selected VCCs with further substitution on the carbonate ring (Scheme 3.6). VCC **3.1k** (incorporating a spiro-fused cyclohexyl group) was first chosen and combined with several Hantzsch esters furnishing **3.3ka**-**3.3kg**. In these sterically frustrated transformations, the b:l ratios remained in most cases practical allowing to isolate the pure, branched homoallylic alcohols in moderate to good yields (48-72%). Furthermore, the conversion of **3.1k** proceeded smoothly with a quantum yield 6.8% leading to complete conversion within 20 min (see Experimental section).[18]

Despite the more complex nature of these couplings compared to the ones presented in Scheme 3.5, slightly higher enantiomeric ratios of up to 92.5:7.5 were noted. Increasing the size of the spiro-cycloalkyl group in the VCC (**3.3la**, **3.3lb** and **3.3ld**) was feasible and the protocol was effective towards the formation of chiral homoallylic alcohol products in reasonable yields and with *er* values of up to 94:6. Next, an acyclic substitution on the tetrasubstituted VCC substrates was examined (*i.e.*, **3.1m**) delivering the target products **3.3ma** and **3.3mb** with slightly higher b:l ratios and isolated yields (for **3.3ma**, 74%, and **3.3mb**, 86%).

(18) The oxidation of **2a** to its corresponding pyridine proceeds with a quantum yield of 7.5%, indicating that the coupling reaction proceeds immediately once the alkyl radicals are released using >90% of the radicals productively.

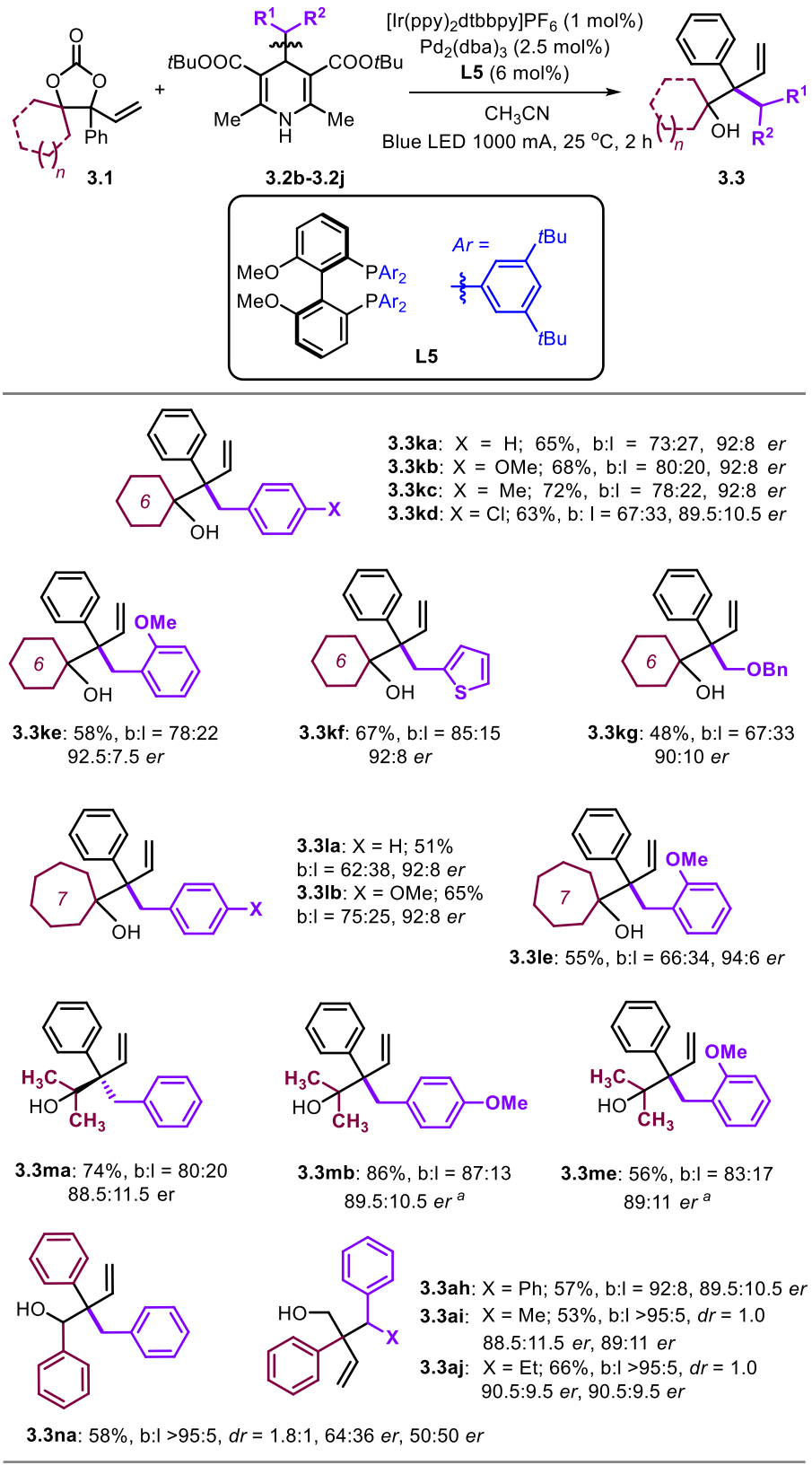

Scheme 3.6. Product scope using various VCCs to generate chiral homoallylic alcohols having vicinal tetrasubstituted carbon centers. Reaction conditions and analyses are the same as in Scheme 3.5. [a] Reaction time was 4 h. [b] The corresponding Hantzsch nitrile was used.

We also studied the use of a trisubstituted VCC (**3.1n**). Despite the excellent regioselectivity, the enantiocontrol was significantly lower while producing the product **3.3na** with low diastereocontrol.[19] Finally, we used Hantzsch esters that would produce secondary radicals under the experimental conditions, leading to products with vicinal quaternary-tertiary carbons through a different route. In all these cases (**3.3ah**, **3.3ai** and **3.3aj**), the products were formed with high regiocontrol and *er* values adding further diversity to the developed methodology. The absolute configuration of the major enantiomer of compound **3.3ma** was determined to be (*R*) by X-ray diffraction (See experimental section).[20]

The synthesis of homoallylic alcohol **3.3ka** could be conveniently scaled up (10-fold) as shown in Scheme 3.7a. We then used **3.3aa** and **3.3ka** for product diversification studies (Scheme 3.7b). Hydroboration/oxidation of **3.3aa** provided access to 1,4-diol **3.4** in 72%; X-ray analysis revealed that the absolute configuration of the major enantiomer was (*S*).[21] A metathesis/cyclization of **3.3aa** in the presence of acryloyl chloride gave unsaturated lactone **3.5** (79%). Under similar reaction conditions as for **3.4**, the hydroboration/oxidation of **3.3ka** gave a Markovnikov type product (1,3-diol **3.6**, 94%)[22] as an approximate 2:1 mixture of diastereoisomers. Dehydration of **3.3ka** using thionyl chloride produced 1,4-diene **3.7** in 88% yield.

(19) Low diastereocontrol is a general phenomenon in the creation of vicinal quaternary/tetrasubstituted carbon stereocenters; see, for instance, ref. **3b**.
(20) This configuration was determined for several crystals that were independently analyzed by X-ray diffraction; see the experimental section for details.
(21) This configuration was determined for several crystals that were independently analyzed by X-ray diffraction; see the experimental section for details.
(22) The discrepancy between the hydroboration/oxidation of **3.3aa** and **3.3ka** is suggested to arise from a directing-group effect of the conformationally more restricted tertiary OH in **3.3ka**.

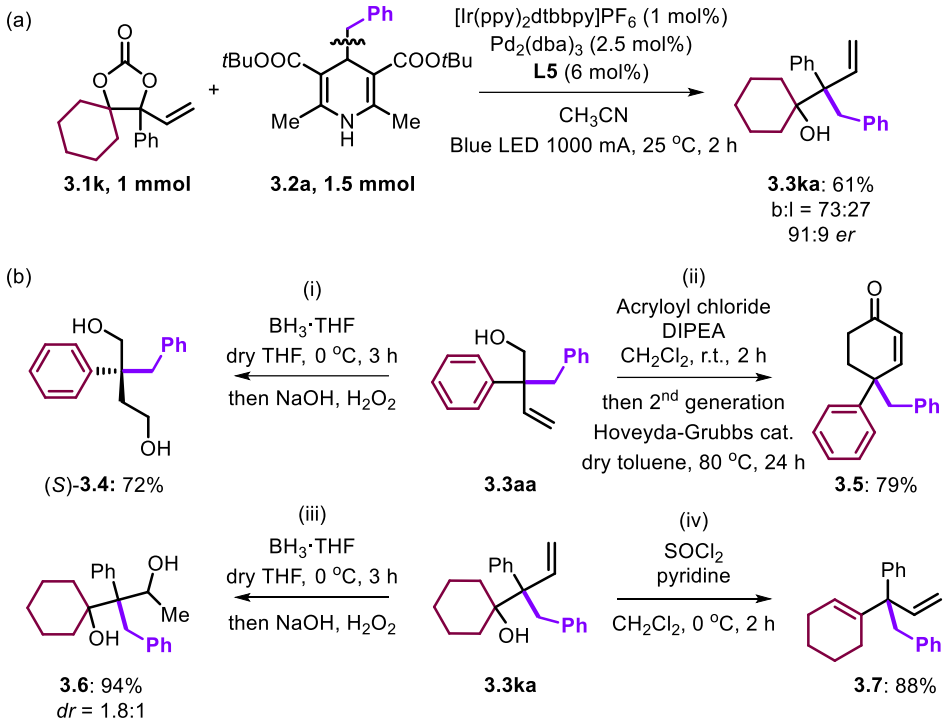

Scheme 3.7. (a) Scale-up and (b) product diversification. Reaction conditions: (i) BH_3·THF, dry THF, 0 ºC, 3 h; then NaOH, H_2O_2. (ii) acryloyl chloride, DIPEA, CH_2Cl_2, r.t., 2 h; then H_2O + work up; then 2nd generation Hoveyda-Grubbs cat. (10 mol%), dry toluene, 80 ºC, 24 h. (iii) same as under (i). (iv) $SOCl_2$ (2 equiv.), pyridine (5 equiv.), CH_2Cl_2, 0 ºC, 2 h; then H_2O at 0 ºC. See the Experimental section for further details.

3.3. Conclusions

In this chapter, we describe a Pd-mediated dual catalysis approach that allows for transformation of previously unreactive VCCs into chiral homoallylic alcohols featuring vicinal, highly congested carbon atoms. The developed protocol combines an atypical preference for the formation of branched regioisomers in a sterically challenging allylic substitution event, and produces the products with enantiomeric ratios of up to 94:6. The present results mark a significant step forward in the use of modular VCCs in challenging enantioselective syntheses.

3.4. Experimental section

3.4.1. General information

Commercially available reagents were used as received without further purification. $Pd_2(dba)_3$ was purchased from Aldrich, ligands were purchased from Aldrich and Strem, anhydrous solvents were taken from a commercial SPS solvent dispenser. ^{1}H NMR, ^{13}C NMR and ^{19}F NMR spectra were recorded on a Bruker AV-300 MHz, a Bruker AV-400 MHz or a Bruker AV-500 MHz at 20°C and referenced to the residual deuterated solvent signals. All reported NMR data are given in parts per million (ppm). FT-IR measurements were carried out using a Bruker Optics FTIR Alpha spectrometer. Optical rotations were measured with a Jasco P-1030 Polarimeter. HRMS were recorded by the Research Support Area (RSA) at ICIQ on a MicroTOF II (Bruker Daltonics) using an electrospray ionization (ESI) source or MaXis impact (Bruker Daltonics) using an atmospheric pressure chemical ionization (APCI) source. X-ray diffraction analysis were performed by the Research Support Area (RSA) at ICIQ on a Bruker Kappa Apex II DUO diffractometer equipped with a Cryostream 700 plus low temperature device, a microsource anode with Mo *Kα* (λ = 0.71073 Å). UPC2 analyses were performed by the Research Support Area (RSA) at ICIQ. UV-Vis spectra were measured on a Shimadzu UV1700PC spectrophotometer with a photomultiplier detector and D2 and W light sources. Fluorescence measurements were performed on a Fluorolog Horiba Jobin Yvon spectrofluorimeter equipped with photomultiplier detector, double monochromator and Xenon light source.

Photochemistry set-up: all photochemical reactions were performed in a parallel photoreactor with 8 spots using flat-bottom J-young Schlenk flasks (see Figure S1). The flasks were placed inside a thermostated (Huber Rotacool) aluminum block, and irradiated from the bottom using OSRAM Oslon SSL 80 royal-blue LEDs mounted on a star (λ = 445 nm). The LEDs were powered in series using a current limited power supply (RS Pro RS-3005D) and cooled passively by a heatsink.

Figure 3.1: Photoreactor setup and power supply to control the light intensity

3.4.2. General procedure for the preparation of vinyl cyclic carbonates

Please refer to section 2.4.2 for more details.

3.4.3. General procedure for the preparation of substituted DHP esters

4-alkyl-1,4-dihydropyridines (**3.2**) were prepared according to literature procedures.[23] Compounds **3.2a**–**3.2c**, **3.2d**–**3.2i** are known, **3.2e** and **3.2j** are new compounds and were prepared following **General procedure I**. Compound **3.2h** is a known compound and was prepared following **General procedure II**.

General procedure I: To a flask charged with *t*-butyl acetoacetate (20 mmol, 3.3 mL), the aldehyde (10 mmol) and ethanol (20 mL) was added an aqueous ammonia solution (60 mmol, 28%, 4.0 mL). The mixture was heated at 100 ºC with an oil bath for 12 h. The reaction mixture was allowed to cool to room temperature. The solution was concentrated under reduced pressure. A mixture of water and CH_2Cl_2 were added to the concentrated residue and the layers were separated. The aqueous layer was extracted 3 times with CH_2Cl_2. The combined organic layers were washed with brine, dried, and filtered. The filtrate was concentrated under reduced pressure. The residue was purified by

(23) a) W. Chen, Z. Liu, J. Tian, J. Li, J. Ma, X. Cheng, G. Li, *J. Am. Chem. Soc.* **2016**, *138*, 12312-12315; b) F. F. de Assis, X. Huang, M. Akiyama, R. A. Pilli, E. Meggers, *J. Org. Chem.* **2018**, *83*, 10922-10932; c) F. Gu, W. Huang, X. Liu, W. Chen, X. Cheng, *Adv. Synth. Catal.* **2018**, *360*, 925-931.

chromatography using silica gel as stationary phase. The obtained solid product was further washed with PE/EA (95:5, v/v) where required.

General procedure II: A reaction flask was charged with 3-aminocrotononitrile (1.6 g, 20 mmol, 2.0 equiv.), the aldehyde (10 mmol, 1.0 equiv.) and acetic acid (10 mL). The reaction mixture was heated at 110 ºC with an oil bath while stirring for 3 h. The crude reaction mixture was allowed to cool to room temperature, diluted with water and extracted 3 times with EtOAc. The combined organic layers were neutralized with a saturated solution of $NaHCO_3$ until complete removal of the acetic acid was achieved, washed with brine, dried over Na_2SO_4, and filtered. The filtrate was concentrated under reduced pressure. The residue was purified by chromatography using silica gel as stationary phase. The obtained solid product was washed with PE/EA (95:5, v/v) where required.

3.4.4. Typical procedure for photoredox and Pd catalyzed asymmetric allylic alkylation reactions featuring tertiary and quaternary carbon centers

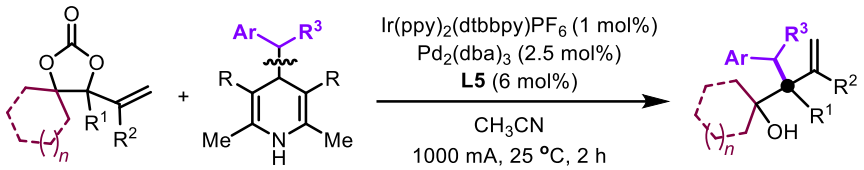

3.1 **3.2** **3.3**

To a sealed tube charged with **3.1** (0.1 mmol, 1.0 equiv.), **3.2** (0.15 mmol, 1.5 equiv.), $Ir(ppy)_2(dtbbpy)PF_6$ (1 mol%, 0.9 mg), $Pd_2(dba)_3$ (2.5 mol%, 2.3 mg), (*R*)-3,5-*t*Bu-MeOBIPHEP (6 mol%, 6.2 mg), CH_3CN (2 mL) was added. The tube was degassed three times and filled with argon. The mixture was then stirred at 25 ℃ for 2 h under blue LED irradiation (1000 mA) as controlled by an external power supply. The organic phase was concentrated and purified by flash chromatography on silica gel (hexane/acetic acid 250/1 to 250/2 or hexane/ethyl acetate 40/1 to 10/1, v/v).

3.4.5. General procedure for the preparation of racemic samples

To a sealed tube charged with **3.1** (0.1 mmol, 1.0 equiv.), **3.2** (0.15 mmol, 1.5 equiv.), $Ir(ppy)_2(dtbbpy)PF_6$ (1 mol%, 0.9 mg), $Pd_2(dba)_3$ (2.5 mol%, 2.3 mg), (*R*)-DTBM-SegPhos (3 mol%, 3.8 mg), (*S*)-DTBM-SegPhos (3 mol%, 3.8 mg), CH_3CN (2 mL) was added. The tube was degassed three times and filled with argon. The mixture was stirred

at 25 ℃ for 2 h under blue LED irradiation (1.0 A) as controlled by an external power supply. The organic phase was concentrated and purified by flash chromatography on silica gel.

3.4.6. Scale-up reaction for product 3.3ka

To a sealed tube charged with **3.1k** (1.0 mmol, 258 mg, 1.0 equiv.), **3.2a** (1.5 mmol, 600 mg, 1.5 equiv.), $Ir(ppy)_2(dtbbpy)PF_6$ (1 mol%, 9.0 mg), $Pd_2(dba)_3$ (2.5 mol%, 23.0 mg), (*R*)-3,5-*t*Bu-MeOBIPHEP (6 mol%, 62.0 mg), CH_3CN (6 mL) was added. The tube was degassed three times and filled with argon. The mixture was stirred at 25 ℃ for 12 h under blue LED irradiation (1.0 A) as controlled by an external power supply. The organic phase was concentrated and purified by flash chromatography on silica gel (hexane/acetic acid 250:1 v/v) to afford the desired product **3.3ka** in 61% yield (186.5 mg) with a b:l ratio of 73:27 and a 91:9 *er* value.

3.4.7. Characterization data for all new compounds

4-phenyl-4-vinyl-1,3-dioxaspiro[4.5]decan-2-one (3.1k)

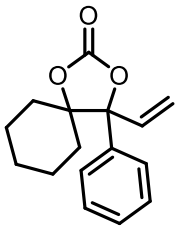

White solid; 2.2 g, 85% yield; **^{1}H NMR** (400 MHz, $CDCl_3$) δ 7.47-7.29 (m, 5H), 6.26 (dd, J = 16.9, 10.9 Hz, 1H), 5.49 (dd, J = 16.9, 0.6 Hz, 1H), 5.34 (dd, J = 10.9, 0.6 Hz, 1H), 2.26-2.09 (m, 1H), 1.75-1.41 (m, 7H), 1.19-0.96 (m, 1H), 0.97-0.78 (m, 1H) ppm; **^{13}C NMR** (101 MHz, $CDCl_3$) δ 153.3, 136.5, 134.6, 128.6, 128.2, 124.7, 116.0, 89.9, 89.0, 33.2, 31.6, 24.6, 22.3, 21.5 ppm; **IR** (neat) ν = 2937, 2849, 1791, 1492, 1446, 1407, 1225, 1124, 1021, 924, 761 cm^{-1}; **HRMS (ESI)** *m/z*: $[M+Na]^+$ Calcd for $C_{16}H_{18}NaO_3^+$ 281.1148, found 281.1157.

4-phenyl-4-vinyl-1,3-dioxaspiro[4.6]undecan-2-one (3.1l)

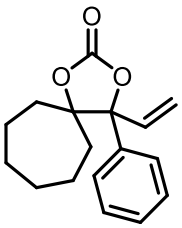

Colorless solid; 0.41 g, 82% yield; **^{1}H NMR** (400 MHz, $CDCl_3$) δ 7.45-7.29 (m, 5H), 6.31 (dd, *J* = 16.9, 10.9 Hz, 1H), 5.46 (d, *J* = 16.9 Hz, 1H), 5.34 (d, *J* = 10.9 Hz, 1H), 2.37-2.24 (m, 1H), 2.02-1.90 (m, 1H), 1.74-1.36 (m, 9H), 1.20-1.08 (m, 1H) ppm; **^{13}C NMR** (101 MHz, $CDCl_3$) δ 153.6, 136.3, 135.0, 128.6, 128.3, 125.1, 116.4, 92.5, 90.7, 35.8, 35.6, 28.6, 28.3, 22.7, 21.2 ppm; **IR** (neat) ν = 3064, 2931, 2861, 1795, 1494, 1452, 1242, 1023, 935, 766 cm^{-1}; **HRMS (ESI)** *m/z*: $[M+Na]^+$ Calcd for $C_{17}H_{20}NaO_3^+$ 295.1305, found 295.1308.

4,5-diphenyl-4-vinyl-1,3-dioxolan-2-one (3.1n)

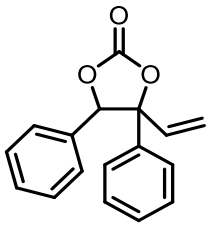

Yellowish oil; 2.07 g, 82% yield; **^{1}H NMR** (400 MHz, $CDCl_3$) δ 7.24-7.06 (m, 6H), 7.00-6.85 (m, 4H), 6.39 (ddd, J = 17.1, 10.8, 0.8 Hz, 1H), 5.75 (s, 1H), 5.67 (dd, J = 17.1, 0.8 Hz, 1H), 5.52 (dd, J = 10.9, 0.8 Hz, 1H) ppm; **^{13}C NMR** (101 MHz, $CDCl_3$) δ 154.0, 136.7, 135.5, 132.9, 129.1, 128.2, 128.1, 128.0, 126.7, 125.7, 117.6, 89.1, 87.1, 77.3, 77.0, 76.7 ppm; **IR** (Neat) ν = 3066, 3037, 1783, 1601, 1496, 1450, 1183, 1035, 940, 688 cm^{-1}; **HRMS (ESI)** *m/z*: $[M+Na]^+$ Calcd for $C_{17}H_{14}NaO_3^+$ 289.0835, found 289.0844.

Di-*tert*-butyl-4-(2-methoxybenzyl)-2,6-dimethyl-1,4-dihydropyridine-3,5-dicarboxylate (3.2e)

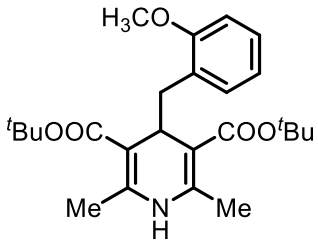

White solid; 2.2 g, 25% yield; **^{1}H NMR** (400 MHz, $CDCl_3$) δ 7.11 (ddd, *J* = 8.1, 7.4, 1.8 Hz, 1H), 6.92 (dd, *J* = 7.4, 1.8 Hz, 1H), 6.82 – 6.69 (m, 2H), 5.21 (s, 1H), 4.19 (t, *J* = 5.6 Hz, 1H), 3.73 (s, 3H), 2.61 (d, *J* = 5.6 Hz, 2H), 2.13 (s, 6H), 1.43 (s, 18H) ppm; **^{13}C NMR** (101 MHz, $CDCl_3$) δ 167.3, 158.2, 144.1, 132.1, 127.9, 126.8, 119.5, 109.5, 103.3, 78.9, 55.1, 35.1, 34.8, 28.2, 19.1 ppm; **IR** (neat) ν = 3343, 2974, 2931, 2837, 1716, 1684, 1618, 1489, 1457, 1238, 1158, 1097, 1017 cm^{-1}; **HRMS (ESI)** *m/z*: $[M+Na]^+$ Calcd for $C_{25}H_{35}NNaO_5^+$ 452.2407, found 452.2410.

Di-*tert*-butyl 2,6-dimethyl-4-(1-phenylpropyl)-1,4-dihydropyridine-3,5-dicarboxylate (3.2j)

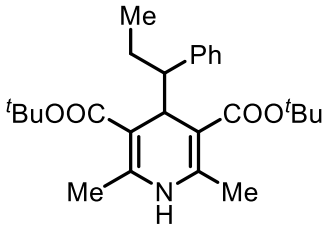

White solid; 1.5 g, 23% yield; **^{1}H NMR** (300 MHz, $CDCl_3$) δ 7.19-7.07 (m, 3H), 7.04-6.88 (m, 2H), 5.00 (s, 1H), 4.27 (d, *J* = 5.0 Hz, 1H), 2.35 (dt, *J* = 10.3, 5.4 Hz, 1H), 2.08 (s, 3H), 2.04 (s, 3H), 1.78-1.62 (m, 2H), 1.51 (s, 9H), 1.43 (s, 9H), 0.75 (t, *J* = 7.3 Hz, 3H) ppm; **^{13}C NMR** (75 MHz, $CDCl_3$) δ 168.0, 167.5, 144.4, 143.8, 142.3, 129.4, 126.8, 125.6, 102.5, 101.7, 79.3, 79.3, 54.5, 39.0, 28.4, 28.2, 28.2, 23.6, 19.1, 19.1, 12.8 ppm; **IR** (neat) ν = 3345, 2973, 2931, 2875, 1718, 1688, 1486, 1453, 1161, 1109, 1031 cm^{-1}; **HRMS (ESI)** *m/z*: $[M+Na]^+$ Calcd for $C_{26}H_{37}NNaO_4^+$ 450.2615, found 450.2617.

2-benzyl-2-phenylbut-3-en-1-ol (3.3aa)

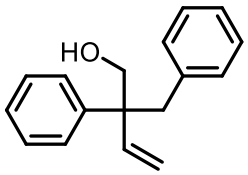

Colorless oil, 17.9 mg, 75%; 89:11 *er*, $[\alpha]_D^{25}$ = +52.89 (c 0.74, $CHCl_3$); (hexane/acetic acid 250:1.5 – 250:2 v/v). **^{1}H NMR** (400 MH $CDCl_3$) δ 7.35-7.11 (m, 9H), 6.87 (dd, *J* = 6.7, 2.8 Hz, 2H), 6.02 (dd, *J* = 17.8, 11.0 Hz, 1H), 5.39 (dd, *J* = 11.0, 1.0 Hz, 1H), 5.19 (dd, *J* = 17.8, 1.1 Hz, 1H), 3.87 (d, *J* = 10.9 Hz, 1H), 3.77 (d, *J* = 10.9 Hz, 1H), 3.19 (d, *J* = 13.0 Hz, 1H), 3.09 (d, *J* = 13.0 Hz, 1H), 1.27 (s, 1H) ppm; **^{13}C NMR** (101 MHz, $CDCl_3$) δ 143.0, 142.7, 137.4, 130.9, 128.4, 127.9, 127.7, 126.8, 128.3, 116.3, 65.3, 51.2, 41.7 ppm; **IR** (neat) ν = 3445, 3028, 2925, 2856, 1635, 1600, 1494, 1449, 1048, 917, 698 cm^{-1}; **HRMS (APCI)** *m/z*: $[M-OH]^+$ Calcd for $C_{17}H_{17}^+$ 221.1325, found 221.1323; the

enantiomeric excess was determined by UPC2 analysis on Chiralpak IG, mobile phase: CO_2:EtOH 70:30, flow rate 2 mL/min, ABPR 2000 psi, t_R = 2.17 min (major), t_R = 4.85 min (minor).

2-Benzyl-2-(4-methoxyphenyl)but-3-en-1-ol (3.3ba)

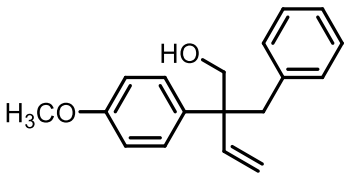

Colorless oil, 18.5 mg, 69%, 88:12 *er*, $[\alpha]_D^{25}$ = +62.68 (c 0.66, $CHCl_3$); (Hexane/EA 40:1, v/v). **^{1}H NMR** (400 MHz, $CDCl_3$) δ 7.21-7.04 (m, 5H), 6.95-6.79 (m, 4H), 5.99 (dd, *J* = 17.8, 11.0 Hz, 1H), 5.36 (d, *J* = 11.0 Hz, 1H), 5.16 (d, *J* = 17.8 Hz, 1H), 3.81 (s and d overlap, 4H), 3.73 (d, *J* = 10.9 Hz, 1H), 3.15 (d, *J* = 12.9 Hz, 1H), 3.05 (d, *J* = 12.9 Hz, 1H), 1.26 (s, 1H) ppm; **^{13}C NMR** (101 MHz, $CDCl_3$) δ 158.4, 143.2, 137.5, 134.6, 131.0, 129.0, 127.7, 126.3, 116.0, 113.7, 65.4, 55.4, 50.6, 41.8 ppm; **IR** (neat) ν = 3446, 3029, 2927, 2858, 1607, 1511, 1458, 1247, 1182, 1036, 830, 704 cm^{-1}; **HRMS (ESI)** *m/z*: $[M+Na]^+$ Calcd for $C_{18}H_{20}NaO_2^+$ 291.1356, found 291.1348; the enantiomeric excess was determined by UPC2 analysis on Chiralpak IG, mobile phase: CO_2:IPA 70:30, flow rate 2 mL/min, ABPR 2000 psi, t_R = 2.23 min (major), t_R = 3.37 min (minor).

2-Benzyl-2-(4-(trifluoromethyl)phenyl)but-3-en-1-ol (3.3ca)

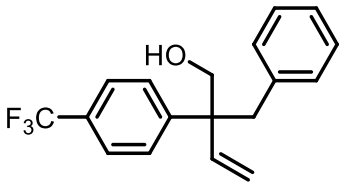

Colorless oil, 19.1 mg, 62%; 85:15 *er*, $[\alpha]_D^{25}$ = +48.24 (c 0.30, $CHCl_3$); (Hexane/EA 30:1 – 20:1, v/v). **^{1}H NMR** (400 MHz, $CDCl_3$) δ 7.55 (d, *J* = 8.2 Hz, 2H), 7.30 (d, *J* = 8.2 Hz, 2H), 7.20-7.10 (m, 3H), 6.85-6.83 (m, 2H), 6.01 (dd, *J* = 17.7, 11.0 Hz, 1H), 5.44 (d, *J* = 11.0 Hz, 1H), 5.20 (d, *J* = 17.8 Hz, 1H), 3.89 (d, *J* = 11.0 Hz, 1H), 3.80 (d, *J* = 11.0 Hz, 1H), 3.20 (d, *J* = 13.1 Hz, 1H), 3.08 (d, *J* = 13.1 Hz, 1H), 1.26 (s, 1H) ppm; ^{19}F NMR (376 MHz, $CDCl_3$) δ -62.17 ppm; **^{13}C NMR** (101 MHz, $CDCl_3$) δ 147.1, 142.3, 136.7, 130.8, 129.0 (q, *J* = 32.3 Hz), 128.5, 127.9, 126.6, 125.1 (q, *J* = 3.8 Hz), 124.3 (q, *J* = 272.6 Hz), 117.2, 65.1, 51.4, 41.9 ppm; **IR** (neat) ν = 3422, 3030, 2926, 2856, 1616, 1494, 1454, 1411, 1325, 1165, 1120, 922, 706 cm^{-1}; **HRMS (APCI)** *m/z*: $[M-OH]^+$ Calcd for $C_{18}H_{16}F_3^+$ 289.1199, found 289.1195; the enantiomeric excess was determined by UPC2 analysis on Chiralpak IG, mobile phase: CO_2:IPA 85:15, flow rate 2 mL/min, ABPR 2000 psi, t_R = 1.68 min (major), t_R = 2.36 min (minor).

2-Benzyl-2-(4-chlorophenyl)but-3-en-1-ol (3.3da)

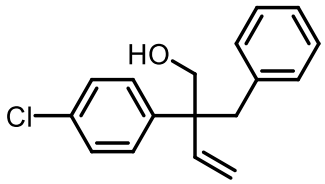

Colorless oil, 18.4 mg, 67%; 81:19 *er*, $[\alpha]_D^{25}$ = +71.38 (c 0.36, $CHCl_3$); (hexane/acetic acid 250:1.5 – 250:2 v/v). **^{1}H NMR** (400 MHz, CDCl3) δ 7.33-7.23 (m, 2H), 7.22-7.05 (m, 5H), 6.94-6.78 (m, 2H), 5.99 (dd, *J* = 17.8, 11.0 Hz, 1H), 5.41 (dd, *J* = 11.0, 0.9 Hz, 1H), 5.19 (dd, *J* = 17.8, 0.9 Hz, 1H), 3.84 (d, *J* = 11.0 Hz, 1H), 3.75 (d, *J* = 10.9 Hz, 1H), 3.17 (d, *J* = 13.0 Hz, 1H), 3.04 (d, *J* = 13.0 Hz, 1H), 1.26 (s, 1H) ppm; **^{13}C NMR** (101 MHz, $CDCl_3$) δ 142.6, 141.3, 136.9, 132.6, 130.9, 129.5, 128.4, 127.9, 126.5, 116.8, 65.1, 51.0, 41.8 ppm; **IR** (neat) ν = 3433, 3029, 2923, 2854, 1635, 1492, 1453, 1095, 1050, 920, 825, 702 cm^{-1}; **HRMS (APCI)** *m/z*: $[M\text{-}OH]^+$ Calcd for $C_{17}H_{16}Cl^+$ 255.0935, found 255.0932; the enantiomeric excess was determined by UPC2 analysis on Chiralpak IG, mobile phase: CO_2:IPA 75:25, flow rate 2 mL/min, ABPR 2000 psi, t_R = 2.17 min (major), t_R = 3.09 min (minor).

2-(Benzo[d][1,3]dioxol-5-yl)-2-benzylbut-3-en-1-ol (3.3ea)

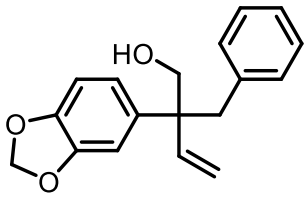

Colorless oil, 16.9 mg, 60%; 81:19 *er*, $[\alpha]_D^{25}$ = +64.11 (c 0.76, $CHCl_3$); (Hexane/EA 40:1 – 20:1, v/v). **^{1}H NMR** (400 MHz, $CDCl_3$) δ 7.20-7.12 (m, 3H), 6.94-6.86 (m, 2H), 6.77-6.70 (m, 2H), 6.62 (dd, *J* = 8.2, 1.9 Hz, 1H), 6.05-5.89 (m, 3H), 5.36 (dd, *J* = 11.0, 1.0 Hz, 1H), 5.16 (dd, *J* = 17.8, 1.0 Hz, 1H), 3.78 (d, *J* = 10.9 Hz, 1H), 3.70 (d, *J* = 10.9 Hz, 1H), 3.13 (d, *J* = 13.0 Hz, 1H), 3.04 (d, *J* = 13.0 Hz, 1H), 1.50-1.37 (*br* m, 1H) ppm; **^{13}C NMR** (101 MHz, $CDCl_3$) δ 147.8, 146.3, 143.0, 137.3, 136.6, 130.9, 127.8, 126.3, 121.0, 116.1, 108.7, 107.9, 101.1, 65.5, 51.0, 41.8 ppm; **IR** (neat) ν = 3441, 3027, 2924, 2888, 1604, 1486, 1434, 1238, 1038, 931, 810, 705 cm^{-1}; **HRMS (ESI)** *m/z*: $[M+Na]^+$ Calcd for $C_{18}H_{18}NaO_3^+$ 305.1148, found 305.1162; the enantiomeric excess was determined by UPC2 analysis on Chiralpak IG, mobile phase: CO_2:IPA 70:30, flow rate 2 mL/min, ABPR 2000 psi, t_R = 2.38 min (major), t_R = 3.70 min (minor).

2-Benzyl-2-(3-(benzyloxy)phenyl)but-3-en-1-ol (3.3fa)

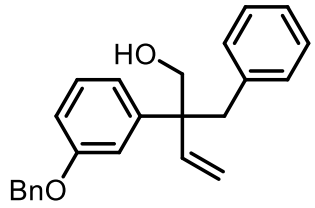

Colorless oil, 23.2 mg, 67%; 85:15 *er*, $[\alpha]_D^{25}$ = +36.99 (c 1.04, $CHCl_3$); (Hexane/EA 40:1 – 20:1, v/v). **^{1}H NMR** (400 MHz, $CDCl_3$) δ 7.46-7.29 (m, 5H), 7.22 (t, *J* = 7.9 Hz, 1H), 7.19-7.13 (m, 3H), 6.93-6.77 (m, 5H), 6.00 (dd, *J* = 17.8, 11.0 Hz, 1H), 5.37 (dd, *J* = 11.0, 1.0 Hz, 1H), 5.17 (dd, *J* = 17.8, 1.0 Hz, 1H), 5.02 (s, 2H), 3.83 (d, *J* = 10.0 Hz, 1H), 3.74 (d, *J* = 10.9 Hz, 1H), 3.16 (d, *J* = 12.9 Hz, 1H), 3.07 (d, *J* = 13.0 Hz, 1H), 1.50-1.35 (*br* m, 1H) ppm; **^{13}C NMR** (101 MHz, $CDCl_3$) δ 158.8, 144.5, 142.7, 137.4, 137.1, 130.9, 129.3, 128.7, 128.1, 127.7, 127.7, 126.3, 120.5, 116.2, 115.4, 112.9, 70.1, 65.4, 51.3, 41.6 ppm; **IR** (neat) ν = 3441, 3027, 2924, 2888, 1604, 1486, 1434, 1238, 1038, 931, 810, 705 cm^{-1}; **HRMS (ESI)** *m/z*: $[M+Na]^+$ Calcd for $C_{24}H_{24}NaO_2^+$ 367.1669, found 367.1673; the enantiomeric excess was determined by UPC2 analysis on Chiralpak IG, mobile phase: CO_2:IPA 75:35, flow rate 2 mL/min, ABPR 2000 psi, t_R = 2.48 min (major), t_R = 3.47 min (minor).

2-Benzyl-2-(2-methoxyphenyl)but-3-en-1-ol (3.3ga)

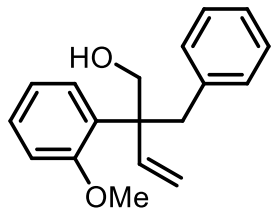

Colorless oil, 21.1 mg, 78%; 82.5:18.5 *er*, $[\alpha]_D^{25}$ = +55.06 (c 0.55, $CHCl_3$); (hexane/acetic acid 250:2 v/v). **^{1}H NMR** (400 MHz, $CDCl_3$) δ 7.25-7.20 (m, 1H), 7.13-7.05 (m, 3H), 7.00-6.88 (m, 2H), 6.88-6.76 (m, 3H), 6.08 (dd, *J* = 17.8, 10.9 Hz, 1H), 5.29 (dd, *J* = 10.9, 1.2 Hz, 1H), 5.10 (dd, *J* = 17.8, 1.2 Hz, 1H), 3.91 (s, 2H), 3.78 (s, 3H), 3.32 (d, *J* = 13.1 Hz, 1H), 3.21 (d, *J* = 13.0 Hz, 1H),), 1.26 (s, 1H) ppm; **^{13}C NMR** (101 MHz, $CDCl_3$) δ 158.2, 143.8, 138.2, 130.8, 130.7, 129.5, 128.2, 127.6, 126.0, 120.7, 114.2, 112.1, 64.9, 55.3, 50.8, 39.8 ppm; **IR** (neat) ν = 3440, 3028, 2926, 2856, 1491, 1457, 1240, 1024, 752, 703 cm^{-1}; **HRMS (ESI)** *m/z*: $[M+Na]^+$ Calcd for $C_{18}H_{20}NaO_2^+$ 291.1356, found 291.1348; the enantiomeric excess was determined by UPC2 analysis on Chiralpak IG, mobile phase: CO_2:MeOH 75:25, flow rate 2 mL/min, ABPR 2000 psi, t_R = 2.39 min (major), t_R = 3.12 min (minor).

2-Benzyl-2-(thiophen-2-yl)but-3-en-1-ol (3.3ha)

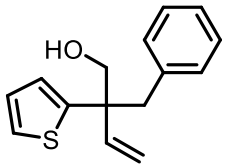

Yellowish oil, 9.5 mg, 39%; 72:28 *er*, $[\alpha]_D^{25}$ = +6.95 (c 0.28, $CHCl_3$); (hexane/acetic acid 250:1.5 – 250:2 v/v). **^{1}H NMR** (400 MHz, $CDCl_3$) δ 7.33-7.12 (m, 5H), 7.09-6.87 (m, 3H), 6.80 (dd, *J* = 3.6, 1.2 Hz, 1H), 6.02 (dd, *J* = 17.7, 10.9 Hz, 1H), 5.31 (dd, *J* = 10.9, 0.8 Hz, 1H), 5.14 (dd, *J* = 17.7, 0.8 Hz, 1H), 3.77 (q, *J* = 11.0 Hz, 2H), 3.18 (q, *J* = 13.0 Hz, 2H), 1.26 (s, 1H) ppm; **^{13}C NMR** (101 MHz, $CDCl_3$) δ 147.8, 141.8, 136.8, 130.8, 127.7, 126.7, 126.4, 124.9, 124.3, 116.0, 66.5, 49.9, 43.1 ppm; **IR** (neat) ν = 3435, 3029, 2923, 2854, 1494, 1453, 1410, 1238, 1050, 921, 803, 697 cm^{-1}; **HRMS (APCI)** *m/z*: $[M\text{-}OH]^+$ Calcd for $C_{15}H_{15}S^+$ 227.0889, found 227.0890; the enantiomeric excess was determined by UPC2 analysis on Chiralpak IG, mobile phase: CO_2:IPA 70:30, flow rate 2 mL/min, ABPR 2000 psi, t_R = 1.93 min (major), t_R = 3.17 min (minor).

2-Benzyl-2-(naphthalen-2-yl)but-3-en-1-ol (3.3ia)

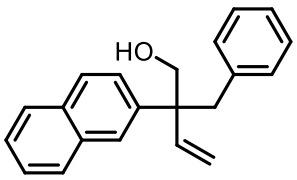

Colorless oil, 14.3 mg, 50%; 86:14 *er*, $[\alpha]_D^{25}$ = +56.51 (c 0.25, $CHCl_3$); (hexane/acetic acid 250:1.5 – 250:2 v/v). **^{1}H NMR** (400 MHz, $CDCl_3$) δ 7.86-7.79 (m, 2H), 7.77-7.75 (m, 1H), 7.63-7.56 (m, 1H), 7.51-7.44 (m, 2H), 7.42 (dd, *J* = 8.7, 1.9 Hz, 1H), 7.16-7.08 (m, 3H), 6.91-6.88 (m, 2H), 6.08 (dd, *J* = 17.8, 11.0 Hz, 1H), 5.43 (dd, *J* = 11.0, 1.0 Hz, 1H), 5.21 (dd, *J* = 17.7, 1.0 Hz, 1H), 3.97 (d, *J* = 11.0 Hz, 1H), 3.88 (d, *J* = 11.0 Hz, 1H), 3.28 (d, *J* = 13.0 Hz, 1H), 3.23 (d, *J* = 13.0 Hz, 1H), 1.26 (s, 1H) ppm; **^{13}C NMR** (101 MHz, $CDCl_3$) δ 142.9, 140.1, 137.3, 133.3, 132.3, 130.9, 128.2, 127.9, 127.8, 127.6, 126.7, 126.4, 126.3, 126.2, 126.0, 116.6, 65.4, 51.4, 41.7 ppm; **IR** (neat) ν = 3456, 3027, 2923, 2853, 1599, 1498, 1454, 1261, 1050, 918, 814, 704 cm^{-1}; **HRMS (ESI)** *m/z*: $[M+Na]^+$ Calcd for $C_{21}H_{20}NaO^+$ 311.1406, found 311.1410; the enantiomeric excess was determined by UPC2 analysis on Chiralpak IG, mobile phase: CO_2:IPA 65:35, flow rate 2 mL/min, ABPR 2000 psi, t_R = 2.37 min (major), t_R = 3.07 min (minor).

2-Benzyl-2,3-diphenylbut-3-en-1-ol (3.3ja)

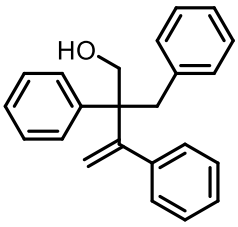

Yellowish solid, 10.5 mg, 33%; 62.5:37.5 *er*, $[\alpha]_D^{25}$ = +13.89 (c 0.35, $CHCl_3$); (hexane/acetic acid 250:1 – 250:1.5 v/v). **^{1}H NMR** (400 MHz, $CDCl_3$) δ 7.34-7.22 (m, 3H), 7.20-7.07 (m, 8H), 6.83-6.81 (m, 2H), 6.78-6.64 (m, 2H), 5.55 (dd, *J* = 10.6, 0.8 Hz, 2H), 3.81 (d, *J* = 10.6 Hz, 1H), 3.75 (d, *J* = 10.6 Hz, 1H), 3.39 (d, *J* = 12.6 Hz, 1H), 3.29 (d, *J* = 12.6 Hz, 1H), 1.26 (s, 1H) ppm; **^{13}C NMR** (101 MHz, $CDCl_3$) δ 153.1, 142.3, 142.0, 137.5, 130.8, 128.3, 128.2, 127.83, 127.79, 127.5, 127.2, 126.7, 126.1, 118.2, 63.2, 52.9, 41.6 ppm; **IR** (neat) ν = 3457, 3057, 3027, 2924, 2854, 1600, 1493, 1448, 1034, 910, 778, 701 cm^{-1}; **HRMS (ESI)** *m/z*: $[M+Na]^+$ Calcd for $C_{23}H_{22}NaO^+$ 337.1563, found 337.1560; the enantiomeric excess was determined by UPC2 analysis on Chiralpak IG, mobile phase: CO_2:EtOH 65:35, flow rate 2 mL/min, ABPR 2000 psi, t_R = 2.02 min (minor), t_R = 2.61 min (major).

1-(1,2-Diphenylbut-3-en-2-yl)cyclohexan-1-ol (3.3ka)

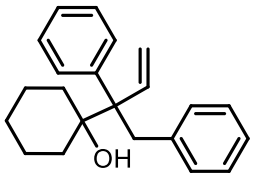

White solid, 19.8 mg, 65%; 92:8 *er*, $[\alpha]_D^{25}$ = -79.45 (c 0.30, $CHCl_3$); (hexane/acetic acid 250:1 v/v). **^{1}H NMR** (400 MHz, $CDCl_3$) δ 7.54-7.42 (m, 2H), 7.33-7.11 (m, 4H), 7.10-6.95 (m, 3H), 6.95 – 6.84 (m, 2H), 6.67 (ddd, *J* = 17.7, 11.3, 1.2 Hz, 1H), 5.41 (dd, *J* = 11.3, 1.2 Hz, 1H), 5.12 (dd, *J* = 17.7, 1.2 Hz, 1H), 3.84 (d, *J* = 16.6 Hz, 1H), 3.51 (d, *J* = 16.6 Hz, 1H), 1.80-1.40 (m, 10H), 1.10-0.92 (*br* m, 1H) ppm; **^{13}C NMR** (101 MHz, $CDCl_3$) δ 141.2, 139.7, 139.5, 130.7, 130.0, 127.7, 127.5, 126.3, 125.1, 118.1, 76.0, 56.6, 35.4, 32.5, 32.0, 25.8, 22.2, 22.1 ppm; **IR** (neat) ν = 3572, 3058, 3026, 2927, 2855, 1601, 1495, 1449, 1260, 1026, 919, 700 cm^{-1}; **HRMS (ESI)** *m/z*: $[M+Na]^+$ Calcd for $C_{22}H_{26}NaO^+$ 329.1876, found 329.1879; the enantiomeric excess was determined by UPC2 analysis on Chiralpak IB, mobile phase: CO_2:IPA 90:10, flow rate 3 mL/min, ABPR 1500 psi, t_R = 1.65 min (major), t_R = 1.95 min (minor).

1-(1-(4-Methoxyphenyl)-2-phenylbut-3-en-2-yl)cyclohexan-1-ol (3.3kb)

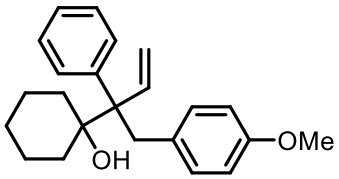

Colorless oil, 22.8 mg, 68%; 92:8 *er*, $[\alpha]_D^{25}$ = -57.65 (c 0.78, $CHCl_3$); (hexane/acetic acid 250:1 v/v). **^{1}H NMR** (400 MHz, $CDCl_3$) δ 7.53-7.47 (m, 2H), 7.31-7.24 (m, 2H), 7.23-7.16 (m, 1H), 6.86-6.80 (m, 2H), 6.69-6.62 (m, 1H), 6.62-6.58 (m, 2H), 5.42 (dd, *J* = 11.4, 1.2 Hz, 1H), 5.12 (dd, *J* = 17.8, 1.3 Hz, 1H), 3.77 (d, *J* = 16.1 Hz, 1H), 3.70 (s, 3H), 3.43 (d, *J* = 16.3 Hz, 1H), 1.83-1.40 (m, 10H), 1.14-0.95 (*br* m, 1H) ppm; **^{13}C NMR** (101 MHz, $CDCl_3$) δ 157.0, 141.1, 139.6, 131.4, 131.1, 129.9, 127.5, 126.1, 118.0, 112.8, 75.9, 56.7, 55.0, 34.5, 32.3, 31.9, 25.6, 22.0, 21.9 ppm; **IR** (neat) ν = 3564, 2928, 2855, 1609, 1510, 1447, 1245, 1179, 1035, 964, 808, 703 cm^{-1}; **HRMS (APCI)** *m/z*: $[M\text{-}OH]^+$ Calcd for $C_{23}H_{27}O^+$ 319.2056, found 319.2051; the enantiomeric excess was determined by UPC2 analysis on Chiralpak IG, mobile phase: CO_2:MeOH 60:40, flow rate 2 mL/min, ABPR 2000 psi, t_R = 3.66 min (minor), t_R = 4.22 min (major).

1-(2-Phenyl-1-(p-tolyl)but-3-en-2-yl)cyclohexan-1-ol (3.3kc)

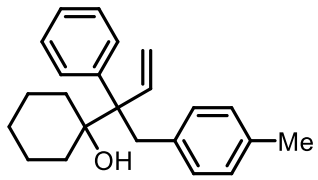

Colorless oil, 23.2 mg, 72%; 92:8 *er*, $[\alpha]_D^{25}$ = -63.95 (c 0.86, $CHCl_3$); (hexane/acetic acid 250:1 v/v). **^{1}H NMR** (400 MHz, $CDCl_3$) δ 7.52-7.43 (m, 2H), 7.30-7.22 (m, 2H), 7.22-7.15 (m, 1H), 6.89-6.75 (m, 4H), 6.65 (ddd, *J* = 17.8, 11.4, 1.2 Hz, 1H), 5.40 (dd, *J* = 11.4, 1.2 Hz, 1H), 5.11 (dd, *J* = 17.8, 1.2 Hz, 1H), 3.79 (d, *J* = 16.4 Hz, 1H), 3.45 (d, *J* = 16.5 Hz, 1H), 2.19 (s, 3H), 1.81-1.37 (m, 10H), 1.11-0.93 (*br* m, 1H) ppm; **^{13}C NMR** (101 MHz, $CDCl_3$) δ 141.1, 139.6, 136.0, 134.3, 130.4, 129.8, 128.1, 127.5, 126.1, 117.9, 75.8, 56.5, 34.9, 32.3, 31.9, 25.6, 22.04, 21.95, 20.8 ppm; **IR** (neat) ν = 3569, 3020, 2928, 2856, 1514, 1447, 1350, 1259, 1020, 964, 919, 756, 702 cm^{-1}; **HRMS (ESI)** *m/z*: $[M+Na]^+$ Calcd for $C_{23}H_{28}NaO^+$ 343.2034, found 343.2035; the enantiomeric excess was determined by UPC2 analysis on Chiralpak IC, mobile phase: CO_2:MeOH 90:10, flow rate 3 mL/min, ABPR 1500 psi, t_R = 1.17 min (major), t_R = 1.90 min (minor).

1-(1-(4-Chlorophenyl)-2-phenylbut-3-en-2-yl)cyclohexan-1-ol (3.3kd)

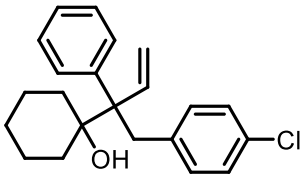

White solid, 21.5 mg, 63%; 89.5:10.5 *er*, $[\alpha]_D^{25}$ = -62.38 (c 0.91, $CHCl_3$); (hexane/acetic acid 250:1 v/v). **^{1}H NMR** (400 MHz, $CDCl_3$) δ 7.46-7.40 (m, 2H), 7.33-7.14 (m, 3H), 7.05-6.91 (m, 2H), 6.89-6.75 (m, 2H), 6.65 (ddd, *J* = 17.8, 11.3, 1.2 Hz, 1H), 5.40 (dd, *J* = 11.4, 1.1 Hz, 1H), 5.06 (dd, *J* = 17.7, 1.1 Hz, 1H), 3.80 (d, *J* = 16.7 Hz, 1H), 3.44 (d, *J* = 16.7 Hz, 1H), 1.78-1.35 (m, 10H), 1.10-0.94 (*br* m, 1H) ppm; **^{13}C NMR** (101 MHz, $CDCl_3$) δ 140.6, 139.2, 137.8, 131.9, 130.6, 129.7, 127.7, 127.4, 126.3, 118.0, 75.8, 56.4, 34.4, 32.4, 31.8, 25.5, 22.0, 21.9 ppm; **IR** (neat) ν = 3570, 3057, 3027, 2929, 2856, 1491, 1448, 1094, 1015, 964, 920, 800, 747, 702 cm^{-1}; **HRMS (ESI)** *m/z*: $[M+Na]^+$ Calcd for $C_{22}H_{25}ClNaO^+$ 363.1486, found 363.1488; the enantiomeric excess was determined by UPC2 analysis on Chiralpak IC, mobile phase: CO_2:EtOH 95:5, flow rate 3 mL/min, ABPR 1500 psi, t_R = 1.88 min (major), t_R = 2.23 min (minor).

1-(1-(2-Methoxyphenyl)-2-phenylbut-3-en-2-yl)cyclohexan-1-ol (3.3ke)

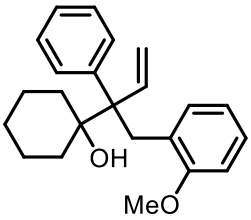

Colorless oil, 19.5 mg, 58%; 92.5:7.5 *er*, $[\alpha]_D^{25}$ = -104.79 (c 0.88, $CHCl_3$); (hexane/acetic acid 250:1 – 250:1.5 v/v). **^{1}H NMR** (400 MHz, $CDCl_3$) δ 7.50-7.40 (m, 2H), 7.29-7.12 (m, 3H), 7.05-6.94 (m, 1H), 6.81-6.75 (m, 1H), 6.69 (ddd, *J* = 17.7, 11.3, 1.1 Hz, 1H), 6.54-6.41 (m, 2H), 5.36 (dd, *J* = 11.3, 1.3 Hz, 1H), 5.10 (dd, *J* = 17.7, 1.3 Hz, 1H), 3.88 (s, 3H), 3.70 (d, *J* = 17.3 Hz, 1H), 3.39 (d, *J* = 17.3 Hz, 1H), 1.78-1.37 (m, 10H), 1.10-0.93 (*br* m, 1H) ppm; **^{13}C NMR** (101 MHz, $CDCl_3$) δ 157.7, 141.7, 140.0, 132.0, 129.6, 127.5, 126.0, 125.8, 119.2, 117.2, 109.3, 75.9, 56.0, 55.2, 32.1, 32.1, 28.7, 25.7, 22.1, 22.0 ppm; **IR** (neat) ν = 3553, 2930, 1597, 1491, 1461, 1237, 1109, 1028, 966, 749, 704 cm^{-1}; **HRMS (APCI)** *m/z*: $[M-OH]^+$ Calcd for $C_{23}H_{27}O^+$ 319.2056, found 319.2055; the enantiomeric excess was determined by UPC2 analysis on Chiralpak IC, mobile phase: CO_2:EtOH 95:5, flow rate 3 mL/min, ABPR 1500 psi, t_R = 1.93 min (major), t_R = 2.29 min (minor).

1-(2-Phenyl-1-(thiophen-2-yl)but-3-en-2-yl)cyclohexan-1-ol (3.3kf)

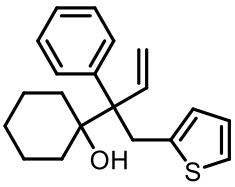

Colorless oil, 21.1 mg, 67%; 92:8 *er*, $[\alpha]_D^{25}$ = -21.10 (c 0.97, $CHCl_3$); (hexane/acetic acid 250:1 – 250:1.5 v/v). **^{1}H NMR** (400 MHz, $CDCl_3$) δ 7.57-7.51 (m, 2H), 7.34-7.28 (m, 2H), 7.27-7.21 (m, 1H), 6.93-6.87 (m, 1H), 6.75-6.68 (m, 1H), 6.61-6.48 (m, 2H), 5.42 (dd, *J* = 11.4, 1.1 Hz, 1H), 5.21 (dd, *J* = 17.8, 1.1 Hz, 1H), 3.96 (d, *J* = 16.0 Hz, 1H), 3.63 (d, *J* = 16.0 Hz, 1H), 1.77-1.39 (m, 10H), 1.12-0.92 (*br* m, 1H) ppm; **^{13}C NMR** (101 MHz, $CDCl_3$) δ 142.3, 140.6, 138.9, 130.0, 127.6, 127.1, 126.5, 125.6, 123.2, 118.2, 75.7, 57.4, 32.5, 31.9, 31.3, 25.5, 22.0, 21.9 ppm; **IR** (neat) ν = 3559, 3060, 3026, 2927, 2855, 1494, 1444, 1259, 1039, 963, 920, 847, 752, 693 cm^{-1}; **HRMS (APCI)** *m/z*: $[M\text{-}OH]^+$ Calcd for $C_{20}H_{23}S^+$ 295.1515, found 295.1508; the enantiomeric excess was determined by UPC2 analysis on Chiralpak IB, mobile phase: CO_2:EtOH 90:10, flow rate 3 mL/min, ABPR 1500 psi, t_R = 1.75 min (major), t_R = 2.29 min (minor).

1-(1-(Benzyloxy)-2-phenylbut-3-en-2-yl)cyclohexan-1-ol (3.3kg)

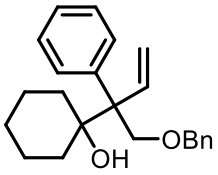

Colorless oil, 16.2 mg, 48%; 90:10 *er*, $[\alpha]_D^{25}$ = -41.25 (c 0.35, $CHCl_3$); (hexane/acetic acid 250:1 – 250:1.5 v/v). **^{1}H NMR** (400 MHz, $CDCl_3$) δ 7.50-7.43 (m, 2H), 7.38-7.18 (m, 8H), 6.53 (dd, *J* = 17.8, 11.3 Hz, 1H), 5.36 (dd, *J* = 11.3, 1.2 Hz, 1H), 5.09 (dd, *J* = 17.8, 1.2 Hz, 1H), 4.64-4.46 (m, 2H), 4.17 (d, *J* = 9.5 Hz, 1H), 3.96 (d, *J* = 9.5 Hz, 1H), 1.72-1.29 (m, 10H), 1.04-0.89 (*br* m, 1H) ppm; **^{13}C NMR** (101 MHz, $CDCl_3$) δ 142.2, 140.6, 137.5, 129.7, 128.4, 127.8, 127.8, 127.3, 126.3, 116.6, 75.6, 74.6, 73.8, 56.1, 33.2, 32.4, 25.7, 21.7, 21.6 ppm; **IR** (neat) ν = 3490, 3060, 3029, 2927, 2855, 1493, 1448, 1262, 1089, 1024, 969, 747, 701 cm^{-1}; **HRMS (APCI)** *m/z*: $[M\text{-}OH]^+$ Calcd for $C_{23}H_{27}O^+$ 319.2056, found 319.2054; the enantiomeric excess was determined by UPC2 analysis on Chiralpak IG, mobile phase: CO_2:EtOH 85:15, flow rate 2 mL/min, ABPR 2000 psi, t_R = 3.03 min (minor), t_R = 3.32 min (major).

1-(1,2-Diphenylbut-3-en-2-yl)cycloheptan-1-ol (3.3la)

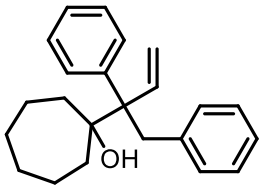

White solid, 16.3 mg, 51%; 92:8 *er*, $[\alpha]_D^{25}$ = -58.71 (c 0.41, $CHCl_3$); (hexane/acetic acid 250:1 v/v). **^{1}H NMR** (400 MHz, $CDCl_3$) δ 7.58-7.46 (m 2H), 7.31-7.12 (m, 3H), 7.08-6.95 (m, 3H), 6.95-6.84 (m, 2H), 6.60 (ddd, *J* = 17.8, 11.3, 1.0 Hz, 1H), 5.40 (dd, *J* = 11.4, 1.2 Hz, 1H), 5.13 (dd, *J* = 17.8, 1.2 Hz, 1H), 3.79 (d, *J* = 16.3 Hz, 1H), 3.48 (d, *J* = 16.3 Hz, 1H), 1.97-1.81 (m, 2H), 1.81-1.67 (m, 1H), 1.61-1.32 (m, 10H) ppm; **^{13}C NMR** (101 MHz, $CDCl_3$) δ 141.5, 140.0, 139.4, 130.6, 129.8, 127.6, 127.4, 126.1, 125.0, 117.6, 79.6, 57.7, 37.1, 37.0, 36.4, 29.6, 29.4, 23.1, 23.1 ppm; **IR** (neat) ν = 3569, 3058, 3026, 2922, 2855, 1600, 1494, 1453, 1016, 917, 701 cm^{-1}; **HRMS (ESI)** *m/z*: $[M+Na]^+$ Calcd for $C_{23}H_{28}NaO^+$ 343.2032, found 343.2033; the enantiomeric excess was determined by UPC2 analysis on Chiralpak IE, mobile phase: CO_2:MeOH 93:7, flow rate 2 mL/min, ABPR 2000 psi, t_R = 2.09 min (minor), t_R = 2.35 min (major).

1-(1-(4-Methoxyphenyl)-2-phenylbut-3-en-2-yl)cycloheptan-1-ol (3.3lb)

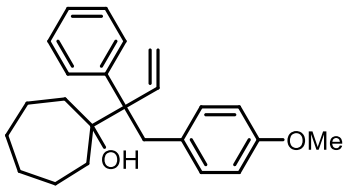

Colorless oil, 22.9 mg, 65%; 92:8 *er*, $[\alpha]_D^{25}$ = -54.13 (c 1.05, $CHCl_3$); (hexane/acetic acid 250:1 – 250:1.5 v/v). **^{1}H NMR** (400 MHz, $CDCl_3$) δ 7.60-7.46 (m, 2H), 7.29-7.16 (m, 3H), 6.88-6.73 (m, 2H), 6.65-6.48 (m, 3H), 5.40 (dd, *J* = 11.3, 1.3 Hz, 1H), 5.13 (dd, *J* = 17.8, 1.3 Hz, 1H), 3.71 (overlapped, d, *J* = 15.8 Hz, 1H), 3.69 (overlapped, s, 3H), 3.39 (d, *J* = 16.0 Hz, 1H), 1.95-1.81 (m, 2H), 1.78-1.68 (m, 1H), 1.61-1.29 (m, 10H) ppm; **^{13}C NMR** (101 MHz, $CDCl_3$) δ 157.1, 141.7, 140.2, 131.4, 131.2, 130.0, 127.5, 126.1, 117.5, 112.8, 79.6, 57.9, 55.0, 37.2, 37.1, 35.8, 29.6, 29.4, 23.1, 23.1 ppm; **IR** (neat) ν = 3556, 2923, 2854, 1609, 1510, 1459, 1245, 1179, 1035, 917, 808, 759, 704 cm^{-1}; **HRMS (ESI)** *m/z*: $[M+Na]^+$ Calcd for $C_{24}H_{30}NaO_2^+$ 373.2138, found 373.2124; the enantiomeric excess was determined by UPC2 analysis on Chiralpak IA, mobile phase: CO_2:IPA 85:15, flow rate 3 mL/min, ABPR 1500 psi, t_R = 2.72 min (major), t_R = 3.13 min (minor).

1-(1-(2-Methoxyphenyl)-2-phenylbut-3-en-2-yl)cycloheptan-1-ol (3.3le)

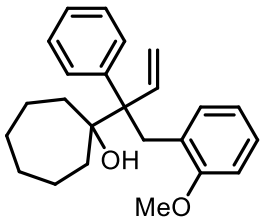

Colorless oil, 19.1 mg, 55%; 94:6 *er*, $[\alpha]_D^{25}$ = -95.43 (c 0.67, $CHCl_3$); (hexane/acetic acid 250:1.5 v/v). **^{1}H NMR** (400 MHz, $CDCl_3$) δ 7.50 (s, 2H), 7.27-7.13 (m, 3H), 7.05-6.96 (m, 1H), 6.81-6.75 (m, 1H), 6.60 (dd, *J* = 17.7, 11.3 Hz, 1H), 6.50 (t, *J* = 7.5 Hz, 1H), 6.42 (d, *J* = 7.6 Hz, 1H), 5.36 (dd, *J* = 11.2, 1.2 Hz, 1H), 5.11 (dd, *J* = 17.7, 1.3 Hz, 1H), 3.88 (s, 3H), 3.66 (d, *J* = 16.8 Hz, 1H), 3.33 (d, *J* = 16.8 Hz, 1H), 1.94-1.35 (m, 13H) ppm; **^{13}C NMR** (101 MHz, $CDCl_3$) δ 157.5, 142.2, 140.6, 132.3, 129.7, 127.6, 127.4, 126.0, 126.0, 119.3, 116.8, 109.4, 79.5, 57.3, 55.2, 37.0, 36.9, 30.2, 29.6, 29.5, 23.3, 23.1 ppm; **IR** (neat) ν = 3492, 2923, 2855, 1597, 1491, 1461, 1237, 1110, 1026, 917, 744, 703 cm^{-1}; **HRMS (ESI)** *m/z*: $[M+Na]^+$ Calcd for $C_{24}H_{30}NaO_2^+$ 373.2138, found 373.2144; the enantiomeric excess was determined by UPC2 analysis on Chiralpak IC, mobile phase: CO_2:IPA 88:12, flow rate 3 mL/min, ABPR 1500 psi, t_R = 1.37 min (major), t_R = 1.70 min (minor).

(*R*)-3-Benzyl-2-methyl-3-phenylpent-4-en-2-ol, (*R*)-3.3ma

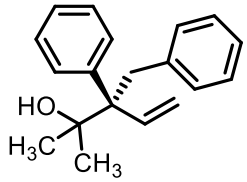

White solid, 19.7 mg, 74%; 88.5:11.5 *er*, $[\alpha]_D^{25}$ = -41.53 (c 0.67, $CHCl_3$); (hexane/acetic acid 250:1 v/v). **^{1}H NMR** (400 MHz, $CDCl_3$) δ 7.52 (d, *J* = 7.6 Hz, 2H), 7.31-7.23 (m, 2H), 7.23-7.16 (m, 1H), 7.09-6.96 (m, 3H), 6.96-6.88 (m, 2H), 6.60 (dd, *J* = 17.8, 11.4 Hz, 1H), 5.40 (dd, *J* = 11.3, 1.1 Hz, 1H), 5.15 (dd, *J* = 17.8, 1.1 Hz, 1H), 3.82 (d, *J* = 16.4 Hz, 1H), 3.48 (d, *J* = 16.4 Hz, 1H), 1.78-1.45 (*br* m, 1H), 1.28 (s, 3H), 1.20 (s, 3H) ppm; **^{13}C NMR** (101 MHz, $CDCl_3$) δ 141.4, 139.9, 139.3, 130.7, 129.8, 127.8, 127.6, 126.4, 125.3, 118.0, 75.5, 56.2, 36.4, 26.5, 26.4 ppm; **IR** (neat) ν = 3469, 3026, 2975, 2927, 2856, 1493, 1452, 1368, 1166, 923, 701 cm^{-1}; **HRMS (ESI)** *m/z*: $[M+Na]^+$ Calcd for $C_{19}H_{22}NaO^+$ 289.1563, found 289.1550; the enantiomeric excess was determined by UPC2 analysis on Chiralpak IG, mobile phase: CO_2:MeOH 75:25, flow rate 2 mL/min, ABPR 2000 psi, t_R = 2.41 min (minor), t_R = 3.61 min (major).

3-(4-Methoxybenzyl)-2-methyl-3-phenylpent-4-en-2-ol (3.3mb)

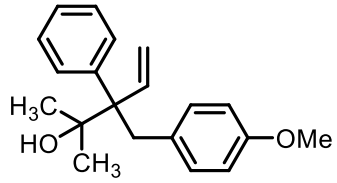

Colorless oil, 25.5 mg, 86%; 89.5:10.5 *er*, $[\alpha]_D^{25}$ = -58.11 (c 0.51, $CHCl_3$); (hexane/acetic acid 250:1.5 – 250:2 v/v). **^{1}H NMR** (400 MHz, $CDCl_3$) δ 7.54-7.49 (m, 2H), 7.30-7.24 (m, 2H), 7.23=7.16 (m, 1H), 6.87-6.76 (m, 2H), 6.64-6.48 (m, 3H), 5.39 (dd, *J* = 11.4, 1.2 Hz, 1H), 5.13 (dd, *J* = 17.8, 1.2 Hz, 1H), 3.73 (d, *J* = 16.1 Hz, 1H), 3.69 (s, 3H), 3.39 (d, *J* = 16.1 Hz, 1H), 1.62-1.54 (*br* s, 1H), 1.26 (s, 3H), 1.19 (s, 3H) ppm; **^{13}C NMR** (101 MHz, $CDCl_3$) δ 157.1, 141.4, 139.9, 131.4, 131.0, 129.8, 127.6, 126.2, 117.8, 112.9, 75.4, 56.2, 55.0, 35.6, 26.4, 26.3 ppm; **IR** (neat) ν = 3559, 2926, 2854, 1609, 1511, 1460, 1245, 1178, 1033, 923, 811, 703 cm^{-1}; **HRMS (ESI)** *m/z*: $[M+Na]^+$ Calcd for $C_{20}H_{24}NaO_2^+$ 319.1669, found 319.1673; the enantiomeric excess was determined by UPC2 analysis on Chiralpak IC, mobile phase: CO_2:MeOH 95:5, flow rate 3 mL/min, ABPR 1500 psi, t_R = 2.18 min (major), t_R = 2.78 min (minor).

3-(2-Methoxybenzyl)-2-methyl-3-phenylpent-4-en-2-ol (3.3me)

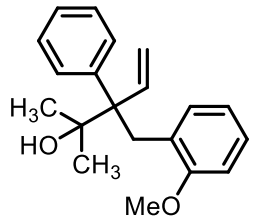

Colorless oil, 16.7 mg, 56%; 89:11 *er*, $[\alpha]_D^{25}$ = -99.60 (c 0.28, $CHCl_3$); (hexane/acetic acid 250:1.5 – 250:2 v/v). **^{1}H NMR** (400 MHz, $CDCl_3$) δ 7.52-7.44 (m, 2H), 7.29-7.21 (m, 2H), 7.21-7.14 (m, 1H), 7.06-6.97 (m, 1H), 6.79 (dd, *J* = 8.2, 1.2 Hz, 1H), 6.62 (ddd, *J* = 17.8, 11.3, 1.0 Hz, 1H), 6.55-6.48 (m, 1H), 6.48-6.42 (m, 1H), 5.36 (dd, *J* = 11.3, 1.2 Hz, 1H), 5.13 (dd, *J* = 17.7, 1.2 Hz, 1H), 3.88 (s, 3H), 3.67 (d, *J* = 17.0 Hz, 1H), 3.38 (d, *J* = 17.0 Hz, 1H), 1.63-1.46 (*br* s, 1H), 1.28 (s, 3H), 1.20 (s, 3H) ppm; **^{13}C NMR** (101 MHz, $CDCl_3$) δ 157.6, 142.0, 140.4, 132.1, 129.5, 127.5, 127.4, 126.11, 126.06, 119.4, 117.0, 109.5, 75.4, 55.7, 55.2, 29.9, 26.4, 26.1 ppm; **IR** (neat) ν = 3476, 2925, 2854, 1597, 1491, 1462, 1238, 1110, 1028, 922, 752 704 cm^{-1}; **HRMS (ESI)** *m/z*: $[M+Na]^+$ Calcd for $C_{20}H_{24}NaO_2^+$ 319.1669, found 319.1673; the enantiomeric excess was determined by UPC2 analysis on Chiralpak IA, mobile phase: CO_2:IPA 90:10, flow rate 3 mL/min, ABPR 1500 psi, t_R = 1.64 min (minor), t_R = 1.99 min (major).

2-Benzyl-1,2-diphenylbut-3-en-1-ol (3.3na)

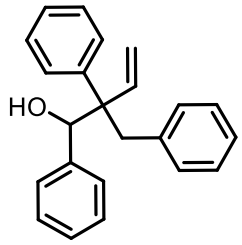

Colorless oil, 18.3 mg, 58%, *dr* = 1.85/1; 64:36 *er*, 50:50 *er*; $[\alpha]_D^{25}$ = +3.928 (c 0.54, $CHCl_3$); (hexane/acetic acid 250:1 – 250:1.5 v/v). **^{1}H NMR** (400 MHz, $CDCl_3$) δ 7.28-7.06 (m, 19H), 7.01-6.83 (m, 4H), 6.28-6.08 (m, 1.5H), 5.57 (dd, *J* = 11.2, 1.0 Hz, 0.52H), 5.51 (dd, *J* = 17.9, 1.0 Hz, 0.52H), 5.44 (dd, *J* = 11.2, 1.1 Hz, 1H), 5.20 (s, 0.53H), 5.17-5.09 (m, 2H), 3.57 (d, *J* = 14.0 Hz, 0.54H), 3.34 (d, *J* = 14.1 Hz, 1H), 3.10 (d, *J* = 14.1 Hz, 1H), 2.97 (d, *J* = 14.0 Hz, 0.59H), 1.26 (s, 1H) ppm; **^{13}C NMR** (101 MHz, CDCl3) δ 141.21, 141.18, 140.5, 140.4, 140.2, 140.1, 137.8, 137.7, 131.1, 130.9, 129.33, 129.30, 128.7, 128.4, 127.8, 127.7, 127.49, 127.45, 127.4, 127.29, 127.27, 126.7, 126.6, 125.9, 125.8, 118.0, 117.1, 78.6, 77.1, 55.2, 54.6, 42.0, 41.6 ppm; **IR** (neat) ν = 3451, 3058, 3028, 2924, 1600, 1494, 1449, 1185, 1024, 919, 699 cm^{-1}; **HRMS (ESI)** *m/z*: $[M+Na]^+$ Calcd for $C_{23}H_{22}NaO^+$ 337.1563, found 337.1577; the enantiomeric excess was determined by UPC2 analysis on Chiralpak OJ, mobile phase: CO_2: ACN 90:10, flow rate 2 mL/min, ABPR 2000 psi, t_R = 1.74 min (major), t_R = 2.37 min (major), t_R = 3.93 min (major), t_R = 4.31 min (major).

2-Benzhydryl-2-phenylbut-3-en-1-ol (3.3ah)

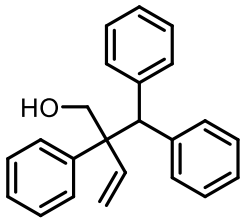

Colorless oil, 17.8 mg, 57%; 89.5:10.5 *er*, $[\alpha]_D^{25}$ = +29.19 (c 0.71, $CHCl_3$); (Hexane/EA 40:1 – 30:1, v/v). **^{1}H NMR** (400 MHz, $CDCl_3$) δ 7.37-7.32 (m, 2H), 7.30-7.18 (m, 8H), 7.13-7.06 (m, 3H), 7.04-6.98 (m, 2H), 6.47 (dd, *J* = 18.0, 11.4 Hz, 1H), 5.47 (dd, *J* = 11.4, 1.1 Hz, 1H), 5.12 (dd, *J* = 18.0, 1.1 Hz, 1H), 4.81 (s, 1H), 3.86 (d, *J* = 11.3 Hz, 1H), 3.75 (d, *J* = 11.3 Hz, 1H), 1.27 (*br* s, 1H) ppm; **^{13}C NMR** (101 MHz, $CDCl_3$) δ 142.2, 141.4, 141.0, 140.0, 130.7, 130.4, 129.0, 128.0, 127.8, 127.7, 126.7, 126.5, 126.0, 117.9, 67.8, 57.1, 53.9 ppm; **IR** (neat) ν = 3442, 3058, 3026, 2924, 2855, 1599, 1493, 1448, 1038, 922, 746, 700 cm^{-1}; **HRMS (APCI)** *m/z*: $[M-OH]^+$ Calcd for $C_{23}H_{21}^+$ 297.1638, found 297.1635; the enantiomeric excess was determined by UPC2 analysis on Chiralpak IG, mobile phase: CO_2:EtOH 75:25, flow rate 2 mL/min, ABPR 2000 psi, t_R = 2.80 min (major), t_R = 4.00 min (minor).

2-Phenyl-2-(1-phenylethyl)but-3-en-1-ol (3.3ai)

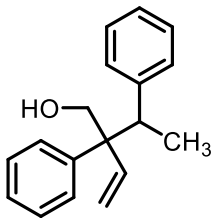

Colorless oil, 13.3 mg, 53%; *dr* = 1.1/1; 88.5:11.5 *er*, 89:11 *er*, $[\alpha]_D^{25}$ = +15.72 (c 0.54, $CHCl_3$); (hexane/acetic acid 250:0.5 v/v). **^{1}H NMR** (400 MHz, $CDCl_3$) δ 7.50-7.43 (m, 2H), 7.42-7.34 (m, 2H), 7.32-7.20 (m, 10H), 7.15-7.08 (m, 4H), 6.82-6.74 (m, 2H), 6.25 (dd, *J* = 18.1, 11.4 Hz, 1H), 6.07 (dd, *J* = 17.9, 11.1 Hz, 1H), 5.54 (dd, *J* = 11.1, 1.2 Hz, 1H), 5.44 (dd, *J* = 11.3, 1.2 Hz, 1H), 5.30 (dd, *J* = 17.8, 1.2 Hz, 1H), 4.96 (dd, *J* = 18.1, 1.2 Hz, 1H), 3.78 (s, 2H), 3.72-3.60 (m, 2H), 3.52 (d, *J* = 11.1 Hz, 1H), 3.37 (q, *J* = 7.2 Hz, 1H), 1.63-1.51 (*br* m, 2H), 1.22 (d, *J* = 7.2 Hz, 3H), 1.19 (d, *J* = 7.3 Hz, 3H) ppm; **^{13}C NMR** (101 MHz, $CDCl_3$) δ 142.5, 142.5, 142.1, 141.7 140.0, 138.0, 129.6, 129.5, 129.4, 128.42, 128.40, 127.6, 127.5, 127.3, 126.7, 126.6, 126.5, 126.4, 117.8, 117.5, 67.7, 65.2, 54.8, 54.0, 44.3, 43.8, 16.6, 16.4 ppm; **IR** (neat) ν = 3456, 3058, 3028, 2971, 2929, 2880, 1600, 1494, 1450, 1032, 919, 767, 700 cm^{-1}; **HRMS (APCI)** *m/z*: $[M\text{-}OH]^+$ Calcd for $C_{18}H_{19}^+$ 235.1481, found 235.1480; the enantiomeric excess was determined by UPC2 analysis on Chiralpak IG, mobile phase: CO_2:EtOH 75:25, flow rate 2 mL/min, ABPR 2000 psi, t_R = 2.25 min (major), t_R = 2.92 min (minor), t_R = 3.59 min (major), t_R = 4.02 min (minor).

2,3-Diphenyl-2-vinylpentan-1-ol (3.3aj)

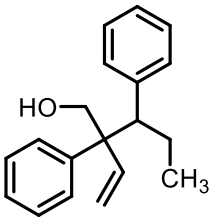

Colorless oil, 17.7 mg, 66%; *dr* = 1.1/1; 90.5:9.5 *er*, 90.5:9.5 *er*, $[\alpha]_D^{25}$ = +29.02 (c 0.77, $CHCl_3$); (hexane/acetic acid 250:1.5 – 250:2 v/v). **^{1}H NMR** (400 MHz, $CDCl_3$) δ 7.52-7.44 (m, 2H), 7.43-7.36 (m, 2H), 7.31 – 7.23 (m, 9H), 7.18-7.06 (m, 5H), 6.76-6.68 (m, 2H), 6.23 (dd, *J* = 18.1, 11.3 Hz, 1H), 6.09 (dd, *J* = 17.8, 11.1 Hz, 1H), 5.53 (dd, *J* = 11.1, 1.2 Hz, 1H), 5.44 (dd, *J* = 11.4, 1.1 Hz, 1H), 5.24 (dd, *J* = 17.8, 1.2 Hz, 1H), 4.96 (dd, *J* = 18.1, 1.2 Hz, 1H), 3.80-3.63 (m, 2H), 3.58 (d, *J* = 11.1 Hz, 1H), 3.45 (d, *J* = 11.1 Hz, 1H), 3.32 (dd, *J* = 11.0, 3.6 Hz, 1H), 3.00 (dd, *J* = 12.2, 2.7 Hz, 1H), 1.96-1.81 (m, 1H), 1.71-1.57 (m, 3H), 1.31-1.21 (s, 2H) 0.65 (overlapped, double t, *J* = 7.4 Hz, 6H) ppm; **^{13}C NMR** (101 MHz, $CDCl_3$) δ 143.1, 142.9, 140.4, 139.8, 139.8, 138.4, 130.2, 129.6, 128.5, 128.2, 127.5, 127.44, 127.40, 126.6, 126.6, 126.5, 126.4, 117.7, 117.2, 67.9, 65.1, 55.2, 54.4, 53.3, 52.5, 23.6, 23.3, 12.8, 12.7 ppm; **IR** (neat) ν = 3454, 3059, 3028, 2961, 2929, 2874, 1600, 1494, 1451, 1041, 919, 761, 699 cm^{-1}; **HRMS (APCI)** *m/z*: $[M\text{-}OH]^+$ Calcd for $C19H21^+$ 249.1638, found 249.1636; the enantiomeric excess was

determined by UPC2 analysis on Chiralpak IG, mobile phase: CO_2:EtOH 80:20, flow rate 2 mL/min, ABPR 2000 psi, t_R = 2.14 min (major), t_R = 2.68 min (minor), t_R = 2.97 min (major), t_R = 3.17 min (minor).

3.4.8. Post-synthetic transformations

(*S*)-2-Benzyl-2-phenylbutane-1,4-diol (*S*)-3.4

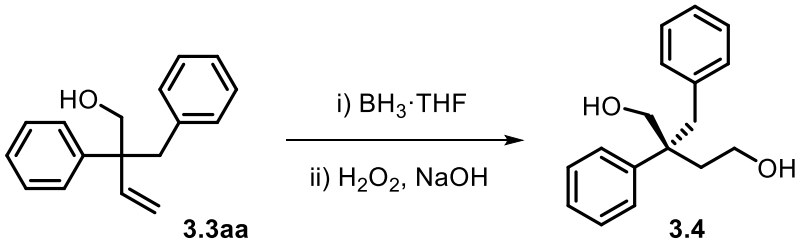

3.3aa **3.4**

A solution of **3.3aa** (23.8 mg, 0.1 mmol, 1.0 equiv.) in 1 mL dry THF was cooled in an ice-water bath for several minutes and charged with a borane solution (1M, 0.2 mmol, 2.0 equiv.). The reaction mixture was stirred at 0 °C in an ice bath for 3 h and quenched with 15% sodium hydroxide (1.0 ml) and 30% hydrogen peroxide (1.0 mL). After stirring for 16 h, ethyl acetate was added. The organic layer was washed with brine and dried over anhydrous Na_2SO_4. After concentration under reduced pressure, the crude product was purified through flash silica gel chromatography (Hexane/EA 10:1 – 5:1, v/v) to afford the desired product **3.4** (white solid, 18.4 mg, 72%).[24] $[\alpha]_D^{25}$ = +8.63 (c 0.31, $CHCl_3$); **^{1}H NMR** (400 MHz, $CDCl_3$) δ 7.36-7.28 (m, 2H), 7.25-7.20 (m, 1H), 7.19-7.07 (m, 5H), 6.79-6.67 (m, 2H), 4.00 (d, *J* = 11.5 Hz, 1H), 3.86 (d, *J* = 11.5 Hz, 1H), 3.82-3.71 (m, 1H), 3.71-3.53 (m, 1H), 2.94 (s, 2H), 2.34 (*br* s, 2H), 2.25-2.11 (m, 1H), 2.11-1.97 (m, 1H) ppm; **^{13}C NMR** (101 MHz, $CDCl_3$) δ 142.8, 137.2, 130.5, 128.4, 127.6, 127.2, 126.3, 126.1, 66.6, 59.2, 46.7, 45.8, 38.5 ppm; **IR** (neat) ν = 3337, 3229, 3059, 3029, 2918, 2856, 1493, 1447, 1333, 1042, 1002, 750, 694 cm^{-1}; **HRMS (ESI)** *m/z*: $[M+Na]^+$ Calcd for $C_{17}H_{20}NaO_2^+$ 279.1356, found 279.1359.

(24) S. Guduguntla, J.-B. Gualtierotti, S. S. Goh, B. L. Feringa, *ACS Catal.* **2016**, *6*, 6591-6595.

5-Benzyl-5-phenyl-5,6-dihydro-2H-pyran-2-one (3.5)

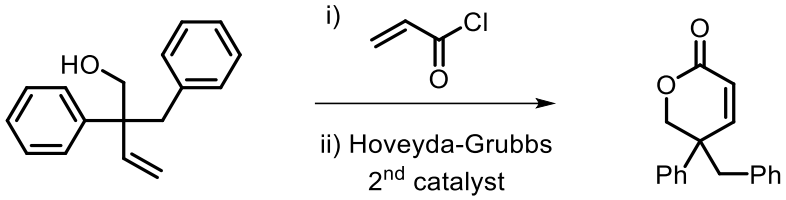

3.3aa **3.5**

To a solution of **3.3aa** (23.8 mg, 0.1 mmol, 1.0 equiv.) in CH_2Cl_2 (1.0 mL) at 0 °C, then was added dropwise DIPEA (0.1 mL, 0.6 mmol, 6.0 equiv.) followed by acryloyl chloride (24 µL, 0.3 mmol, 3.0 equiv.). The resulting reaction mixture was stirred at room temperature for 2 h and then quenched with water (10 mL). The aqueous layer was extracted with CH_2Cl_2. The combined organic layers were dried over anhydrous Na_2SO_4, filtered and concentrated under reduced pressure to afford the desired ester. Then, to a solution of this ester (0.1 mmol, 1.0 equiv.) in anhydrous toluene (0.02 M) was added Hoveyda-Grubbs II catalyst (10 mol %, 6.3 mg). The resulting mixture was heated at 80 °C with an oil bath for 24 h. After this time, all volatiles were removed under reduced pressure. The crude material was purified by column chromatography on silica gel (Hexane/EA 10:1, v/v) to afford the desired α,β-unsaturated lactone **3.5** (yellowish oil, 20.8 mg) in 79% yield.[25] $[\alpha]_D^{25}$ = +13.47 (c 0.93, $CHCl_3$); **^{1}H NMR** (400 MHz, $CDCl_3$) δ 7.40-7.28 (m, 3H), 7.25-7.11 (m, 6H), 6.84-6.75 (m, 2H), 6.12 (d, *J* = 9.9 Hz, 1H), 4.58-4.45 (m, 2H), 3.33-3.06 (m, 2H) ppm; **^{13}C NMR** (101 MHz, $CDCl_3$) δ 163.3, 152.8, 139.8, 135.1, 130.2, 128.8, 128.1, 127.6, 127.0, 126.6, 120.3, 74.4, 44.0, 43.5 ppm; **IR** (neat) *ν* = 3060, 3029, 2926, 2857, 1725, 1601, 1495, 1450, 1228, 1075, 831, 758, 700 cm^{-1}; **HRMS (ESI)** *m/z*: $[M+Na]^+$ Calcd for $C_{18}H_{16}NaO_2^+$ 287.1043, found 287.1046.

(25) Y. Xiong, G. Zhang, *J. Am. Chem. Soc.* **2018**, *140*, 2735-2738.

1-(3-Hydroxy-1,2-diphenylbutan-2-yl)cyclohexan-1-ol (3.6)

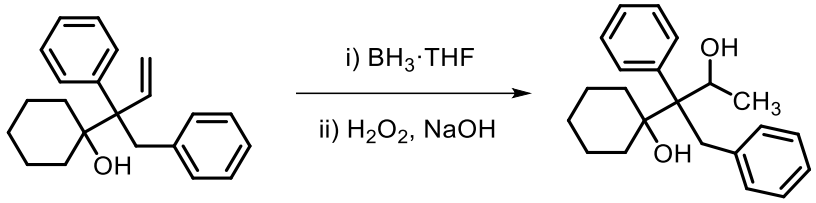

3.3ka **3.6**

A solution of **3.3ka** (30.5 mg, 0.1 mmol, 1.0 equiv.) in 1 mL dry THF was cooled in an ice-water bath for several minutes and charged with a borane solution (1M, 0.2 mmol, 2.0 equiv.). The reaction mixture was stirred at 0 °C in an ice bath for 3 h and quenched with 15% sodium hydroxide (1.0 ml) and 30% hydrogen peroxide (1.0 mL). After another 2 h, ethyl acetate was added. The organic layer was washed with brine and dried over anhydrous Na_2SO_4. After concentration under reduced pressure, the crude product was purified through flash silica gel chromatography (Hexane/EA 20:1 – 15:1, v/v) to afford the desired product **3.6**.[24]

Diastereomer 1 (white solid, 10.6 mg, 34%): $[\alpha]_D^{25}$ = +7.55 (c 0.43, $CHCl_3$); **^{1}H NMR** (400 MHz, $CDCl_3$) δ 7.92 (d, *J* = 7.7 Hz, 2H), 7.47-7.12 (m, 10H), 4.69 (q, *J* = 6.3 Hz, 1H), 3.39 (d, *J* = 14.7 Hz, 1H), 3.25 (d, *J* = 14.7 Hz, 1H), 2.08-1.93 (m, 1H), 1.78-1.41 (m, 9H), 1.26 (s, 2H), 0.99 (d, *J* = 6.3 Hz, 3H) ppm; **^{13}C NMR** (101 MHz, $CDCl_3$) δ 139.3, 139.3, 131.2, 130.8, 128.2, 127.6, 126.8, 126.5, 78.0, 71.7, 56.7, 38.7, 33.0, 31.5, 25.6, 22.2, 21.5, 20.2 ppm; **IR** (neat) ν = 3321, 3058, 3027, 2928, 2855, 1496, 1449, 1262, 1089, 1029, 963, 803, 743, 701 cm^{-1}; **HRMS (ESI)** *m/z*: $[M+Na]^+$ Calcd for $C_{22}H_{28}NaO_2^+$ 347.1982, found 347.1982.

Diastereomer 2 (white solid, 18.6 mg, 60%): $[\alpha]_D^{25}$ = +56.39 (c 0.61, $CHCl_3$); **^{1}H NMR** (400 MHz, $CDCl_3$) δ 7.54 (d, *J* = 7.2 Hz, 2H), 7.38-7.24 (m, 5H), 7.19-7.06 (m, 3H), 5.19 (q, *J* = 6.6 Hz, 1H), 3.76 (d, *J* = 15.2 Hz, 1H), 3.69 (d, *J* = 15.2 Hz, 1H), 3.19 (*br* s, 2H), 2.11-1.87 (m, 2H), 1.63-1.45 (m, 5H), 1.31-1.20 (m, 2H), 1.15-1.05 (m, 1H), 0.77 (d, *J* = 6.6 Hz, 3H) ppm; **^{13}C NMR** (101 MHz, $CDCl_3$) δ 141.3, 140.9, 131.2, 130.6, 127.9, 127.1, 126.4, 126.0, 79.0, 71.3, 56.8, 32.7, 32.5, 31.8, 25.2, 22.0, 21.6, 21.2 ppm; **IR** (neat) ν = 3197, 3089, 3026, 2922, 2854, 1493, 1446, 1263, 1093, 1044, 950, 697 cm^{-1}; **HRMS (ESI)** *m/z*: $[M+Na]^+$ Calcd for $C_{22}H_{28}NaO_2^+$ 347.1982, found 347.1983.

(2-(Cyclohex-1-en-1-yl)but-3-ene-1,2-diyl)dibenzene (3.7)

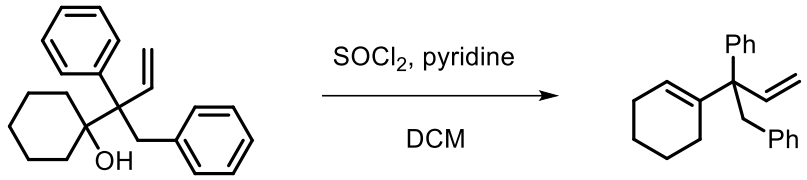

3.3ka **3.7**

To a solution of **3.3ka** (30.6 mg, 0.1 mmol, 1.0 equiv.) in dry CH_2Cl_2 (0.5 mL) at 0 °C in an ice bath under argon were gradually added pyridine (40 µL, 0.5 mmol, 5.0 equiv.) and $SOCl_2$ (40 µL, 0.2 mmol, 2.0 equiv.). The mixture was stirred at 0 °C for 2 h and then poured into ice water. The organic layer was separated, and the aqueous phase was extracted with CH_2Cl_2. The combined extracts were washed with saturated solution of $NaHCO_3$ and brine, and then dried (Na_2SO_4). Evaporation of the solvent left a crude, which was purified by flash chromatography on silica gel (Hexane/EA 50:1, v/v) to afford the desired, skipped alkene **3.7** (colorless oil, 25.5 mg) in 88% yield.[26] $[\alpha]_D^{25}$ = +29.19 (c 0.71, $CHCl_3$); **^{1}H NMR** (400 MHz, $CDCl_3$) δ 7.33-7.19 (m, 6H), 7.17-7.11 (m, 3H), 6.95-6.80 (m, 2H), 6.12 (dd, *J* = 17.5, 10.7 Hz, 1H), 5.82-5.66 (m, 1H), 5.16 (dd, *J* = 10.7, 1.8 Hz, 1H), 4.83 (dd, *J* = 17.5, 1.8 Hz, 1H), 3.36-3.15 (m, 2H), 2.28-2.03 (m, 2H), 1.85-1.71 (m, 2H), 1.66-1.52 (m, 4H) ppm; **^{13}C NMR** (101 MHz, $CDCl_3$) δ 144.4, 143.1, 140.6, 138.3, 130.9, 128.5, 127.7, 127.6, 125.9, 125.8, 124.1, 114.6, 55.4, 45.0, 27.0, 25.8, 23.2, 22.6 ppm; **IR** (neat) ν = 3056, 3027, 2926, 2855, 1600, 1493, 1447, 920, 758, 696 cm^{-1}; **HRMS (APCI)** *m/z*: $[M+H]^+$ Calcd for $C_{22}H_{25}^+$ 289.1951, found 289.1949.

(26) A. Fernández-Mateos, A. I. Ramos Silvo, R. Rubio González, M. S. J. Simmonds, *Tetrahedron* **2006**, *62*, 7809-7816.

3.4.9. Mechanistic studies

3.4.9.1. Quantum yield determination

The kinetics of the reaction were followed by monitoring characteristic IR bands corresponding to reagent **3.1k** and **3.2a**, and the pyridine-based byproduct **Py**. For this purpose, a Mettler Toledo FTIR ReactIR 15 spectrometer equipped with a MTC detector and a diamond AgX Fiber Probe was used. To a three-neck flat-bottom flask, charged with **3.2a** (60.0 mg, 0.15 mmol, 1.5 equiv.), $Ir(ppy)_2(dtbbpy)PF_6$ (1 mol%, 0.9 mg), $Pd_2(dba)_3$ (2.5 mol%, 2.3 mg), (*R*)-3,5-*t*Bu-MeOBIPHEP **L5** (6 mol%, 6.2 mg), was added **3.1k** (25.8 mg, 0.1 mmol, 1.0 equiv.) in CH_3CN (2 mL). The ReactIR probe was inserted into the reaction mixture and the mixture was then deaerated by purging with nitrogen at 25 ℃ for 10 minutes. The mixture was stirred at 25 ℃ for 2 h under the radiation of blue LED (1.0 A, 1.6 μeinstein/s) and IR spectra were measured every 30 seconds. For **3.1k** and **3.2a**, their extinction coefficients were calculated by their known concentrations at $t = 0$, and for **Py** the final absorbance was assumed to correspond to a 1 to 1 conversion of **3.2a** into **Py**. For quantum yield determination, the number of moles of consumption of **3.1k** or **3.2a,** or production of **Py**, per second was calculated by linear regression over 5 minutes and divided by the photon flux, determined by standard ferrioxalate actinometry.[27]

(27) C. G. Hatchard, C. A. Parker, E. J. Bowen, *Math. Phys. Sci.* **1956**, *235*, 518-536.

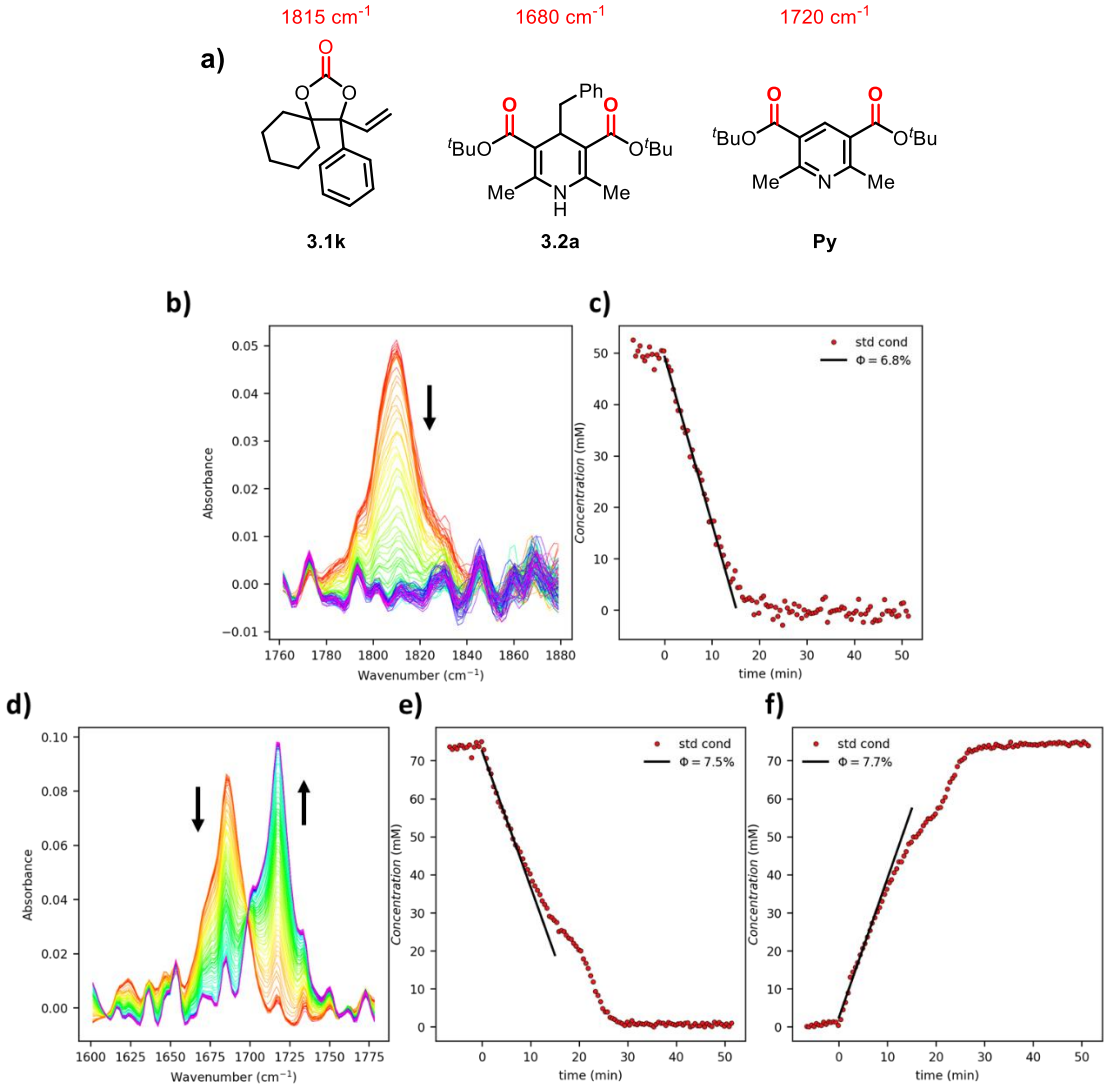

Figure 3.2. a) Structures of the compounds quantifiable by IR-spectroscopy. **b)** IR-band of the carbonate **3.1k** disappearing over time. **c)** kinetics trace of the maximum of **3.1k** (1815 cm^{-1}) as a function of time, and linear regression corresponding to a quantum yield of 6.8%. **d)** IR-band of the **3.2a** converting into **Py**. **e)** kinetics trace of the maximum of **3.2a** (1680 cm^{-1}) as a function of time, and linear regression corresponding to a quantum yield of 7.5%. **f)** kinetics trace of the maximum of **Py** (1720 cm^{-1}) as a function of time, and linear regression corresponding to a quantum yield of 7.7%. Conditions: **3.1k** (0.10 mmol), **3.2a** (0.15 mmol), $Ir(ppy)_2(dtbbpy)PF_6$ (1 µmol), $Pd_2(dba)_3$ (2.5 µmol), L* (6.0 µmol), CH_3CN (2.0 mL), 25 °C under blue LED radiation (445 nm, 1000 mA, corresponding to a photon flux of 1.6 µeinstein / s) for 2 h.

3.4.9.2. Radical trapping experiment

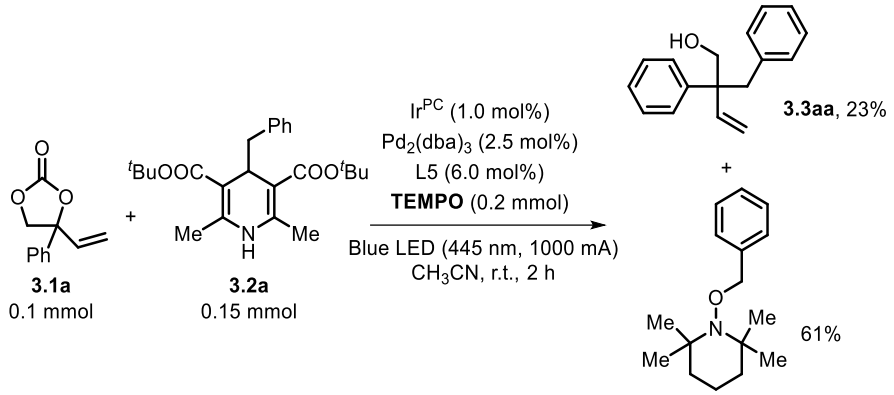

To a sealed tube charged with **3.1a** (0.1 mmol, 19.1 mg), **3.2a** (0.15 mmol, 60.0 mg), $Ir(ppy)_2(dtbbpy)PF_6$ (1 mol%, 0.9 mg), $Pd_2(dba)_3$ (2.5 mol%, 2.3 mg), (*R*)-3,5-*t*Bu-MeOBIPHEP (6 mol%, 6.2 mg), TEMPO (0.2 mmol, 31.3 mg), CH_3CN (2 mL) was added. The tube was degassed three times and filled with argon. The mixture was then stirred at 25 °C for 2 h under blue LED irradiation (1000 mA) as controlled by an external power supply. The organic phase was concentrated and purified by flash chromatography on silica gel (hexane/ethyl acetate 40/1 to 30/1, v/v) to give TEMPO-trapped product in 61% yield (22.4 mg). The spectroscopic characterization matched with the data reported in the literature.[28]

3.4.9.3. Phosphorescence quenching experiment

Stern-Volmer plot for emission quenching of $Ir(ppy)_2(dtbbpy)PF_6$ with **3.1a** and **3.2a** was shown in CH_3CN in Figure S2. Samples containing a solution of $Ir(ppy)_2(dtbbpy)PF_6$ in CH_3CN (1.83 mg in 100 mL, to obtain an absorbance of 0.1 at 445 nm over a pathlength of 1 cm) were deoxygenated through argon purge in a cuvette sealed by septum. The emission spectrum was measured by excitation at 445 nm. Then, aliquots of quencher compound (**3.1a** or **3.2a**) dissolved in the same $Ir(ppy)_2(dtbbpy)PF_6$ solution were added, thus remaining the absorbance of the solution while increasing the concentration of quencher. the averaged emission intensity between 580 and 590 nm without quencher divided by the emission intensity with quencher was then plotted as a function of the concentration of quencher to obtain the Stern-Volmer plot.

(28) Y. Yasu, T. Koike, M. Akita, *Adv. Synth. Catal.* **2012**, *354*, 3414-3420.

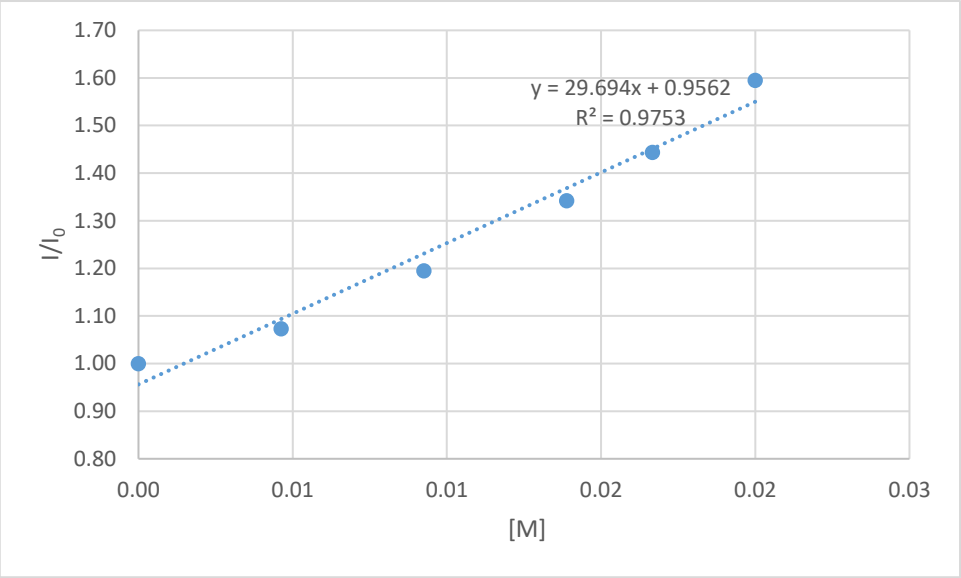

Figure 3.3 Phosphorescence quenching of $Ir(ppy)_2(dtbbpy)PF_6$ with excitation at 445 nm by **3.2a** in CH_3CN.

3.4.9.4. Proposed mechanism

Based on the results presented in section 3.4.9 and in line with previous work,[12f, 29] a plausible mechanism is proposed below. The reductive quenching process of the visible-light excited Ir(III)* by benzyl-DHP ester **3.2a** initially generates a low-valent Ir(II) complex and simultaneously delivers a radical cation, which rapidly fragments to give the corresponding alkyl radical and an aromatized pyridine derivative.[12f, 29-30] The Pd(0) precursor undergoes oxidative addition by **3.1a** to afford a π-allyl-Pd(II) species, following the addition of the alkyl radical to generate a π-allyl-Pd(III) intermediate. Subsequent reductive elimination yields the desired product **3.3aa**. The resulting Pd(I) species is then reduced to Pd(0)L by Ir(II), thereby regenerating the initial species for subsequent turnover.[12f, 29]

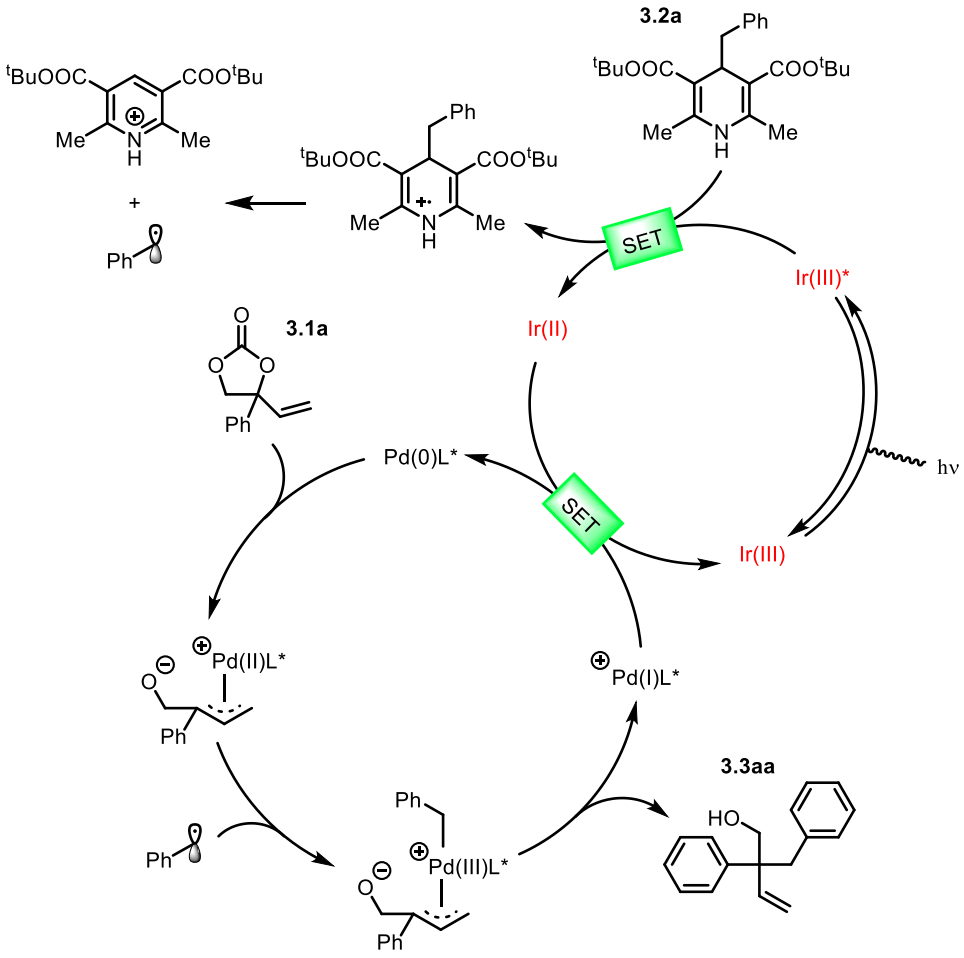

(30) a) K. Nakajima, S. Nojima, Y. Nishibayashi, *Angew. Chem. Int. Ed.* **2016**, *55*, 14106-14110; b) H.-H. Zhang, S. Yu, *J. Org. Chem.* **2017**, *82*, 9995-10006; c) B. M. Trost, M. R. Machacek, A. Aponick, *Acc. Chem. Res.* **2006**, *39*, 747-760.

In general, Pd catalyzed allylic alkylation reactions tend to favor the addition of nucleophiles on the less substituted allylic carbon center. According to the mechanism proposed, we believe that the ligand has a crucial influence on the regioselectivity. Through the investigation of various ligands over the years, a tendency towards the formation of "branched" products has demonstrated that more sterically frustrated and more electron-rich ligands give higher reactivity, branched regioselectivity and enantioselectivity. Pd intermediates coordinated with bulky diphosphine ligands representing good π-acidic ligands favor the nucleophilic addition at the more substituted allyl terminus.[30c] The ligand we have used in this study obeys the same rules, showing high steric demand as well as containing electron-rich substituents, therefore preferring the branched product, in line with previous research.[29]

3.4.10. X-ray crystallographic studies

The experimental procedure for measuring the single crystals of compounds **3.3ma** and **3.4** by X-ray diffraction is detailed in chapter 2.

Comments for the X-ray measurements for 3.3ma: With the aim to confirm the absolute configuration of the major fraction of this sample having an optical purity of 77% *ee*, different crystals were selected from the same sample vial. Finally five different crystals were measured and all of them crystallized in the same orthorhombic chiral space group $P2_12_12_1$. From the measured crystals, three corresponded to complete datasets suitable for absolute structure determination. The data of these three structure determinations are provided in CIF format. The Flack values based on Parsons' quotients were 0.04(9), 0.11(5) and 0.04(6) (references: H. D. Flack, *Acta Cryst*. **1983**, A39, 876; S. Parsons, H. Flack, *Acta Cryst*. **2004**, *A39*, S61; S. Parsons, H. D. Flack, T. Wagner, *Acta Cryst*. **2013**, *B69*, 249; the Flack *x* parameter was determined using 1698 quotients [(I+)-(I-)]/[(I+)+(I-)]). The Flack (Parsons or Hooft) parameter value for the correct absolute structure determination should be 0; the inverted structure would give 1 taking into account the standard deviation. The absolute configuration based on the structure of the measured crystals was in each case determined as (*R*) at C1 and in this way, the absolute configuration of the majority fraction is unambiguously confirmed. The three individual structures have excellent quality (no A- or B-alerts) with R_1 values of 0.0257, 0.0234 and 0.0247.

<u>Crystallographic data for 3.3ma (one selected example):</u>

$C_{19}H_{22}O$, M_r = 266.36, orthorhombic, $P2_12_12_1$, a = 6.0440(2) Å, b = 12.2290(3) Å, c = 19.7944(5) Å, $\alpha = \beta = \gamma = 90°$, V = 1463.05(7) Å^3, Z = 4, ρ = 1.209 mg·M^{-3}, μ = 0.554 mm^{-1}, λ = 0.71073 Å, T = 100(2) K, F(000) = 576, crystal size = 0.50 × 0.04 × 0.03 mm, 2θ(min) = 4.249°, 2θ(max) = 66.679°, 7612 reflections collected, 2522 reflections unique (R_{int} = 0.0282), GoF = 1.077, R_1 = 0.0247 and wR_2 = 0.0640 [$I > 2\sigma(I)$], R_1 = 0.0248 and wR_2 = 0.0641 (all indices), Flack (x) = 0.04(6), min/max residual density = −0.117/0.124 [e·Å^{-3}]. Completeness to 2θ(66.679°) = 98%. CCDC number 2077795.

Comments for the X-ray measurements for 3.4: With the aim to confirm the absolute configuration of the major fraction of this sample having with an optical purity of 78% *ee*, different crystals selected from the same sample vial were measured. Finally six different crystals (blocks and needles) were measured. Blocks crystallized in the monoclinic chiral space group $P2_1$ and the needles in the orthorhombic chiral space group $P2_12_12_1$. Both crystal forms corresponded to the same compound thus being polymorphic forms. From the measured crystals, three (1 block and two needles) corresponded to complete datasets suitable for absolute structure determination. The absolute configuration could be reliable determined for all three crystals with Flack parameter values based on Parsons' quotients of -0.04(12), 0.11(6) and 0.08(10) (references: H. D. Flack, *Acta Cryst*. **1983**, A39, 876; S. Parsons, H. Flack, *Acta Cryst*. **2004**, *A39*, S61; S. Parsons, H. D. Flack, T. Wagner, *Acta Cryst*. **2013**, *B69*, 249; the Flack *x* parameter was determined using 1698 quotients [(I+)-(I-)]/[(I+)+(I-)]). The Flack (Parsons or Hooft) parameter value for the correct absolute structure determination should be 0; the inverted structure would give 1 taking into account the standard deviation. The absolute configuration based on the structure of the measured crystals was in each of the cases determined as (*S*) at C1 and in this way, the absolute configuration of the majority fraction is unambiguously confirmed. The structures were of excellent quality (no A- or B-alerts) with R_1 values of 0.032, 0.026 and 0.028.

Crystallographic data for 3.4:

$C_{17}H_{20}O_2$, M_r = 256.33, monoclinic, $P2_1$, a = 6.42520(10) Å, b = 7.17910(10) Å, c = 15.22900(10) Å, α = 90º, β = 100.1620(10)º, γ = 90º, V = 691.451(15) Å^3, Z = 2, ρ = 1.231 mg·M^{-3}, μ = 0.079 mm^{-1}, λ = 0.71073 Å, T = 100(2) K, F(000) = 276, crystal size = 0.20 × 0.20 × 0.10 mm, θ(min) = 2.718°, θ(max) = 43.354°, 53054 reflections collected, 10421 reflections unique (R_{int} = 0.0230), GoF = 1.081, R_1 = 0.0322 and wR_2 = 0.0890 [$I > 2\sigma(I)$], R_1 = 0.0347 and wR_2 = 0.0904 (all indices), Flack (x) = -0.04(12), min/max residual density = −0.193/0.569 [e·Å^{-3}]. Completeness to θ(43.354°) = 99.7%. CCDC number 2077798.

Chapter 4.

Dual Cobalt/Organophotoredox Catalysis for Diastereo- and Regio selective 1,2-Difunctionalization of 1,3-Diene Surrogates Creating Quaternary Carbon Centers

The results described in this chapter are based on the following manuscript to be submitted:

S. Xue,[+] À. Cristòfol,[+] B. Limburg, A. W Kleij, A Dual Cobalt/Organophotoredox Catalyst for Diastereo- and Regio selective 1,2-Difunctionalization of 1,3-Diene Surrogates Creating Quaternary Carbon Centers.

4.1. Introduction

4.1.1. Difunctionalization of unsymmetrical 1,3-dienes

Catalytic intermolecular difunctionalization of unsymmetrical 1,3-dienes provides a straight-forward and atom-economical access to more complex motifs through π-allyl-metal species.[1] The addition of the latter to carbonyl reagents is one of the most useful methodologies for the formation of homoallylic alcohols,[2] while 1,3-dienes serving as π-allyl-metal precursors provide a more ideal platform than the use of stoichiometric organometallic reagents. Although significant progress has been made in stereoselective allylation of carbonyl compounds using 1,3-dienes in the recent decades,[3] diastereo- and regio-selective 1,2-difunctionalization (hydro- or alkyl-hydroxyalkylation) of unsymmetrical 1,3-dienes (and more specifically 2-substituted dienes) to construct homoallylic alcohols featuring a quaternary carbon center still remains underdeveloped and challenging (Scheme 4.1a).[4]

Most of the synthetic efforts focused on conversion of readily available 2-alkyl-1,3-dienes,[5] while the 1,2-difunctionalization of 2-aryl-1,3-dienes remains elusive. Krische and co-workers established highly efficient reductive diene-aldehyde couplings mediated by hydrogen auto-transfer under Ru-[6] and Ir-catalysis (Scheme 4.1b).[7] Despite being attractive, these processes have important limitations in scope and require expensive transition metal catalysts. Recently, sequential alkylation and carbonyl allylation of 1,3-

(1) a) G. J. P. Perry, T. Jia, D. J. Procter, *ACS Catal.* **2020**, *10*, 1485-1499; b) G. Li, X. Huo, X. Jiang, W. Zhang, *Chem. Soc. Rev.* **2020**, *49*, 2060-2118; c) H.-M. Huang, P. Bellotti, F. Glorius, *Chem. Soc. Rev.* **2020**, *49*, 6186-6197; d) X. Wu, L.-Z. Gong, *Synthesis* **2019**, *51*, 122-134; e) Y. Xiong, Y. Sun, G. Zhang, *Tetrahedron Lett.* **2018**, *59*, 347-355; f) M. Holmes, L. A. Schwartz, M. J. Krische, *Chem. Rev.* **2018**, *118*, 6026-6052.

(2) a) M. Yus, J. C. González-Gómez, F. Foubelo, *Chem. Rev.* **2013**, *113*, 5595-5698; b) K. Spielmann, G. Niel, R. M. de Figueiredo, J.-M. Campagne, *Chem. Soc. Rev.* **2018**, *47*, 1159-1173.

(3) a) M. Kimura, H. Fujimatsu, A. Ezoe, K. Shibata, M. Shimizu, S. Matsumoto, Y. Tamaru, *Angew. Chem. Int. Ed.* **1999**, *38*, 397-400; b) R. Sawaki, Y. Sato, M. Mori, *Org. Lett.* **2004**, *6*, 1131-1133; c) Y. Sato, Y. Hinata, R. Seki, Y. Oonishi, N. Saito, *Org. Lett.* **2007**, *9*, 5597-5599; d) Y. Yang, S. F. Zhu, H. F. Duan, C. Y. Zhou, L. X. Wang, Q. L. Zhou, *J. Am. Chem. Soc.* **2007**, *129*, 2248-2249; e) M. Xiang, D. E. Pfaffinger, M. J. Krische, *Chem. Eur. J.* **2021**, *27*, 13107-13116; f) M. M. Parsutkar, T. V. RajanBabu, *J. Am. Chem. Soc.* **2021**, *143*, 12825-12835.

(4) a) J. R. Zbieg, J. Moran, M. J. Krische, *J. Am. Chem. Soc.* **2011**, *133*, 10582-10586; b) Y.-L. Li, W.-D. Li, Z.-Y. Gu, J. Chen, J.-B. Xia, *ACS Catal.* **2020**, *10*, 1528-1534.

(5) a) S. Ogoshi, K. I. Tonomori, M. A. Oka, H. Kurosawa, *J. Am. Chem. Soc.* **2006**, *128*, 7077-7086; b) M. Kimura, A. Ezoe, M. Mori, K. Iwata, Y. Tamaru, *J. Am. Chem. Soc.* **2006**, *128*, 8559-8568.

(6) a) H. Han, M. J. Krische, *Org. Lett.* **2010**, *12*, 2844-2846; b) A. Köpfer, B. Sam, B. Breit, M. J. Krische, *Chem. Sci.* **2013**, *4*, 1876-1880.

(7) K. D. Nguyen, D. Herkommer, M. J. Krische, *J. Am. Chem. Soc.* **2016**, *138*, 14210-14213.

dienes was realized by Zhang,[8] Shi[9] and Glorius.[10] However, these methodologies (Scheme 4.1c) do not offer general access towards regio- and diastereo- selective 1,2-alkylation/hydroxyalkylation of a wider variety of 2- substituted dienes, and seldom report products with a quaternary carbon center.

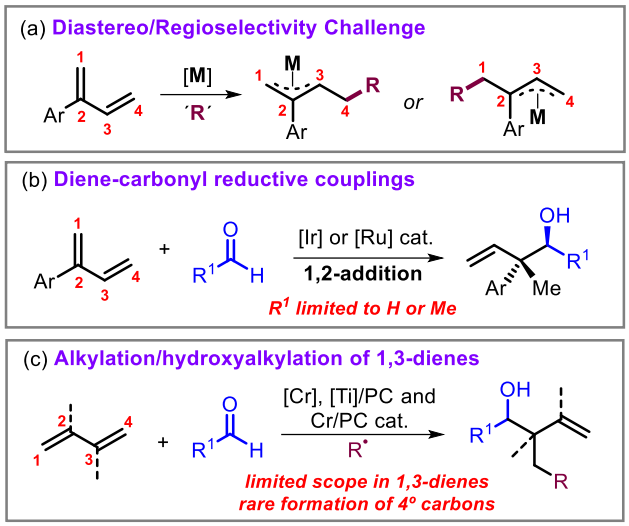

Scheme 4.1. Difunctionalization of unsymmetrical 1,3-diene and its challenge.

4.1.2. Aims and objectives

Vinylethylene carbonates (VCCs, Scheme 1d) have recently emerged as versatile substrates in allylic substitution (Scheme 1d, using NuH)[11] and cycloaddition chemistry (Scheme 1d, using E^+). [12] Despite these well-established typically Pd-catalyzed decarboxylative transformations of VCCs, their use as versatile, in situ generated 1,3-diene reagents remains undeveloped.[13] Substituted 1,3-dienes are not easily accessible,

(8) Y. Xiong, G. Zhang, *J. Am. Chem. Soc.* **2018**, *140*, 2735-2738.
(9) F. Li, S. Lin, Y. Chen, C. Shi, H. Yan, C. Li, C. Wu, L. Lin, C. Duan, L. Shi, *Angew. Chem. Int. Ed.* **2021**, *60*, 1561-1566.
(10) J. L. Schwarz, H.-M. Huang, T. O. Paulisch, F. Glorius, *ACS Catal.* **2020**, *10*, 1621-1627.
(11) a) A. Cai, W. Guo, L. Martínez-Rodríguez, A. W. Kleij, *J. Am. Chem. Soc.* **2016**, *138*, 14194-14197; b) W. Guo, L. Martínez-Rodríguez, R. Kuniyil, E. Martin, E. C. Escudero-Adán, F. Maseras, A. W. Kleij, *J. Am. Chem. Soc.* **2016**, *138*, 11970-11978; c) J. Xie, W. Guo, A. Cai, E. C. Escudero-Adán, A. W. Kleij, *Org. Lett.* **2017**, *19*, 6388-6391; d) S. Xue, B. Limburg, D. Ghorai, J. Benet-Buchholz, A. W. Kleij, *Org. Lett.* **2021**, *23*, 4447-4451; e) A. Khan, H. Zhao, M. Zhang, S. Khan, D. Zhao, *Angew. Chem. Int. Ed.* **2020**, *59*, 1340-1345; f) A. Khan, S. Khan, I. Khan, C. Zhao, Y. Mao, Y. Chen, Y. J. Zhang, *J. Am. Chem. Soc.* **2017**, *139*, 10733-10741; g) L. Shi, Y. He, J. Gong, Z. Yang, *Asian J. Org. Chem.* **2019**, *8*, 823-827.
(12) a) W. Guo, J. E. Gómez, À. Cristòfol, J. Xie, A. W. Kleij, *Angew. Chem. Int. Ed.* **2018**, *57*, 13735-13747; b) A. Khan, Y. J. Zhang, *Synlett* **2015**, *26*, 853-860; c) Q.-Z. Li, Y. Liu, M.-Z. Li, X. Zhang, T. Qi, J.-L. Li, *Org. Biomol. Chem.* **2020**, *18*, 3638-3648; d) K. Liu, I. Khan, J. Cheng, Y. J. Hsueh, Y. J. Zhang, *ACS Catal.* **2018**, 11600-11604; e) L.-C. Yang, Z. Y. Tan, Z.-Q. Rong, R. Liu, Y.-N. Wang, Y. Zhao, *Angew. Chem. Int. Ed.* **2018**, *57*, 7860-7864.
(13) For the transformation of VCCs via a two-step [4+2] cycloaddition pathway involving silylated precursors, see: a) W. Feng, L. Xu, D. Y. Li, P. N. Liu, *Org. Lett.* **2020**, *22*, 5094-5098; for the Pd-

and their direct preparation from VCCs under appropriate conditions can provide new incentives for the creation of otherwise difficult to prepare quaternary carbon centers through 1,2-difunctionalization. We envisioned a scenario in which metal/photoredox dual catalysis could provide the necessary impetus to realize this challenging cascade of events (Scheme 4.2, below). Metallaphotoredox catalysis has recently emerged as a powerful approach enabling carbon–carbon bond formation under mild conditions,[14] though cobalt-catalyzed protocols remain relatively unmapped.[15] In this realm, the allylation of aldehydes enabled by a nucleophilic allyl-Co^{II} species has recently been studied by various groups,[16] and we showed that 1,3-diols featuring quaternary carbon centers can be prepared from VCCs under high diastereocontrol.[16c]

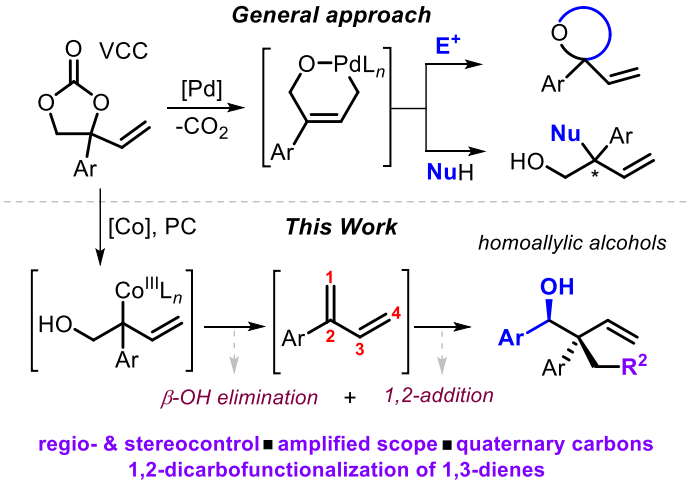

Scheme 4.2. Conceptual framework for the regio- and stereoselective conversion of VCCs into 2-aryl-substituted 1,3-dienes via Co/PC dual catalysis.

catalyzed reductive synthesis of dienes from allylic esters, see: b) H. Hattori, M. Katsukawa, Y. Kobayashi, *Tetrahedron Lett.* **2005**, *46*, 5871-5875.

(14) a) T. P. Yoon, M. A. Ischay, J. Du, *Nat. Chem.* **2010**, *2*, 527-532; b) Y. Y. Gui, L. Sun, Z. P. Lu, D. G. Yu, *Org. Chem. Front.* **2016**, *3*, 522-526; c) J. Twilton, C. Le, P. Zhang, M. H. Shaw, R. W. Evans, D. W. C. MacMillan, *Nat. Rev. Chem.* **2017**, *1*, 0052-0052; d) K. N. Lee, M. Y. Ngai, *Chem. Commun.* **2017**, *53*, 13093-13112; e) M. De Abreu, P. Belmont, E. Brachet, *Eur. J. Org. Chem.* **2020**, *2020*, 1327-1378.

(15) a) J. F. Han, P. Guo, X. G. Zhang, J. B. Liao, K. Y. Ye, *Org. Biomol. Chem.* **2020**, *18*, 7740-7750; b) A. Guérinot, J. Cossy, *Acc. Chem. Res.* **2020**, *53*, 1351-1363; c) M. Kojima, S. Matsunaga, *Trends Chem.* **2020**, *2*, 410-426; d) S. M. Thullen, T. Rovis, *J. Am. Chem. Soc.* **2017**, *139*, 15504-15508; e) P. Rai, K. Maji, B. Maji, *Org. Lett.* **2019**, *21*, 3755-3759; f) K. Takizawa, T. Sekino, S. Sato, T. Yoshino, M. Kojima, S. Matsunaga, *Angew. Chem. Int. Ed.* **2019**, *58*, 9199-9203.

(16) a) A. Gualandi, G. Rodeghiero, R. Perciaccante, T. P. Jansen, C. Moreno-Cabrerizo, C. Foucher, M. Marchini, P. Ceroni, P. G. Cozzi, *Adv. Synth. Catal.* **2021**, *363*, 1105-1111; b) C. Shi, F. Li, Y. Chen, S. Lin, E. Hao, Z. Guo, U. T. Wosqa, D. Zhang, L. Shi, *ACS Catal.* **2021**, *11*, 2992-2998; c) À. Cristòfol, B. Limburg, A. W. Kleij, *Angew. Chem. Int. Ed.* **2021**, *60*, 15266-15270; d) L. Wang, L. Wang, M. Li, Q. Chong, F. Meng, *J. Am. Chem. Soc.* **2021**, *143*, 12755-12765.

Inspired by recent contributions involving Co^{III} mediated β-hydroxide elimination as a key step,[17] we questioned whether we could harness this potential to enable the selective formation of 2-aryl substituted 1,3-dienes[18] from structurally versatile VCCs by a decarboxylation/β-hydroxide sequence (Scheme 4.2), followed by Co-catalyzed 1,2-difunctionalization. Here we show that the use of dual Co/organophotocatalysis can overcome the current limitation in 1,3-diene diversity, and allows to convert them into homoallylic alcohol products having quaternary carbon centers under both high regio- and stereocontrol.

(17) a) Y. Suzuki, B. Sun, K. Sakata, T. Yoshino, S. Matsunaga, M. Kanai, *Angew. Chem. Int. Ed.* **2015**, *54*, 9944-9947; b) T. Gensch, S. Vásquez-Céspedes, D. G. Yu, F. Glorius, *Org. Lett.* **2015**, *17*, 3714-3717; c) Y. Bunno, N. Murakami, Y. Suzuki, M. Kanai, T. Yoshino, S. Matsunaga, *Org. Lett.* **2016**, *18*, 2216-2219; d) D. Kalsi, R. A. Laskar, N. Barsu, J. R. Premkumar, B. Sundararaju, *Org. Lett.* **2016**, *18*, 4198-4201; e) M. Sen, P. Dahiya, J. R. Premkumar, B. Sundararaju, *Org. Lett.* **2017**, *19*, 3699-3702.

(18) 2-Substituted-1,3-dienes are unstable and tend to self-dimerize via Diels-Alder reactions, see: D. Fiorito, S. Folliet, Y. Liu, C. Mazet, *ACS Catal.* **2018**, *8*, 1392-1398.

4.2. Results and discussion

4.2.1. Optimization studies

In our previous work,[16c] we found that by using MeCN as solvent and DPEPhos as ligand, apart from the 1,3-diol product **4.3aa-OH** small amounts of a product was formed that was identified as **4.3aa**. Presumably, **4.3aa** is formed through addition of a [Co-H][15c] to the diene intermediate with subsequent C–C bond formation through a Zimmerman-Traxler transition state (*vide infra*). At the onset of our screening (Table 4.3, Experimental section), we selected VCC **4.1a** and benzaldehyde **4.2a** as representative substrates to develop a protocol towards the target compounds. We noted that the use of 2,2´-bipyridine (bpy) was more beneficial towards the formation of **4.3aa** (Scheme 4.3a), and after some preliminary optimization of the base, ligand and electron donor, the yield of **4.3aa** was increased to 52%.

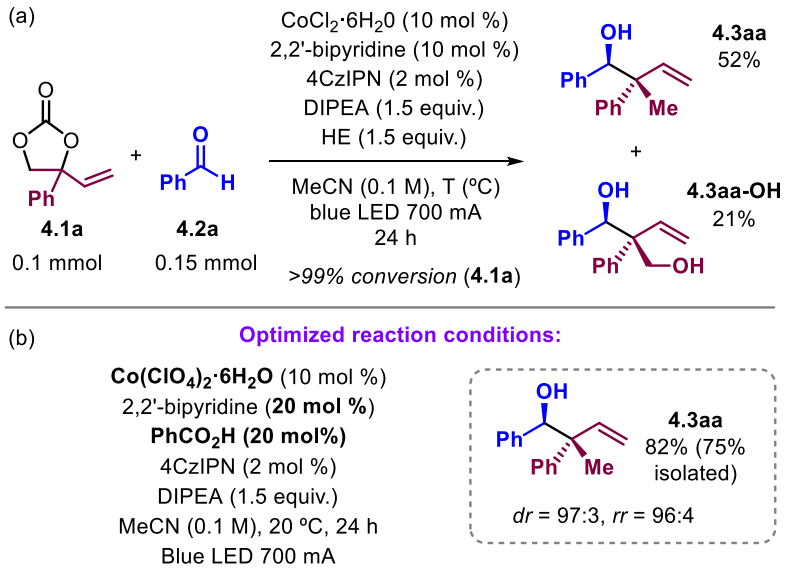

Scheme 4.3. Preliminary results (a) and optimized results (b) for the coupling of VCC **4.1a** and benzaldehyde **4.2a**.

Further optimization of the protocol was achieved by screening various base additives, photocatalysts (PCs), electron donors (EDs), cobalt precursors, ligands, solvents and acid additives (please refer to the Experimental section, Tables 4.3-4.10). The desired product **4.3aa** could be prepared in 82% yield (75% isolated, Scheme 4.3b), and with high diastereo- (*dr* = 97:3) and regio-selectivity (*rr* = 96:4). A series of control experiments (Table 4.1) showed the necessity of all the reagents.

Table 4.1. Control reactions.[a]

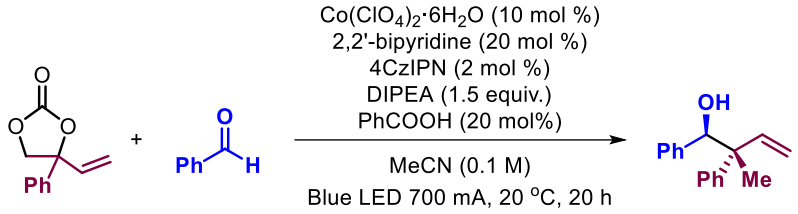

4.1a 0.1 mmol | **4.2a** 0.15 mmol | **4.3aa**

Entry	Change to std. condition	Yield (%)[b]
1	Without $PhCO_2H$	60
2	Without 2,2'-bipyridine	<5
3	Without $Co(ClO_4)_2·6H_2O$	<5
4	Without 4CzIPN	<5
5	Without light (Dark)	<5
6	Under air	<5

[a] $Co(ClO_4)_2·6H_2O$ (10 mol%), 2,2´-bipyridine (20 mol %), 4CzIPN (2 mol%), DIPEA (1.5 equiv.), $PhCO_2H$ (20 mol%), MeCN (0.1 M), freshly distilled benzaldehyde was used, 700 mA blue LED, 20 ℃ for 20 h. [b] Yields were determined by ^1H NMR using mesitylene as internal standard.

4.2.2. Scope of aldehyde partners

With the optimized condition in hand, we then started to investigate the scope of aldehyde reaction partners in this dual Co/organophotoredox catalyzed cross-coupling reaction (Scheme 4.4).

The use of aryl aldehydes with electron-withdrawing and -donating *para*-substituents was productive leading to the target products in appreciable yields (**4.3aa**-**4.3ae**: up to 76%) and with high diastereo- and regio-control. The presence of *meta*- (**4.3af**) and *ortho*-substituents (**4.3ag**) was also tolerated leading to the products in good yields and selectivities. Somewhat more elaborate aldehyde reagents were then tested (preparation of **4.3aj**-**4.3al**), adding further value to the protocol. The utilization of (unsaturated) alkyl aldehydes is also feasible (**4.3am**, 74%, >95:5 *dr*, >99:1 *rr*), giving a 1:1 mixture of diastereomers with regard to the distant tertiary chiral center already present in **4.2m**.

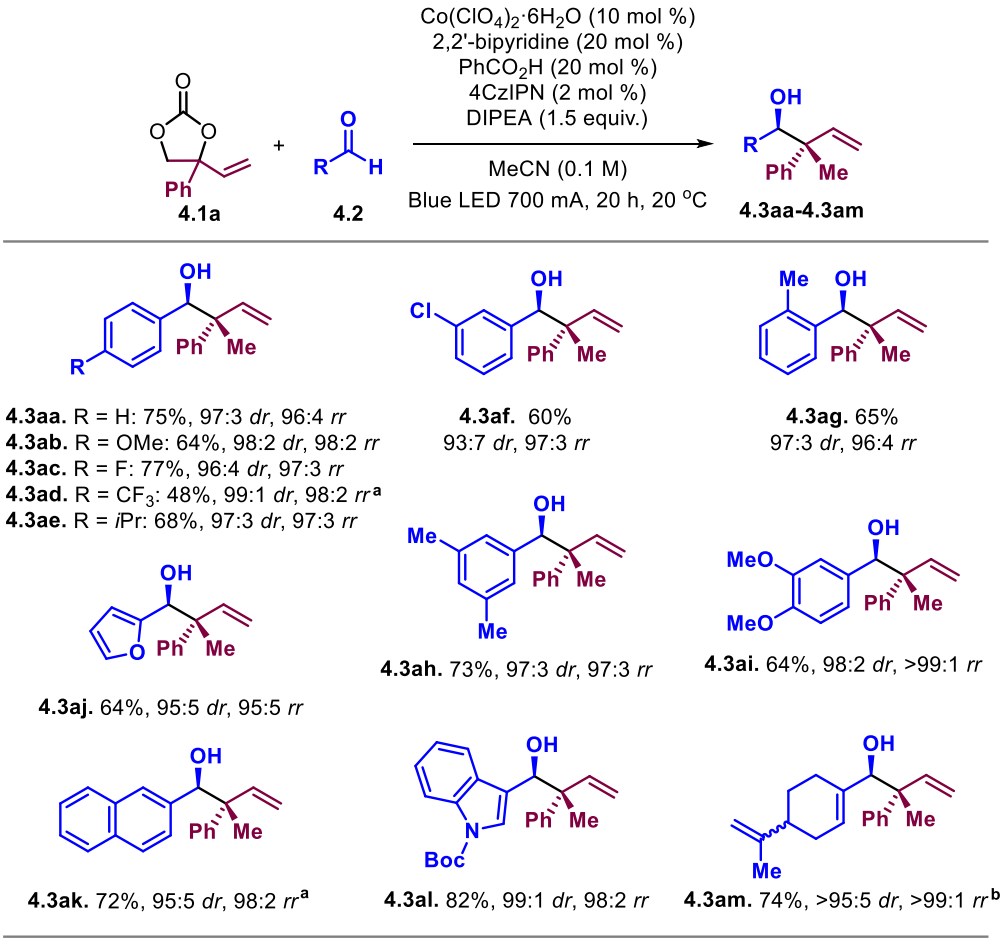

Scheme 4.4. Scope of aldehyde partners **4.2** in the dual Co/organophotoredox catalyzed 1,2-hydroalkylation of 2-phenyl-1,3-diene derived from VCC **4.1aa**. Reaction condition: all reactions performed under the optimized reaction conditions reported in Scheme 4.3b. [a] DIPEA (2.0 equiv.). [b] (*S*)-(−)-perillaldehyde was used. The reported selectivities determined for **4.3am** refer to the 1,2-hydroalkylation process.

4.2.3. Scope of VCCs

Next, we examined various VCCs **4.1** in the formation of a wider series of homoallylic alcohols (Scheme 4.5, **4.3ba-4.3pa**). Aryl-vinyl carbonates with different ring-substituents (R^1) were screened and showed that *para*-, *meta*- and *ortho*-groups (**4.3ba-4.3la**) are tolerated providing the target products in good yields (up to 76%, **3da**) and excellent *dr* and *rr* values. The yields for **4.3ga** and **4.3ha** are likely lower due to some electronic bias, whereas the low yield for **4.3ba** is explained by the competitive formation of a similar amount of a 1,3-diol byproduct (cf., **4.3aa-OH**, Scheme 4.3a).

VCC reagents equipped with other aromatic groups such as 2-naphthyl and 2-thiophenelyl represent productive substrates and provided **4.3ma** (76%) and **4.3na** (52%)

in appreciable yield and high stereo- (≥ 95:5 *dr*) and regio-selectivity (≥ 98:2 *rr*). The benzofuran-based product **4.3oa** could only be isolated in 28% though retaining high stereo/regio-fidelity. A sterically demanding phenyl substitution in the vinyl group of the VCC reagent (**4.3pa**, 29%, *dr* >99:1) was feasible though with significant corrosion of the product yield. X-ray analysis of **4.3da** (Scheme 4.5, inset) provided further support for the proposed diastereo- and regio-isomeric control in this cascade protocol.

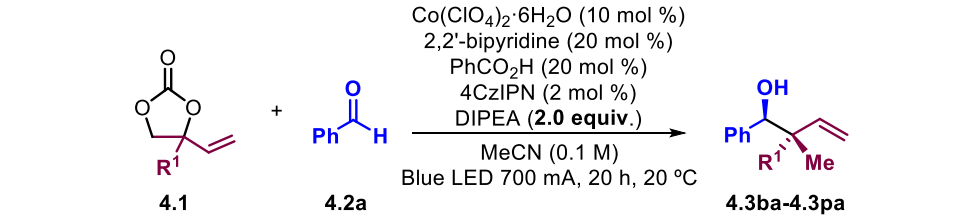

4.3ba. R = OMe: 29%, 96:4 *dr*, >99:1 *rr*
4.3ca. R = Me: 67%, 97:3 *dr*, 98:2 rr
4.3da. R = Ph: 76%, 96:4 *dr*, 98:2 *rr*
4.3ea. R = F: 74%, 97:3 *dr*, 99:1 *rr*
4.3fa. R = Cl: 69%, 95:5 *dr*, >99:1 *rr*
4.3ga. R = CF_3: 58%, 93:7 *dr*, 99:1 *rr*
4.3ha. R = SO_2Me: 46% 90:10 *dr*, 84:16 *rr*

4.3ia. R = Me: 77%
97:3 *dr,* 98:2 *rr*

4.3ja. R = OBn: 62%
96:4 *dr*, 98:2 *rr*

4.3ka. 58%
99:1 *dr*, >99:1 *rr* [a]

4.3ma. 76%, 96:4 *dr*, 98:2 *rr*

4.3na. 52%
95:5 *dr*, >99:1 *rr*

4.3la. 68%
97:3 *dr*, 99:1 *rr*

4.3oa. 28%, 97:3 *dr,* >99:1 *rr*

X-ray of **4.3da**
CCDC-2111527

4.3pa. 21%, >99:1 *dr*

Scheme 4.5. Scope of VCCs **4.1** in the Co/organophotoredox catalyzed 1,2-hydroalkylation of 2-aryl-1,3-dienes using aldehyde **4.2a**. Reaction condition: all reactions were performed under the optimized reaction conditions of Scheme 4.3b unless stated otherwise. [a] DIPEA (1.5 equiv.) was used.

4.2.4. Scope of alkyl dihydropyridines coupling partners

Inspired by the results reported in Schemes 4.4 and 4.5, we then considered the possibility of using alkyl-substituted dihydropyridines (4-alkyl-DHPs, **4.4**) to intercept the hypothesized 2-aryl-1,3-diene intermediate by alkyl radicals and to extent the catalytic protocol towards a formal 1,2-dicarbofunctionalization.

Table 4.2. Preliminary studies[a]

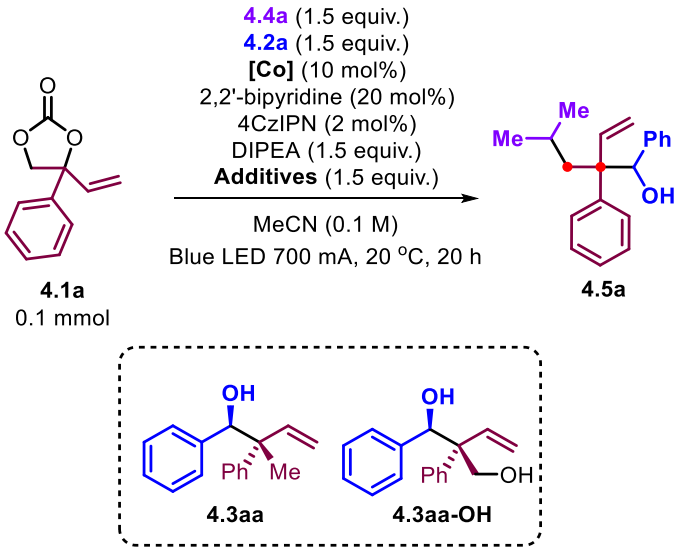

Entry	[Co]	Add.	Conv. (%)	Y. 4.5a (%)[b]	Y. 4.3aa (%)[b]	Y. 4.3aa-OH (%)[b]
1	$Co(ClO_4)_2{\cdot}6H_2O$	$NaHCO_3$	>99	22	13	14
2	$Co(ClO_4)_2{\cdot}6H_2O$	-	>99	19	5	15
3[c]	$Co(ClO_4)_2{\cdot}6H_2O$	$NaHCO_3$	>99	-	-	-
4[d]	$Co(ClO_4)_2{\cdot}6H_2O$	$NaHCO_3$	>99	50	20	-
5	**$Co(OAc)_2$**	**-**	**>99**	**22**	**47**	**-**
6[e]	$Co(OAc)_2$	-	>99	20	40	-
7[e]	$Co(OAc)_2$	4Å MS	>99	22	41	-
8[e]	$Co(OAc)_2$	dry Na_2SO_4	>99	22	39	-

[a] General procedure A: [Co] (10 mol%), 2,2´-bipyridine (20 mol %), 4CzIPN (2 mol%), DIPEA (1.5 equiv.), Additives (1.5 equiv.), MeCN, 700 mA blue LED, 20 ℃ for 20 h. [b] Yields were determined by ^1H NMR using mesitylene as internal standard. [c] In the absence of DIPEA. [d] 2-phenyl-1,3-butadiene **4.A** was used as substrate instead of **4.1a**. [e] Dry MeCN was used. Note that Y. stands for yield.

Encouragingly, preliminary studies focused on the coupling of **4.4a** and benzaldehyde **4.2a** delivered the 1,2-dicarbofunctionalization product **4.5a** in 22% yield (Table 4.2, entry 1). When 2-phenyl-1,3-diene **4.A** (Scheme 4.6) was subjected to the same latter conditions, product **4.5a** was produced in a 50% yield (Table 4.2, entry 4). Further optimization could be achieved (Experimental section, Tables 4.11-4.16), with the final conditions (Scheme 4.6, top) being used to explore the scope of 4-alkyl-DHPs.

The use of secondary alkyl substituted DHPs proved to be productive towards the preparation of various homoallylic alcohol products **4.5a**-**4.5g** using a 1-pot 2-step procedure in substantial yields and under high selectivity control, with **4.5f** and **4.5g** isolated as 1:1 mixtures of diastereoisomers (>95:5 *dr* with respect to the newly generated vicinal carbon stereocenters) as a result of the presence of a third stereogenic center. Apart from the use of secondary radical precursors, also 4-alkyl-DHPs that would in situ generate tertiary and primary radicals were tested (**4.5h**-**4.5k**). As expected, the coupling of tertiary radicals (**4.5h**, 18%) showed some limitation, whereas the coupling of primary radicals was effective providing **4.5i** and **4.5j** in reasonable yields and with high stereo/regio-selectivity. The coupling of a benzyl radical (**4.5k**, 29%) proved to be less selective.

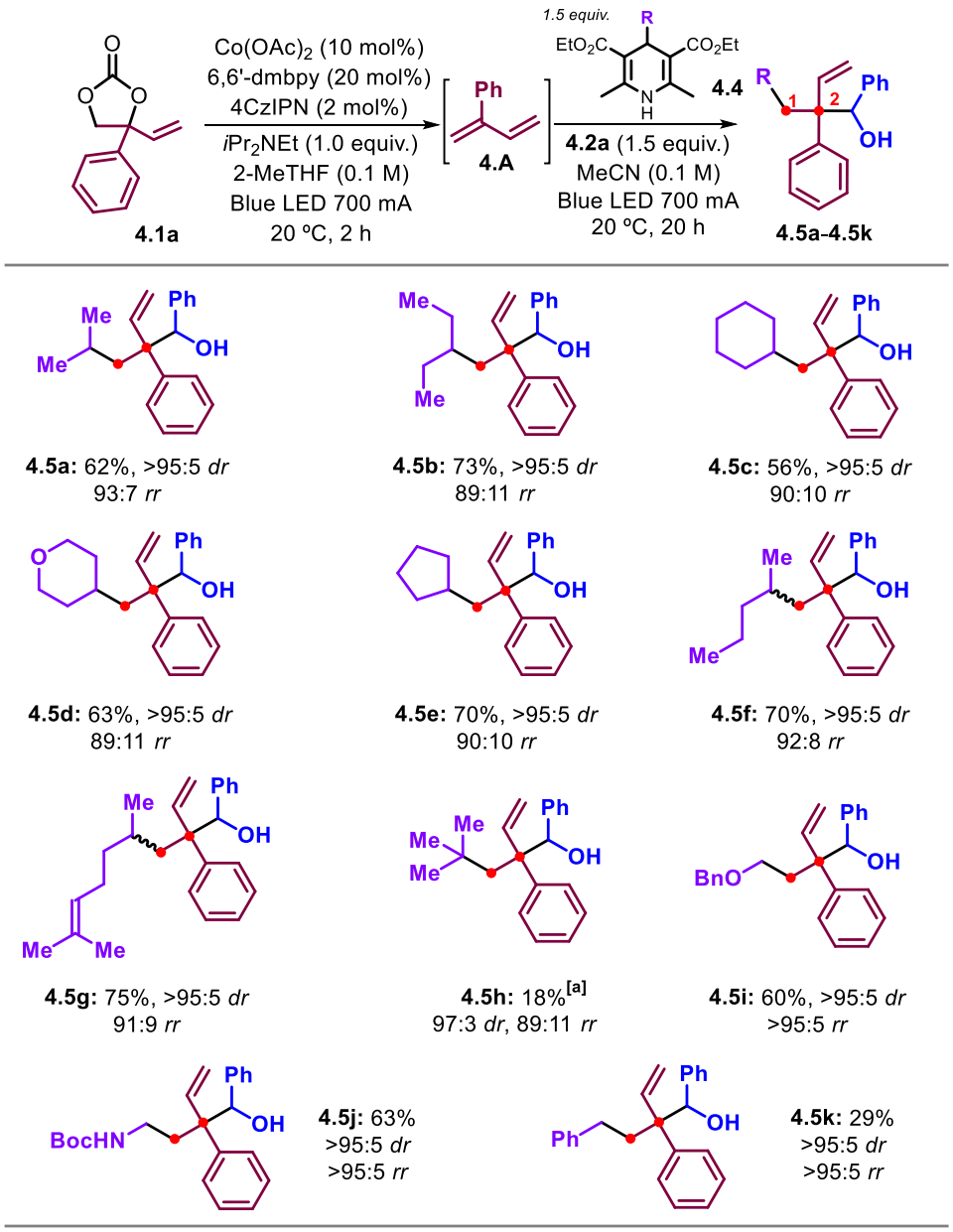

Scheme 4.6. Scope of alkyl dihydropyridines coupling partners **4.4** in the Co/organophotoredox catalyzed 1,2-dicarboalkylation of 2-phenyl-1,3-diene **4.A** derived from VCC **4.1a**. Reaction condition: all reactions performed using **4.1a** (0.1 mmol) followed by the addition of aldehyde **4.2a** (0.15 mmol) and alkyl-DHP **4.4** (0.15 mmol) in MeCN (0.1 M). [a] The corresponding Hantzsch nitrile was used.

4.2.5. Mechanistic studies

In order to gain more insights into the intermediacy of a 1,3-diene and the unusual combination of 1,3-diene formation and in situ 1,2-difunctionalization, in a first approximation, 2-phenyl-1,3-diene **4.A** was observed in a reaction mixture based on the coupling between **4.1a** and **4.2a** after 1 h by GC, together with DIPEA-derived oxidation

products acetaldehyde and diisopropylamine (see the Experimental section for more details). A detailed kinetic profile for this reaction as determined by GC (Scheme 6a) shows a near quantitative conversion of VCC **4.1a** into **4.A** within 100 minutes, while shortly hereafter the concentration of 1,3-diene **4.A** reaches a maximum (quantum yield: 1.2%). Subsequently, the concentration of **4.A** gradually decreases over time, along with slow formation of homoallylic alcohol **4.3aa** (quantum yield: 0.1%). Interestingly, the overall cascade transformation features a high mass balance with 78% of **4.3aa** being formed after 995 min (end of the kinetic trace) with 7% of unreacted 1,3-diene **4.A**.

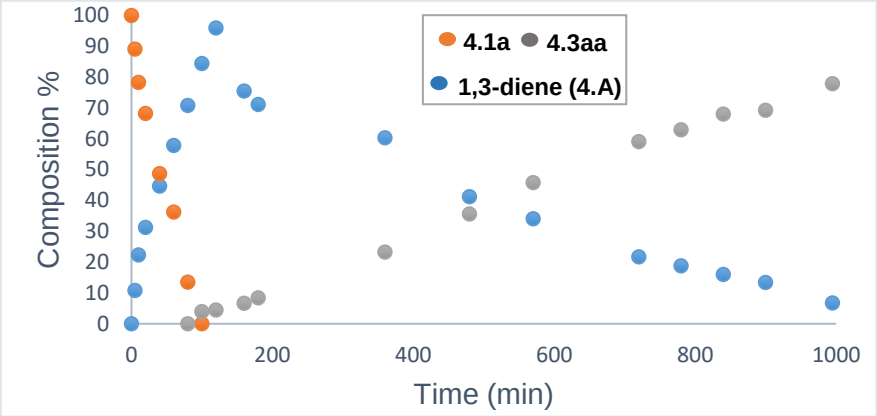

Figure 4.1. Kinetic profiles for **4.1a**, **4.3aa** and 1,3-diene **4.A** under the optimized conditions of Schemes 4.4.

To further corroborate that **4.A** is the precursor to the homoallylic product, an authentic sample of 1,3-diene was directly used as a substrate under similar reaction conditions (Scheme 4.7a) providing virtually quantitative yield (99%) of **4.3aa**. When the 1,3-diene **4.A** was subjected to the optimized conditions of the 1,2-dicarbofunctionalization (Scheme 4.7b), product **4.5a** was isolated in 41% yield, while changing the (pre)catalyst to $Co(ClO_4)_2 \cdot 6H_2O$/bpy, **4.5a** was produced in 57% yield. Altogether, these data (Figure 4.1 and Scheme 4.7) clearly demonstrate the intermediacy of **4.A** in the formation of the homoallylic alcohol end-product.

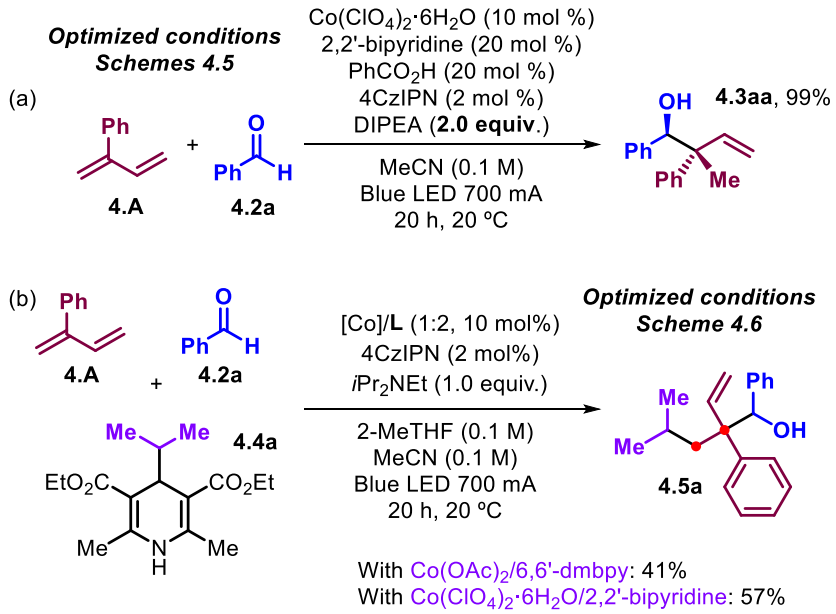

Scheme 4.7. Control experiments using 1,3-diene **4.A** as substrate.

The final control experiment in Scheme 4.8 refers to the first step of the optimized protocol of Scheme 4.6. Following these conditions, a 85% yield of 1,3-diene **4.A** species was calculated from the GC analysis performed after 2 h while deviation from the optimized reaction conditions led to no observable conversion of **4.1a**, which indicated that all the reagents were required to form the 1,3-diene **4.A**.

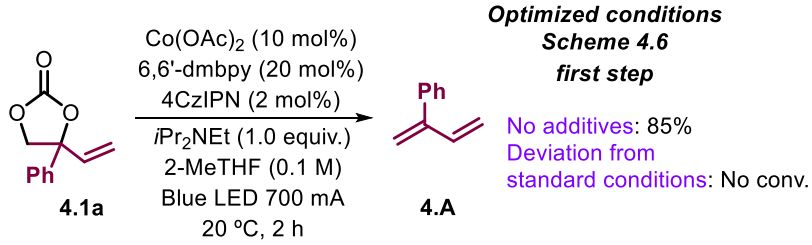

Scheme 4.8. Control experiments of the formation of 1.3-diene **4.A**.

Electrochemical analysis,[19] both cyclic voltammetry and square wave voltammetry (see Experimental section for more details),[20] ascertained that the waves at –0.98 V and –1.55 V vs $Fc|Fc^+$ correspond to the redox couples $(L)_2Co^{II/I}$ and $LCo^{II/I}$, respectively (L

(19) a) D. P. Hickey, C. Sandford, Z. Rhodes, T. Gensch, L. R. Fries, M. S. Sigman, S. D. Minteer, *J. Am. Chem. Soc.* **2019**, *141*, 1382-1392; b) T. Tang, C. Sandford, S. D. Minteer, M. S. Sigman, *Chem. Sci.* **2021**, *12*, 4771-4778.

(20) In order to further examine the reduction processes taking place at –0.98 V and –1.55 V vs $Fc|Fc^+$, square wave voltammetric analysis was performed.

= 6,6´-dmbpy).[21] The cyclic voltammograms of the $Co^{II/I}$ redox couple with increasing equivalent of VCC **4.1a** showed the absence of the re-oxidation peaks of both Co species, which indicates that the Co^{I} species generated by electrochemical reduction are likely in a dynamic equilibrium, and are fully consumed in an oxidative event to furnish prospectively an allyl-Co^{III} complex.

Due to the thermally activated delay fluorescence (TADF), time-correlated single photon counting was used to separate the biexponential decay, originating from prompt fluorescence (PF) and TADF. Their individual rate constants were assessed to determine the Stern-Volmer relationship (see the SI). The results revealed that the excited photocatalyst 4CzIPN* can be efficiently quenched by DIPEA, **4.4a** and the $Co(ClO_4)_2 \cdot 6H_2O$/6,6´-dmbpy catalyst through both PF and TADF, with DIPEA being the most efficient quencher.

On the basis of the experimental evidence and literature precedents, a plausible mechanism is proposed in Scheme 4.9. Upon irradiation with visible light, the excited state photocatalyst 4CzIPN* (E_{red}^{*} = 1.35 V vs SCE in MeCN)[22] induces single electron transfer (SET) by DIPEA ($E_{1/2}^{ox}$ = 0.65 V vs SCE in MeCN)[23] or R-DHP ($E_{1/2}^{ox}$ = 1.10 V vs SCE in MeCN)[24] to give the corresponding radical cation DIPEA$^{\cdot+}$ or R-DHP$^{\cdot+}$ as well as 4CzIPN$^{\cdot-}$.[25] The latter species (E_{red} = –1.21 V vs SCE in MeCN) is oxidized by the Co^{II} species **I** ($E_{1/2}(L_2Co^{II/I})$ = –0.58 V, $E_{1/2}(LCo^{II/I})$ = –1.15 V vs SCE in MeCN; L = 6,6´-dmbpy) and regenerates 4CzIPN closing the photoredox catalytic cycle.

The resultant radical cation DIPEA$^{\cdot+}$ would then release a hydrogen atom through HAT or an electron and proton (cf., 1,2-hydroalkylation) to afford an iminium cation,[26]

(21) The obtained value was referenced to $Fc|Fc^{+}$ and converted to saturated calomel electrode (SCE) values by adding 0.40 V. See: Connelly, N. G.; Geiger, W. E. *Chem. Rev*. **1996**, *96*, 877-910.
(22) M. A. Bryden, E. Zysman-Colman, *Chem. Soc. Rev.* **2021**, *50*, 7587-7680.
(23) T. Chatterjee, N. Iqbal, Y. You, E. J. Cho, *Acc. Chem. Res.* **2016**, *49*, 2284-2294.
(24) J.-P. Cheng, Y. Lu, X.-Q. Zhu, Y. Sun, F. Bi, J. He, *J. Org. Chem.* **2000**, *65*, 3853-3857.
(25) Alternatively, DIPEA may serve as an electron shuttle between R-DHP and the photocatalyst, see ref. 4b and: L. Qi, Y. Chen, *Angew. Chem. Int. Ed.* **2016**, *55*, 13312-13315.
(26) a) C. K. Prier, D. A. Rankic, D. W. C. MacMillan, *Chem. Rev.* **2013**, *113*, 5322-5363; b) J.-J. Zhong, Q.-Y. Meng, B. Liu, X.-B. Li, X.-W. Gao, T. Lei, C.-J. Wu, Z.-J. Li, C.-H. Tung, L.-Z. Wu, *Org. Lett.* **2014**, *16*, 1988-1991; c) K. Nakajima, Y. Miyake, Y. Nishibayashi, *Acc. Chem. Res.* **2016**, *49*, 1946-1956; d) Q. Yang, L. Zhang, C. Ye, S. Luo, L. Z. Wu, C. H. Tung, *Angew. Chem. Int. Ed.* **2017**, *56*, 3694-3698; e) Q. Y. Meng, T. E. Schirmer, K. Katou, B. König, *Angew. Chem. Int. Ed.* **2019**, *58*, 5723-5728.

while R-DHP$^{\cdot+}$ would give rise to the formation of an alkyl radical R$^{\cdot}$ (cf., 1,2-dicarbofunctionalization).[27]

Oxidative addition of the VCC to the Co^{I} species **II** produces the π-allyl-Co^{III} species **III**, and following β-hydroxy elimination yields Co^{III} complex **V**. Ligand exchange and SET reduction delivers a 1,3-diene intermediate and releases a Co^{II} species **I** for additional turnover. The 1,3-diene then enters a second Co-cycle affording first the π-allyl-Co^{III} species **VII** after combining with the 1,3-diene and a radical intermediate R$^{\cdot}$ (i.e., in the case of using DHP esters, see Scheme 5). With respect to the 1,2-hydroalkylation process (Schemes 4.4 and 4.5), the electron and proton are then captured by Co^{II} to afford a Co^{I} and a Co^{III}-H species, followed by the migratory insertion of 1,3-diene into the Co^{III}-H bond forming the π-allyl-Co^{III} species **VII**.[15c, 26] This π-allyl-Co^{III} species is then reduced by SET furnishing a nucleophilic allyl-Co^{II} species (**VIII**). The stereoselective coupling of the allyl-Co^{II} species to the aldehyde reagent through a Zimmerman-Traxler transition state (**IX**) followed by protonolysis releases the *anti*-configured[16b, 16c] homoallylic alcohol product.

(27) a) W. Huang, X. Cheng, *Synlett* **2017**, *28*, 148-158; b) P.-Z. Wang, J.-R. Chen, W.-J. Xiao, *Org. Biomol. Chem.* **2019**, *17*, 6936-6951; c) J. A. Milligan, J. P. Phelan, S. O. Badir, G. A. Molander, *Angew. Chem. Int. Ed.* **2019**, *58*, 6152-6163.

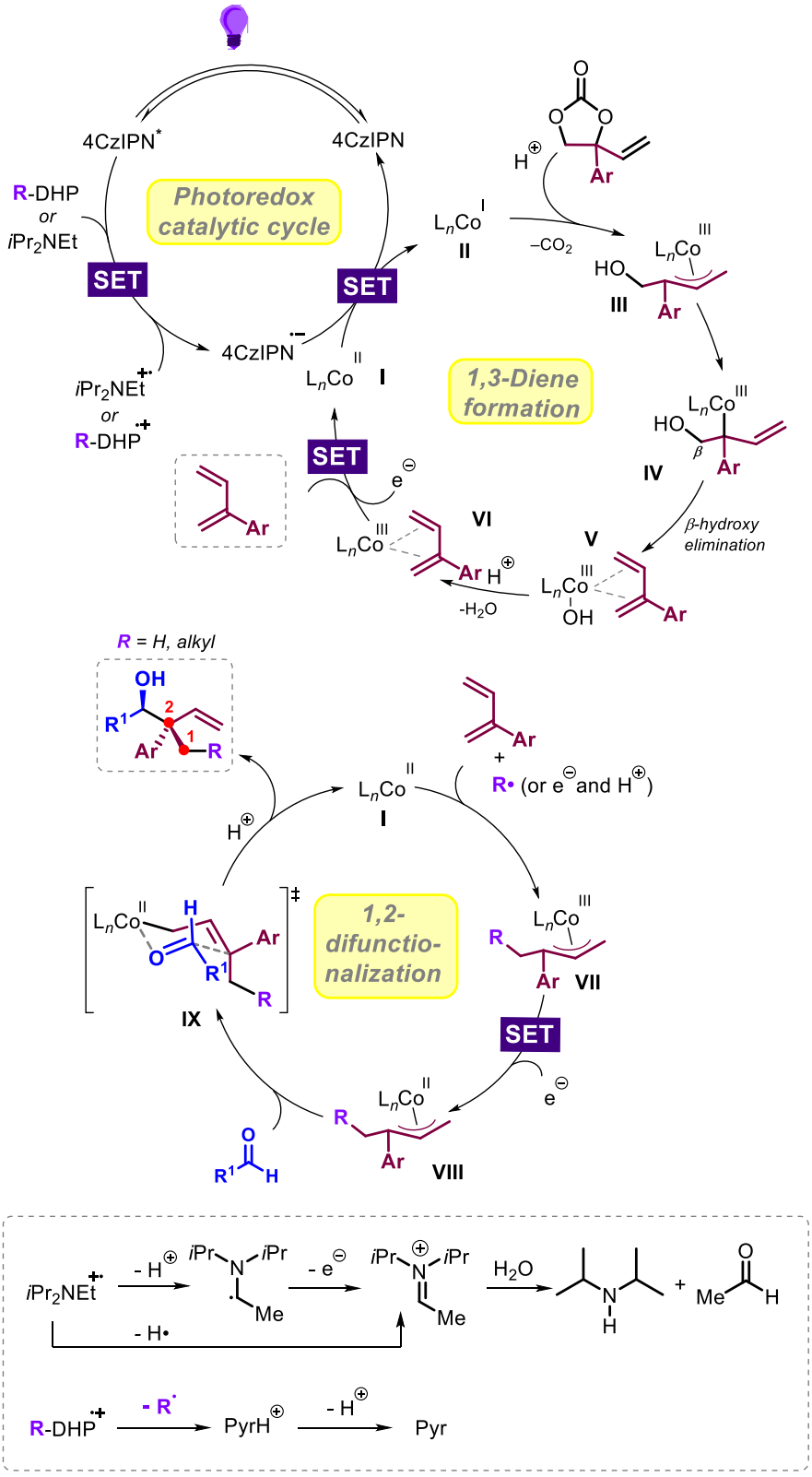

Scheme 4.9. Proposed mechanism for the catalytic cascade synthesis of homoallylic alcohols from VCCs, aldehydes and DHPs/proton source

4.3. Conclusions

The creation of sterically encumbered quaternary carbon stereocenters is among the greatest synthetic challenges in organic chemistry. The stereo- and regio-selective difunctionalization of 2-substituted 1,3-dienes has remained elusive with important limitations for existing methodologies in terms of creating such stereogenic centers. We present here an important step forward in this area by using a conceptually new dual Co/organophotoredox approach that allows to perform cascade transformations using vinyl cyclic carbonates as versatile and modular 1,3-diene surrogates. In this cascade process, a variety of 2-arylated 1,3-dienes are conveniently prepared in situ, and are selective transformed through catalytic and formal 1,2-hydroalkylation and 1,2-dicarbofunctionalization providing a wide scope of homoallylic alcohols featuring quaternary carbon centers. The manifold leading to these products is proposed to follow a pathway that involves photo-mediated SET reduction of a Co^{II} precursor allowing for oxidative addition of the VCC substrate, and producing the 1,3-diene via β-OH elimination. The present work thus unlocks new synthetic potential for the use of substituted 1,3-dienes in other types of quaternary carbon bond formation reactions.

4.4. Experimental section

4.4.1. General information

Air and water-sensitive reactions were carried out in heat-gun-dried glassware under an Ar or N_2 atmosphere using standard Schlenk manifold techniques. Reactions were monitored by TLC and/or ^{1}H NMR. TLC was carried out on 0.25 mm Merck aluminum backed sheets coated with 60 F_{254} silica gel. Visualization of the silica plates was achieved using a UV lamp (λ = 254 nm) and/or by heating plates that were dipped in a $KMnO_4$ stain or ceric ammonium molybdate stain. Flash chromatography was carried out on Sigma-Aldrich silica gel 60 (70-230 mesh) using the indicated eluent system. LED photon fluxes were measured by standard ferrioxalate actinometry.[28]

Commercially available reagents and solvents were purchased from Sigma-Aldrich, TCI, Fluorochem, Strem Chemicals, Abcr GmbH, Acros Organics or Alfa Aesar, and were used without further purification. Benzaldehyde, *p*-anisaldehyde and isobutyraldehyde were distilled under reduced pressure before use. 4CzIPN was synthesized according to a previously reported procedure.[29] Solvents were dried using an Innovative Technology PURE SOLV solvent purification system.

^{1}H NMR, ^{13}C NMR, DEPT-90, DEPT-135, and related 2D NMR (gCOSY90, gHMQC, gHMBC, gNOESY) spectra were recorded at room temperature on a Bruker AV-300, AV-400 or AV-500 spectrometer and referenced to their residual deuterated solvent signals. Coupling constants (*J*) are reported in hertz with the following splitting abbreviations: s = singlet, d = doublet, t = triplet, q = quadruplet, quint = quintet, sextet = sext, heptet = hept, br = broad and app = apparent. All reported NMR values are given in parts per million (ppm). FT-IR measurements were carried out on a Bruker Optics FTIR Alpha spectrometer. Mass spectrometric and X-ray analyses were performed by the Research Support Group at ICIQ. UV-Vis measurements were carried out on a Shimadzu UV1700PC spectrophotometer equipped with a photomultiplier detector, double beam optics and D2 and W light sources. Fluorescence measurements were carried out on a Fluorolog Horiba Jobin Yvon spectrofluorimeter equipped with photomultiplier detector, double monochromator and Xenon light source. Lifetime measurements were carried out on an Edinburgh Instruments LifeSpec-II based on the time-correlated single photon

(28) C. G. Hatchard, C. A. Parker, *Proc. R. Soc. Lond. A.* **1956**, *235*, 518-536.
(29) J. Luo, J. Zhang, *ACS Catal.* **2016**, *6*, 873-877.

counting (TCSPC) technique, equipped with a PMT detector, double subtractive monochromator and a picosecond pulsed diode laser source with a wavelength of 405 nm. Cyclic voltammetry (CV) studies and square wave voltammograms (SWVs) were carried out on a Princeton Applied Research PARSTAT 2273 potentiostat.

4.4.2. Optimization studies of 1,2-hydro/hydroxyalkylation of 2-aryl 1,3-diene deriving from VCCs

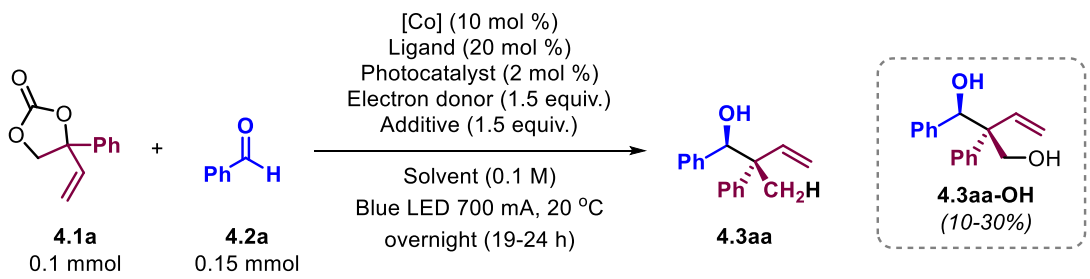

4.1a 0.1 mmol + **4.2a** 0.15 mmol → **4.3aa**

PC (2 mol%), [Co] (10 mol%) and ligand (20 mol%), base (1.5 equiv.) and ED (1.5 equiv.) were weighed in a flat-bottom Schlenk flask. Then, solvent (1 mL), VCC **4.1a** (0.1 mmol) and benzaldehyde **4.2a** (0.15 mmol) were added. The flask was sealed with a Teflon cap and the mixture was freeze-pump-thawed 3 times and stirred under N_2 at room temperature for 5–20 minutes after which it was irradiated for 20 hours at 20 °C using a single high-power blue LED (λ_{em} = 445 nm, 1.2 µeinstein s^{-1}) from the bottom. After the irradiation was stopped, the mixture was directly filtered through basic Al_2O_3 (3 cm, Ø = 0.5 cm) eluting with CH_2Cl_2/MeOH (9:1, 2.5 mL). The filtrate was evaporated to dryness and the residue was dissolved in $CDCl_3$ and analyzed by ^1H NMR using mesitylene as internal standard.

Table 4.3. Preliminary screening results[a]

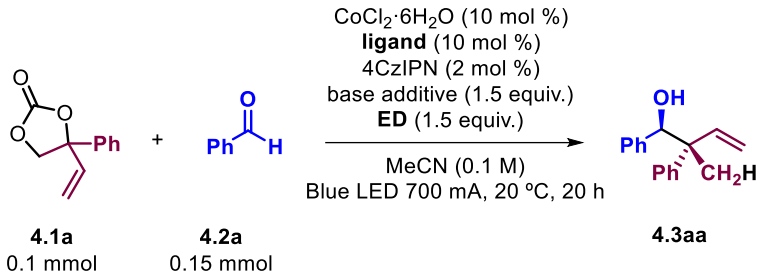

4.1a 0.1 mmol | **4.2a** 0.15 mmol | **4.3aa**

Entry	Ligand	Base	ED	Conv. (%)[b]	Yield (%)[b]
1	DPEPhos	K_3PO_4	HE	>99	0
2	DPEPhos	K_3PO_4	DIPEA	87	22
3	Bipy	K_3PO_4	DIPEA	95	36
4	dtbbpy	K_3PO_4	DIPEA	>99	28
5	Phen	K_3PO_4	DIPEA	>99	7
6	Bipy	K_3PO_4	TEA	>99	31
7	Bipy	K_3PO_4	TEOA	>99	10
8	**Bipy**	**DIPEA**	**HE**	**>99**	**52**

[a] **4.1a** (0.1 mmol), **4.2a** (aged benzaldehyde, 0.15 mmol), $CoCl_2·6H_2O$ (10 mol%), **ligand** (10 mol %), 4CzIPN (2 mol%), **base** (1.5 equiv.), **ED** (1.5 equiv.), MeCN (0.1 M), 700 mA blue LED, 20 ºC for 20 h. [b] Yields/conversions were determined by ^1H NMR using mesitylene as internal standard. ED stands for electron donor, HE is Hantzsch ester. Dtbbpy = 4,4´-di-*tert*-butyl-2,2´-dipyridine, Phen = phenanthroline, TEA = triethyl amine, TEOA = triethanol amine.

Table 4.4. Screening of additives[a]

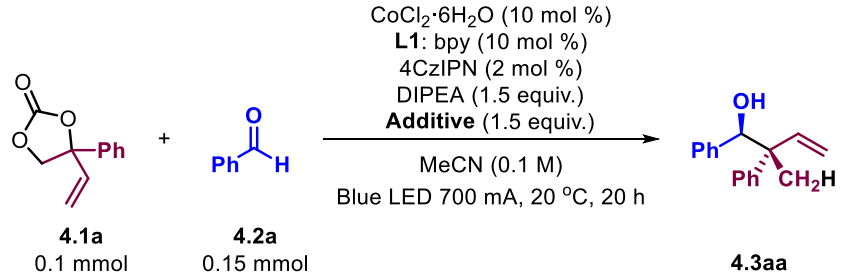

4.1a 0.1 mmol | **4.2a** 0.15 mmol | **4.3aa**

Entry	Additive	Yield (%)[b]
1	K_3PO_4	36
2	2,4,6-collidine	42
3	Cs_2CO_3	20
4	**$NaHCO_3$**	**50**
5	HE	52
6	$B(OH)_3$	42
7	Na_2HPO_4	50

[a] **4.1a** (0.1 mmol), **4.2a** (aged benzaldehyde, 0.15 mmol), $CoCl_2·6H_2O$ (10 mol%), bpy (10 mol %), 4CzIPN (2 mol%), DIPEA (1.5 equiv.), Additives (1.5 equiv.), MeCN (0.1 M), 700 mA blue LED, 20 ºC for 20 h. [b] Yields were determined by ^1H NMR using mesitylene as internal standard.

Table 4.5. Screening of electron donors[a]

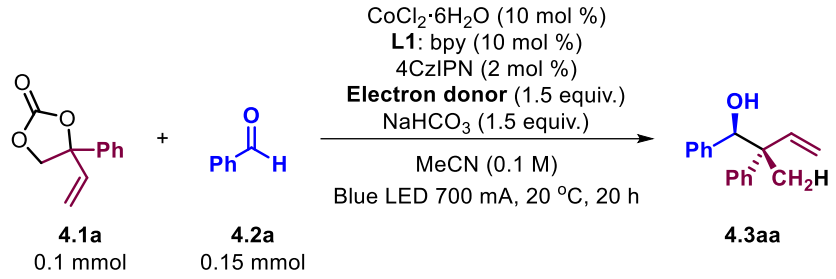

4.1a 0.1 mmol | **4.2a** 0.15 mmol | **4.3aa**

Entry	Electron Donor	Yield (%)[b]
1	**DIPEA**	**50**
2	*n*-Bu_3N	42
3	DMIPA	18
4[c]	*N*-Me-TMP	11
5[d]	TEA	31
6[d]	TEOA	10

[a] **4.1a** (0.1 mmol), **4.2a** (aged benzaldehyde, 0.15 mmol), $CoCl_2·6H_2O$ (10 mol%), bpy (10 mol %), 4CzIPN (2 mol%), $NaHCO_3$(1.5 equiv.), electron donor (1.5 equiv.), MeCN (0.1 M), 700 mA blue LED, 20 °C for 20 h. [b] Yields were determined by ^1H NMR using mesitylene as internal standard. [c] $CoCl_2(bpy)_2·3H_2O$ was used. [d] Using K_3PO_4 instead of $NaHCO_3$.

Table 4.6. Screening of cobalt sources[a]

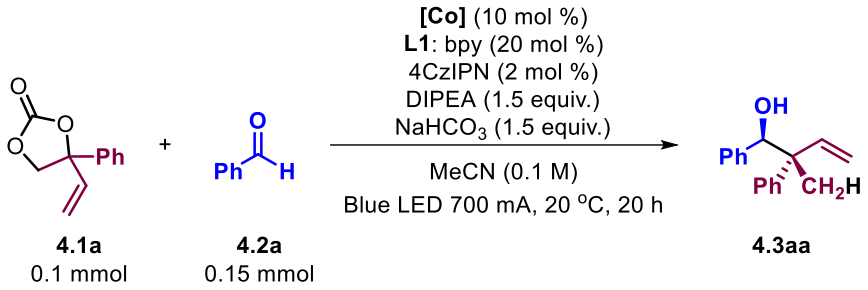

4.1a 0.1 mmol | **4.2a** 0.15 mmol | **4.3aa**

Entry	[Co]	Yield (%)[b]
1[c]	$CoCl_2·6H_2O$	50
2[d]	$CoCl_2(bpy)$	51
3[d]	$CoCl_2(bpy)_2·3H_2O$	70
4	CoF_2	<5
5	$CoBr_2$	29
6	CoI_2	30
7	$Co(OAc)_2$	80
8	$Co(NO_3)_2·6H_2O$	55
9	$Co(BF_4)_2·6H_2O$	82
10	$CoSO_4·7H_2O$	11
11	$Co(acac)_2$	34
12	**$Co(ClO_4)_2·6H_2O$**	**84**

[a] **4.1a** (0.1 mmol), **4.2a** (aged benzaldehyde, 0.15 mmol), [Co] (10 mol%), **L1**: bpy (20 mol %), 4CzIPN (2 mol%), $NaHCO_3$(1.5 equiv.), DIPEA (1.5 equiv.), MeCN (0.1 M), 700 mA blue LED, 20 ºC for 20 h. [b] Yields were determined by ^1H NMR using mesitylene as internal standard. [c] 10 mol% bpy was used. [d] Without adding exogenous bpy.

Table 4.7. Screening of ligands[a]

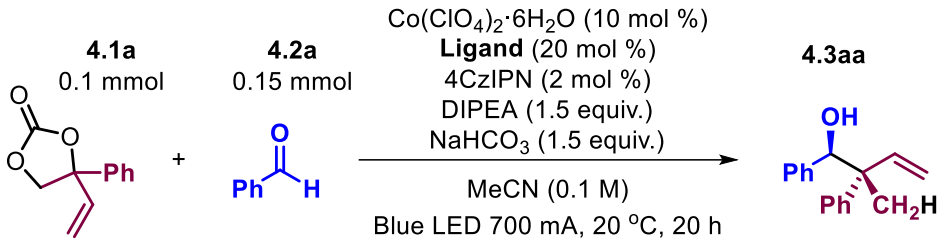

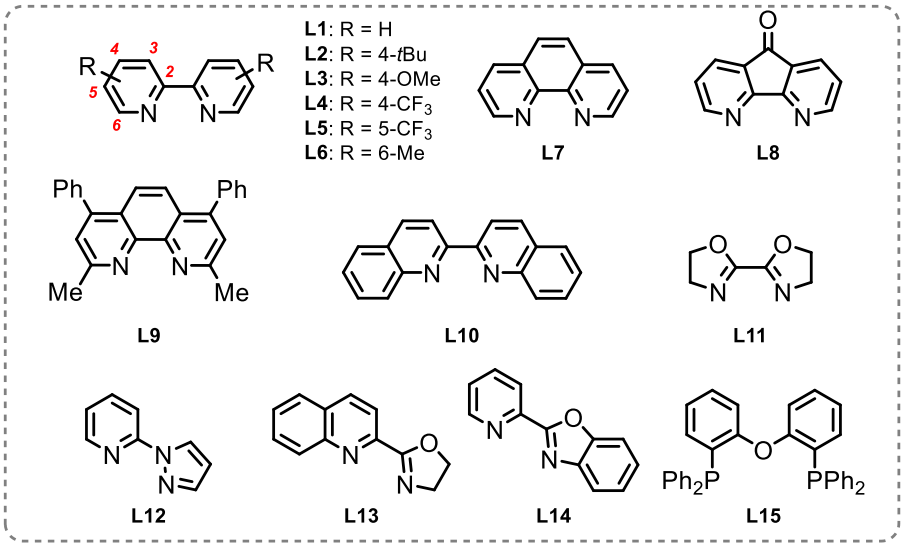

Entry	Ligand	Yield (%)[b]	Entry	Ligand	Yield (%)[b]
1	**L1**	**84**	9	**L9**	22
2	**L2**	41	10	**L10**	<5
3	**L3**	35	11	**L11**	<5
4	**L4**	8	12	**L12**	23
5	**L5**	34	13	**L13**	22
6	**L6**	31	14	**L14**	<5
7	**L7**	21	15[c]	**L15**	22
8	**L8**	27			

[a] **4.1a** (0.1 mmol), **4.2a** (aged benzaldehyde, 0.15 mmol), $Co(ClO_4)_2·6H_2O$ (10 mol%), ligand (20 mol %), 4CzIPN (2 mol%), $NaHCO_3$(1.5 equiv.), DIPEA (1.5 equiv.), MeCN (0.1 M), 700 mA blue LED, 20 ºC for 20 h. [b] Yields were determined by ^1H NMR using mesitylene as internal standard. [c] Using $CoCl_2·6H_2O$ and K_3PO_4 instead of $Co(ClO_4)_2·6H_2O$ and $NaHCO_3$.

Table 4.8. Screening of photocatalysts[a]

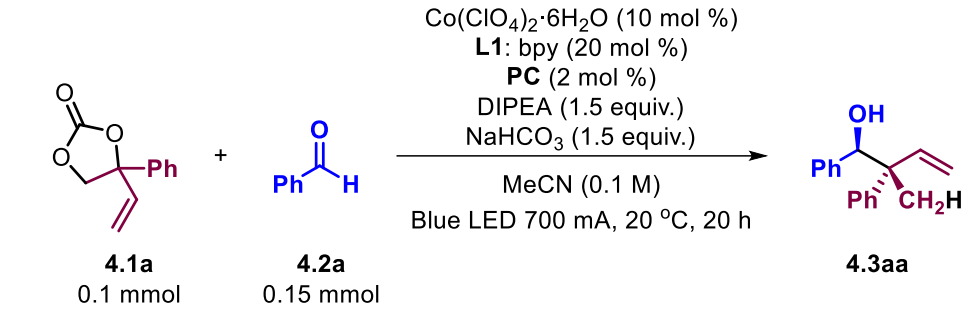

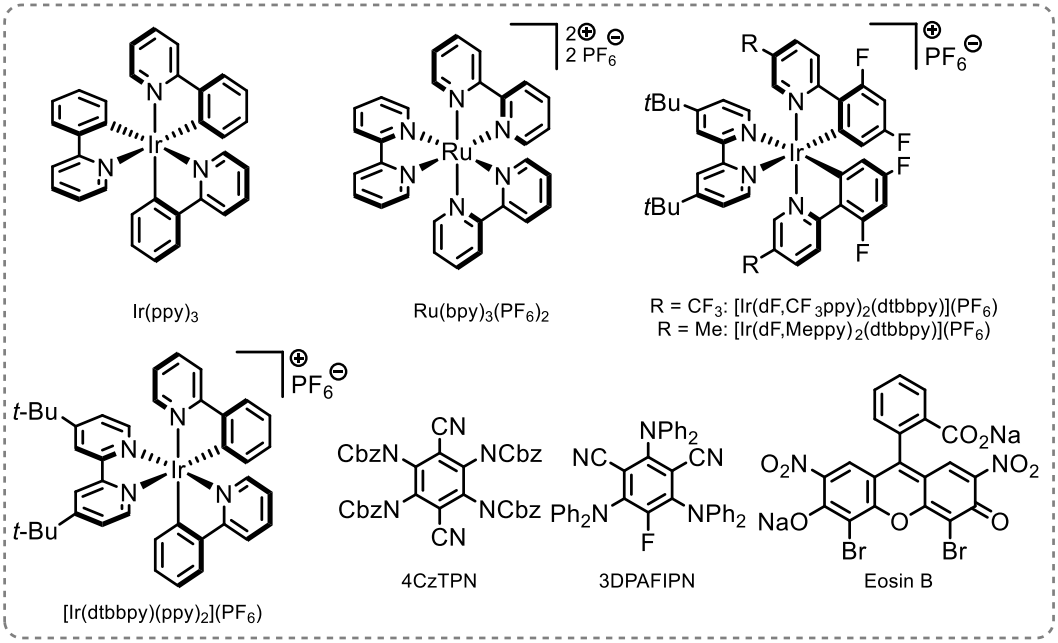

Entry	PC	Yield (%)[b]
1	**4CzIPN**	**84**
2	Eosin B	<5
3	$Ir(ppy)_3$	<5
4	$Ru(bpy)_3(PF_6)_2$	11
5	$[Ir(dF,CF_3ppy)_2(dtbbpy)](PF_6)$	47
6	$[Ir(dF,Meppy)_2(dtbbpy)](PF_6)$	41
7	$[Ir(dtbbpy)(ppy)_2](PF_6)$	<5
8	4CzTPN	5
9	3DPAFIPN	<5

[a] **4.1a** (0.1 mmol), **4.2a** (aged benzaldehyde, 0.15 mmol), $Co(ClO_4)_2·6H_2O$ (10 mol%), **L1** (20 mol %), PC (2 mol%), $NaHCO_3$(1.5 equiv.), DIPEA (1.5 equiv.), MeCN (0.1 M), 700 mA blue LED, 20 ºC for 20 h. [b] Yields were determined by ^1H NMR using mesitylene as internal standard.

Table 4.9. Screening of solvents[a]

4.1a 0.1 mmol + **4.2a** 0.15 mmol → **4.3aa**

Entry	Solvent	Yield (%)[b]
1	**MeCN**	**84**
2	DMF	<5
3	DMF/H_2O (9:1)	41
4	NMP	13
5	DCE	<5
6	TPGS-750-M	<5
7[c]	MeCN	36
8[c]	MeCN/THF (9:1)	13
9[c]	DMSO	27
10[c]	DMA	30
11[c]	Acetone	31
12[c]	MeOH	13
13[c]	MeCN/HFIP (20:1)	41

[a] **4.1a** (0.1 mmol), **4.2a** (aged benzaldehyde, 0.15 mmol), $Co(ClO_4)_2·6H_2O$ (10 mol%), **L1** (20 mol %), 4CzIPN (2 mol%), $NaHCO_3$(1.5 equiv.), DIPEA (1.5 equiv.), Solvent (0.1 M), 700 mA blue LED, 20 ºC for 20 h. [b] Yields were determined by ^1H NMR using mesitylene as internal standard. [c] Used $CoCl_2·6H_2O$, K_3PO_4 and bpy (10 mol %) instead of $Co(ClO_4)_2·6H_2O$, $NaHCO_3$ and bpy (20 mol %).

Table 4.10. Screening of acid additives[a]

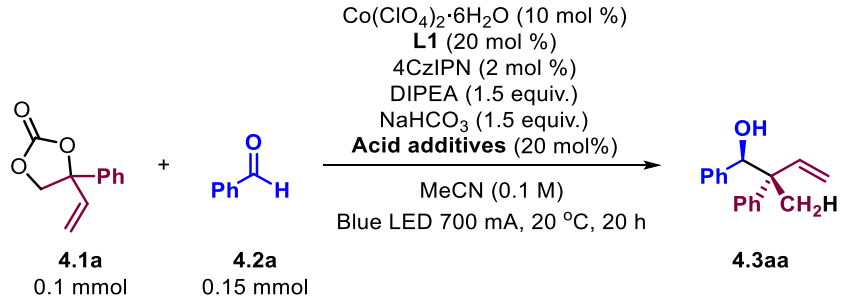

4.1a 0.1 mmol | **4.2a** 0.15 mmol | **4.3aa**

Entry	Acid (20 mol %)	Yield (%)[b]
1[c]	aged benzaldehyde	84%
2	$PhCO_2H$	82%
3	AcOH	79%
4	TFA	60%
5	Oxalic Acid	45%
6	PivOH	78%
7	$MesCO_2H$	81%
8	1-$AdCO_2H$	74%
9	*p*-TsOH·H_2O	<5%
10[d]	**$PhCO_2H$**	**82%**
11[d]	Without $PhCO_2H$	60%

[a] **4.1a** (0.1 mmol), **4.2a** (0.15 mmol), $Co(ClO_4)_2·6H_2O$ (10 mol%), **L1** (20 mol %), 4CzIPN (2 mol%), $NaHCO_3$(1.5 equiv.), DIPEA (1.5 equiv.), MeCN (0.1 M), freshly distilled benzaldehyde was used, 700 mA blue LED, 20 ºC for 20 h. [b] Yields were determined by ^1H NMR using mesitylene as internal standard. [c] Without external $PhCO_2H$, aged benzaldehyde (1.5 equiv.) was used which could contain a lot of $PhCO_2H$. [d] Reaction run without $NaHCO_3$.

4.4.3. Optimization studies of 1,2-alkyl/hydroxyalkylation of 2-aryl 1,3-diene deriving from VCCs

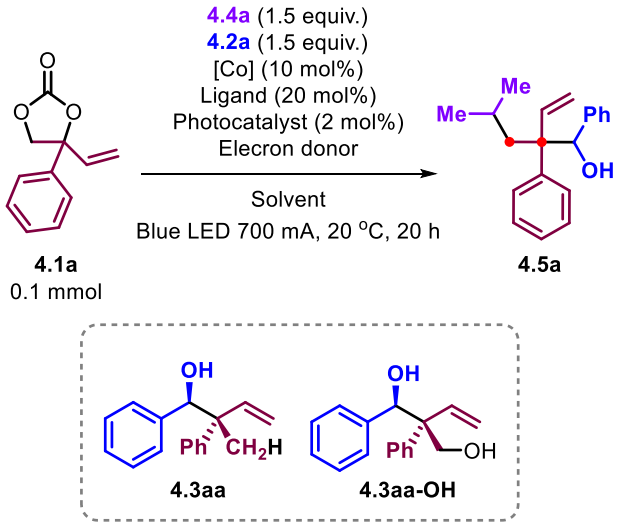

General procedure A:

Alkyl-DHP esters **4.4a** (1.5 equiv.), PC (2 mol%), [Co] (10 mol%), ligand (20 mol%) and electron donor (1.5 equiv.) were weighed in a flat-bottom Schlenk flask. Then, solvent (1 mL), **4.1a** (0.1 mmol) and benzaldehyde **4.2a** (0.15 mmol) were added. The flask was sealed with a Teflon cap and the mixture was freeze-pump-thawed 3 times and stirred under N_2 at room temperature for 5–20 minutes after which it was irradiated for 20 hours at 20 °C using a single high-power blue LED (λ_{em} = 445 nm, 1.2 μeinstein s^{-1}) from the bottom. After stopping the irradiation, the mixture was extracted with ethyl acetate, washed with brine, dried over anhydrous Na_2SO_4, and the organic phases were concentrated *in vacuo*. The residue was dissolved in $CDCl_3$ and analyzed by ^1H NMR using mesitylene as internal standard.

General procedure B:

PC (2 mol%), [Co] (10 mol%) and ligand (20 mol%), electron donor (1.5 equiv.) were weighed in a flat-bottom Schlenk flask (first mixture). Then, to a second Schlenk flask solvent (1 mL) and **4.1a** (0.1 mmol) were added. A. The solids were dissolved in 2-MeTHF (1 mL), and **4.1a** (0.1 mmol) was added. To another Schlenk flask, alkyl-DHP ester **4.4a** (0.15 mmol) and benzaldehyde **4.2a** (15.2 μL, 0.15 mmol) were dissolved in MeCN (1 mL). Both flasks were sealed with a Teflon cap and the mixtures were freeze-pump-thawed 3 times. The mixture of the first Schlenk flask was stirred under N_2 at room temperature for 5 minutes, after which it was irradiated for 2 hours at 20 °C using a single

high-power blue LED (λ_{em} = 445 nm, 700 mA, 1.2 μeinstein s^{-1}) from the bottom. Then, the mixture in the second Schlenk flask was added to the first one under Ar, followed by irradiation for 20 hours at the same conditions mentioned above. After stopping the irradiation, the mixture was extracted with ethyl acetate, washed with brine, dried over anhydrous Na_2SO_4, and the organic phases were concentrated *in vacuo*. The residue was dissolved in $CDCl_3$ and analyzed by ^1H NMR using mesitylene as internal standard.

Table 4.11. Screening of photocatalyst[a]

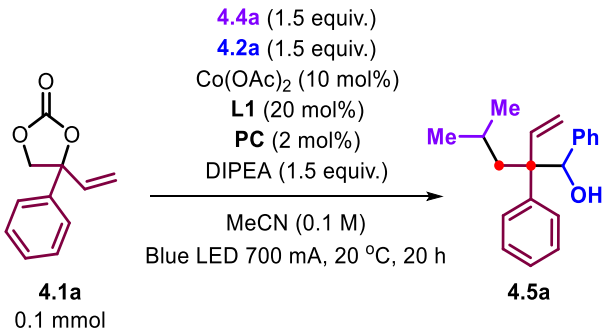

Entry	PC	Conv. (%)	Y. 4.5a (%)[b]	Y. 4.3aa (%)[b]	Y. 4.3aa-OH (%)[b]
1	**4CzIPN**	**>99**	**22**	**47**	**-**
2	$[Ir(dF,CF_3ppy)_2(dtbbpy)](PF_6)$	>99	18	25	11
3	$[Ir(dtbbpy)(ppy)_2]PF_6$	>99	3	25	-

[a] General procedure A: **4.1a** (0.1 mmol), **4.2a** (0.15 mmol), **4.4a** (0.15 mmol), $Co(OAc)_2$ (10 mol%), **L1** (20 mol %), PC (2 mol%), DIPEA (1.5 equiv.), MeCN, 700 mA blue LED, 20 °C for 20 h. [b] Yields were determined by ^1H NMR using mesitylene as internal standard. Y. stands for yield.

Table 4.12. Screening of electron donor[a]

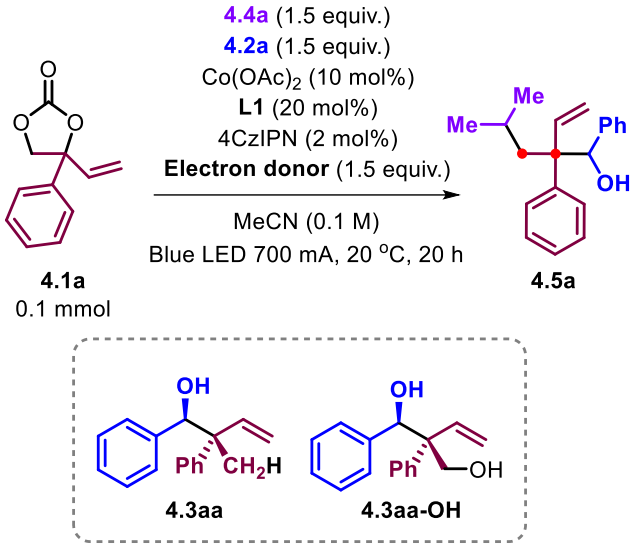

Entry	Electron donor	Conv. (%)	Yield 4.5a (%)[b]	Yield 4.3aa (%)[b]	Yield 4.3aa-OH (%)[b]
1	**DIPEA**	**>99**	**22**	**47**	–
2	TEA	>99	13	33	16
3	TMEDA	>99	9	10	13
4	*n*Bu$_3$N	>99	13	–	–

[a] General procedure A: **4.1a** (0.1 mmol), **4.2a** (0.15 mmol), **4.4a** (0.15 mmol), $Co(OAc)_2$ (10 mol%), **L1** (20 mol %), 4CzIPN (2 mol%), electron donor (1.5 equiv.), MeCN, 700 mA blue LED, 20 ºC for 20 h. [b] Yields were determined by ^{1}H NMR using mesitylene as internal standard.

Table 4.13. Screening of solvent[a]

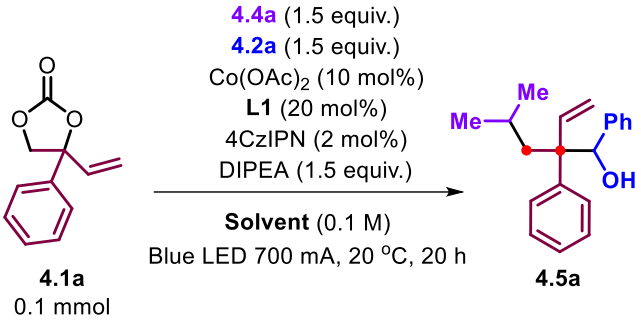

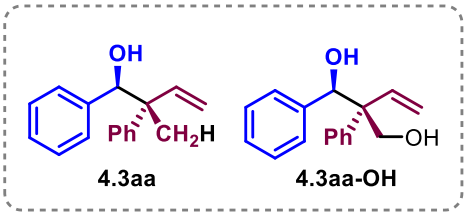

Entry	Solvent	Conv. (%)	Yield 4.5a (%)[b]	Yield 4.3aa (%)[b]	Yield 4.3aa-OH (%)[b]
1	MeCN	>99	22	47	–
2	THF	>99	29	15	17
3	DMF	>99	25	24	11
4	dioxane	>99	29	5	18
5	**2-MeTHF**	**>99**	**31**	**7**	**23**

[a] General procedure A: **4.1a** (0.1 mmol), **4.2a** (0.15 mmol), **4.4a** (0.15 mmol), $Co(OAc)_2$ (10 mol%), **L1** (20 mol %), 4CzIPN (2 mol%), DIPEA (1.5 equiv.), solvent, 700 mA blue LED, 20 ºC for 20 h. Yields were determined by ^1H NMR using mesitylene as internal standard.

Table 4.14. Screening of ligands[a]

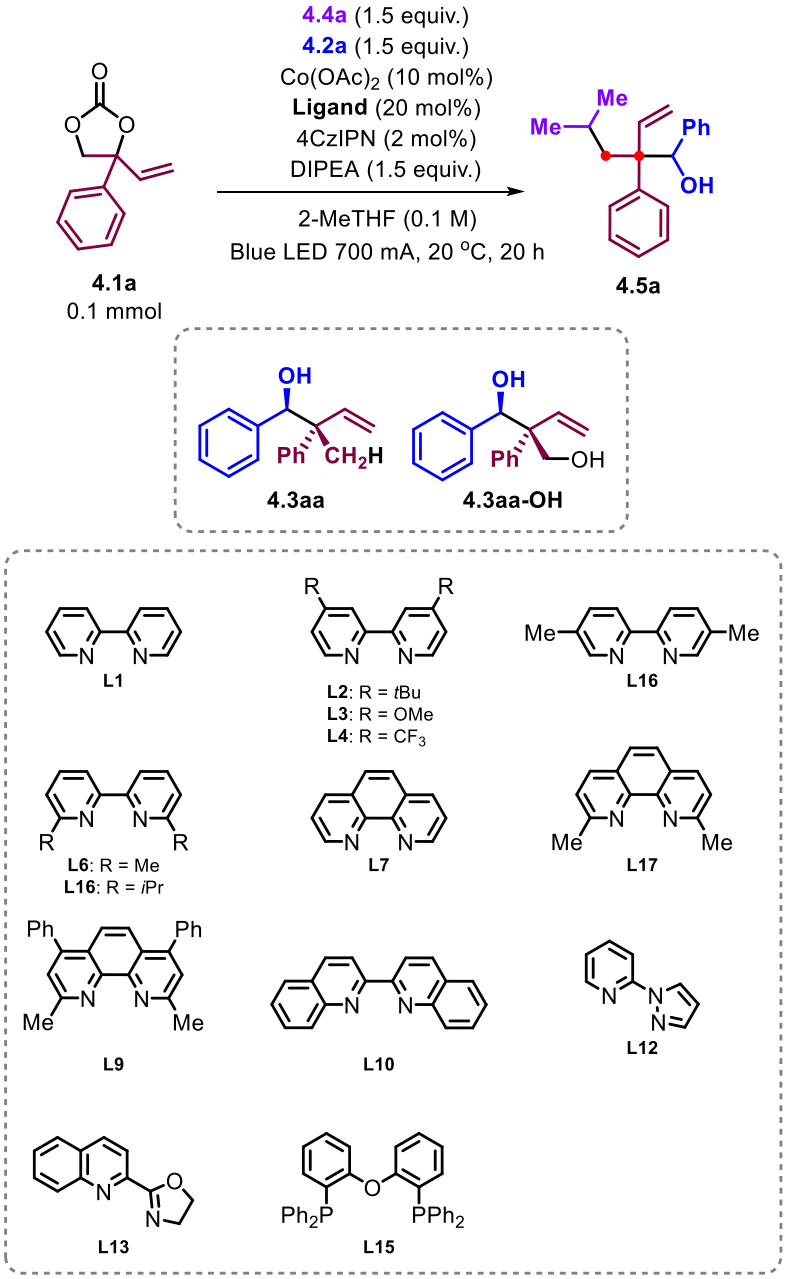

- See for the catalytic data the next page -

Entry	Ligand	Conv. (%)	Yield 4.5a (%)[b]	Yield 4.3aa (%)[b]	Yield 4.3aa-OH (%)[b]
1	**L1**	>99	31	7	23
2	**L2**	>99	33	5	10
3	**L3**	>99	8	3	9
4	**L4**	>99	0	-	-
5	**L16**	>99	42	-	9
6	**L6**	**>99**	**39**	**0**	**0**
15[c]	**L6**	>99	28	0	-
7	**L16**	>99	23	0	16
8	**L7**	>99	<5	-	-
9	**L17**	>99	18	0	-
10	**L9**	>99	33	10	<5
11	**L10**	-	0	0	0
12	**L12**	>99	0	0	0
13	**L13**	56	0	0	0
14	**L15**	>99	<5	-	-

[a] General procedure A: **4.1a** (0.1 mmol), **4.2a** (0.15 mmol), **4.4a** (0.15 mmol), $Co(OAc)_2$ (10 mol%), ligand (20 mol %), 4CzIPN (2 mol%), DIPEA (1.5 equiv.), 2-MeTHF, 700 mA blue LED, 20 ºC for 20 h. [b] Yields were determined by ^1H NMR using mesitylene as internal standard. [c] 6,6'-dmbpy (10 mol%).

Table 4.15. Screening of the amount of DIPEA[a]

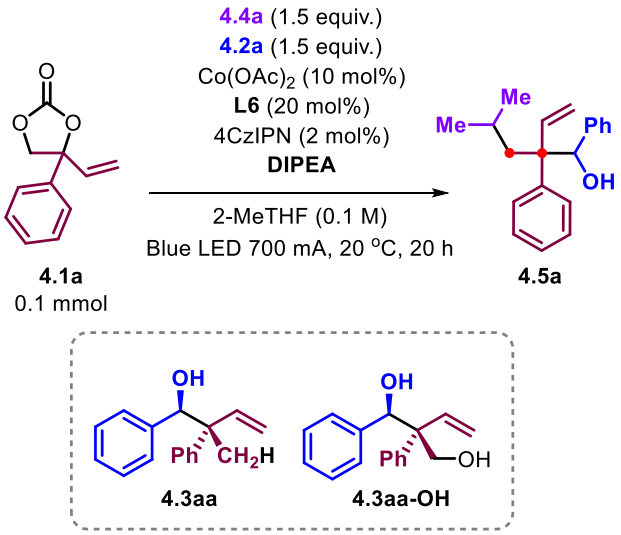

Entry	DIPEA (equiv.)	Conv. (%)	Y. 4.5a (%)[b]	Y. 4.3aa (%)[b]	Y. 4.3aa-OH (%)[b]
1	1.5	>99	39	0	16
2	1.2	>99	45	0	14
3	1.0	>99	49	0	15
4	0.8	>99	36	0	10
5	0.5	>99	31	0	10
6[c]	1.0	>99	38	0	0
7[d]	1.0	>99	46	0	18
8[e]	1.0	>99	39	0	0
9[f]	**1.0**	**>99**	**49**	**0**	**5**

[a] General procedure A: **4.1a** (0.1 mmol), **4.2a** (0.15 mmol), **4.4a** (0.15 mmol), $Co(OAc)_2$ (10 mol%), **L6** (20 mol %), 4CzIPN (2 mol%), DIPEA (1.5 equiv.), 2-MeTHF, 700 mA blue LED, 20 ºC for 20 h. [b] Yields were determined by ^1H NMR using mesitylene as internal standard. [c] 2-MeTHF 0.05 M was used. [d] **4.4a** (1.0 eq.), **4.1a** (1.5 eq.), calculating the yield on the basis of **4.4a**. [e] **L6** (10 mol%). [f] general procedure B: the solution of **4.4a** and **4.2a** in 2-MeTHF (1 mL) was added after 2 h, 2-MeTHF 0.05 M was used.

Table 4.16. Screening of solvent[a]

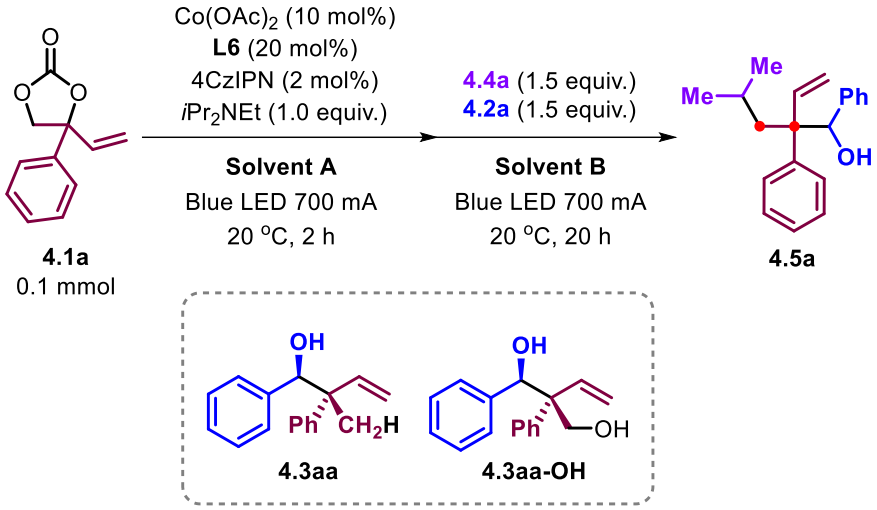

Entry	Solvents (mL+mL)	Conv. (%)	Y 4.5a (%)[b]	Y 4.3aa (%)[b]	Y 4.3aa-OH (%)[b]
1	2-MeTHF, 2	>99	49	0	5
2	2-MeTHF/THF, 1+1	>99	43	10	0
3	**2-MeTHF/MeCN, 1+1**	**>99**	**65**[c]	**0**	**0**
4	2-MeTHF/DMF, 1+1	>99	60	0	0
5	MeCN/2-MeTHF, 1+1	>99	53	4	0
6	2-MeTHF/DMA, 1+1	>99	40	0	0
7	2-MeTHF/DMSO, 1+1	>99	29	0	0
8	2-MeTHF/Dioxane, 1+1	>99	43	0	0
10	2-MeTHF/ MeCN, 1.5+0.5	>99	40	0	0
11	2-MeTHF/ MeCN, 0.5+1.5	>99	42	trace	0
12	2-MeTHF/MeCN, 1+0.5	>99	57	4	0
13	MeCN, 2	>99	63	4	0

[a] General procedure B: **4.1a** (0.1 mmol), $Co(OAc)_2$ (10 mol%), **L6** (20 mol %), 4CzIPN (2 mol%), DIPEA (1.5 equiv.) in solvent A was stirring at 20 ºC under the radiation of 700 mA blue LED for 2 h, followed by the addition of the solution of **4.4a** (0.15 mmol) and **4.2a** (0.15 mmol) in solution B for another 20 h. [b] Yields were determined by ^1H NMR using mesitylene as internal standard. [c] isolated yield was 62%. Y stands for yield.

4.4.4. General procedure for the preparation of starting materials

Substituted vinyl cyclic carbonates were prepared according to a previously reported procedure.[11a,11b,11d] All alkyl dihydropyridines (alkyl-DHP) are known derivatives and were prepared following previously reported procedures.[10] Compounds **4.4a**-**4.4g** and **4.4i**-**4.4k** were prepared following **General Procedure A**, while compound **4.4h** was prepared following **General Procedure B**. In the case of known products, analytical data were consistent with the literature.[10,30]

General procedure for the synthesis of alkyl DHPs:

General Procedure A: To an oven-dried Schlenk tube containing a magnetic stirring bar, ethylene glycol (2.5 M), the respective aldehyde (1.0 equiv.) ethyl 3-aminocrotonate (1.0 equiv.) and ethyl acetoacetate (1.0 equiv.) were added. Then, *n*-Bu_4HSO_4 (12 mol%) was added in one portion. The reaction mixture was stirred at 80 ºC for 16 h. The reaction mixture was allowed to cool to r.t., quenched with brine and extracted with EtOAc. The combined organics were dried over $MgSO_4$, concentrated under reduced pressure. Then the obtained residue was washed with hexane/EA (95:5, v/v) and purified by column chromatography on silica gel to afford the respective target.

General Procedure B: A reaction flask was charged with 3-aminocrotononitrile (1.6 g, 20 mmol, 2.0 equiv.), the aldehyde (10 mmol, 1.0 equiv.) and acetic acid (10 mL). The reaction mixture was heated at 110 ºC with an oil bath while stirring for 3 h. The crude reaction mixture was allowed to cool to r.t., diluted with water and extracted 3 times with EtOAc. The combined organic layers were neutralized with a saturated solution of $NaHCO_3$ until complete removal of acetic acid was achieved, washed with brine, dried over Na_2SO_4, and filtered. The filtrate was concentrated under reduced pressure. The residue was purified by chromatography using silica gel as stationary phase. The obtained solid product was washed with PE/EA (95:5, v/v) where needed.

(30) a) L. Buzzetti, A. Prieto, S. R. Roy, P. Melchiorre, *Angew. Chem. Int. Ed.* **2017**, *56*, 15039-15043; b) G. Li, R. Chen, L. Wu, Q. Fu, X. Zhang, Z. Tang, *Angew. Chem. Int. Ed.* **2013**, *52*, 8432-8436; c) H.-H. Zhang, J.-J. Zhao, S. Yu, *J. Am. Chem. Soc.* **2018**, *140*, 16914-16919.

4.4.5. General procedure for the synthesis of homoallylic alcohols

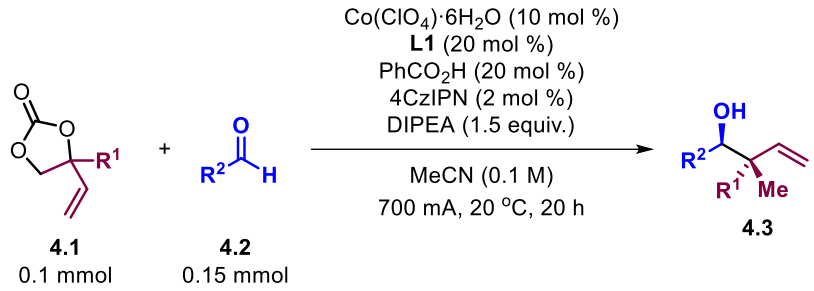

Method A: $Co(ClO_4)_2 \cdot 6H_2O$ (10 µmol, 3.7 mg), **L1** (20 µmol, 3.2 mg), $PhCO_2H$ (20 µmol, 2.4 mg) and 4CzIPN (2 µmol, 1.6 mg) were weighed in a flat-bottom Schlenk flask. The solids were dissolved in MeCN (1 mL), and DIPEA (26.1 µL, 0.15 mmol), **4.1** (0.1 mmol) and aldehyde **4.2** (0.15 mmol) were added affording an orange solution. The flask was sealed with a Teflon cap and the mixture was freeze-pump-thawed 3 times and stirred under N_2 at room temperature for 5–20 minutes after which it was irradiated for 20 hours at 20 °C using a single high-power blue LED (λ_{em} = 445 nm, 700 mA, 1.2 µeinstein s^{-1}) from the bottom. After stopping the irradiation, the mixture was evaporated to dryness and the residue was purified by column chromatography (SiO_2, EtOAc/hexanes) to afford product **4.3**.

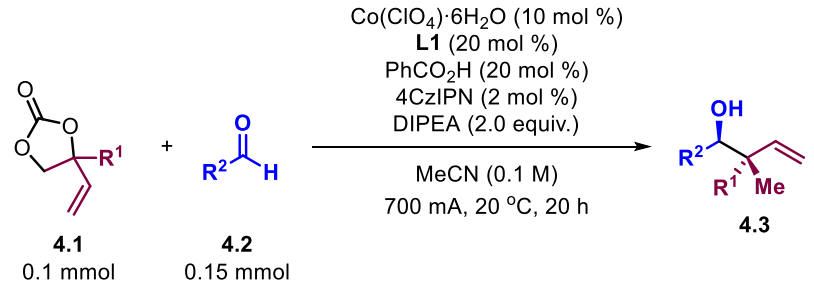

Method B: $Co(ClO_4)_2 \cdot 6H_2O$ (10 µmol, 3.7 mg), **L1** (20 µmol, 3.2 mg), $PhCO_2H$ (20 µmol, 2.4 mg) and 4CzIPN (2 µmol, 1.6 mg) were weighed in a flat-bottom Schlenk flask. The solids were dissolved in MeCN (1 mL) and DIPEA (35.7 µL, 0.2 mmol), **4.1** (0.1 mmol) and aldehyde **4.2** (0.15 mmol) were added affording an orange solution. The flask was sealed with a Teflon cap and the mixture was freeze-pump-thawed 3 times and stirred under N_2 at r.t. for 5–20 minutes after which it was irradiated for 20 hours at 20 °C using a single high-power blue LED (λ_{em} = 445 nm, 700 mA, 1.2 µeinstein s^{-1}) from the bottom. After stopping the irradiation, the mixture was evaporated to dryness and the residue was purified by column chromatography (SiO_2, EtOAc/hexanes) to afford product **4.3**.

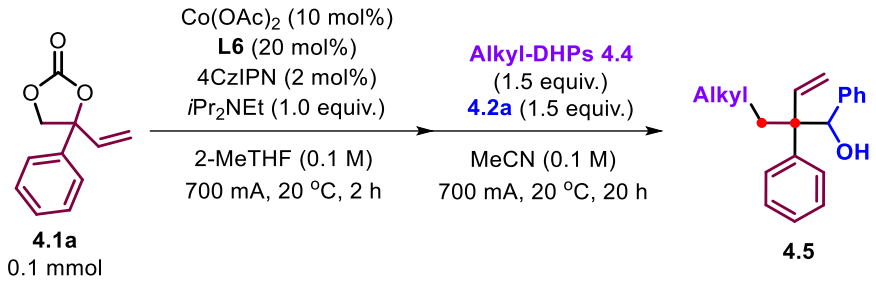

Method C: $Co(OAc)_2$ (10 µmol, 1.8 mg), **L6** (20 µmol, 3.7 mg) and 4CzIPN (2 µmol, 1.6 mg) were weighed in a flat-bottom Schlenk flask (first mixture). The solids were dissolved in 2-MeTHF (1 mL), and DIPEA (0.1 mmol, 17.4 µL) and **4.1a** (0.1 mmol) were added affording an orange solution. Another Schlenk flask (second vessel) was charged with alkyl-DHP esters **4.4** (0.15 mmol) and benzaldehyde **4.2a** (15.2 µL, 0.15 mmol) in MeCN (1 mL). Both flasks were sealed with a Teflon cap and the mixtures were freeze-pump-thawed 3 times. Hereafter, the first Schlenk flask was stirred under N_2 at r.t. for 5 minutes, after which it was irradiated for 2 hours at 20 °C using a single high-power blue LED (λ_{em} = 445 nm, 700 mA, 1.2 µeinstein s^{-1}) from the bottom. Then the mixture in the second Schlenk flask was added to first one under Ar, followed by irradiation for 20 hours under the same conditions. Subsequently, the mixture was evaporated to dryness and the residue purified by column chromatography (SiO_2, EtOAc/hexanes) to afford product **4.5**.

4.4.6. Characterization data for new compounds

2-methyl-1,2-diphenylbut-3-en-1-ol (4.3aa)[31]

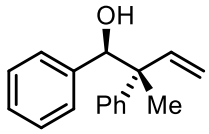

Yellowish oil (Method A, 17.9 mg, 75% yield, 96:4 *dr*, 95:5 *rr*); **^{1}H NMR** (400 MHz, $CDCl_3$) (major) δ 7.42 – 7.36 (m, 2H), 7.36 – 7.29 (m, 2H), 7.27 – 7.19 (m, 4H), 7.15 – 7.08 (m, 2H), 6.57 (dd, *J* = 17.7, 10.9 Hz, 1H), 5.33 (dd, *J* = 10.9, 1.2 Hz, 1H), 5.11 (dd, *J* = 17.6, 1.2 Hz, 1H), 5.08 (s, 1H), 2.07 (*br* s, 1H), 1.30 (s, 3H); **^{1}H NMR** (400 MHz, $CDCl_3$) **(minor diastereoisomer**, **diagnostic peaks)** δ 6.26 (dd, *J* = 17.5, 10.9 Hz, 1H), 5.17 (dd, *J* = 10.9, 1.1 Hz, 1H), 5.04 – 4.98 (m, 2H); **^{1}H NMR** (400 MHz, $CDCl_3$) **(minor regioisomer**, **diagnostic peaks)** δ 5.41 (d, *J* = 1.0 Hz, 1H), 5.23 (d, *J* = 1.2 Hz, 1H), 4.71 (d, *J* = 3.7 Hz, 1H), 3.21 – 3.09 (m, 1H); **^{13}C NMR** (101 MHz, $CDCl_3$) (major) δ 145.1, 142.2, 140.2, 128.4, 128.1, 127.6, 127.4, 127.3, 126.7, 115.7, 80.4, 50.4, 20.7.

1-(4-methoxyphenyl)-2-methyl-2-phenylbut-3-en-1-ol (4.3ab)

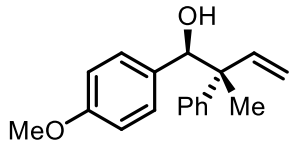

Yellowish oil (17.1 mg, 64% yield, 98:2 *dr*, 98:2 *rr*); **^{1}H NMR** (500 MHz, $CDCl_3$) (major) δ 7.40 – 7.35 (m, 2H), 7.35 – 7.29 (m, 2H), 7.25 – 7.21 (m, 1H), 7.06 – 7.01 (m, 2H), 6.78 – 6.72 (m, 2H), 6.56 (dd, *J* = 17.7, 10.9 Hz, 1H), 5.33 (dd, *J* = 10.9, 1.2 Hz, 1H), 5.11 (dd, *J* = 17.7, 1.3 Hz, 1H), 5.03 (s, 1H), 3.77 (s, 3H), 2.02 (*br* s, 1H), 1.28 (s, 3H); **^{1}H NMR** (500 MHz, $CDCl_3$) (**minor diastereomer**, **diagnostic peaks**) δ 6.25 (dd, *J* = 17.5, 10.8 Hz, 1H); **^{1}H NMR** (500 MHz, $CDCl_3$) (**regioisomers**, **diagnostic peaks**) δ 3.16 – 3.09 (m, 1H); **^{13}C NMR** (126 MHz, $CDCl_3$) (major) δ 159.0, 145.3, 142.3, 132.3, 129.1, 128.4, 127.4, 126.6, 115.7, 112.8, 80.1, 55.3, 50.5, 20.8; **IR** (neat) ν = 3473, 3084, 3057, 2978, 2934, 2836, 1610, 1511, 1444, 1245, 1174, 1030, 917, 831, 699 cm^{-1}; **HRMS** (ESI/TOF) *m/z*: $[M + Na]^+$ Calcd for. $C_{18}H_{20}NaO_2^+$ 291.1356; found 291.1359.

1-(4-fluorophenyl)-2-methyl-2-phenylbut-3-en-1-ol (4.3ac)

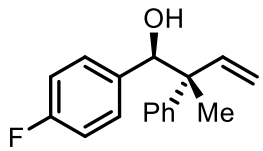

Yellowish oil (Method A, 19.8 mg, 77% yield, 96:4 *dr*, 97:3 *rr*); **^{1}H NMR** (400 MHz, $CDCl_3$) δ 7.41 – 7.29 (m, 4H), 7.28 – 7.20 (m, 1H), 7.11 – 7.01 (m, 2H), 6.93 – 6.82 (m, 2H), 6.53 (dd, *J* = 17.6, 10.9 Hz, 1H), 5.34 (dd, *J* = 10.9, 1.1 Hz, 1H), 5.12 (dd, *J* = 17.7, 1.1 Hz, 1H), 5.06 (s, 1H), 2.12 (*br* s, 1H), 1.28 (s, 3H); ^{1}H NMR (400 MHz, $CDCl_3$) **(minor diastereoisomer**,

(31) J. R. Zbieg, E. L. McLnturff, J. C. Leung, M. J. Krische, *J. Am. Chem. Soc.* **2011**, *133*, 1141-1144.

diagnostic peaks) δ 6.23 (dd, *J* = 17.5, 10.9 Hz, 1H), 5.18 (dd, *J* = 10.9, 1.1 Hz, 1H), 5.04 – 4.98 (m, 2H). ^{1}H NMR (400 MHz, $CDCl_3$) **(minor regioisomer**, **diagnostic peaks)** δ 5.40 (d, *J* = 1.0 Hz, 1H), 5.21 (d, *J* = 1.2 Hz, 1H), 4.66 (d, *J* = 3.9 Hz, 1H), 3.17 – 3.04 (m, 1H); **^{13}C NMR** (101 MHz, $CDCl_3$) δ 163.51, 161.07, 144.79, 142.09, 135.77, 135.74, 129.58, 129.50, 128.51, 127.34, 126.79, 115.95, 114.27, 114.06, 79.73, 77.48, 77.16, 76.84, 50.46, 20.31; **^{19}F NMR** (376 MHz, $CDCl_3$) δ -115.40; **IR** (neat) ν = 3451, 3084, 3059, 2979, 2929, 1603, 1507, 1446, 1222, 1158, 1035, 921, 833, 699 cm^{-1}; **HRMS** (ESI/TOF) *m/z*: $[M + Na]^+$ Calcd. for $C_{17}H_{17}FNaO^+$ 279.1156; found 279.1149.

2-methyl-2-phenyl-1-(4-(trifluoromethyl)phenyl)but-3-en-1-ol (4.3ad)[6]

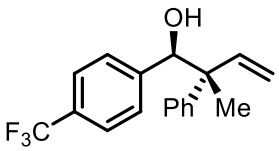

Yellowish oil (Method B,14.6 mg, 48% yield, 94:6 *dr*, >99:1 *rr*); **^{1}H NMR** (400 MHz, $CDCl_3$) δ 7.47 – 7.40 (m, 2H), 7.38 – 7.31 (m, 4H), 7.29 – 7.23 (m, 1H), 7.22 – 7.15 (m, 2H), 6.53 (dd, *J* = 17.6, 10.9 Hz, 1H), 5.35 (dd, *J* = 10.9, 1.1 Hz, 1H), 5.17 – 5.09 (m, 2H), 2.18 (d, *J* = 2.2 Hz, 1H), 1.29 (s, 3H); ^{1}H NMR (400 MHz, $CDCl_3$) **(minor diastereoisomer**, **diagnostic peaks)** δ 6.22 (dd, *J* = 17.5, 10.9 Hz, 1H), 5.20 (dd, *J* = 10.9, 1.0 Hz, 1H), 5.08 (d, *J* = 3.0 Hz, 1H), 5.02 (dd, *J* = 17.5, 1.0 Hz, 1H); **^{13}C NMR** (101 MHz, $CDCl_3$) δ 144.37, 144.02, 141.80, 129.66 (q, *J* = 32.3 Hz), 128.64, 128.30, 127.32, 126.98, 124.35 (q, *J* = 271.3 Hz), 124.22 (q, *J* = 3.8 Hz), 116.26, 79.76, 77.48, 77.16, 76.84, 50.46, 20.05; **^{19}F NMR** (376 MHz, $CDCl_3$) δ -62.15.

1-(4-isopropylphenyl)-2-methyl-2-phenylbut-3-en-1-ol (4.3ae)

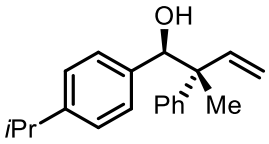

Yellowish oil (Method A, 19.1 mg, 68% yield, 97:3 *dr*, 97:3 *rr*); **^{1}H NMR** (400 MHz, $CDCl_3$) δ 7.44 – 7.37 (m, 2H), 7.37 – 7.28 (m, 2H), 7.28 – 7.20 (m, 1H), 7.11 – 7.01 (m, 4H), 6.59 (dd, *J* = 17.7, 10.9 Hz, 1H), 5.33 (dd, *J* = 10.9, 1.3 Hz, 1H), 5.10 (dd, *J* = 17.7, 1.3 Hz, 1H), 5.05 (s, 1H), 2.87 (hept, *J* = 6.9 Hz, 1H), 2.03 (*br* s, 1H), 1.30 (s, 3H), 1.23 (d, *J* = 6.9 Hz, 6H); **^{1}H NMR** (400 MHz, $CDCl_3$) **(minor diastereoisomer**, **diagnostic peaks)** δ 6.26 (dd, *J* = 17.5, 10.9 Hz, 1H), 5.16 (dd, *J* = 10.9, 1.2 Hz, 1H), 5.02 – 4.97 (m, 2H); ^{1}H NMR (400 MHz, $CDCl_3$) **(minor regioisomer**, **diagnostic peaks)** δ 5.39 (d, *J* = 1.1 Hz, 1H), 5.22 (d, *J* = 1.2 Hz, 1H), 4.68 (d, *J* = 3.9 Hz, 1H), 3.19 – 3.09 (m, 1H); **^{13}C NMR** (101 MHz, $CDCl_3$) δ 148.13, 145.42, 142.24, 137.68, 128.35, 128.00, 127.45, 126.55, 125.44, 115.65, 80.41, 77.48, 77.16, 76.84, 50.39, 33.85, 24.12, 24.07, 21.13; **IR** (neat) ν = 3451, 3085, 3056, 2906, 2926, 2872, 1602, 1495, 1451, 1414, 1373, 1035, 1021, 918, 832, 699

cm^{-1}; **HRMS** (ESI/TOF) *m/z*: $[M + Na]^+$ Calcd. for $C_{20}H_{24}NaO^+$ 303.1719; found 303.1715.

1-(3-chlorophenyl)-2-methyl-2-phenylbut-3-en-1-ol (4.3af)

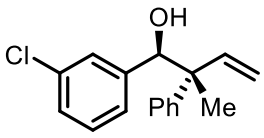

Yellowish oil (Method A, 16.5 mg, 60% yield, 93:7 *dr*, 97:3 *rr*); **^{1}H NMR** (400 MHz, $CDCl_3$) δ 7.39 – 7.29 (m, 4H), 7.29 – 7.23 (m, 1H), 7.21 – 7.16 (m, 1H), 7.15 – 7.07 (m, 2H), 6.94 – 6.88 (m, 1H), 6.52 (dd, J = 17.7, 10.9 Hz, 1H), 5.35 (dd, J = 11.0, 1.1 Hz, 1H), 5.13 (dd, J = 17.7, 1.1 Hz, 1H), 5.04 (s, 1H), 2.13 (*br* s, 1H), 1.29 (s, 3H); **^{1}H NMR** (400 MHz, $CDCl_3$) **(minor diastereoisomer**, **diagnostic peaks)** δ 6.23 (dd, *J* = 17.5, 10.9 Hz, 1H), 5.19 (dd, *J* = 10.8, 1.0 Hz, 1H); **^{1}H NMR** (400 MHz, $CDCl_3$) **(minor regioisomer**, **diagnostic peaks)** δ 5.44 – 5.42 (m, 1H), 5.23 (d, *J* = 1.2 Hz, 1H), 4.65 (d, *J* = 3.5 Hz, 1H), 3.23 – 3.06 (m, 1H); **^{13}C NMR** (101 MHz, $CDCl_3$) δ 144.58, 142.15, 141.84, 133.35, 128.56, 128.50, 128.14, 127.66, 127.32, 126.90, 126.23, 116.11, 79.74, 50.43, 20.32; **IR** (neat) ν = 3439, 3083, 3060, 2979, 2925, 1597, 1574, 1437, 1376, 1190, 1030, 920, 743, 695 cm^{-1}; **HRMS** (ESI/TOF) *m/z*: $[M + Na]^+$ Calcd. for $C_{17}H_{17}ClNaO^+$ 295.0860; found 295.0864.

2-methyl-2-phenyl-1-(o-tolyl)but-3-en-1-ol (4.3ag)

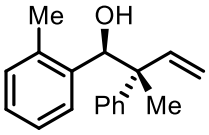

Yellowish oil (Method A, 16.4 mg, 65% yield, 97:3 *dr*, 96:4 *rr*); **^{1}H NMR** (400 MHz, $CDCl_3$) δ 7.44 – 7.12 (m, 8H), 7.08 – 7.00 (m, 1H), 6.63 (dd, *J* = 17.7, 11.0 Hz, 1H), 5.41 (dd, *J* = 11.0, 1.2 Hz, 1H), 5.35 (d, *J* = 2.0 Hz, 1H), 5.17 (dd, *J* = 17.7, 1.2 Hz, 1H), 2.08 (*br* s, 3H), 1.96 (d, *J* = 2.7 Hz, 1H), 1.36 (s, 3H); ^{1}H NMR (400 MHz, $CDCl_3$) **(minor diastereoisomer**, **diagnostic peaks)** δ 6.21 (dd, *J* = 17.5, 10.8 Hz, 1H), 5.10 (dd, *J* = 10.9, 1.2 Hz, 1H), 4.94 (dd, *J* = 17.5, 1.2 Hz, 1H); ^{1}H NMR (400 MHz, $CDCl_3$) **(minor regioisomer**, **diagnostic peaks)** δ 5.28 – 5.26 (m, 1H), 4.82 (d, *J* = 3.3 Hz, 1H), 3.14 – 3.05 (m, 1H); **^{13}C NMR** (101 MHz, $CDCl_3$) δ 145.37, 142.17, 138.84, 136.45, 130.00, 128.39, 128.28, 127.62, 127.51, 126.64, 125.33, 115.91, 77.48, 77.16, 76.84, 75.30, 50.86, 21.26, 20.01; **IR** (neat) ν = 3445, 3058, 3024, 2975, 1600, 1491, 1447, 1437, 1023, 918, 737, 697 cm^{-1}; **HRMS** (ESI/TOF) *m/z*: $[M + Na]^+$ Calcd. for $C_{18}H_{20}NaO^+$ 275.1406; found 275.1405.

1-(3,5-dimethylphenyl)-2-methyl-2-phenylbut-3-en-1-ol (4.3ah)

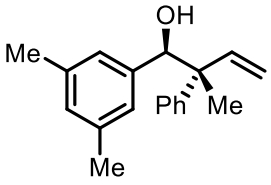

Yellowish solid (Method A, 19.5 mg, 73% yield, 97:3 *dr*, 97:3 *rr*); **^{1}H NMR** (400 MHz, $CDCl_3$) δ 7.41 – 7.36 (m, 2H), 7.36 – 7.29 (m, 2H), 7.27 – 7.20 (m, 1H), 6.89 – 6.82 (m, 1H), 6.74 – 6.67 (m, 2H), 6.57 (dd, J = 17.7, 10.9 Hz, 1H), 5.33 (dd, J = 10.9, 1.3 Hz, 1H), 5.11 (dd, J = 17.7, 1.3 Hz, 1H), 4.99 (s, 1H), 2.24 (s, 6H), 2.02 (s, 1H), 1.30 (s, 3H); **^{1}H NMR** (400 MHz, $CDCl_3$) **(minor diastereoisomer**, **diagnostic peaks)** δ 6.27 (dd, *J* = 17.5, 10.9 Hz, 1H), 5.17 (dd, *J* = 10.9, 1.2 Hz, 1H), 5.03 (d, *J* = 1.2 Hz, 0.5H), 4.94 (s, 1H); **^{1}H NMR** (400 MHz, $CDCl_3$) **(minor regioisomer**, **diagnostic peaks)** δ 5.40 (d, *J* = 1.1 Hz, 1H), 5.24 – 5.22 (m, 1H), 4.64 (d, *J* = 3.6 Hz, 1H), 3.14 (dd, *J* = 7.0, 3.7 Hz, 1H); **^{13}C NMR** (101 MHz, $CDCl_3$) δ 145.35, 142.30, 140.11, 136.67, 129.12, 128.31, 127.49, 126.56, 125.92, 115.57, 80.49, 50.36, 21.42, 20.94; **IR** (neat) ν = 3455, 3056, 3015, 2976, 2918, 1603, 1493, 1448, 1374, 1051, 916, 948, 698 cm^{-1}; **HRMS** (ESI/TOF) *m/z*: $[M + Na]^+$ Calcd. for $C_{19}H_{22}NaO^+$ 289.1563; found 289.1556.

1-(3,4-dimethoxyphenyl)-2-methyl-2-phenylbut-3-en-1-ol (4.3ai)

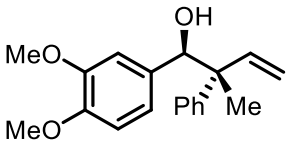

Yellowish oil (Method A, 19.1 mg, 64% yield, 98:2 *dr*, >99:1 *rr*); **^{1}H NMR** (400 MHz, $CDCl_3$) δ 7.40 – 7.17 (m, 5H), 6.77 – 6.67 (m, 2H), 6.54 (dd, *J* = 17.6, 10.9 Hz, 1H), 6.46 – 6.39 (m, 1H), 5.33 (dd, *J* = 10.9, 1.2 Hz, 1H), 5.16 (dd, *J* = 17.6, 1.2 Hz, 1H), 5.00 (s, 1H), 3.84 (s, 3H), 3.65 (s, 3H), 2.11 (*br* s, 1H), 1.30 (s, 3H); **^{13}C NMR** (101 MHz, $CDCl_3$) δ 148.31, 147.77, 145.05, 142.85, 132.70, 128.34, 127.55, 126.58, 120.15, 115.54, 111.30, 110.00, 80.11, 55.89, 55.70, 50.49, 19.91; **IR** (neat) ν = 3516, 3082, 3057, 2933, 2836, 1595, 1512, 1459, 1259, 1233, 1137, 1024, 918, 811, 739, 700 cm^{-1}; **HRMS** (ESI/TOF) *m/z*: $[M + Na]^+$ Calcd. for $C_{19}H_{22}NaO_3^+$ 321.1461; found 321.1451.

1-(furan-2-yl)-2-methyl-2-phenylbut-3-en-1-ol (4.3aj)[6]

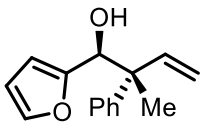

Yellowish oil (Method A, 14.2 mg, 62% yield, 93:7 *dr*, 96:4 *rr*); **^{1}H NMR** (400 MHz, $CDCl_3$) δ 7.39 – 7.29 (m, 5H), 7.25 – 7.19 (m, 1H), 6.48 (dd, J = 17.7, 10.9 Hz, 1H), 6.27 (dd, J = 3.3, 1.8 Hz, 1H), 6.10 – 6.03 (m, 1H), 5.34 (dd, J = 10.9, 1.2 Hz, 1H), 5.15 (dd, J = 17.6, 1.2 Hz, 1H), 5.09 (d, J = 3.3 Hz, 1H), 2.09 (d, J = 4.2 Hz, 1H), 1.41 (s, 3H); **^{1}H NMR** (400 MHz, $CDCl_3$) **(minor diastereoisomer**, **diagnostic peaks)** δ 5.28 (dd, *J* = 10.9, 1.2 Hz, 1H), 5.04 (d, *J* = 5.9 Hz, 1H); **^{1}H NMR** (400 MHz, $CDCl_3$) **(minor regioisomer**, **diagnostic peaks)** δ 4.74 –

4.68 (m, 1H), 3.36 – 3.23 (m, 1H); **^{13}C NMR** (101 MHz, $CDCl_3$) δ 154.12, 144.69, 142.22, 141.54, 128.38, 127.32, 126.67, 115.63, 110.20, 107.90, 74.73, 50.20, 21.51.

2-methyl-1-(naphthalen-2-yl)-2-phenylbut-3-en-1-ol (4.3ak)

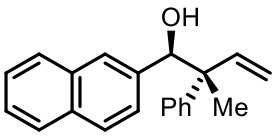

Yellowish oil (Method B, 20.7 mg, 72% yield, 95:5 *dr*, 98:2 *rr*); **^{1}H NMR** (400 MHz, $CDCl_3$) δ 7.85 – 7.71 (m, 2H), 7.69 – 7.57 (m, 2H), 7.51 – 7.37 (m, 4H), 7.37 – 7.30 (m, 2H), 7.29 – 7.23 (m, 1H), 7.19 (dd, J = 8.5, 1.8 Hz, 1H), 6.63 (dd, J = 17.7, 10.9 Hz, 1H), 5.35 (dd, J = 10.9, 1.2 Hz, 1H), 5.24 (s, 1H), 5.12 (dd, J = 17.6, 1.2 Hz, 1H), 2.23 (*br* s, 1H), 1.35 (s, 3H); **^{1}H NMR** (400 MHz, $CDCl_3$) **(minor diastereoisomer**, **diagnostic peaks)** δ 6.32 (dd, *J* = 17.5, 10.9 Hz, 1H), 5.21 – 5.17 (m, 2H), 5.03 (dd, *J* = 17.5, 1.1 Hz, 1H). **^{1}H NMR** (400 MHz, $CDCl_3$) **(minor regioisomer**, **diagnostic peaks)** δ 5.44 (d, *J* = 1.0 Hz, 1H), 5.28 – 5.27 (m, 1H), 4.87 (d, *J* = 3.4 Hz, 1H), 3.33 – 3.22 (m, 1H); **^{13}C NMR** (101 MHz, $CDCl_3$) δ 145.04, 142.22, 137.80, 133.01, 132.75, 128.47, 128.18, 127.64, 127.46, 127.00, 126.72, 126.67, 126.26, 125.89, 125.84, 115.88, 80.49, 50.63, 20.69; **IR** (neat) ν = 3452, 3055, 3023, 2977, 2926, 1599, 1496, 1445, 1367, 1266, 1026, 918, 819, 743, 698 cm^{-1}; **HRMS** (ESI/TOF) *m/z*: $[M + Na]^+$ Calcd. for $C_{21}H_{20}NaO^+$ 311.1406; found 311.1397.

tert-butyl 1-hydroxy-2-methyl-2-phenylbut-3-en-1-yl)-1*H*-indole-1-carboxylate (4.3al)

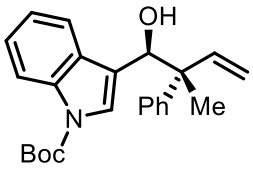

Yellowish oil (Method A, 30.8 mg, 82% yield, 99:1 *dr*, 98:2 *rr*); **^{1}H NMR** (400 MHz, $CDCl_3$) δ 8.13 (d, *J* = 8.3 Hz, 1H), 7.51 – 7.43 (m, 3H), 7.38 – 7.24 (m, 5H), 7.21 – 7.12 (m, 1H), 6.63 (dd, *J* = 17.7, 11.0 Hz, 1H), 5.44 – 5.36 (m, 2H), 5.23 (dd, *J* = 17.7, 1.2 Hz, 1H), 2.12 (*br* s, 1H), 1.67 (s, 9H), 1.46 (s, 3H); ^{1}H NMR (400 MHz, $CDCl_3$) **(minor regioisomer**, **diagnostic peaks)** δ 4.97 (d, *J* = 4.5 Hz, 1H), 3.45 – 3.28 (m, 1H); **^{13}C NMR** (101 MHz, $CDCl_3$) δ 149.76, 145.11, 142.25, 135.00, 130.28, 128.47, 127.48, 126.74, 124.56, 124.16, 122.47, 120.31, 115.96, 115.08, 83.72, 74.44, 50.73, 28.31, 21.40; **IR** (neat) ν = 3538, 3083, 3055, 2978, 2930, 1729, 1603, 1451, 1368, 1255, 1153, 1081, 1015, 921, 739, 699 m^{-1}; **HRMS** (ESI/TOF) *m/z*: $[M + Na]^+$ Calcd. for $C_{24}H_{27}NNaO_3^+$ 400.1883; found 400.1879.

2-methyl-2-phenyl-1-(4-(prop-1-en-2-yl)cyclohex-1-en-1-yl)but-3-en-1-ol (4.3am)

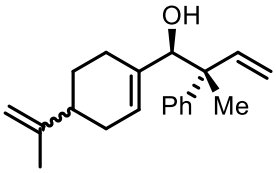

Yellowish oil (Method A, 20.9 mg, 74% yield, >95:5 *dr*, >99:1 *rr*); **^{1}H NMR** (400 MHz, $CDCl_3$) δ 7.45 – 7.37 (m, 4H), 7.36 – 7.28 (m, 4H), 7.25 – 7.17 (m, 2H), 6.59 – 6.41 (m, 2H), 5.76 – 5.63 (m, 2H), 5.32 (dd, J = 10.9, 1.3 Hz, 1H), 5.28 (dd, J = 10.9, 1.3 Hz, 1H), 5.21 (dd, J = 8.9, 1.3 Hz, 1H), 5.16 (dd, J = 8.8, 1.3 Hz, 1H), 4.74 – 4.61 (m, 4H), 4.36 (d, J = 13.6 Hz, 2H), 2.24 – 1.75 (m, 11H), 1.74 – 1.70 (m, 7H), 1.38 (s, 6H), 1.35 – 1.20 (m, 4H); **^{13}C NMR** (101 MHz, $CDCl_3$) δ 150.02, 149.87, 146.01, 145.60, 143.63, 143.33, 137.44, 137.06, 128.36, 127.30, 127.25, 126.49, 126.47, 126.00, 125.08, 114.67, 114.51, 108.67, 82.31, 81.89, 49.62, 49.49, 41.29, 40.94, 30.82, 30.66, 27.90, 27.64, 27.43, 26.88, 21.58, 20.92, 20.86, 20.35; **IR** (neat) ν = 3446, 3082, 3060, 2970, 2924, 1641, 1600, 1494, 1443, 1372, 1024, 917, 888, 699 cm^{-1}; **HRMS** (ESI/TOF) *m/z*: $[M + Na]^+$ Calcd. for $C_{20}H_{26}NaO^+$ 305.1876; found 305.1866.

2-(4-methoxyphenyl)-2-methyl-1-phenylbut-3-en-1-ol (4.3ba)[16d]

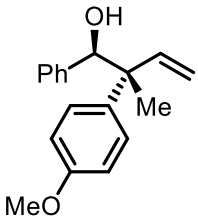

Yellowish oil (Method B, 7.9 mg, 29% yield, 96:4 *dr*, >99:1 *rr*); **^{1}H NMR** (400 MHz, $CDCl_3$) δ 7.28 (d, *J* = 8.9 Hz, 2H), 7.24 – 7.16 (m, 3H), 7.14 – 7.07 (m, 2H), 6.85 (d, *J* = 8.9 Hz, 2H), 6.52 (dd, *J* = 17.6, 10.9 Hz, 1H), 5.30 (dd, *J* = 10.9, 1.2 Hz, 1H), 5.09 (dd, *J* = 17.7, 1.2 Hz, 1H), 5.02 (s, 1H), 3.80 (s, 3H), 2.03 (*br* s, 1H), 1.27 (s, 3H); **^{1}H NMR** (400 MHz, $CDCl_3$) **(minor diastereomer**, **diagnostic peaks)** δ 6.23 (dd, *J* = 17.5, 10.8 Hz, 1H), 5.14 (dd, *J* = 10.9, 1.2 Hz, 1H), 4.97 (s, 1H); **^{13}C NMR** (101 MHz, $CDCl_3$) δ 158.25, 142.49, 140.26, 137.02, 128.50, 128.07, 127.52, 127.35, 115.44, 113.75, 55.39, 49.81, 20.79.

2-methyl-1-phenyl-2-(p-tolyl)but-3-en-1-ol (4.3ca)

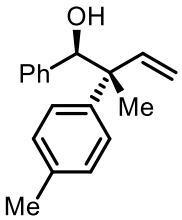

Yellowish oil (Method B, 17.0 mg, 67% yield, 97:3 *dr*, 98:2 *rr*); **^{1}H NMR** (400 MHz, $CDCl_3$) δ 7.28 (d, *J* = 8.3 Hz, 3H), 7.28 – 7.16 (m, 5H), 7.14 (d, *J* = 8.5 Hz, 4H), 6.56 (dd, *J* = 17.7, 10.9 Hz, 1H), 5.31 (dd, *J* = 10.9, 1.3 Hz, 1H), 5.13 – 5.02 (m, 2H), 2.35 (s, 3H), 2.08 (s, 1H), 1.28 (s, 4H); **^{1}H NMR** (400 MHz, $CDCl_3$) **(minor diastereomer**, **diagnostic peaks)** δ 6.24 (dd, *J* = 17.5, 10.8 Hz, 1H), 5.14 (dd, *J* = 10.8, 1.2 Hz, 1H), 5.01 (s, 1H), 4.98 (dd, *J* = 17.5, 1.2 Hz, 1H); ^{1}H NMR (400 MHz, $CDCl_3$) **(minor regioisomer, diagnostic peaks)** δ 5.40 (d, *J* = 1.1 Hz, 1H), 5.18 (d, *J* = 1.4 Hz, 1H), 4.72 (d, *J* = 3.5 Hz, 1H), 3.18

– 3.09 (m, 1H); **^{13}C NMR** (101 MHz, $CDCl_3$) δ 142.22, 142.14, 140.27, 136.20, 129.16, 128.10, 127.52, 127.33, 127.26, 115.56, 80.48, 50.10, 21.04, 20.99; **IR** (neat) ν = 3451, 3085, 3059, 3027, 2977, 2922, 1605, 1512, 1453, 1375, 1188, 1019, 915, 811, 724, 701 cm^{-1}; **HRMS** (ESI/TOF) *m/z*: $[M + Na]^+$ Calcd. for $C_{18}H_{20}NaO^+$ 275.1406; found 275.1402.

2-([1,1'-biphenyl]-4-yl)-2-methyl-1-phenylbut-3-en-1-ol (4.3da)

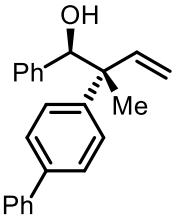

Yellowish solid (Method B, 24.0 mg, 76% yield, 96:4 *dr*, 98:2 *rr*); **^{1}H NMR** (400 MHz, $CDCl_3$) δ 7.65 – 7.56 (m, 4H), 7.51 – 7.42 (m, 4H), 7.41 – 7.33 (m, 1H), 7.28 – 7.22 (m, 3H), 7.21 – 7.14 (m, 2H), 6.62 (dd, *J* = 17.7, 10.9 Hz, 1H), 5.37 (dd, *J* = 10.9, 1.2 Hz, 1H), 5.18 – 5.10 (m, 2H), 2.14 (d, *J* = 2.3 Hz, 1H), 1.35 (s, 3H); **^{1}H NMR** (400 MHz, $CDCl_3$) **(minor diastereomer**, **diagnostic peaks)** δ 6.31 (dd, *J* = 17.5, 10.8 Hz, 1H), 5.20 (dd, *J* = 10.9, 1.1 Hz, 2H), 5.08 – 5.02 (m, 2H); **^{1}H NMR** (400 MHz, $CDCl_3$) **(minor regioisomer**, **diagnostic peaks)** δ 5.49 (d, *J* = 1.0 Hz, 1H), 5.27 (d, *J* = 1.1 Hz, 1H), 4.77 (d, *J* = 3.7 Hz, 1H), 3.25 – 3.17 (m, 1H); **^{13}C NMR** (101 MHz, $CDCl_3$) δ 144.31, 142.04, 140.82, 140.23, 139.39, 128.89, 128.09, 127.84, 127.62, 127.39, 127.36, 127.14, 127.03, 115.84, 80.45, 50.24, 20.97; **IR** (neat) ν = 3556, 3079, 3060, 3027, 2978, 2924, 1602, 1484, 1449, 1409, 1257, 1074, 1019, 924, 842, 724, 694 cm^{-1}; **HRMS** (ESI/TOF) *m/z*: $[M + Na]^+$ Calcd. for $C_{23}H_{22}NaO^+$ 337.1563; found 337.1563.

2-(4-fluorophenyl)-2-methyl-1-phenylbut-3-en-1-ol (4.3ea)[16d]

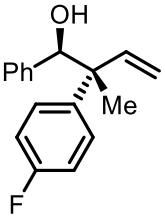

Yellowish oil (Method B, 17.0 mg, 67% yield, 97:3 *dr*, 98:2 *rr*); **^{1}H NMR** (400 MHz, $CDCl_3$) δ 7.35 – 7.28 (m, 2H), 7.24 – 7.17 (m, 3H), 7.11 – 7.05 (m, 2H), 7.03 – 6.95 (m, 2H), 6.50 (dd, *J* = 17.7, 10.9 Hz, 1H), 5.33 (dd, *J* = 10.9, 1.1 Hz, 1H), 5.12 (dd, *J* = 17.7, 1.1 Hz, 1H), 5.01 (s, 1H), 2.08 (*br* s, 1H), 1.30 (s, 3H); **^{1}H NMR** (400 MHz, $CDCl_3$) **(minor diastereomer**, **diagnostic peaks)** δ 6.25 (dd, *J* = 17.5, 10.9 Hz, 1H), 5.18 (d, *J* = 1.1 Hz, 0.5H), 5.05 (d, *J* = 1.1 Hz, 0.5H), 4.95 (s, 1H); **^{1}H NMR** (400 MHz, $CDCl_3$) **(minor regioisomer**, **diagnostic peaks)** δ 5.20 (d, *J* = 1.1 Hz, 1H), 4.67 (d, *J* = 4.0 Hz, 1H), 3.15 – 3.00 (m, 1H); **^{13}C NMR** (101 MHz, $CDCl_3$) δ 162.79, 160.35, 142.29, 140.75, 140.72, 140.13, 129.15, 129.07, 128.07, 128.01, 127.67, 127.49, 127.43, 115.80, 115.10, 114.89, 80.40, 49.94, 20.79; **^{19}F NMR** (376 MHz, $CDCl_3$) δ -116.86.

2-(4-chlorophenyl)-2-methyl-1-phenylbut-3-en-1-ol (4.3fa)[16d]

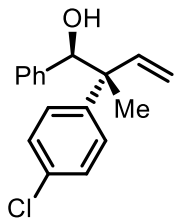

Yellowish oil (Method B, 18.8 mg, 69% yield, 95:5 *dr*, >99:1 *rr*); **^{1}H NMR** (400 MHz, $CDCl_3$) δ 7.31 – 7.27 (m, 4H), 7.25 – 7.19 (m, 3H), 7.13 – 7.06 (m, 2H), 6.49 (dd, *J* = 17.6, 10.9 Hz, 1H), 5.33 (dd, *J* = 10.9, 1.1 Hz, 1H), 5.11 (dd, *J* = 17.7, 1.1 Hz, 1H), 5.01 (s, 1H), 2.03 (*br* s, 1H), 1.29 (s, 3H); **^{1}H NMR** (400 MHz, $CDCl_3$) **(minor diastereomer, diagnostic peaks)** δ 6.23 (dd, *J* = 17.5, 10.9 Hz, 1H), 5.19 (dd, *J* = 10.9, 1.0 Hz, 1H), 5.04 (d, *J* = 1.0 Hz, 0.5H), 5.00 (d, *J* = 1.1 Hz, 0.5H), 4.96 (s, 1H); **^{13}C NMR** (101 MHz, $CDCl_3$) δ 143.71, 141.93, 140.07, 132.45, 128.98, 128.38, 128.03, 127.76, 127.50, 116.07, 80.31, 50.07, 20.81.

2-methyl-1-phenyl-2-(4-(trifluoromethyl)phenyl)but-3-en-1-ol (4.3ga)

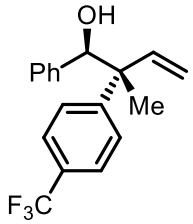

Yellowish oil (Method B, 17.7 mg, 58% yield, 93:7 *dr*, 99:1 *rr*); **^{1}H NMR** (400 MHz, $CDCl_3$) δ 7.56 (d, *J* = 8.3 Hz, 2H), 7.49 (d, *J* = 8.0 Hz, 2H), 7.23 (dd, *J* = 5.0, 2.0 Hz, 3H), 7.15 – 7.07 (m, 2H), 6.53 (dd, *J* = 17.7, 10.9 Hz, 1H), 5.37 (dd, *J* = 11.0, 1.1 Hz, 1H), 5.12 (dd, *J* = 17.7, 1.1 Hz, 1H), 5.07 (s, 1H), 2.06 (s, 1H), 1.32 (s, 3H); **^{1}H NMR** (400 MHz, $CDCl_3$) **(minor diastereomer, diagnostic peaks)** δ 6.27 (dd, *J* = 17.5, 10.9 Hz, 1H), 5.21 (dd, *J* = 10.9, 1.0 Hz, 1H), 5.05 – 4.99 (m, 2H); **^{13}C NMR** (101 MHz, $CDCl_3$) δ 149.54, 141.50, 140.06, 128.81 (q, *J* = 32.7 Hz), 128.02, 127.94, 127.90, 127.57, 125.15 (q, *J* = 3.8 Hz), 124.37 (q, *J* = 271.7 Hz), 116.46, 80.29, 50.48, 21.14; ^{19}F NMR (376 MHz, $CDCl_3$) δ -62.52. **IR** (neat) ν = 3438, 3085, 3065, 3031, 2981, 2928, 1616, 1493, 1455, 1411, 1324, 1164, 1117, 1075, 1016, 921, 840, 725, 702 cm^{-1}; **HRMS** (APCI/TOF) *m/z*: $[M - OH]^+$ Calcd. for $C_{18}H_{16}F_3^+$ 289.1199; found 289.1195.

2-methyl-2-(4-(methylsulfonyl)phenyl)-1-phenylbut-3-en-1-ol (4.3ha)

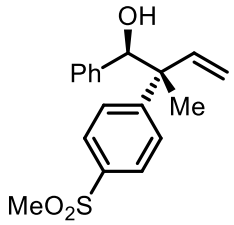

White solid (Method A, 14.5 mg, 46% yield, 90:10 *dr*, 84:16 *rr*); **^{1}H NMR** (500 MHz, $CDCl_3$) (major) δ 7.88-7.83 (m, 2H), 7.61-7.56 (m, 2H), 7.25-7.17 (m, 3H), 7.14-7.08 (m, 2H), 6.52 (dd, *J* = 17.7, 10.9 Hz, 1H), 5.38 (dd, *J* = 11.0, 1.0 Hz, 1H), 5.11 (dd, *J* = 17.6, 1.0 Hz, 1H), 5.07 (s, 1H), 3.04 (s, 3H), 2.12 (*br* s, 1H), 1.32 (s, 3H); **^{1}H NMR** (500 MHz, $CDCl_3$) (**minor diastereomer**, **diagnostic peaks**) δ 6.27 (dd, *J* = 17.5, 10.9 Hz, 1H), 5.22 (dd, *J* = 10.9, 0.9 Hz, 1H); **^{1}H NMR** (500 MHz, $CDCl_3$) (**regioisomers**, **diagnostic peaks**) δ 4.63 (d, *J* = 4.8 Hz, 1H), 4.60 (d, *J* = 8.2 Hz, 1H); **^{13}C NMR** (101 MHz, CDCl3) (major)

δ 152.2, 141.1, 140.0, 138.5, 128.7, 128.1, 128.0, 127.7, 127.2, 116.8, 80.2, 50.6, 44.7, 21.5; **IR** (neat) ν = 3491, 2978, 2925, 2870, 1592, 1295, 1146, 1093, 1047, 955, 921, 778, 700 cm^{-1}; **HRMS** (ESI/TOF) *m/z*: $[M + Na]^+$ Calcd. for $C_{18}H_{20}NaO_3S^+$ 339.1025; found 339.1029.

2-methyl-1-phenyl-2-(m-tolyl)but-3-en-1-ol (4.3ia)

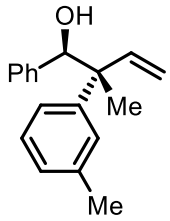

Yellowish oil (Method B, 19.1 mg, 77% yield, 97:3 *dr*, 98:2 *rr*); **^{1}H NMR** (400 MHz, $CDCl_3$) δ 7.25 – 7.18 (m, 6H), 7.18 – 7.11 (m, 2H), 7.09 – 7.03 (m, 1H), 6.58 (dd, *J* = 17.7, 10.9 Hz, 1H), 5.32 (dd, *J* = 11.0, 1.2 Hz, 1H), 5.11 – 5.04 (m, 2H), 2.36 (s, 3H), 2.07 (*br* s, 1H), 1.28 (s, 3H); **^{1}H NMR** (400 MHz, $CDCl_3$) **(minor diastereomer**, **diagnostic peaks)** δ 6.25 (dd, *J* = 17.4, 10.9 Hz, 1H), 5.14 (dd, *J* = 10.9, 1.1 Hz, 2H), 5.03 (s, 1H), 4.98 (dd, *J* = 17.5, 1.1 Hz, 1H); **^{1}H NMR** (400 MHz, $CDCl_3$) **(minor regioisomer**, **diagnostic peaks)** δ 5.40 (d, *J* = 1.1 Hz, 1H), 5.21 (s, 1H), 4.71 (d, *J* = 3.6 Hz, 1H), 3.19 – 3.09 (m, 1H); **^{13}C NMR** (101 MHz, $CDCl_3$) δ 145.18, 142.02, 140.23, 137.95, 128.35, 128.15, 128.11, 127.54, 127.42, 127.31, 124.37, 115.68, 80.49, 77.48, 77.16, 76.84, 50.35, 21.82, 21.12; **IR** (neat) ν = 3455, 3083, 3059, 3029, 2977, 2922, 1603, 1490, 1453, 1375, 1184, 1036, 917, 785, 723, 701 cm^{-1}; **HRMS** (ESI/TOF) *m/z*: $[M + Na]^+$ Calcd. for $C_{18}H_{20}NaO^+$ 275.1406; found 275.1404.

2-(3-(benzyloxy)phenyl)-2-methyl-1-phenylbut-3-en-1-ol (4.3ja)

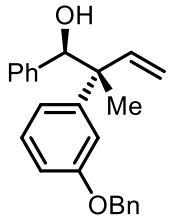

Yellowish oil (Method B, 21.2 mg, 62% yield, 96:4 *dr*, 99:1 *rr*); **^{1}H NMR** (400 MHz, $CDCl_3$) δ 7.48 – 7.37 (m, 4H), 7.37 – 7.31 (m, 1H), 7.29 – 7.20 (m, 4H), 7.17 – 7.10 (m, 2H), 7.01 (dd, *J* = 7.6, 1.1 Hz, 2H), 6.89 – 6.84 (m, 1H), 6.54 (dd, *J* = 17.7, 10.9 Hz, 1H), 5.32 (dd, *J* = 10.9, 1.2 Hz, 1H), 5.09 (dd, *J* = 17.7, 1.2 Hz, 1H), 5.04 (s, 3H), 2.08 (s, 1H), 1.27 (s, 3H); ^{1}H NMR (400 MHz, $CDCl_3$) **(minor diastereomer**, **diagnostic peaks)** δ 6.23 (dd, *J* = 17.4, 10.9 Hz, 1H), 5.15 (dd, *J* = 10.9, 1.1 Hz, 1H), 4.99 (s, 1H), 4.97 (d, *J* = 1.2 Hz, 1H); **^{13}C NMR** (101 MHz, $CDCl_3$) δ 158.85, 146.98, 141.89, 140.14, 137.14, 129.37, 128.72, 128.12, 128.07, 127.73, 127.58, 127.36, 119.98, 115.82, 115.09, 112.47, 80.39, 77.48, 77.16, 76.84, 70.16, 50.49, 20.93; **IR** (neat) ν = 3465, 3062, 3030, 2977, 2925, 2874, 1599, 1581, 1489, 1453, 1289, 1245, 1172, 1021, 917, 728, 697 cm^{-1}; **HRMS** (ESI/TOF) *m/z*: $[M + Na]^+$ Calcd. for $C_{24}H_{24}NaO_2^+$ 367.1669; found 367.1661.

2-(2-methoxyphenyl)-2-methyl-1-phenylbut-3-en-1-ol (4.3ka)[16d]

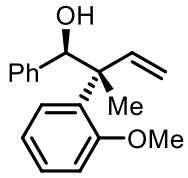

Yellowish oil (Method A, 15.6 mg, 58% yield, >99:1 *dr*, >99:1 *rr*); **^{1}H NMR** (400 MHz, $CDCl_3$) δ 7.26 – 7.20 (m, 1H), 7.18 – 7.12 (m, 3H), 7.11 – 7.02 (m, 3H), 6.96 (dd, *J* = 8.2, 1.2 Hz, 1H), 6.90 – 6.78 (m, 2H), 5.75 (s, 1H), 5.21 (dd, *J* = 10.9, 1.4 Hz, 1H), 5.05 (dd, *J* = 17.7, 1.4 Hz, 1H), 3.94 (s, 3H), 2.17 (*br* s, 1H), 1.35 (s, 3H); **^{13}C NMR** (101 MHz, $CDCl_3$) δ 157.87, 143.06, 141.10, 132.87, 129.24, 128.24, 127.62, 127.17, 127.04, 121.00, 114.67, 111.93, 75.79, 55.38, 50.97, 18.19.

2-(3,5-dimethylphenyl)-2-methyl-1-phenylbut-3-en-1-ol (4.3la)

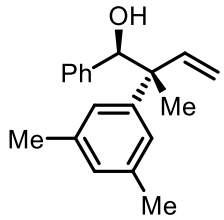

Yellowish oil (Method B, 18.0 mg, 68% yield, 97:3 *dr*, 99:1 *rr*); **^{1}H NMR** (400 MHz, $CDCl_3$) δ 7.26 – 7.22 (m, 3H), 7.21 – 7.15 (m, 2H), 7.04 – 6.99 (m, 2H), 6.93 – 6.86 (m, 1H), 6.58 (dd, *J* = 17.7, 11.0 Hz, 1H), 5.31 (dd, *J* = 10.9, 1.3 Hz, 1H), 5.09 – 4.99 (m, 2H), 2.34 – 2.31 (m, 6H), 2.06 (*br* s, 1H), 1.25 (s, 3H); **^{1}H NMR** (400 MHz, $CDCl_3$) **(minor diastereomer**, **diagnostic peaks)** δ 6.24 (dd, *J* = 17.5, 10.9 Hz, 1H), 5.11 (dd, *J* = 10.8, 1.2 Hz, 1H), 4.95 (dd, *J* = 17.5, 1.2 Hz, 1H); **^{13}C NMR** (101 MHz, $CDCl_3$) δ 145.25, 141.83, 140.27, 137.88, 128.36, 128.17, 127.53, 127.29, 125.14, 115.62, 80.58, 50.27, 21.69, 21.50; **IR** (neat) ν = 3457, 3082, 3058, 3029, 2976, 2917, 2869, 1600, 1490, 1453, 1375, 1183, 1038, 916, 848, 721, 701 cm^{-1}; **HRMS** (ESI/TOF) *m/z*: $[M + Na]^+$ Calcd. for $C_{19}H_{22}NaO^+$ 289.1563; found 289.1561.

2-methyl-2-(naphthalen-2-yl)-1-phenylbut-3-en-1-ol (4.3ma)[16d]

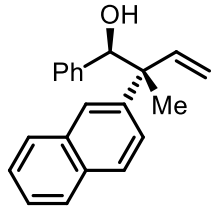

Yellowish oil (Method B, 21.9 mg, 76% yield, 96:4 *dr*, 98:2 *rr*); **^{1}H NMR** (400 MHz, $CDCl_3$) δ 7.89 – 7.74 (m, 4H), 7.60 (dd, *J* = 8.7, 2.0 Hz, 1H), 7.52 – 7.42 (m, 2H), 7.25 – 7.13 (m, 5H), 6.67 (dd, *J* = 17.7, 10.9 Hz, 1H), 5.39 (dd, *J* = 10.9, 1.2 Hz, 1H), 5.22 (s, 1H), 5.15 (dd, *J* = 17.7, 1.2 Hz, 1H), 2.13 (*br* s, 1H), 1.40 (s, 3H); **^{1}H NMR** (400 MHz, $CDCl_3$) **(minor diastereomer**, **diagnostic peaks)** δ 6.34 (dd, *J* = 17.5, 10.9 Hz, 1H), 5.02 (dd, *J* = 17.5, 1.1 Hz, 1H); **^{1}H NMR** (400 MHz, $CDCl_3$) **(minor regioisomer**, **diagnostic peaks)** δ 5.55 (d, *J* = 1.0 Hz, 1H), 5.33 (d, *J* = 1.1 Hz, 1H), 4.76 (d, *J* = 3.8 Hz, 1H), 3.34 – 3.24 (m, 1H); **^{13}C NMR** (101 MHz, $CDCl_3$) δ 142.59, 142.04, 140.21, 133.41, 132.24, 128.25, 128.08, 127.94, 127.61, 127.51, 127.41, 126.37, 126.13, 125.94, 125.65, 116.04, 80.23, 50.62, 21.15.

2-methyl-1-phenyl-2-(thiophen-2-yl)but-3-en-1-ol (4.3na)[16d]

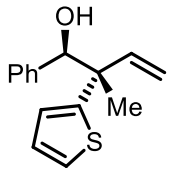

Yellowish oil (Method B, 12.7 mg, 52% yield, 95:5 *dr*, >99:1 *rr*); **^{1}H NMR** (400 MHz, $CDCl_3$) δ 7.26 – 7.19 (m, 4H), 7.18 – 7.10 (m, 2H), 6.96 (dd, *J* = 5.1, 3.6 Hz, 1H), 6.84 (dd, *J* = 3.6, 1.2 Hz, 1H), 6.48 (dd, *J* = 17.5, 10.8 Hz, 1H), 5.31 (dd, *J* = 10.8, 1.0 Hz, 1H), 5.15 (dd, *J* = 17.5, 1.0 Hz, 1H), 4.93 – 4.82 (m, 1H), 2.24 (d, *J* = 2.6 Hz, 1H), 1.38 (s, 3H); **^{1}H NMR** (400 MHz, $CDCl_3$) **(minor diastereomer**, **diagnostic peaks)** δ 6.20 (dd, *J* = 17.3, 10.7 Hz, 1H), 5.03 (dd, *J* = 17.3, 0.9 Hz, 1H); **^{13}C NMR** (101 MHz, $CDCl_3$) δ 150.13, 141.59, 139.79, 127.96, 127.80, 127.49, 126.74, 124.63, 124.06, 115.70, 81.65, 77.48, 77.16, 76.84, 49.50, 21.91.

2-(benzofuran-2-yl)-2-methyl-1-phenylbut-3-en-1-ol (4.3oa)

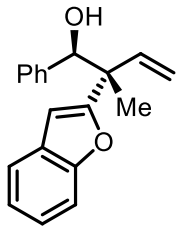

Yellowish solid (Method B, 7.6 mg, 28% yield, 93:7 *dr*, >99:1 *rr*); **^{1}H NMR** (500 MHz, $CDCl_3$) δ 7.52 – 7.45 (m, 2H), 7.29 – 7.25 (m, 1H), 7.22 – 7.17 (m, 4H), 7.15 – 7.08 (m, 2H), 6.53 (dd, *J* = 17.6, 10.8 Hz, 1H), 6.36 (d, *J* = 0.9 Hz, 1H), 5.35 (dd, *J* = 10.8, 1.0 Hz, 1H), 5.24 – 5.17 (m, 2H), 2.33 (d, *J* = 2.8 Hz, 1H), 1.34 (s, 3H); **^{1}H NMR** (500 MHz, $CDCl_3$) **(minor diastereomer**, **diagnostic peaks)** δ 6.15 (dd, *J* = 17.5, 10.7 Hz, 1H), 5.03 (dd, *J* = 17.5, 1.0 Hz, 1H); **^{13}C NMR** (126 MHz, $CDCl_3$) δ 161.32, 154.73, 139.73, 139.59, 128.44, 127.74, 127.63, 127.53, 123.86, 122.82, 120.90, 116.66, 111.16, 103.74, 78.30, 48.98, 17.53; **IR** (neat) ν = 3450, 3084, 3062, 3032, 2979, 2924, 2855, 1579, 1492, 1453, 1252, 1166, 1043, 923, 802, 744, 719, 703 cm^{-1}; **HRMS** (ESI/TOF) *m/z*: $[M + Na]^+$ Calcd. for $C_{19}H_{18}NaO_2^+$ 301.1199; found 301.1210.

2-methyl-1,2,3-triphenylbut-3-en-1-ol (4.3pa)

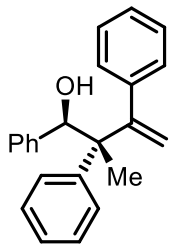

Yellowish solid (Method B, 6.6 mg, 21% yield, >99:1 *dr*, >99:1 *rr*); **^{1}H NMR** (400 MHz, $CDCl_3$) δ 7.25 – 7.00 (m, 11H), 6.83 – 6.73 (m, 4H), 5.82 (s, 1H), 5.55 (s, 1H), 5.46 (s, 1H), 2.67 (s, 1H), 1.25 (s, 3H); **^{13}C NMR** (101 MHz, $CDCl_3$) δ 155.17, 143.05, 142.45, 139.62, 128.28, 128.24, 128.20, 128.14, 127.77, 127.14, 127.08, 126.99, 126.90, 114.94, 78.50, 53.49, 16.62; **IR** (neat) ν = 3459, 3059, 3026, 2923, 2854, 1598, 1491, 1447, 1378, 1182, 1022, 909, 776, 743, 700 cm^{-1}; **HRMS** (ESI/TOF) *m/z*: $[M + Na]^+$ Calcd. for $C_{23}H_{22}NaO^+$ 337.1563; found 337.1559.

4-methyl-1,2-diphenyl-2-vinylpentan-1-ol (4.5a)

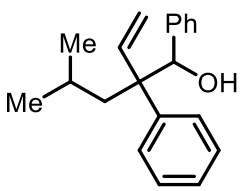

Yellowish oil (Method C, 18.2 mg, 62% yield, >95:5 *dr*, 93:7 *rr*); **^{1}H NMR** (400 MHz, $CDCl_3$) δ 7.50 – 7.42 (m, 2H), 7.39 – 7.31 (m, 2H), 7.31 – 7.22 (m, 4H), 7.24 – 7.16 (m, 3H), 6.27 (dd, *J* = 18.0, 11.2 Hz, 1H), 5.39 (dd, *J* = 11.2, 1.3 Hz, 1H), 5.23 (d, *J* = 1.7 Hz, 1H), 4.97 (dd, *J* = 18.0, 1.3 Hz, 1H), 2.01 (*br* d, *J* = 2.7 Hz, 1H), 1.59 – 1.46 (m, 3H), 0.63 (d, *J* = 6.4 Hz, 3H), 0.43 (d, *J* = 6.4 Hz, 3H); **^{1}H NMR** (400 MHz, $CDCl_3$) **(minor regioisomer**, **diagnostic peaks)** δ 5.43 (d, *J* = 1.1 Hz, 1H), 5.15 (d, *J* = 1.0 Hz, 1H), 4.66 (d, *J* = 4.6 Hz, 1H), 3.08 (dt, *J* = 11.3, 4.0 Hz, 1H), 0.86 (d, *J* = 6.6 Hz, 3H), 0.74 (d, *J* = 6.6 Hz, 3H); **^{13}C NMR** (101 MHz, $CDCl_3$) δ 142.62, 140.52, 139.99, 128.83, 128.77, 128.41, 127.66, 127.27, 126.75, 117.04, 80.06, 54.87, 44.28, 24.87, 24.60, 24.30; **^{13}C NMR** (101 MHz, $CDCl_3$) **(minor regioisomer**, **diagnostic peaks)** δ 114.68, 75.52, 49.79, 36.71, 29.85, 25.40, 21.69; **IR** (neat) ν = 3451, 3084, 3059, 3028, 2979, 2927, 1600, 1493, 1449, 1375, 1188, 1021, 918, 725, 696 cm^{-1}; **HRMS** (ESI/TOF) *m/z*: $[M + Na]^+$ Calcd. for $C_{20}H_{24}NaO^+$ 303.1719; found 303.1716.

4-ethyl-1,2-diphenyl-2-vinylhexan-1-ol (4.5b)

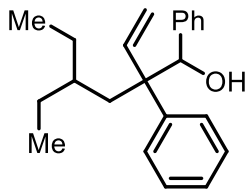

Yellowish oil (Method C, 22.4 mg, 73% yield, >95:5 *dr*, 89:11 *rr*); **^{1}H NMR** (400 MHz, $CDCl_3$) δ 7.48 – 7.42 (m, 2H), 7.38 – 7.31 (m, 2H), 7.30 – 7.24 (m, 4H), 7.23 – 7.17 (m, 2H), 6.22 (dd, *J* = 18.0, 11.3 Hz, 1H), 5.40 (dd, *J* = 11.3, 1.3 Hz, 1H), 5.24 (s, 1H), 5.02 (dd, *J* = 18.0, 1.3 Hz, 1H), 2.05 (*br* s, 1H), 1.65 – 1.51 (m, 2H), 1.25 – 1.12 (m, 2H), 1.10 – 0.96 (m, 1H), 0.82 – 0.72 (m, 2H), 0.64 (t, *J* = 7.4 Hz, 3H), 0.57 (t, *J* = 7.3 Hz, 3H); **^{1}H NMR** (400 MHz, $CDCl_3$) **(minor regioisomer**, **diagnostic peaks)** δ 5.45 (d, *J* = 1.0 Hz, 1H), 5.19 (s, 1H), 4.68 (d, *J* = 4.4 Hz, 1H), 3.09 (dt, *J* = 11.4, 3.8 Hz, 1H); **^{13}C NMR** (101 MHz, $CDCl_3$) δ 142.67, 140.58, 140.21, 128.87, 128.75, 128.31, 127.62, 127.24, 126.73, 117.20, 80.00, 54.92, 39.64, 35.37, 25.82, 25.30, 10.31, 10.20; **^{13}C NMR** (101 MHz, $CDCl_3$) **(minor regioisomer**, **diagnostic peaks)** δ 114.65, 75.46, 49.56, 37.42, 30.45, 26.50, 24.62, 11.33, 9.75; **IR** (neat) ν = 3464, 3085, 3060, 3029, 2961, 2927, 2873, 1569, 1494, 1453, 1386, 1225, 1036, 917, 702 cm^{-1}; **HRMS** (ESI/TOF) *m/z*: $[M + Na]^+$ Calcd. for $C_{22}H_{28}NaO^+$ 331.2032; found 331.2041.

2-(cyclohexylmethyl)-1,2-diphenylbut-3-en-1-ol (4.5c)

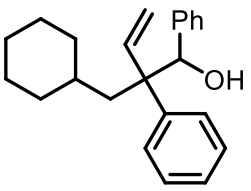

Yellowish oil (Method C, 18.0 mg, 56% yield, >95:5 *dr*, 90:10 *rr*); **^{1}H NMR** (400 MHz, $CDCl_3$) δ 7.44 – 7.39 (m, 2H), 7.34 – 7.28 (m, 2H), 7.25 – 7.20 (m, 4H), 7.19 – 7.12 (m, 2H), 6.24 (dd, *J* = 18.0, 11.2 Hz, 1H), 5.36 (dd, *J* = 11.2, 1.3 Hz, 1H), 5.20 (d, *J* = 1.7 Hz, 1H), 4.96 (dd, *J* = 18.0, 1.3 Hz, 1H), 2.01 (*br* d, *J* = 3.0 Hz, 1H), 1.63 – 1.47 (m, 4H), 1.42 – 1.29 (m, 2H), 1.20 – 1.10 (m, 1H), 1.02 – 0.86 (m, 4H), 0.81 – 0.52 (m, 2H); **^{1}H NMR** (400 MHz, $CDCl_3$) **(minor regioisomer**, **diagnostic peaks)** δ 5.42 (d, *J* = 1.0 Hz, 1H), 5.15-5.13 (m, 1H), 4.63 (d, *J* = 4.4 Hz, 1H), 3.11 (dt, *J* = 11.3, 3.9 Hz, 1H); **^{13}C NMR** (101 MHz, $CDCl_3$) δ 142.73, 140.55, 140.20, 128.82, 128.69, 128.31, 127.61, 127.24, 126.72, 116.94, 80.00, 54.86, 42.89, 35.43, 35.10, 33.82, 26.62, 26.59, 26.45; **IR** (neat) ν = 3450, 3084, 3059, 3029, 2920, 2848, 1600, 1494, 1448, 1263, 1023, 916, 731, 699 cm^{-1}; **HRMS** (ESI/TOF) *m/z*: $[M + Na]^+$ Calcd. for $C_{23}H_{28}NaO^+$ 343.2032; found 343.2027.

1,2-diphenyl-2-((tetrahydro-2H-pyran-4-yl)methyl)but-3-en-1-ol (4.5d)

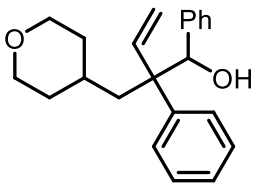

Yellowish oil (Method C, 20.4 mg, 63% yield, >95:5 *dr*, >95:5 *rr*); **^{1}H NMR** (400 MHz, $CDCl_3$) δ 7.48 – 7.42 (m, 2H), 7.37 – 7.32 (m, 2H), 7.27 – 7.23 (m, 4H), 7.21 – 7.16 (m, 2H), 6.29 (dd, *J* = 18.0, 11.2 Hz, 1H), 5.40 (dd, *J* = 11.2, 1.2 Hz, 1H), 5.22 (s, 1H), 3.80 – 3.53 (m, 2H), 3.10 (dtd, *J* = 42.9, 11.5, 2.6 Hz, 2H), 1.67 – 1.54 (m, 2H), 1.45 – 1.39 (m, 1H), 1.20 – 1.13 (m, 2H), 1.05 – 0.93 (m, 1H), 0.70 – 0.61 (m, 1H); **^{13}C NMR** (101 MHz, $CDCl_3$) δ 142.55, 140.37, 139.76, 128.74, 128.56, 128.48, 127.75, 127.33, 126.94, 117.11, 80.18, 68.15, 68.12, 54.57, 42.44, 35.04, 34.80, 31.33; **IR** (neat) ν = 3405, 3084, 3058, 3028, 2922, 2845, 1600, 1494, 1448, 1269, 1088, 1020, 917, 732, 700 cm^{-1}; **HRMS** (ESI/TOF) *m/z*: $[M + Na]^+$ Calcd. for $C_{22}H_{26}NaO_2^+$ 345.1825; found 345.1814.

2-(cyclopentylmethyl)-1,2-diphenylbut-3-en-1-ol (4.5e)

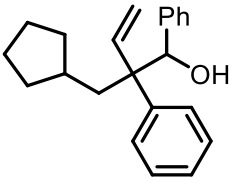

Yellowish oil (Method C, 21.3 mg, 70% yield, >95:5 *dr*, 90:10 *rr*); **^{1}H NMR** (400 MHz, $CDCl_3$) δ 7.47 – 7.42 (m, 2H), 7.38 – 7.32 (m, 2H), 7.29 – 7.24 (m, 4H), 7.24 – 7.19 (m, 2H), 6.30 (dd, *J* = 18.0, 11.2 Hz, 1H), 5.38 (dd, *J* = 11.2, 1.3 Hz, 1H), 5.27 (s, 1H), 4.98 (dd, *J* = 18.0, 1.3 Hz, 1H), 2.11 – 1.92 (m, 1H), 1.74 (d, *J* = 5.5 Hz, 2H), 1.67 – 1.57 (m, 1H), 1.46 – 1.36 (m, 3H), 1.29 – 1.22 (m, 2H), 1.07 – 0.98 (m, 1H), 0.89 – 0.80 (m, 1H), 0.75

– 0.63 (m, 1H); **^{1}H NMR** (400 MHz, $CDCl_3$) **(minor regioisomer**, **diagnostic peaks)** δ 5.44 (d, *J* = 1.1 Hz, 1H), 5.17 (d, *J* = 1.1 Hz, 1H), 4.65 (d, *J* = 4.7 Hz, 1H), 3.06 (dt, *J* = 11.3, 4.1 Hz, 1H); **^{13}C NMR** (101 MHz, $CDCl_3$) δ 142.88, 140.59, 140.06, 128.79, 128.73, 128.37, 127.61, 127.26, 126.70, 116.87, 79.80, 54.81, 42.06, 36.47, 34.73, 34.55, 24.99, 24.83. **^{13}C NMR** (101 MHz, $CDCl_3$) **(minor regioisomer**, **diagnostic peaks)** δ 114.59, 75.63, 51.05, 37.52, 34.02, 33.89, 32.16, 29.84, 25.26; **IR** (neat) ν = 3442, 3083, 3059, 3028, 2943, 2864, 1600, 1494, 1449, 1021, 916, 729, 699 cm^{-1}; **HRMS** (ESI/TOF) *m/z*: $[M + Na]^+$ Calcd. for $C_{22}H_{26}NaO^+$ 329.1876; found 329.1876.

4-methyl-1,2-diphenyl-2-vinylheptan-1-ol (4.5f)

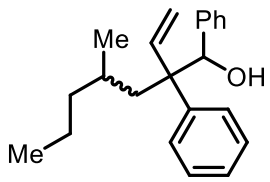

Yellowish oil (Method C, 21.3 mg, 70% yield, >95:5 *dr*, 92:8 *rr*); **^{1}H NMR** (400 MHz, $CDCl_3$) δ 7.47 – 7.41 (m, 4H), 7.36 – 7.30 (m, 4H), 7.26 – 7.16 (m, 12H), 6.31 – 6.18 (m, 2H), 5.40 – 5.33 (m, 2H), 5.25 – 5.17 (m, 2H), 5.02 – 4.90 (m, 2H), 2.06 – 1.96 (*br* m, 2H), 1.65 – 1.57 (m, 2H), 1.53 – 1.43 (m, 2H), 1.39 – 1.30 (m, 2H), 1.18 – 1.08 (m, 2H), 1.03 – 0.95 (m, 2H), 0.93 – 0.86 (m, 2H), 0.70 (t, *J* = 7.2 Hz, 5H), 0.63 (t, *J* = 7.3 Hz, 3H), 0.58 (d, *J* = 6.6 Hz, 3H), 0.33 (d, *J* = 6.6 Hz, 3H); **^{1}H NMR** (400 MHz, $CDCl_3$) **(minor regioisomer**, **diagnostic peaks)** δ 5.14 (d, *J* = 1.0 Hz, 1H), 4.65 (d, *J* = 4.6 Hz, 1H), 3.09 (dt, *J* = 10.9, 4.1 Hz, 1H); **^{13}C NMR** (101 MHz, $CDCl_3$) δ 142.70, 140.56, 140.52, 140.20, 139.98, 128.87, 128.85, 128.79, 128.75, 128.38, 128.37, 127.65, 127.63, 127.26, 127.23, 126.74, 126.70, 117.11, 117.07, 80.16, 79.94, 54.94, 43.23, 43.17, 41.27, 40.84, 28.61, 28.57, 21.29, 20.99, 20.01, 19.97, 14.34, 14.25; **IR** (neat) ν = 3449, 3085, 3060, 3029, 2956, 2926, 2870, 1600, 1494, 1451, 1380, 1022, 916, 730, 700 cm^{-1}; **HRMS** (ESI/TOF) *m/z*: $[M + Na]^+$ Calcd. for $C_{22}H_{28}NaO^+$ 331.2032; found 331.2019.

4,8-dimethyl-1,2-diphenyl-2-vinylnon-7-en-1-ol (4.5g)

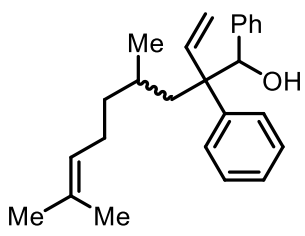

Yellowish oil (Method C, 26.2 mg, 75% yield, >95:5 *dr*, 91:9 *rr*); **^{1}H NMR** (400 MHz, $CDCl_3$) δ 7.46 (d, *J* = 7.6 Hz, 4H), 7.38 – 7.32 (m, 4H), 7.29 – 7.20 (m, 12H), 6.27 (dd, *J* = 18.0, 11.2 Hz, 2H), 5.41 (dd, *J* = 3.4, 1.2 Hz, 1H), 5.39 (dd, *J* = 3.5, 1.3 Hz, 1H), 5.25 (s, 1H), 5.22 (s, 1H), 5.01 (dd, *J* = 11.3, 1.3 Hz, 1H), 4.96 (dd, *J* = 11.3, 1.3 Hz, 1H), 4.94 – 4.89 (m, 1H), 4.88 – 4.80 (m, 1H), 2.04 (*br* s, 2H), 1.86 – 1.76 (m, 2H), 1.71 – 1.66 (m, 2H), 1.64 (s, 6H), 1.60 – 1.54 (m, 2H), 1.52 (s, 6H), 1.42 – 1.19 (m, 4H), 1.15 – 1.05 (m, 1H), 1.00 – 0.90 (m, 1H), 0.87 – 0.78

(m, 2H), 0.63 (d, *J* = 6.6 Hz, 3H), 0.38 (d, *J* = 6.6 Hz, 3H); **^{1}H NMR** (400 MHz, $CDCl_3$) **(minor regioisomer**, **diagnostic peaks)** δ 5.45 – 5.43 (m, 1H), 5.18 – 5.14 (m, 1H), 4.70 – 4.63 (m, 1H), 3.16 – 3.03 (m, 1H); **^{13}C NMR** (101 MHz, $CDCl_3$) δ 142.64, 142.56, 140.54, 140.48, 140.23, 139.85, 131.12, 131.00, 128.85, 128.83, 128.78, 128.76, 128.39, 128.38, 127.65, 127.63, 127.26, 127.22, 126.75, 126.72, 124.88, 124.87, 117.13, 117.10, 80.25, 79.86, 54.93, 54.90, 43.18, 43.09, 39.04, 38.75, 28.56, 28.54, 25.80, 25.49, 25.47, 21.23, 20.92, 17.70, 17.67; **IR** (neat) ν = 3434, 3084, 3060, 3028, 2958, 2926, 2873, 1600, 1494, 1450, 1378, 1232, 1026, 916, 732, 701 cm^{-1}; **HRMS** (ESI/TOF) *m/z*: $[M + Na]^+$ Calcd. for $C_{25}H_{32}NaO^+$ 371.2345; found 371.2329.

4,4-dimethyl-1,2-diphenyl-2-vinylpentan-1-ol (4.5h)

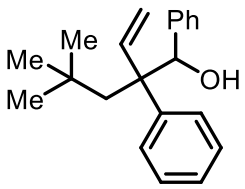

Yellowish oil (Method C, 5.2 mg, 18% yield, 97:3 *dr*, 89:11 *rr*); **^{1}H NMR** (500 MHz, $CDCl_3$) δ 7.57 – 7.51 (m, 2H), 7.36 – 7.30 (m, 3H), 7.24 – 7.22 (m, 3H), 7.18 – 7.13 (m, 2H), 6.15 (dd, *J* = 18.1, 11.4 Hz, 1H), 5.48 (dd, *J* = 11.4, 1.2 Hz, 1H), 5.22 – 5.15 (m, 2H), 2.04 (d, *J* = 3.5 Hz, 1H), 1.89 (d, *J* = 14.6 Hz, 1H), 1.74 (d, *J* = 14.7 Hz, 1H), 0.62 (s, 9H); **^{13}C NMR** (126 MHz, $CDCl_3$) δ 142.03, 140.46, 140.09, 129.40, 129.12, 128.19, 127.55, 127.13, 126.80, 117.79, 81.38, 54.25, 48.39, 32.08, 31.93; **IR** (neat) ν = 3425, 3085, 3060, 3029, 2952, 2867, 1602, 1494, 1451, 1025, 918, 728, 702 cm^{-1}; **HRMS** (ESI/TOF) *m/z*: $[M + Na]^+$ Calcd for. $C_{21}H_{26}NaO^+$ 317.1876; found 317.1861.

2-(2-(benzyloxy)ethyl)-1,2-diphenylbut-3-en-1-ol (4.5i)

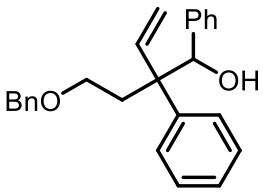

Yellowish oil (Method C, 21.4 mg, 60% yield, >95:1 *dr*, >95:1 *rr*); **^{1}H NMR** (400 MHz, $CDCl_3$) δ 7.36 – 7.15 (m, 13H), 7.11 – 7.03 (m, 2H), 6.31 (dd, *J* = 17.9, 11.2 Hz, 1H), 5.39 (dd, *J* = 11.2, 1.1 Hz, 1H), 5.14 – 5.03 (m, 2H), 4.39 (s, 2H), 3.47 (ddd, *J* = 9.4, 8.0, 6.2 Hz, 1H), 3.25 (ddd, *J* = 9.4, 7.9, 5.8 Hz, 1H), 2.77 (*br* s, 1H), 2.26 – 1.99 (m, 2H), 1.27 (s, 3H); **^{13}C NMR** (101 MHz, $CDCl_3$) δ 142.72, 140.26, 139.85, 138.21, 128.51, 128.36, 128.30, 127.82, 127.76, 127.50, 127.30, 126.75, 116.91, 79.94, 73.29, 67.41, 53.30, 34.35; **IR** (neat) ν = 3426, 30060, 3029, 2923, 2854, 1599, 1494, 1452, 1097, 1046, 920, 701 cm^{-1}; **HRMS** (ESI/TOF) *m/z*: $[M + Na]^+$ Calcd. for $C_{25}H_{26}NaO_2^+$ 381.1825; found 381.1822.

tert-butyl (3-(hydroxy(phenyl)methyl)-3-phenylpent-4-en-1-yl)carbamate (4.5j)

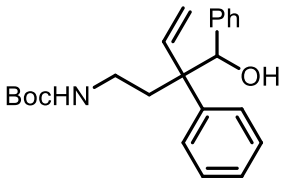

Yellowish oil (Method C, 23.1 mg, 63% yield, >95:5 *dr*, >95:5 *rr*); **^{1}H NMR** (400 MHz, $CDCl_3$) δ 7.42 – 7.27 (m, 5H), 7.24 – 7.19 (m, 3H), 7.17 – 7.07 (m, 2H), 6.33 (dd, *J* = 18.0, 11.2 Hz, 1H), 5.42 (dd, *J* = 11.3, 1.0 Hz, 1H), 5.14 – 5.01 (m, 2H), 4.29 (s, 1H), 3.09 – 2.85 (m, 1H), 2.85 – 2.64 (m, 1H), 2.24 – 2.02 (m, 1H), 1.96 (ddd, *J* = 13.6, 10.7, 5.6 Hz, 1H), 1.85 (ddd, *J* = 13.6, 10.5, 5.1 Hz, 1H), 1.39 (s, 9H); **^{13}C NMR** (101 MHz, $CDCl_3$) δ 155.93, 141.91, 140.05, 138.71, 128.61, 128.44, 128.26, 127.78, 127.39, 126.97, 117.42, 80.34, 79.20, 53.20, 37.03, 34.98, 28.51; **IR** (neat) ν = 3367, 3084, 3059, 3029, 2975, 2932, 1688, 1598, 1501, 1451, 1365, 1247, 1165, 1043, 921, 734, 701 cm^{-1}; **HRMS** (ESI/TOF) *m/z*: $[M + Na]^+$ Calcd. for $C_{23}H_{29}NNaO_3^+$ 390.2040; found 390.2043.

2-phenethyl-1,2-diphenylbut-3-en-1-ol (4.5k)

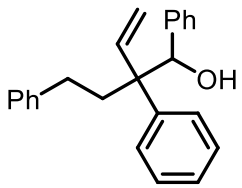

Yellowish oil (Method C, 9.6 mg, 29% yield, >95:5 *dr*, >95:5 *rr*); **^{1}H NMR** (400 MHz, $CDCl_3$) δ 7.50 – 7.44 (m, 2H), 7.43 – 7.37 (m, 2H), 7.32 – 7.27 (m, 1H), 7.24 – 7.11 (m, 8H), 7.05 – 6.99 (m, 2H), 6.41 (dd, *J* = 18.0, 11.2 Hz, 1H), 5.46 (dd, *J* = 11.2, 1.2 Hz, 1H), 5.21 – 5.16 (m, 1H), 5.09 (dd, *J* = 18.0, 1.2 Hz, 1H), 2.40 (td, *J* = 13.1, 4.8 Hz, 1H), 2.23 (td, *J* = 13.0, 4.7 Hz, 1H), 2.11 – 1.90 (m, 3H); **^{13}C NMR** (101 MHz, $CDCl_3$) δ 142.86, 142.45, 140.29, 139.22, 128.57, 128.52, 128.49, 128.44, 128.33, 127.77, 127.43, 126.83, 125.82, 117.26, 80.30, 54.55, 36.88, 30.89; **IR** (neat) ν = 3450, 3083, 3059, 3027, 2926, 2858, 1600, 1494, 1450, 1388, 1024, 918, 731, 699 cm^{-1}; **HRMS** (ESI/TOF) *m/z*: $[M + Na]^+$ Calcd. for $C_{24}H_{24}NaO^+$ 351.1719; found 351.1722.

4.4.7. Mechanistic studies

4.4.7.1. Role of the 1,3-diene 4.A in the catalytic cycle

Control experiment 1: Deviation from standard condition for the formation of diene **4.A**

Table 4.17. Deviation from the standard conditions for the formation of diene **4.A**[a]

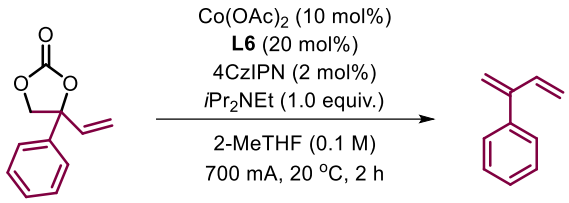

4.1a **4.A**

Entry	4CzIPN	$Co(OAc)_2$	L6	*i*Pr_2NEt	Blue LED	Yield (%)
1	–	√	√	√	√	0
2	√	–	√	√	√	0
3	√	√	–	√	√	0
4	√	√	√	–	√	0
5	√	√	√	√	–	0
6	**√**	**√**	**√**	**√**	**√**	**85%**

[a] Standard conditions: **4.1a** (0.1 mmol), $Co(OAc)_2$ (10 mol%), **L6** (20 mol%), 4CzIPN (2 mol%), DIPEA (1.0 equiv.), MeCN (0.1 M) under the radiation of 700 mA blue LED for 2 h. The yield was determined by GC analysis, using decane as internal standard.

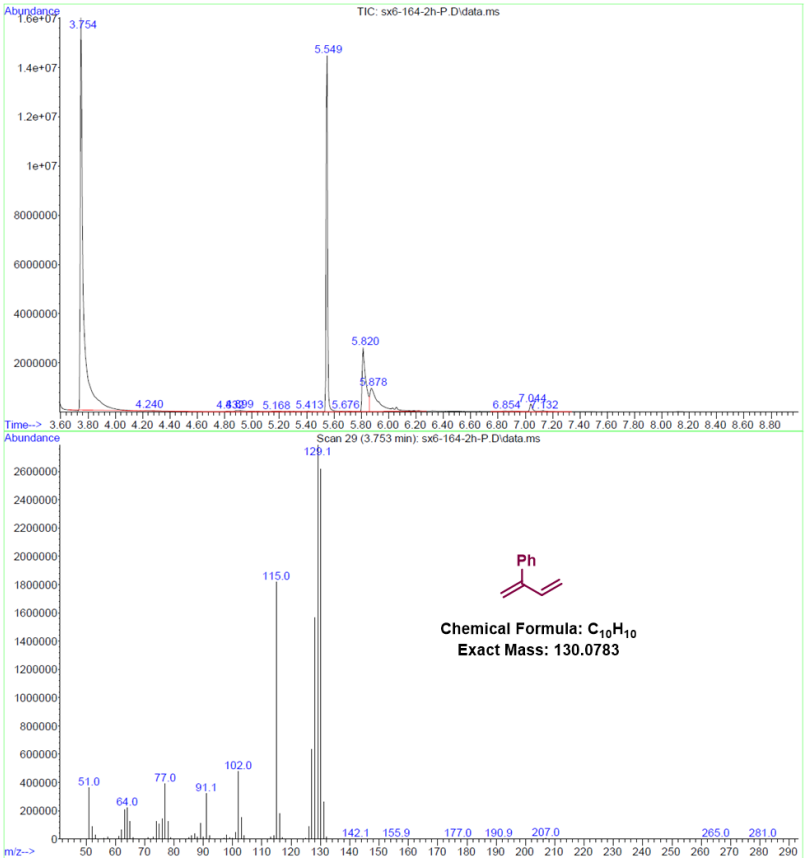

Figure 4.2. GC-MS analysis for the reaction mixture

Procedure related to the standard conditions of entry 6: $Co(OAc)_2$ (10 µmol, 1.8 mg), **L6** (20 µmol, 3.7 mg) and 4CzIPN (2 µmol, 1.6 mg) were weighed in a flat-bottom Schlenk flask. The solids were dissolved in 2-MeTHF (1 mL), then DIPEA (0.1 mmol, 17.4 µL) and **4.1a** (0.1 mmol) were added affording an orange solution. The flask was sealed with a Teflon cap and the mixture was freeze-pump-thawed 3 times and stirred under N_2 at r.t. for 5–20 minutes, after which it was irradiated for 2 hours at 20 °C using a single high-power blue LED (λ_{em} = 445 nm, 700 mA, 1.2 µeinstein s^{-1}) from the bottom. GC-MS analysis was conducted for the mixture attained in entry 6, see Figure 4.2.

Control experiments 2: 1,3-Diene **4.A** as substrate under the standard conditions.

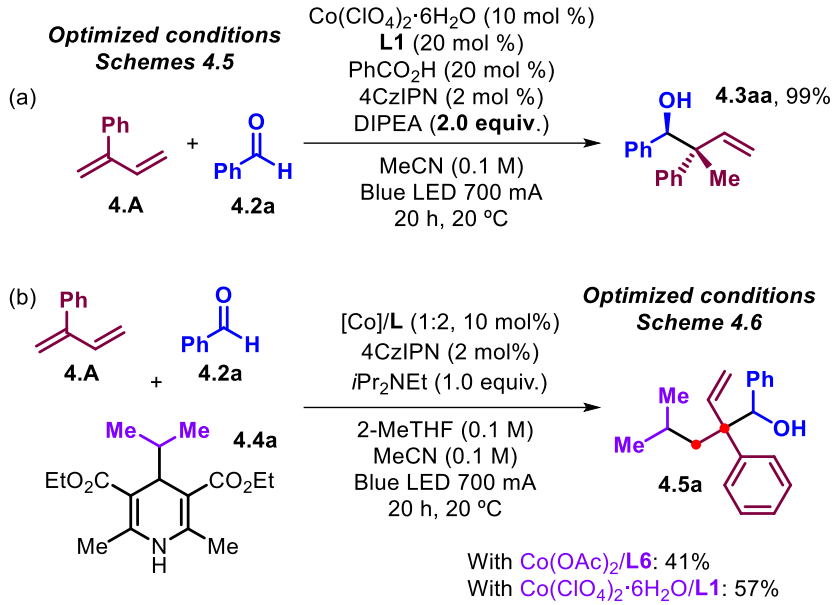

Scheme 4.10. Employing 1,3-diene **4.A** as substrate under standard conditions.

Procedure (a): To a flat-bottom Schlenk flask, $Co(ClO_4)_2 \cdot 6H_2O$ (10 µmol, 3.7 mg), **L1** (20 µmol, 3.2 mg), $PhCO_2H$ (20 µmol, 2.4 mg) and 4CzIPN (2 µmol, 1.6 mg) were added, followed by the addition of 1,3-diene **4.A** in MeCN (1 mL), DIPEA (0.15 mmol, 26.1 µL) as well as aldehyde **4.2a** (0.15 mmol, 15.2 µL). The flask was sealed with a Teflon cap and the mixture was freeze-pump-thawed 3 times and stirred under N_2 at r.t. for 5–20 minutes after which it was irradiated for 20 hours at 20 ºC using a single high-power blue LED (λ_{em} = 445 nm, 700 mA, 1.2 µeinstein s^{-1}) from the bottom. After stopping the irradiation, the yield was determined by ^1H NMR using mesitylene as internal standard.

Procedure (b): $Co(OAc)_2$ (10 µmol, 1.8 mg) and **L6** (20 µmol, 3.7 mg) ***or*** $Co(ClO_4)_2 \cdot 6H_2O$ (10 µmol, 3.7 mg) and **L1** (20 µmol, 3.2 mg) were combined with 4CzIPN (2 µmol, 1.6 mg) as well as **4.4a** (0.15 mmol, 44.3 mg) into a flat-bottom Schlenk flask. 1,3-Diene **4.A** in MeCN (1 mL) dissolved in MeCN/2-MeTHF (1 mL, 1 mL) and DIPEA (17.4 µL, 0.1 mmol) was added affording an yellow solution. The flask was sealed with a Teflon cap and the mixture was freeze-pump-thawed 3 times and stirred under N_2 at r.t. for 5–20 minutes after which it was irradiated for 20 hours at 20 °C using a single high-power blue LED (λ_{em} = 445 nm, 700 mA, 1.2 µeinstein s^{-1}) from the bottom. After stopping the irradiation, the yield was determined by ^1H NMR using mesitylene as internal standard.

4.4.7.2. Investigation of the cycle related to the 1,2-difunctionalization step

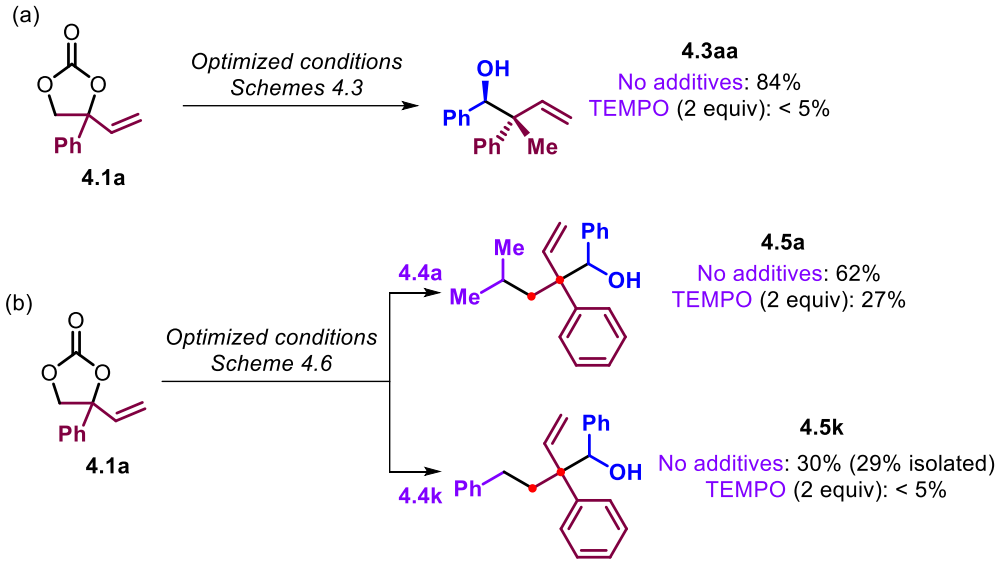

Scheme 4.11. Radical scavenger experiments

Procedure (a): $Co(ClO_4)_2 \cdot 6H_2O$ (10 µmol, 3.7 mg), **L1** (20 µmol, 3.2 mg), $PhCO_2H$ (20 µmol, 2.4 mg), 4CzIPN (2 µmol, 1.6 mg) and TEMPO (0.2 mmol) were weighed in a flat-bottom Schlenk flask. The solids were dissolved in MeCN (1 mL) and DIPEA (0.15 mmol, 26.1 µL), **4.1a** (0.1 mmol, 19.1 mg) and aldehyde **4.2a** (0.15 mmol, 15.2 µL) were added affording an orange solution. The flask was sealed with a Teflon cap and the mixture was freeze-pump-thawed 3 times and stirred under N_2 at r.t. for 5–20 minutes after which it was irradiated for 20 hours at 20 °C using a single high-power blue LED (λ_{em} = 445 nm, 700 mA, 1.2 µeinstein s^{-1}) from the bottom. After stopping the irradiation, the yield of product was determined by ^1H NMR using mesitylene as internal standard. GC-MS analysis was also conducted to detect the formation of possible intermediates, see Figures S4-5.

Procedure (b): $Co(OAc)_2$ (10 µmol, 1.8 mg), **L6** (20 µmol, 3.7 mg) and 4CzIPN (2 µmol, 1.6 mg) were weighed in a flat-bottom Schlenk flask I. The solids were dissolved in 2-MeTHF (1 mL), and DIPEA (17.4 µL, 0.1 mmol) and **4.1a** (0.1 mmol) were added affording a yellow solution. Another Schlenk flask was charged with *i*Pr-DHP **4.4a** (0.15 mmol, 44.3 mg) or **4.4k** (0.15 mmol, 51.5 mg), **4.2a** (0.15 mmol, 15.2 µL) and TEMPO (0.2 mmol) in MeCN (1 mL). Both flasks were sealed with a Teflon cap and the mixture were freeze-pump-thawed 3 times and the mixture in the first Schlenk vessel was stirred under N_2 at r.t. for 5 minutes after which it was irradiated for 2 hours at 20 °C using a single high-power blue LED (λ_{em} = 445 nm, 700 mA, 1.2 µeinstein s^{-1}) from the bottom.

Then the mixture in the second Schlenk flask was added to the first one under Ar, followed by irradiation for 20 hours under the same conditions. After stopping the irradiation, the yield of product was determined by ^{1}H NMR using mesitylene as internal standard.

4.4.7.3. Kinetics of the reaction between VCC 4.1a, 1,3-diene 4.A and 4.3aa, and quantum yield determination

$Co(ClO_4)_2 \cdot 6H_2O$ (10 µmol, 3.7 mg), **L1** (20 µmol, 3.2 mg), $PhCO_2H$ (20 µmol, 2.4 mg) and 4CzIPN (2 µmol, 1.6 mg) were weighed in a flat-bottom Schlenk flask. The solids were dissolved in MeCN (1 mL), and DIPEA (0.15 mmol, 26.1 µL), **4.1a** (0.1 mmol, 19.1 mg), aldehyde **4.2a** (0.15 mmol, 15.2 µL) and decane (0.1 mmol, 14.5 mg) were added affording an orange solution. The flask was sealed with a Teflon cap and the mixture was freeze-pump-thawed 3 times and stirred under N_2 at r.t. for 5–20 minutes, after which it was irradiated at 20 °C using a single high-power blue LED (λ_{em} = 445 nm, 700 mA, 1.2 µeinstein s^{-1}). A small portion of the reaction mixture (around 50 µL) was diluted with 300 µL EA and analyzed by GC (Figure 4.3 below).

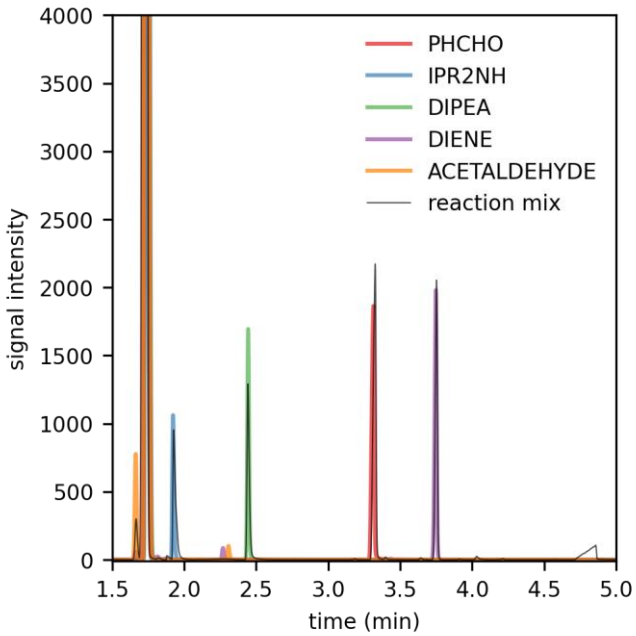

Figure 4.3. GC analysis for the reaction mixture obtained after 1 hour.

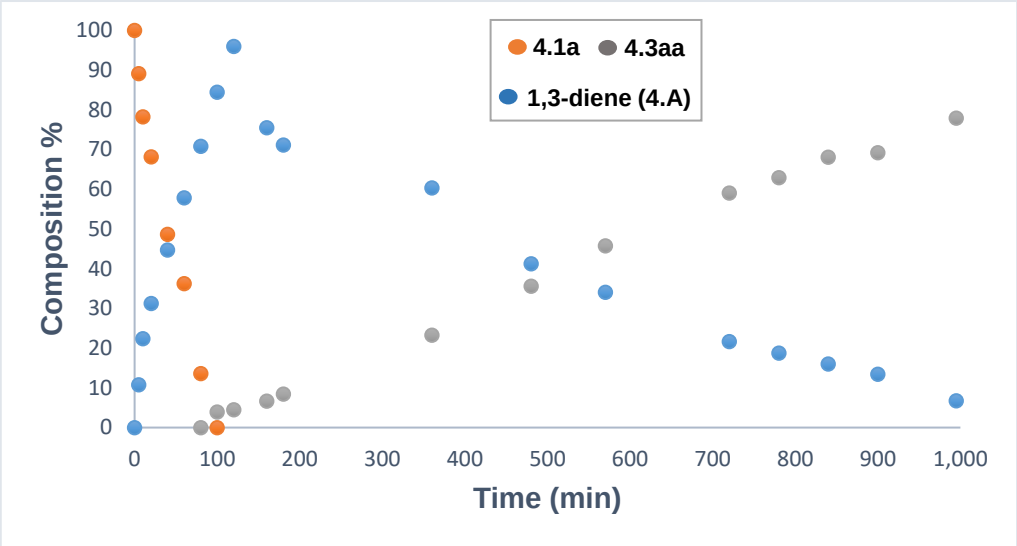

Figure 4.4. Kinetic profiles for the yield of 1,3-diene **4.A** and **4.3aa** (%) and remaining amount of **4.1a** (%) over time.

The quantum yield was determined using equation (1) where the photon flux is 1.2 μeinstein s^{-1}. An absorption spectrum of the reaction mixture gave an absorbance value of >3 at 450 nm, indicating that essentially all the incident light (f_R > 0.999) is absorbed by the photocatalyst.

$$\Phi = \frac{n(product)}{Photon\ Flux * t * f_R} = \frac{Rate\ of\ Product\ formation}{Photon\ Flux} \qquad (1)$$

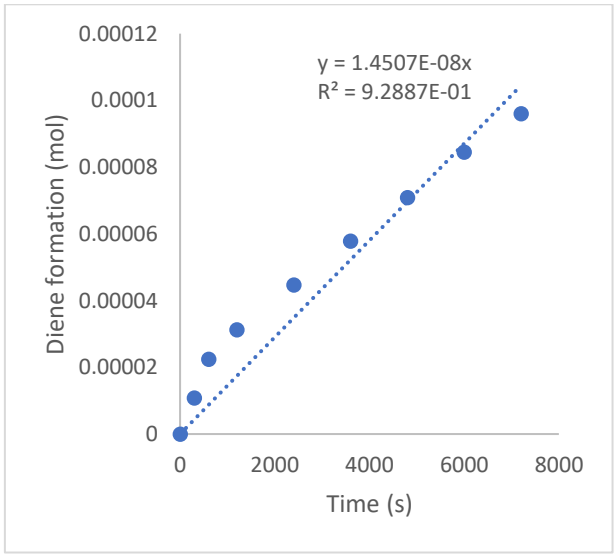

Figure 4.4. Graphical representation of the moles of diene **4.A** formed as a function of time during the quantum yield studies.

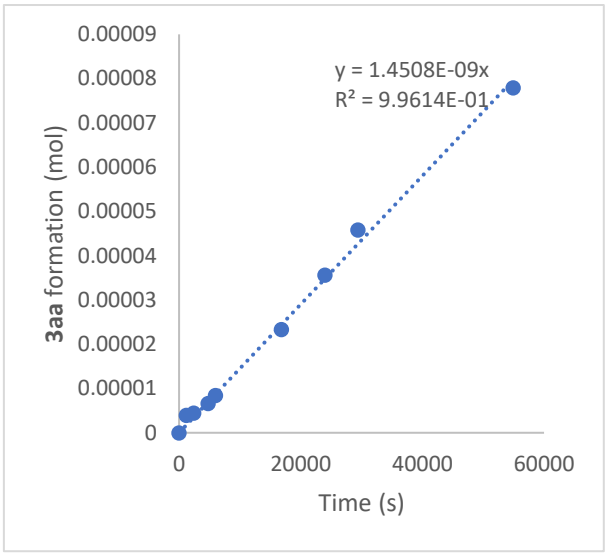

Figure 4.5. Graphical representation of the moles of **4.3aa** formed as a function of time during the quantum yield studies.

From these data, the following quantum yields were determined:

$$\Phi_{\text{diene } \mathbf{6} \text{ formation}} = \frac{1.45*10^{-8}\ mol{\cdot}s^{-1}}{1.2*10^{-6}\ \text{einstein}\ s^{-1}} = 0.012$$

$$\Phi_{\mathbf{3aa} \text{ formation}} = \frac{1.45*10^{-9}\ mol{\cdot}s^{-1}}{1.2*10^{-6}\ \text{einstein}\ s^{-1}} = 0.0012$$

4.4.7.4. Stern-Volmer plots

Stern-Volmer analysis was performed as well as time-correlated single-photon counting (TCSPC). For the TCSPC analysis, samples containing a solution of 4CzIPN in MeCN (1.6 mg in 100 mL, to obtain an absorbance of 0.1 at 450 nm over a pathlength of 1 cm) were deoxygenated through argon purging in a cuvette sealed by a septum. Then, aliquots of the quencher compound (*i.e.*, DIPEA, $Co(ClO_4)_2 \cdot 6H_2O$/**L1** (1/2), **4.1a**, **4.2a,** *i*Pr-DHP **4.4a** or 1,3-diene **4.A**) dissolved in the same 4CzIPN solution were added, thus maintaining the absorbance of the solution while increasing the concentration of quencher. The TCSPC decay was monitored at λ_{em} = 550 nm and fitted biexponentially to obtain the decay-constants of the prompt fluorescence and the thermally-activated delayed fluorescence. The lifetime of either the PF or TADF without quencher divided by the lifetime in the presence of quencher was plotted as a function of quencher to obtain the Stern-Volmer plot, according to formula below. The UV-vis spectrum of each sample was measured prior to and after TCSPC measurements to ensure that no decomposition had taken place during the measurement, and to ensure a stable absorbance.

$$\frac{\tau_0}{\tau} = 1 + \tau_0 k_q [Q]$$

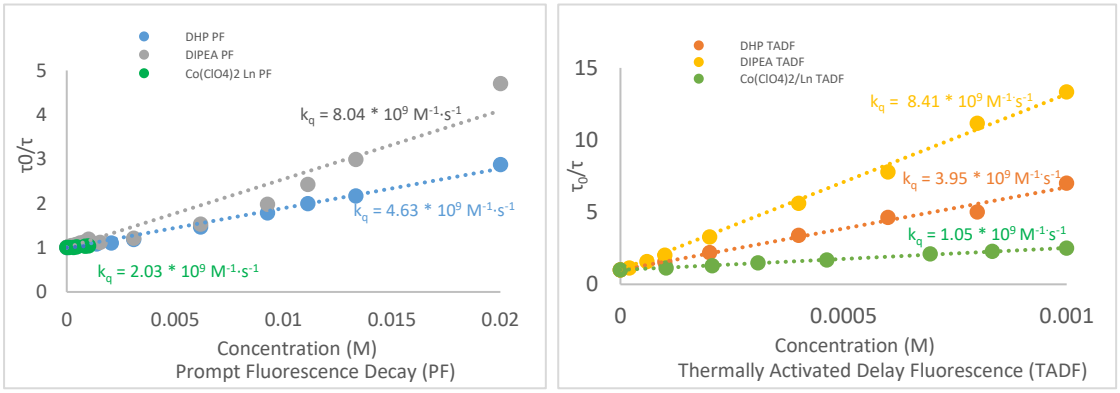

Figure 4.6. Stern-Volmer plots for the quenching of the thermally activated delayed fluorescence decay (TADF) and prompt fluorescence decay (PF) states of 4CzIPN by DIPEA, **4.4a** and $Co(ClO_4)_2 \cdot 6H_2O$/**L1** (1/2).

4.4.7.5. Electrochemical studies

Cyclic voltammograms were collected on a Princeton Applied Research PARSTAT 2273 potentiostat using a glassy carbon disk electrode and a platinum disk as counter-electrode. A silver wire coated with AgCl immersed in a 3 M aqueous solution of NaCl and separated from the analyte by a fritted glass disk was employed as the reference electrode. Voltammograms were taken at r.t. in a 100 mM MeCN solution of tetrabutylammonium hexafluorophosphate (using ferrocene as the internal standard) under an Argon atmosphere. Square wave voltammetry (SWV) was performed with a pulse height of 25 mV, a pulse width of 2 ms and a step height of 2 mV.

To prevent the catalytically active Co^{I} from deleterious disproportionation, 6,6'-dmbpy was used for the measurement, which is the same ligand used in Scheme 4.6. Instead of using $Co(OAc)_2$, $Co(ClO_4)_2 \cdot 6H_2O$ was used here for solubility reasons. Electrochemical investigations on Co-based bipy complexes have been previously conducted based on the work outlined by Minteer and Sigman.[19]

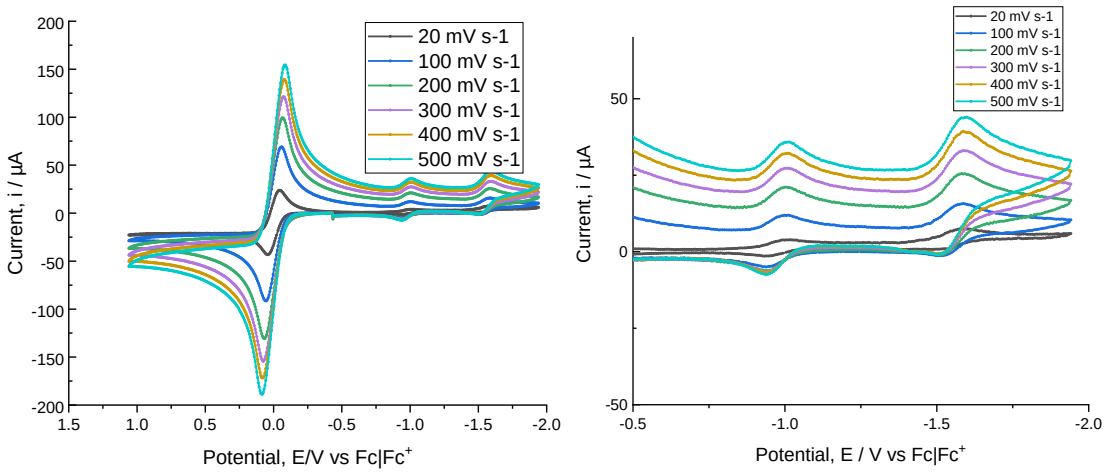

Figure 4.7. CVs of 1.0 mM $Co(ClO_4)_2$ with 2.0 mM **L6** at varying scan rates in a 100 mM solution of NBu_4PF_6 in acetonitrile.

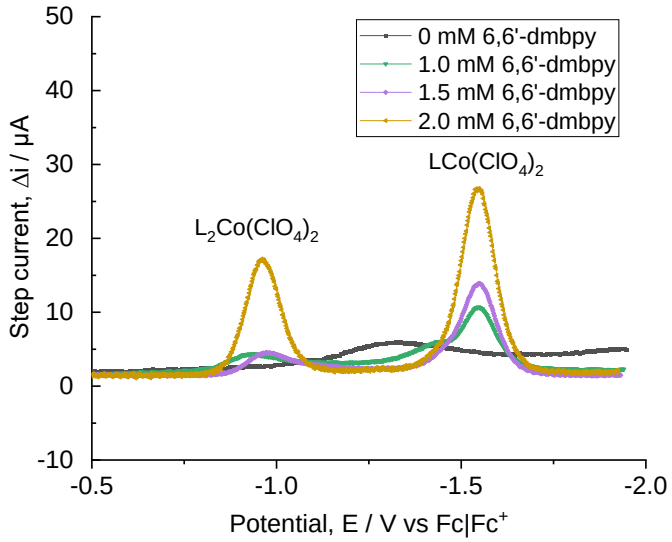

Figure 4.8. Square wave voltammograms of 1 mM $Co(ClO_4)_2 \cdot 6H_2O$ in the presence of 0.0, 1.0, 1.5 and 2.0 mM **L6** in a 100 mM solution of NBu_4PF_6 in acetonitrile.

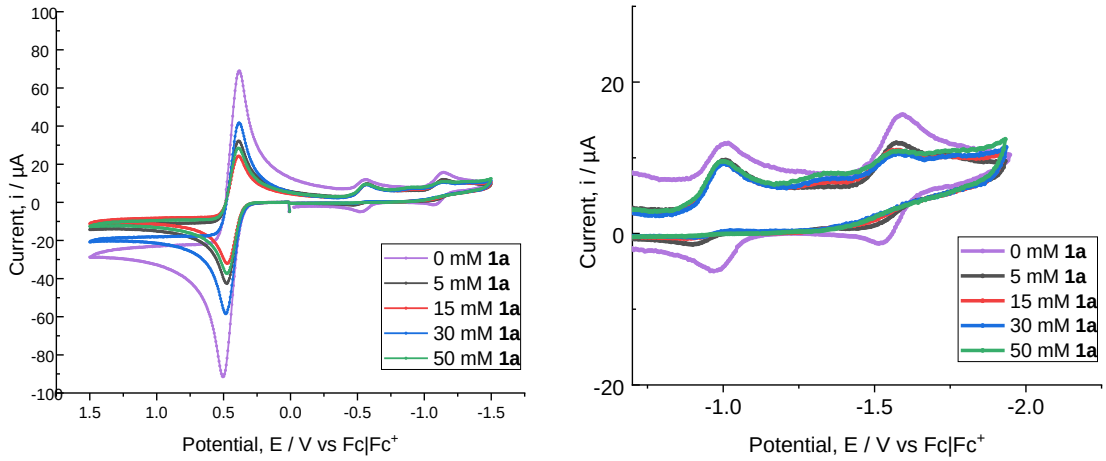

Figure 4.9. CVs of 1.0 mM $Co(ClO_4)_2$ with 2.0 mM **L6** in the presence of varying equivalents of **1a** at 100 $mV \cdot s^{-1}$ in a 100 mM solution of NBu_4PF_6 in acetonitrile.

Chapter 5.

Summary and General Conclusions

Quaternary carbon stereocenters are ubiquitous in bioactive and pharmaceutically relevant molecules. However, the construction of C–C bonds leading to chiral quaternary carbons still remains underdeveloped. Our group has explored allylic substitution reactions by employing vinyl cyclic carbonates (VCCs) as privileged substrate motifs, thereby enabling the versatile formation of stereo-defined building blocks. However, at the time of the start of this thesis work, the focus had been merely on preparative methods giving rise to tetrasubstituted C–X (X = N, B, S and O) bonds. Therefore, in order to expand the repertoire of methodologies that lead to sterically demanding carbon centers, the main objective of this doctoral dissertation was the development of novel enantioselective and/or diastereoselective synthetic protocols that involve C–C bond formations that give access to quaternary carbon stereocenters via dual TM catalyzed or dual photoredox/TM catalyzed allylic alkylation reactions.

It was hypothesized that dual catalytic methods could help to bridge the known reactivity of electrophilic allylic-Pd species with their nucleophilic congeners, whereas the merger of photoredox and TM catalysis should allow for direct cross-coupling of VCCs and otherwise inaccessible reactive radical species. These alternative reactivity paradigms should create new impetus for the conception of elusive quaternary carbon stereocenters in the area of allylic substitution that go beyond the current limitations.

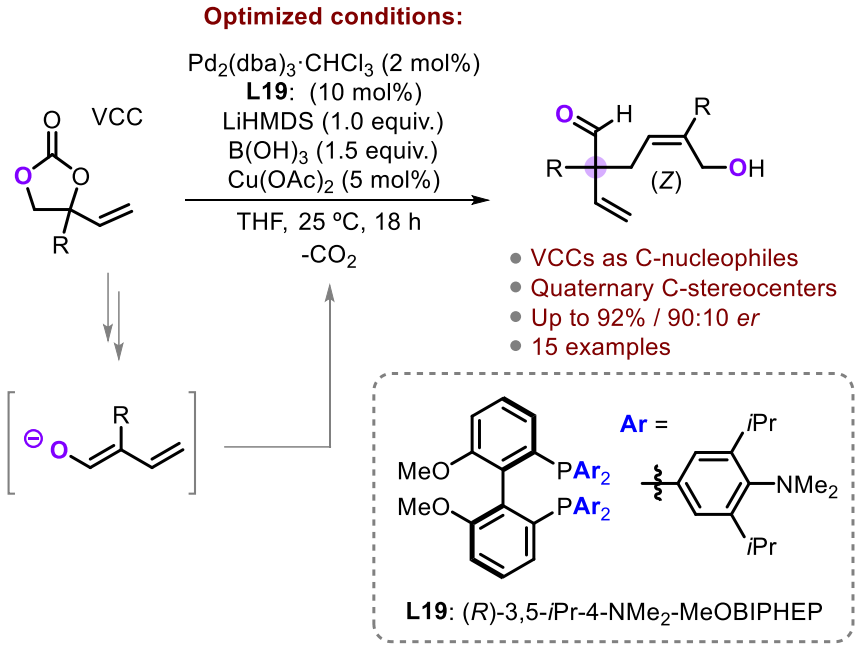

Scheme 5.1. Pd/Cu dual catalyzed asymmetric synthesis of highly functional all carbon quaternary stereocenters from vinyl cyclic carbonates.

Chapter 2 discloses an asymmetric synthesis of quaternary carbon stereocenters through an umpolung approach. Upon decarboxylation of the VCC, a suitable Pd (pre)catalyst transforms it in situ into a nucleophilic dienolate species, which then allowed to react this nucleophilic species with a second molecule of decarboxylated VCC (cf., an electrophilic allyl-Pd complex) to forge an enantioenriched product bearing a quaternary carbon stereocenter (Scheme 5.1). Essentially these transformations can be regarded as cross-electrophile coupling reactions. The enantioinduction was accomplished by a judicious optimization of the chiral ligand structure. Notably, the additives were required to provide additional substrate activation/stabilization giving as a result access to a series of compounds featuring densely functionalized, elusive quaternary carbon stereocenters in appreciable yield and with enantiomeric ratios of up to 90:10. A number of control experiments were conducted in order to rationalize the role of the additives.

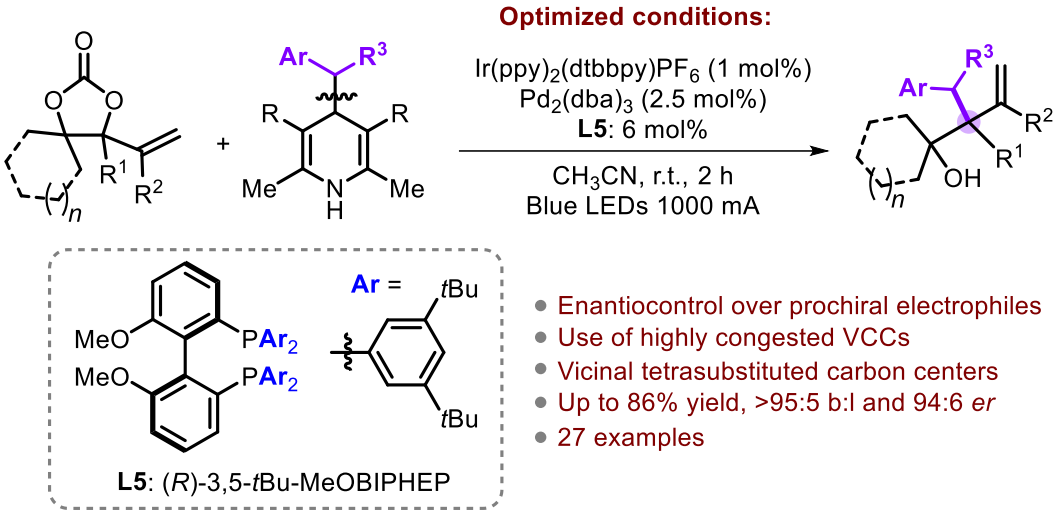

Scheme 5.2. Dual Pd/photocatalytic formation of homoallylic alcohols featuring vicinal tetrasubstituted carbon centers.

In **Chapter 3**, by combining photoredox and Pd catalysis, we were able to establish the decarboxylative asymmetric synthesis of vicinal α,β-tri/tetra and α,β-tetrasubstituted homoallylic alcohols using benzyl-substituted Hantzsch esters as radical precursors (Scheme 5.2). This mild methodology enabled the construction of C–C bonds in appreciable yields, high branch selectivity and enantiomeric ratios of up to 94:6. The protocol is a rare example of using prochiral electrophiles for the creation of vicinal congested carbon centers.

In **Chapter 4**, we present a dual Co/photoredox catalyzed cascade approach that enables the *in situ* conversion of modular vinyl cyclic carbonates into 2-aryl-1,3-diene intermediates, and their subsequent regio- and stereo-selective 1,2-hydroalkylation and 1,2-dicarbonfunctionalization (*only the latter* is shown in Scheme 5.3). The 1,3-diene species are conveniently converted into nucleophilic Co(allyl) intermediates that can be intercepted by aldehyde reagents to afford homoallylic alcohols with ample scope in the reaction partners. The developed protocol marks a significant step forward in the use of structurally versatile 1,3-dienes (which are neither easily accessible nor commercially available) under attractive catalytic conditions.

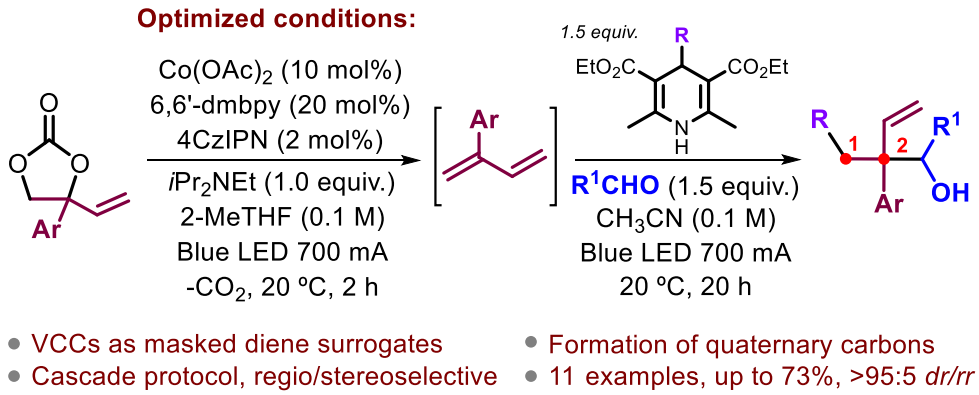

Scheme 5.3. Dual Co/photocatalytic formation of homoallylic alcohols prepared by a domino approach that involves in situ 2-aryl-1,3-diene formation from VCCs and its subsequent 1,2-dicarbofunctionalization.

The **General Conclusion** from this doctoral thesis work is that the obtained results contribute to new synthetic possibilities to construct challenging quaternary carbon stereocenters either in a diastereoselective or enantioselective fashion. Dual metal or TM metal/photoredox catalysis approaches are complementary to existing protocols but offer a way to expand the synthetic toolbox in this area. The nature of the key substrate, a VCC, has been crucial and vindicates its privileged position in the field of organic synthesis by serving as a new type of masked 1,3-diene surrogate, and its transformation to complex building blocks. Such potential should offer a tangible starting point for the diffusion of these VCCs in other synthetic campaigns that focus on the preparation of small molecule synthons.

UNIVERSITAT
ROVIRA i VIRGILI